Deutsche Entomologische Zeitschrift

65 (**1**) 2018

PENSOFT

museum für naturkunde

ISSN 1435-1951 (print), ISSN 1860-1324 (online)
Dtsch. Entomol. Z. 65 (1) 2018, 1–115

Deutsche Entomologische Zeitschrift

An International Journal of Systematic Etymology

Instructions for authors

Scope

Deutsche Entomologische Zeitschrift *is an international peer-reviewed journal of systematic entomology. It publishes original research papers in English on systematics, taxonomy, phylogeny, comparative and functional morphology, as well as biogeography of insects. Other arthropods are only considered where of relevance to the biology of insects. The geographical scope of the journal is worldwide. Priority is given to revisional work and comprehensive studies of phylogenetic, biological or zoogeographical relevance. The journal also welcomes review articles pertaining to systematics and biology of insects.*

Authors and submission

- *Conflicts of interest: Authors must disclose relevant competing interests, both financial and personal.*
- *Ownership: Authors must declare that the submitted work is their own and that copyright has not been breached in seeking its publication.*
- *Originality: Authors must declare that the submitted work has not previously been published, and is not being consid- ered for publication elsewhere.*

Language and style

- *The language of publication is English. There is no general limitation of the length of manuscripts, but please contact the editor before submitting papers exceeding 30 printed pages (approximately 60 manuscript pages including figures).*
- *Manuscripts should be written in a clear, straightforward style and must not have been published or submitted elsewhere.*
- *The text should be 12 pt, double-spaced, one-sided, left justified and with a margin of at least 3 cm.*
- *Use a standard typeface, e.g. Times New Roman as little formatted as possible (without tabulators, several blank spaces, etc.). Avoid footnotes.*
- *Divide the text into sections using headlines and subheadlines. Do not number the headlines. Inline headers should be set in italics and followed by a full stop.*
- *The names of genera and species must be in italics.*
- *Taxonomic descriptions must comply with the rules of the 4th edition of the ICZN (see http://www.iczn.org/).*
- *Enter the page number on every page.*
- *Submit figures with a minimum resolution of 300 dpi.*
- *The preferred file formats are PSD (Photoshop) and TIFF for colour and grayscale illustrations, and EPS for vector graphics.*
- *JPG files are only accepted in high resolution.*

General manuscript structure

If appropriate, the manuscript should be structured using headlines and sub-headlines, but without numbering, according to the following sections:

- *Title page*
- *Abstract*
- *Introduction*
- *Materials and Methods*
- *Results*
- *Discussion*
- *Acknowledgements*
- *References*
- *Tables with captions*
- *Figure captions*

The publication process

Peer reviewing

Manuscripts are subject to peer review. All manuscripts submitted will be reviewed by at least two experts. Authors are welcome to make suggestions for competent reviewers.

Proofs

Prior to publication of your manuscript you will receive proofs in PDF format. Please correct and return the proofs within two weeks to the editorial office.
We recommend using the standard proofreading marks or – in the case of a few corrections – using page and line numbers.
Do not change the contents of your article. Corrections extending beyond production errors will be carried out at the expense of the author.
The editorial office reserves the right to publish your article with only the editor's corrections, if your corrections do not reach us in time.

Publishing

The journal is published in print and online. It is accessible in open access at Pensoft: http://dez.pensoft.net

COPE Membership

This journal endorses the COPE (Committee on Publication Ethics) guidelines and will pursue cases of suspected research and publication misconduct (e.g. falsification, unethical experimentation, plagiarism, inappropriate image manipulation, redundant publication). For further informa- tion about COPE, please see the website for COPE at http://www.publicationethics.org.uk

Deutsche Entomologische Zeitschrift

65 (1) 2018

PENSOFT

museum für naturkunde

Deutsche Entomologische Zeitschrift
An International Journal of Systematic Entomology

Deutsche Entomologische Zeitschrift

2018. Volume 65. Issue 1

ISSN: 1435-1951 (print), 1860-1324 (online)
Abbreviated keys title: Dtsch. Entomol. Z.

In Focus

The cover picture shows *Mecyclothorax* (*Meonochilus*) *amplipennis* (Broun).

See paper of **Liebherr JK** Cladistic classification of *Mecyclothorax* Sharp (Coleoptera, Carabidae, Moriomorphini) and taxonomic revision of the New Caledonian subgenus *Phacothorax* Jeannel

Cover design
Pensoft

PENSOFT

Deutsche Entomologische Zeitschrift
An International Journal of Systematic Entomology

Content of volume **65** (**1**) 2018

Liebherr JK
Cladistic classification of *Mecyclothorax* Sharp (Coleoptera, Carabidae, Moriomorphini) and taxonomic revision of the New Caledonian subgenus *Phacothorax* Jeannel 1

Baranek B, Kuba K, Bauder J, Krenn HW
Mouthpart dimorphism in male and female wasps of *Vespula vulgaris* and *Vespula germanica* (Vespidae, Hymenoptera) 65

Mey W
Vansoniella chirindensis gen. n., sp. n. – an unusual taxon with translucent wings from Zimbabwe (Lepidoptera, Limacodidae) 75

Bidzilya OV, Mey W
Review of the genus *Tricerophora* Janse, 1958 (Lepidoptera, Gelechiidae) with description of six new species 81

Arriaga-Varela E, Wong SY, Kirejtshuk A, Fikáček M
Review of the flower-inhabiting water scavenger beetle genus *Cycreon* (Coleoptera, Hydrophilidae), with descriptions of new species and comments on its biology 99

Abstract & Indexing Information

Biological Abstracts® (Thompson ISI)
BIOSIS Previews® (Thompson ISI)
Camgridge Scientific Abstracts (CSA/CIG)
Web of Science® (Thompson ISI)
Zoological Record™ (Thompson ISI)

Dtsch. Entomol. Z. 65 (1) 2018, 1–63 | DOI 10.3897/dez.65.21000

PENSOFT museum für naturkunde

Cladistic classification of *Mecyclothorax* Sharp (Coleoptera, Carabidae, Moriomorphini) and taxonomic revision of the New Caledonian subgenus *Phacothorax* Jeannel

James K. Liebherr[1]

1 *Cornell University Insect Collection, John H. and Anna B. Comstock Hall, Cornell University, Ithaca, NY 14853-2601, USA*

http://zoobank.org/73DEE0F3-2BB0-4A21-B445-5E168FE50F54

Corresponding author: *James K. Liebherr* (JKL5@cornell.edu)

Received 14 September 2017
Accepted 15 December 2017
Published 18 January 2018

Academic editor:
Dominique Zimmermann

Key Words

aptery
conservation prioritization
endemism
genitalic variation
revisionary systematics

Abstract

The 15 species of *Mecyclothorax* Sharp precinctive to New Caledonia are revised and shown by cladistic analysis to comprise a monophyletic lineage, here treated as subgenus *Phacothorax* Jeannel. The New Caledonian species of subgenus *Phacothorax* include *Mecyclothorax fleutiauxi* (Jeannel), *M. najtae* Deuve, and 13 newly described species: *M. jeanneli* **sp. n.**, *M. laterobustus* **sp. n.**, *M. laterorectus* **sp. n.**, *M. laterosinuatus* **sp. n.**, *M. laterovatulus* **sp. n.**, *M. manautei* **sp. n.**, *M. megalovatulus* **sp. n.**, *M. octavius* **sp. n.**, *M. paniensis* **sp. n.**, *M. picdupinsensis* **sp. n.**, *M. plurisetosus* **sp. n.**, and two jointly authored species; *M. kanak* Moore & Liebherr **sp. n.,** and *M. mouensis* Moore & Liebherr **sp. n.**. Subgenus *Phacothorax* is one of five subgenera recognized within genus *Mecyclothorax* based on cladistic analysis of 65 exemplar taxa utilizing information from 137 morphological characters. The four other monophyletic subgenera include the precinctive Australian *Eucyclothorax* **subgen. n.** (type species *Mecyclothorax blackburni* [Sloane]), the precinctive Queensland *Qecyclothorax* **subgen. n.** (type species *Mecyclothorax storeyi* Moore), the precinctive New Zealand *Meonochilus* Liebherr & Marris **status n.**, and the geographically widespread and very diverse nominate subgenus, distributed from St. Paul and Amsterdam Islands, eastward across Australia and New Guinea, and in the Sundas, Timor Leste, Lord Howe and Norfolk Islands, New Zealand, and the Society and Hawaiian Islands. The biogeographic history of *Mecyclothorax* can be derived from the parsimony cladogram time-calibrated by times of origin of particular geographic areas inhabited by resident representative species. Based on sister-group status of subgenus *Phacothorax* and subgenus *Mecyclothorax*, and occupation of Lord Howe Island–an island originating no earlier than 6 Ma–by the earliest divergent lineage within subgenus *Mecyclothorax,* the ancestor of present-day *Phacothorax* spp. is hypothesized to have colonized New Caledonia 6 Ma, subsequent both to Cretaceous Gondwanan vicariance as well as any Oligocene submergence. Area relationships among the New Caledonian *Phacothorax* point to earliest diversification incorporating the northern massifs, and most recent diversification on the ultramafic volcanic substrates in the south of Grand Terre. Flight wing loss has played an important role in shaping the various island faunas, both in their morphology as well as their diversity. The retention of flight capability in only a few of the many hundred *Mecyclothorax* spp. is presented in light of how populations evolve from macropterous colonizing propagules to vestigially winged specialists. Interspecific differences in genitalic structures for the sister-species pair *M. fleutiauxi* + *M. jeanneli* are shown to involve functional complementarity of male and female structures. Extensive geographic variation of male genitalia is demonstrated for several New Caledonian *Mecyclothorax* spp. This variation deviates from the geographically uniform male genitalia exhibited by species in the hyperdiverse *Mecyclothorax* radiation of Haleakalā volcano,

Maui, suggesting that extensive sympatry occurring among species in that diverse species swarm selects for stability within this mate recognition system. Conversely, lower levels of sympatry characterizing the depauperate New Caledonian radiation permit the presence of more extensive male genitalic variation, this variation not selected against due to the lower likelihood of interspecific mating mistakes.

Introduction

The carabid beetle fauna of New Caledonia comprises elements ranging from the mundane to the bizarre. Typical of the more mundane representatives of the fauna would be the geographically widespread species *Platycoelus melliei* (Montrouzier), native to Australia and present in New Caledonia likely due to human transport (Will 2011). Somewhat less mundane would be a generalized native such as *Notagonum kanak* (Fauvel), the single New Caledonian representative species of a geographically widespread, southwest Pacific grade of platynine carabid beetles (Darlington 1952), most species of which include flight capable individuals (Liebherr 2017a). Though the New Caledonian *N. kanak* is precinctive to the island, and is the product of speciation within New Caledonia, its presence on the island can tell us little about the history of New Caledonia. Of much more interest both morphologically and potentially biogeographically are those lineages that have radiated in New Caledonia resulting in numerous native, precinctive species. Such biological diversity may belie longer periods of residency by these lineages offering the possibility that earlier geological events influenced their phylogenetic history. *Abacophrastus* Will, an endemic New Caledonian genus of pterostichine Carabidae with seven precinctive New Caledonian species (Will 2011), is a candidate for implicating events of earth history based on the phylogenetic relationships both within and external to the genus. *Cyphocoleus* Chaudoir, a New Caledonian endemic genus described in tribe Platynini, and placed in terminal position with that tribe in catalogues (Csiki 1931, Lorenz 2005) due to its bizarre "platynine" anatomy, is actually an aberrant member of the Odacanthini with relatives in both Australia and South America, suggesting a Cretaceous-aged biogeographic link via an Antarctic pathway (Liebherr 2016). Only phylogenetic analysis of *Cyphocoleus* plus a broad array of potential outgroups allowed such a hypothesis to be proposed. Conversely, immense disparity across an island radiation may evolve adaptively in isolated and restricted island situations over a very short time, such as with *Mecyclothorax* carabid beetles of the Society and Hawaiian Islands (Liebherr 2013, 2015). Characterizing such biological diversity is the first step toward hypothesizing the context within which a particular lineage has evolved. Cladistic analysis of the recognized species-level taxa, in light of appropriate outgroups (Hennig 1966), comprises the second step. Only then can biogeographic hypotheses be proposed and tested using area-based methods such as vicariance biogeography (Nelson and Platnick 1981, Ladiges and Cantrill 2007), or temporal-calibration methods such as lineage divergence dating based on molecular sequence data (Grandcolas et al. 2008, Nattier et al. 2017).

This contribution sets out to establish the phylogenetic context of a taxon of New Caledonian carabid beetles initially proposed as the distinct genus *Phacothorax* Jeannel (1944). Jeannel proposed recognition of this group at the generic level due to its distinct external anatomy, though he noted that *Phacothorax* shared male genitalic characters with the Australian and Hawaiian, geographically widespread genus *Mecyclothorax* Sharp. Once phylogenetic relationships of the *Phacothorax* radiation and its outgroups are established, the sister group relationships of the constituent clades allow a concise hypothesis for time of origin of the New Caledonian radiation. This allows addition of *Phacothorax* spp. to the panoply of New Caledonian taxa for which hypothesized ages of origin range from the Pleistocene to much earlier in the Eocene to Cretaceous (Nattier 2017). In addition to proposing phylogenetic relationships for the *Phacothorax* radiation, all presently known species are validated through species description, with a dichotomous key provided for taxonomic study of this radiation. These species-level treatments establish distributional hypotheses that define areas of endemism appropriate for conservation prioritization, and expose biogeographic factors associated with species diversification. The role of flight wing loss during the evolution of *Mecyclothorax* is investigated. Differences in genitalic morphology both within and between species are presented, these pointing to functional interactions of the male intromittent organ and the female reproductive tract, as well as providing information on the level of cohesion among populations comprising geographically widespread species. This variation is compared to that observed in more diverse Polynesian *Mecyclothorax* radiations, with the differences related to requirements of an evolutionarily stable mate recognition system.

Material and methods

Taxonomic material. Revision of New Caledonian *Mecyclothorax* is based on 676 specimens deposited in 12 institutional or personal collections. The bulk of the material–518 specimens–was collected during various expeditions by Dr. Geoff Monteith and colleagues, Queensland Museum, Brisbane (QMB). Material from the Museum of Natural History, Wrocław University (MNHW) complements the QMB material in the careful annotation of geographic coordinates, elevation, and collecting method

or situation. Use of label data from these two institutional collections provided the principal core of information for characterizing microhabitat occupation for the species. Additional material deposited in the following institutional collections was also studied: B. P. Bishop Museum, Honolulu (BPBM); Canadian National Collection, Agriculture Canada, Ottawa (CNC); Cornell University Insect Collection (CUIC); Essig Museum of Entomology, University of California, Berkeley (EMEC); Hungarian Natural History Museum, Budapest (HNHM); Muséum d'Histoire naturelle, Genève (MHNG); Muséum national d'Histoire naturelle, Paris (MNHN); Naturhistorisches Museum, Wien (NHMW); Queensland Museum, Brisbane (QMB); Martin Baehr personal collection (MBC); Pier M. Giachino personal collection (PMGC).

Material collected by Herbert Franz in 1970 (NHMW) were labeled only with a key code, with the codes deciphered in his field notebook (Jäch, pers. comm.).

All type specimens are labeled as such, with data for holotypes presented verbatim, including typographic spacing and capitalization. Individual lines on a label are separated by a slash "/" and different labels are indicated by a double slash "//". The complete list of scientific names for species included in the cladistic analysis, with authorship, is provided in Table 1, obviating the need to clutter the text with author names.

Laboratory techniques. Dissection and staining techniques are fully described in Liebherr (2015: 18–20). All male and female dissections were photographed using a Microptics (now Visionary Digital®) macrophotographic apparatus, using a Nikon D1X camera, fibre-optic strobe light source, and K-series Microptics lenses. Specimens were slide-mounted and photographed with backlighting provided by a transmitted light stage, or backlighting plus direct lighting provided by multiple fibre-optic cables. All specimens photographed with direct lighting were surrounded with two nested Lucite® tubes lined with translucent plastic drafting film.

Table 1. Species-level taxa included in cladistic analysis. *Mecyclothorax* subgeneric classification based upon results of cladistic analysis. Type species indicated for *Mecyclothorax* generic-level taxa. *Mecyclothorax andersoni* represented by infraspecific aedeagal forms with either a short or long median lobe apex (Liebherr 2017b). *Mecyclothorax* sp. n. D treated as non-valid terminal; species to be described subsequently.

Moriomorphina [secondary outgroup]
Neonomius laevicollis (Sloane)
Amblytelina [primary outgroups]
Amblytelus brevis Blackburn
Amblytelus curtus (F.)
Amblytelus matthewsi Baehr
Dystrichothorax amplipennis (MacLeay)
Epleyx lindensis Blackburn
Paratrichothorax brevistylus Baehr
***Mecyclothorax* Sharp [ingroup]**
subgenus *Eucyclothorax* Liebherr subgen. n
Mecyclothorax (*Eucyclothorax*) *blackburni* (Sloane) [type species]
Mecyclothorax (*Eucyclothorax*) *curtus* (Sloane)
Mecyclothorax (*Eucyclothorax*) *eyrensis* (Blackburn)
Mecyclothorax (*Eucyclothorax*) *lophoides* (Chaudoir)
Mecyclothorax (*Eucyclothorax*) *moorei* Baehr
Mecyclothorax (*Eucyclothorax*) *peryphoides* (Blackburn)
Mecyclothorax (*Eucyclothorax*) *punctatus* (Sloane)
Mecyclothorax (*Eucyclothorax*) sp. n. D
subgenus *Qecyclothorax* Liebherr subgen. n.
Mecyclothorax (*Qecyclothorax*) *impressipennis* Baehr
Mecyclothorax (*Qecyclothorax*) *inflatus* Baehr
Mecyclothorax (*Qecyclothorax*) *lewisensis* Moore
Mecyclothorax (*Qecyclothorax*) *storeyi* Moore [type species]
subgenus *Meonochilus* Liebherr & Marris status n.
Mecyclothorax (*Meonochilus*) *amplipennis* (Broun) [type species]
Mecyclothorax (*Meonochilus*) *bellorum* (Liebherr & Marris)
Mecyclothorax (*Meonochilus*) *eplicatus* (Broun)
Mecyclothorax (*Meonochilus*) *rectus* (Liebherr & Marris)
Mecyclothorax (*Meonochilus*) *spiculatus* (Liebherr & Marris)
subgenus *Phacothorax* Jeannel
Mecyclothorax (*Phacothorax*) *fleutiauxi* (Jeannel) [type species]
Mecyclothorax (*Phacothorax*) *jeanneli* Liebherr sp. n.
Mecyclothorax (*Phacothorax*) *kanak* Moore & Liebherr sp. n.
Mecyclothorax (*Phacothorax*) *laterobustus* Liebherr sp. n.
Mecyclothorax (*Phacothorax*) *laterorectus* Liebherr sp. n.
Mecyclothorax (*Phacothorax*) *laterosinuatus* Liebherr sp. n.
Mecyclothorax (*Phacothorax*) *laterovatulus* Liebherr sp. n.
Mecyclothorax (*Phacothorax*) *manautei* Liebherr sp. n.
Mecyclothorax (*Phacothorax*) *megalovatulus* Liebherr sp. n.
Mecyclothorax (*Phacothorax*) *mouensis* Moore & Liebherr sp. n.
Mecyclothorax (*Phacothorax*) *najtae* Deuve
Mecyclothorax (*Phacothorax*) *octavius* Liebherr sp. n.
Mecyclothorax (*Phacothorax*) *paniensis* Liebherr sp. n.
Mecyclothorax (*Phacothorax*) *picdupinsensis* Liebherr sp. n.
Mecyclothorax (*Phacothorax*) *plurisetosus* Liebherr sp. n.
subgenus *Mecyclothorax* Sharp
Mecyclothorax (*Mecyclothorax*) *amingwiwae* Liebherr
Mecyclothorax (*Mecyclothorax*) *andersoni* Liebherr
Mecyclothorax (*Mecyclothorax*) *andersoni* Liebherr (long aedeagus)
Mecyclothorax (*Mecyclothorax*) *baehri* Guéorguiev
Mecyclothorax (*Mecyclothorax*) *brispex* Liebherr
Mecyclothorax (*Mecyclothorax*) *goweri* Moore
Mecyclothorax (*Mecyclothorax*) *gressitti* Liebherr
Mecyclothorax (*Mecyclothorax*) *howei* Moore
Mecyclothorax (*Mecyclothorax*) *kavanaughi* Liebherr
Mecyclothorax (*Mecyclothorax*) *medioconstrictus* Liebherr
Mecyclothorax (*Mecyclothorax*) *sedlaceki* Darlington
Mecyclothorax (*Mecyclothorax*) *ambiguus* (Erichson)
Mecyclothorax (*Mecyclothorax*) *basipunctus* Louwerens
Mecyclothorax (*Mecyclothorax*) *globicollis* (Mandl)
Mecyclothorax (Mecyclothorax) lateralis (Laporte de Castelnau)
Mecyclothorax (Mecyclothorax) lissus (Andrewes)
Mecyclothorax (*Mecyclothorax*) *marau* Perrault
Mecyclothorax (*Mecyclothorax*) *minutus* (Laporte de Castelnau)
Mecyclothorax (*Mecyclothorax*) *monteithi* Moore
Mecyclothorax (*Mecyclothorax*) *montivagus* (Blackburn) [type species]
Mecyclothorax (*Mecyclothorax*) *oopteroides* Liebherr
Mecyclothorax (*Mecyclothorax*) *otagoensis* Liebherr
Mecyclothorax (*Mecyclothorax*) *punctipennis* (MacLeay)
Mecyclothorax (Mecyclothorax) rectangulus Louwerens
Mecyclothorax (*Mecyclothorax*) *rotundicollis* (White)
Mecyclothorax (*Mecyclothorax*) *sculptopunctatus* (Enderlein)

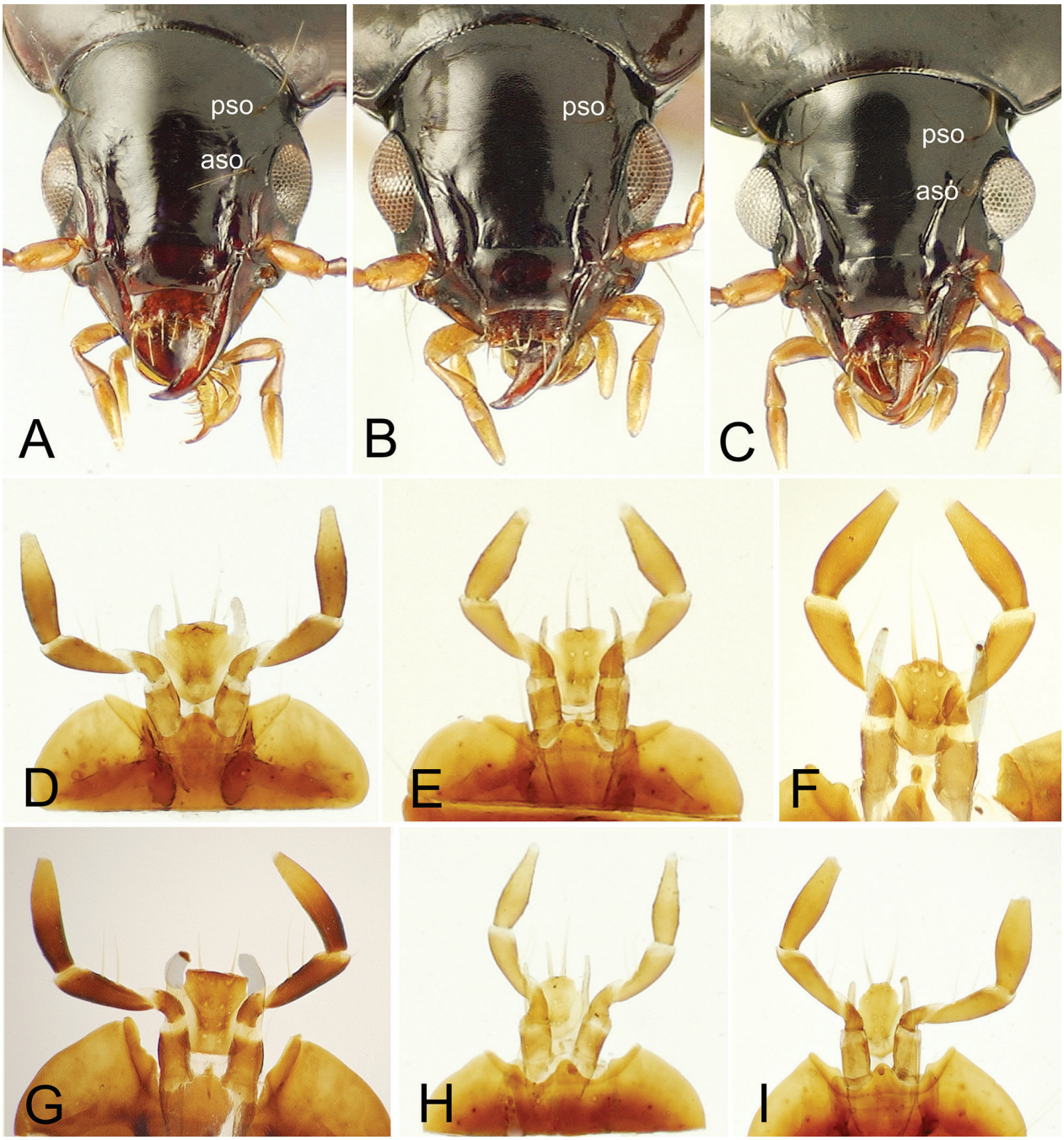

Figure 1. Head and mouthpart structures of *Mecyclothorax* spp. **A–C**. Head capsule, dorsal view: **A**, *M. goweri*; **B**, *M. fleutiauxi*; **C**, *M. laterorectus*. **D–I**, Mentum, labial palps and ligula: **D**, *M. peryphoides*, ventral view; **E**, *M. storeyi*, ventral view; **F**, *M. amplipennis*, dorsal view; **G**, *M. montivagus*, dorsal view; **H**, *M. kanak*, ventral view; **I**, *M. fleutiauxi*, ventral view. Abbreviations include: **aso**, anterior supraorbital seta; **pso**, posterior supraorbital seta.

Descriptive conventions. Several measurements proved useful for diagnosing species. Eye development was quantified by the ocular ratio: MHW/mFW, or maximum head width across eyes divided by the minimum frons width between eyes. The breadth of the eye socket on the head capsule varies from smaller, with the eye covering less of the extended ocular lobe (Fig. 1A), to larger, with the eye covering much of the lateral surface of the ocular lobe (Fig. 1B). This amount of coverage was quantified by the ocular lobe ratio, EyL/OLL, or the diameter of the eye measured in dorsal view divided by the distance from the anterior margin of the eye to the constriction of the head capsule posterad the ocular lobe. Thirdly, the convexity of the outer eye surface was quantified by the eye length measured in dorsal aspect divided by the eye depth, EyL/EyD, measured so that the entire dorsal margin of the eye lay perpendicular in the field of view. This ratio was influenced by the position of the eyes on the head capsule, for some species have eyes placed more dorsally on the head capsule, necessitating determination

of eye depth such that the head was not horizontal when the latter measurement was made.

Elongation of the mandibles was quantified relative to the anterior margin of the labrum by the ratio of the distance from the base of the dorsal (anatomically anterior) condyle of the mandible to the mandibular apex divided by the distance from condylar base to the anterolateral margin of the labrum. Specimens with a non-retracted or angularly retracted labrum were used for this ratio when possible; otherwise the position of a non-retracted labrum was estimated.

Dimensions of the pronotum were routinely used to diagnose several of the species, with four measurements made: **1**, MPW, maximum pronotal (or prothoracic) width, measured either across the pronotum, or across the externally bulging proepisternum if visible in dorsal view; **2**, APW, apical pronotal width, measured between the two most anterior points along the anterior pronotal margin; **3**, BPW, basal pronotal width, measured across the base of the pronotum along the lateral marginal bead; and **4**, PL, pronotal length, or the distance from the apex of the pronotum to the basal margin measured along the midline. These measurements were variously combined into the ratios APW/BPW, MPW/BPW, and MPW/PL, in order to describe prothoracic configuration. Two measurements of the elytra were also used to describe body shape: **1**, MEW, maximal elytral width; and **2**, EL, elytral length, or the distance from the base of the scutellum to the elytral apex, measured parallel to the suture, and to the farther of the two apices if they are separated by a median invagination at the suture. These measurements were combined into the ratio MEW/EL. The ranges of all ratios are used for descriptive purposes only without any statistical connotations. When sufficiently available, at least five specimens were chosen for calculation of ratios, encompassing the largest and smallest specimen available, plus male and female representatives. For widespread species, five specimens from various localities were measured in order to give a view to any infraspecific trends in size or shape. The number of specimens used is presented at the start of each description. The number of male and female dissections used to elucidate male genitalic and female genitalic and reproductive tract characters is provided at the start of those sections of the species treatment.

Standardized body length used to describe body size is the sum of three measurements: **1**, head length measured from the labral medioapical margin to the cervical ridge at the head-pronotal juncture; **2**, pronotal length as measured above; **3**, elytral length as measured above. As this sum of measurements ignores the apical portion of the elongate mandibles (always in variable positions specimen to specimen) and any distended portions of the abdomen (also variable dependent on specimen condition when prepared), the standardized body length measure will be smaller than the size perceived by eye.

Dorsal body setation exhibited by each species is summarized in the diagnosis using a chaetotaxic formula expanded from that first proposed for *Mecyclothorax* by Perrault (1984). The formula designates presence (+) or absence (–) of the anterior supraorbital seta, posterior supraorbital seta, lateral pronotal seta, basal pronotal seta, parascutellar seta, and the subapical and apical elytral seta. The number of dorsal elytral setae associated with the third elytral interval is indicated using Arabic numbers. The positions of these setae are illustrated in Liebherr (2013: fig. 2) and Liebherr (2015: fig. 7). For this contribution, the formula +/+//+/–//+/2/+/+ designates presence of both supraorbitals, presence of the lateral pronotal seta but absence of the basal seta, presence of the parascutellar seta, presence of two dorsal elytral setae, and presence of both subapical and apical elytral setae. The various body regions–head, pronotum, elytra–are separated by double slashes (//). For variable numbers of dorsal elytral setae among individuals, the range of setae present is given. If a seta is variably present or absent, this variation is indicated using "+–."

Comprehensive descriptions to complement the diagnoses are provided for all newly described species. The various ratios that quantify proportions of body somites or their constituent structures–e.g., antennae, mandibles, eyes, pronota, elytra–are presented for all species. All character data were recorded in an Excel® spreadsheet, the characters grouped onto sheets according to body region. This spreadsheet is available from the author upon request. Also, many of the character states used as the basis for taxonomic description are also presented in the cladistic analysis (Fig. 7, Suppl. material 1).

Cladistic analysis

Ingroup circumscription. Based on a tribal analysis of Moriomorphini (Liebherr 2011), it was determined that the genera *Amblytelus* and *Mecyclothorax* constituted components of a monophyletic moriomorphine subtribe Amblytelina. The New Caledonian species were first considered to represent the distinct genus *Phacothorax* Jeannel (Jeannel 1944), though the second-known species was described as *Mecyclothorax najtae* (Deuve 1987). Based on preliminary dissections of the material revised herein, Liebherr and Marris (2009) synonymized *Phacothorax* with *Mecyclothorax*. In order to elucidate the phylogenetic relationships of the revised New Caledonian taxa, and thereby to determine their generic-level classification within Amblytelina, they were analyzed along with a broad array of other *Mecyclothorax* taxa (Table 1). This constituted a broad representation of described Australian taxa, plus representative species from Papua New Guinea, Java, Borneo, New Zealand, St. Paul and Amsterdam Islands, Lord Howe Island, Norfolk Island, and the Society and Hawaiian Islands. Outgroup taxa representing other amblyteline lineages were chosen based on the classification of Baehr (2004), including three species of *Amblytelus* Erichson, *Dystrichothorax amplipennis*, *Epelyx lindenensis*, and *Paratrichothorax brevistylus*. The entire analysis was rooted between the *Amblytelus-Mecyclothorax* ingroup and the outgroup *Neonomius laevicollis,* a

species similar in external appearance to *Mecyclothorax* species, but differing in male and female genitalic characters such that it is properly considered a member of the subtribe Moriomorphina instead of subtribe Amblytelina (Liebherr 2011).

Characters. Information from 137 binary or multistate characters was recorded for 65 moriomorphine taxa; 7 outgroup taxa and 58 terminals assignable to the genus *Mecyclothorax*. In the listing of characters below, multistate characters are presented as either ordered (+) or unordered (–). The initial state descriptions are nearly verbatim relative to the Winclada dataset (Suppl. material 1), although in some instances a more expanded description of the character states supported by illustrations is required. Characters are numbered as per the Winclada default: starting at 0.

0. 3rd antennomere (–): glabrous except for apical ring of setae (0); a few short setae basad distal ring (1); with 3–4 series of elongate setae along shaft (2); setose in apical half (3). This character is treated as unordered so as not to require that the state of a setose apical half of the antennomere be derived only from the state wherein a few setae accompany the apical ring of setae.

1. Antennomere 9 length/width ratio (+): $1.46 < x \leq 1.92$ (0); $2.0 < x < 2.8$ (1); $x \geq 2.89$–3.43 (2). The ratio values for the three states span the limits presented.
2. Labrum front margin (+): straight (0; Fig. 9A); slightly emarginate (1; Fig. 1B–C)); moderately to deeply emarginate (2; Fig. 1A).
3. Mandibular length ratio (+): very short, ratio 1.18–1.55 (0); moderately elongate, ratio of 1.57–1.92 (1; Fig. 1B–C); elongate, ratio of 1.95–2.33 (2; Fig. 1A). The distributional limits of the ratios representing the three states are reflected in the values presented.
4. Apical 2 maxillary palpomeres (+): apparently glabrous (0; Figs 1A–C); with sparse pelage of short setae (1); with pelage of elongate setae (2).
5. Anterior supraorbital seta: present (0; Fig. 1A, C)); absent (1; Fig. 1B).
6. Frontal grooves: very shallow, not evident between eyes (0); shallow to deep, evident between eyes (1).
7. Frontal grooves (–): subparallel (0; Figs 1A, 8D–E); arcuately convergent, then divergent anterad (1; Figs 1B, 8A–B); very deep from front of eye, large lateral callous, pit at frontoclypeal suture (2; Figs 1C, 8C); shallow, convergent from front of eye, no pit at frontoclypeal suture (3).
8. Frontal grooves: not extended onto, or much shallower on clypeus (0; Fig. 8C–E); extended onto clypeus (1; Figs 1, 8A–B).
9. Neck impression (+) absent, dorsum of head convex (0; Figs 1B-C, 8A–B); flat area between hind margins of eye (1); transverse depression behind hind margins of eyes (2; Figs 1A, 8C–E).
10. Ocular lobe assessed behind eye (dorsal view): protruded, meeting gena at obtuse angle (0; Fig. 8A, D–E); little protruded, meeting gena at very obtuse angle (1; Figs 1, 8B–C).
11. Ocular lobe groove behind eye (+): distinct groove present (0; Fig. 8D–E); shallow groove present (1; Figs 1A, 8A–C); no groove present, juncture simple change in angle of surfaces (2; Fig. 1B–C).
12. Mentum tooth: sides acute to subparallel, apex tightly rounded (0; Fig. 1F–I); sides more obtuse, apex broadly rounded (1; Fig. 1D–E).
13. Mentum width/length ratio (+): $2.3 < x < 3.11$ (0); $3.14 < x < 3.5$ (1); $3.70 < x < 4.0$ (2). This ratio is defined as the maximum breadth of the mentum measured across its convex lateral margins divided by the distance from the mentum-submentum suture to the apex of a lateral lobe. The distributional limits of the states are reflected in the values presented.
14. Apex of ligula (+): apically rounded or with narrow concave apex between setae (0; Fig. 1E–F, H–I); broad, longer medially with shorter lateral wings (1; Fig. 1D); broadly truncate, margin straight and heavily sclerotized (2; Fig. 1G).
15. Apical two ligular setae: proximate, separated by 1–2 setal diameters (0; Fig. 1E, F, H–I); distant, separated by 3–4 or more setal diameters (1; Fig. 1D, G).
16. Paraglossae (+): extended only slightly beyond apex of ligula (0); extended 1/2 distance from base to ligular apex beyond apex (1; Fig. 1G, I); extended as far beyond apex as basal length to apex (2; Fig. 1F); extended 2× as far beyond apex as basal length of apex (3; Fig. 1D–E, H).
17. Ocular ratio (+): $1.31 < x \leq 1.42$ (0; Fig. 1A); $1.43 \leq x \leq 1.54$ (1; Fig. 1B–C): $1.55 \leq x < 1.75$ (2). Although the limits of the ratios for the three states were chosen to maximize fidelity to each state, there were seven species that exhibit infraspecific eye development requiring they be coded polymorphic for states 0 and 1: *Mecyclothorax bellorum*, *M. eyrensis*, *M. inflatus*, *M. kanak*, *M. laterostinuatus*, *M. megalovatulus*, and *M. mouensis* (Suppl. material 1)
18. Ocular lobe ratio (+): $0.59 < x < 0.72$ (0; Fig. 1A); $0.73 < x < 0.87$ (1; Fig. 1C); $0.88 < x < 0.97$ (2; Fig. 1B). As for character 17, numerous species exhibit polymorphism in this character: one for states 0 and 1 (*M. spiculatus*); and seven for states 1 and 2 (*M. blackburni*, *M. curtus*, *M.* n sp. D, *M. eyrensis*, *M. laterosinuatus*, *M. montivagus*, and *M. rectus*) (Suppl. material 1).
19. Eye convexity (EyL/EyD) (+): convex or popeyed, $2.0 < x < 2.53$ (0); moderately convex, $2.55 < x < 2.89$ (1; Fig. 1C); little convex, $2.90 < x < 4.18$ (2; Fig. 1A–B). As for the other two eye ratios, six species were coded as polymorphic under this character coding scheme: *M. curtus* for states 0 and 1, and five species–*M. bellorum*, *M. blackburni*, *M. eplicatus*, *M. lophoides*, and *M. peryphoides*–for states 1 and 2 (Suppl. material 1).
20. Number of ommatidia across horizontal diameter of eye (+); 11–15 (0; Fig. 1A, C); 16–20 (1; Fig. 1B); 21–30 (2); 31–40 (3).
21. Pronotum: broad basally, MPW/BPW = 1.23–1.80 (0; Fig. 2A); narrow basally, MPW/BPW = 1.82–3.91 (1;

Fig. 1B). Only *M. eyrensis* failed to adhere to the ratio limits used to define the two states of this character, as individuals exhibited ratios = 1.77–1.82.

22. Pronotal lateral seta: present (0; Fig. 2A–B); absent (1; Fig. 9D–E).
23. Pronotal basal seta: present (0; Fig. 8D–E); absent (1; Fig. 2A–B).
24. Lateral pronotal setal position (if present) (+) with: articulatory socket in or adjoining lateral marginal depression (0); articulatory socket 1/2–2 setal diameters medially from marginal depression (1); articulatory socket 2–4 setal diameters medially from marginal depression (2).
25. Pronotal hind seta (if present): situated at hind angle (0); visibly anterad hind angle (1).
26. Pronotal hind angles (+): nearly right to obtuse, with sides subparallel anterad hind angle (0; Fig. 2A); obtuse, sides divergent anterad hind angle (1); projected denticle on rounded lateral margin (2); obsolete, lateral and basal margins convex (3, Fig. 9D–E).
27. Pronotal hind angle: rounded to right-angled (0; Fig. 2A–B); acute, with acuminate lateral projection at angle (1; Fig. 8C).
28. Pronotal basal margin: straight or convex mesad hind angles (0; Fig. 8C); distinctly sinuate inside hind angles (1; Fig. 8A).
29. Pronotal median base (+): coplanar with disc medially (0; Fig. 2A); depressed relative to disc medially (1; Figs 2B, 8A–B, D); greatly depressed relative to disc medially (2; Fig. 8C, E).
30. Pronotum median base (+): smooth laterally mesad laterobasal depressions (0; Fig. 2A–B); with 3–10 punctures each side mesad laterobasal depressions (1; Fig. 8B); with >12 punctures each side mesad laterobasal depressions (2; Fig. 8A, C–E).
31. Pronotal basal margin: beaded medially (0; Fig. 8A); convex medially, marginal bead only behind laterobasal depression (1; Figs 2A–B, 8B–E).
32. Pronotal basal marginal bead (if present; i.e. state 0, #31): narrow, continuous with lateral bead (0); broader, discontinuous with lateral bead (1).
33. Pronotal median longitudinal impression (+): well defined, continuous on pronotal disc (0; Figs 2B, 8B–C); fine and shallow on disc (1; Figs 2A, 8A, D–E); reduced to small punctures, obsolete, or obscured by punctures (2).
34. Anterior transverse impression (+): obsolete to absent medially, anterior callosity not defined (0; Fig. 16B–C); broad and shallow medially, anterior callosity broadly convex (1; Figs 2A–B, 8A, C); broad and deep medially, anterior callosity well defined posteriorly (2; Fig. 8B, D–E).
35. Anterior transverse impression (+): absent to obsolete laterally (0; Fig. 2A–B); visible only in outer 1/4–1/3 of breadth each side (1); visible in outer 1/2 of breadth each side (2); visible across entire breadth of notum (3; Fig. 8B–E).
36. Pronotal anterior margin: unmargined (0); with marginal bead medially (1).
37. Pronotal front angles (+): not protruded, rounded behind (0; Fig. 8A); slightly protruded, broadly rounded (1; Fig. 8B, D–E); slightly protruded, narrowly to tightly rounded (2; Figs 2A–B, 8C); protruded, obtusely rounded to angulate (3; Fig. 9D–E); protruded, broadly rounded (4).
38. Pronotal lateral marginal depression (at midlength) (+): very narrow, margin beaded (0; Fig. 8A–C); moderately narrow, microsculpture visible at depth (1; Fig. 2A–B); broad to very broad, lateral margin variously explanate, microsculpture evident (2; Fig. 8D–E).
39. Pronotal laterobasal depression (–): broad, smoothly extended to lateral margin (0; Fig. 9D–E); continuous linear broadening of lateral marginal depression (1; Fig. 2B); with median longitudinal/punctate depression and lateral tubercle (2; Fig. 2A); not depressed, surface rugose or punctate (3).
40. Prosternal process: smooth ventrally, rounded behind (0; Fig. 2D–F); margined ventrally, a bead defining ventroposterior margin (1).
41. Proepisternum (+): smooth (0; Fig. 2C, E); with large punctures ventrally along sternum (1; Fig. 2D); covered with large punctures (2; Fig. 2F).
42. Prosternum (+): medially convex anterad and between coxal cavities (0); medially depressed only between coxal cavities (1; Fig. 2D); medially depressed between and anterad coxal cavities (2; Fig. 2C, D–F).
43. Prosternum (+): smooth medially (0; Fig. 2C); with 2 punctures medially (1); with 5–7 punctures medially (2; Fig. 2D–F).
44. Lateral portion of prosternum: impunctate except for anteapical furrow (0; Fig. 2C); irregularly punctate (1; Fig. 2D–F).
45. Prosternal anterior margin (+): without or with very shallow indistinct groove (0); with smooth depression or groove (1; Fig. 2C); with indistinctly punctate groove (2); with distinctly punctate groove (3; Fig. 2D–E); with groove reduced to large, serially isolated punctures (4; Fig. 2F).
46. Prosternal anteapical groove (if present at all in some form; i.e. states 1–4, #45) (+): very short, restricted to dorsodistal surface of prosternum (0); longer, extended from dorsodistal margin ventrad onto lateral surface of prosternum (1); continuous ventrally but shallower or irregular between the lateral reaches of prosternum (2; Fig. 2C–D, F); continuously deep ventrally between sides of prosternum (3; Fig. 2E).
47. Proepimeron (+): with anterior and posterior grooves smooth (0); with anterior groove minutely punctate, posterior smooth (1); with both anterior and posterior grooves irregular or punctate (2).
48. Parascutellar seta: present (0); absent (1).
49. Scutellum: narrower, W/L = 0.83–1.86 (0; Fig. 8A–E); broader, W/L = 2.0–2.5 (1; Fig. 9A). For this ratio, scutellar length is determined along the scutellar midline from the basal transverse depression to the apex, whereas width is determined along a line just apicad that depression.

50. Parascutellar striole: longer, terminated between sutural stria and suture where parallel (0; Fig. 8A, D–E); short, terminated between sutural stria and suture where convergent (1; Fig. 8C).
51. Parascutellar striole (+): present, continuous, smooth or punctate (0; Fig. 8A, C); present, consisting of 3–8 punctures, not connected by stria (1; Fig. 8D–E); present, consisting of 1–2 isolated punctures (2); absent (3; Figs 8B, 9D–E).
52. Dorsal elytral setal count (+): 0 (0); 1 (1; Fig. 8B–C); 2 (2; Fig. 8A, E); 3–5 (3; Fig. 8D).
53. Accessory dorsal setae (+); absent (0); in fifth elytral interval (1); in fifth and seventh elytral intervals (2). The presence of accessory setae in the fifth elytral interval is documented for *M. kavanaughi* (Liebherr 2008a), whereas the presence of accessory setae in both the fifth and seventh interval occurs in *Amblytelus brevis* and *A. curtus* (Fig. 2J).
54. Position of anterior (or single) dorsal elytral seta (–): at anterior 1/5–1/3 of length (0); at midlength (1); in posterior third (2). A single dorsal elytral seta at elytral midlength occurs in *M. storeyi* and *M. lewisensis* (Moore 1984) and other members of subgenus *Qecyclothorax*.
55. Supracarinal elytral seta (basad subapical seta) (+): absent (0; Fig. 2L); present (1); present and doubled (2; Fig. 2J). Additional setae in the seventh elytral interval basad the subapical seta, and mesad the carina associated with the seventh stria is a feature of *Amblytelus brevis* and *A. curtus* (Fig. 2J)
56. Elytral subapical seta: present (0); absent (1). This seta is plesiomorphically present in *Mecyclothorax* and its sister group comprising *Amblytelus* and allied genera, and is situated within the seventh stria (Fig. 2H), or in a position homologous with that stria if the stria is reduced (Fig. 2K)
57. Elytral apical seta: present (0); absent (1). This seta occurs just laterad the mesally curved apex of stria 2 near the elytral sutural apex (Fig. 2G–H).
58. Apex of elytral interval 8 (+): with same curvature as elytral apex (0; Fig. 2G); more convex than rest of elytra (1; Fig. 2H–I); with distinct ridge on inner margin near stria 7 (2; Fig. 2K); distinctly carinate on inner margin near stria 7 (3; Fig. 2J, L).
59. Elytral shape (+): broadly subquadrate, sides subparallel, humeri broad (0; Fig. 8A, D); subquadrate, humeri narrowed (1; Fig. 8E); ellipsoid to ovoid (2; Figs 8B–C, 9D–E).
60. Elytral shape (humeri moderately broad; i.e. state 2 of #59) (+): foreshortened, hemiovoid (0); elongate, ellipsoid (1; Fig. 9D–E); elongate, ovoid (2; Fig. 16A).
61. Elytral dorsal curvature (+): moderately convex, sides sloping to margins, disc flat (0; Fig. 8A, D–E); convex, sides nearly vertical, disc domed (1; Fig. 9D–E); very convex, sides nearly vertical to margins, apex depressed (2; Fig. 8B–C).
62. Elytral basal groove (+): hardly recurved (0; Fig. 8C); recurved (1; Fig. 8B, D); distinctly recurved, an angular hitch at humerus (2; Figs 8A, E).
63. Elytral humeral angle (+): rounded (0: Fig. 8C); tightly rounded to obtuse-angulate (1; Fig. 8D–E); angulate (2; Fig. 8A–B).
64. Elytral humeral angle: with evenly convex margin on base and lateral edge (0); with elevated humeral tooth at angle (1).
65. Elytral striae on disc (+): 1–8 present, complete (0; Fig. 8C); 1–6 present, 7 obsolete to absent (1; Fig. 8D); 1–5 present, 6–7 reduced to obsolete, to absent (2; Fig. 8A); 1–3 to 1–4 shallow, 5–7 progressively obsolete (3; Fig. 8B, E); only sutural stria 1 present, punctate, 2–7 obsolete (4; Fig. 20B); all reduced, obsolete to absent except stria 8 (5; Fig. 9D–E).
66. Elytral striae on apex (+): all present, deep (0; Fig. 2J); 1–7 present, traceable, though they may be shallow apically (1); 1–3 to 1–5 traceable on apex, 7 evident mesad subapical sinuation (2; Figs 2K, 8C–D); only striae 1–2 and 7 visible near apex, 3–6 obsolete (3; Fig. 8E); only sutural stria and 7th traceable near apex, others obsolete (4); only sutural stria traceable near apex (5; Fig. 8B); no striae visible at apex except 8th at subapical sinuation (6; Fig. 16A).
67. Elytral apex along suture: not upraised in a conjoined juncture (0; Fig. 8A, D–E); upraised in a conjoined juncture (1; Fig. 8B–C).
68. Elytral strial punctation (+): absent (0; Fig. 9D–E); small, not expanding strial diameter (1; Fig. 8B–C); larger, elongate or round but little expanding strial diameter (2; Fig. 8D–E); large, deep, expanding strial diameter (3; Fig. 8A).
69. Setal depressions of dorsal elytral setae (+): shallow, extended over 1/4 breadth of interval 3 or less (0; Fig.9D–E); evident, extended over 1/3–1/2 breadth of interval 3 (1; Fig. 8D–E); broad, deep, extended over 3/4 breadth of interval 3 (2).
70. Elytral stria 8 (+): smoothly impressed along midlength (0; Fig. 2K); serially punctate, irregular along midlength (1; Fig. 2L).
71. Elytral lateral marginal depression (+): very narrow throughout length (0; Fig. 8C); narrow to moderately broad, microsculpture visible in deepest part (1; Fig.8A, D–E); broad anteriorly, moderately broad behind (2; Figs 2J, 8B).
72. Subapical sinuation: deep, distinct, more abruptly curved anteriorly (0; Figs 2J, 8D); broad, shallow (1; Figs 2G–I, 8E).
73. Mesepisternal punctures (+): none, surface smooth (0; Fig. 3B); 5–6 small punctures in single curved line (1); 5–9 large punctures in 2–3 rows (2; Fig. 3A); 10 or more large punctures in 3 rows (3).
74. Mesosternal/mesepisternal suture: present (0; Fig. 3A); absent anteriorly, sclerites fused near prothorax (1; Fig. 3B).
75. Metathoracic flight wings (–): fully developed, venated, with reflexed apex (0; Fig. 3C); brachypterous, with reduced apex, venation reduced (1); stenopterous, reduced to a narrow strap longer than metanotum (2; Fig. 3D); vestigial, wing rudiment not extended to apex of metanotum (3).

76. Metepisternal width/length ratio (–): 0.30 < x < 0.60 (0); 0.60 < x < 0.87 (1); 0.87 < x < 1.46 (2; Fig. 3A–B). For this ratio, the metepisternal length is measured along the lateral margin from the juncture with the mesepimeron to the metepimeron. Metepisternal width is the maximal perpendicular distance from this line to the metepisterna-mespimeral-mesosternal 3-point junction, measured with the metepisternum level in the field of view.
77. Metepisternum-metepimeron suture: distinct, a distinct line (0; Fig. 3B); incomplete, reduced laterally (1; Fig. 3A).
78. Tarsomeres: dorsally glabrous (0); dorsally setose (1).
79. Metatarsomeres 4 (+): narrow, with short apical lobes (0); broadly triangular, broader apex with very short lobes (1); broad overall, bilobed, apical lobes broad, elongate (2).
80. Suture between abdominal ventrites 1 and 2: straight to sinuous with ventrite 2 not or only slightly depressed (0); sinuous with ventrite 2 distinctly depressed inside curve (1).
81. Suture between abdominal ventrites 2 and 3: shallow, complete, traceable to margin (0); reduced, incomplete, absent laterally (1).
82. Abdominal ventrites 3–5 (–): with irregular linear plaques in lateral reaches (0); with round, smooth depressed plaques in lateral reaches (1); with surface punctate obscuring any other features (2).
83. Apical abdominal ventrite 6 (male) (–): with 1 seta each side (total of 2) (0); with 2 setae each side (total of 4) (1); with 3 setae each side (total of 6) (2); with 4 setae each side (total of 8) (3).
84. Apical abdominal ventrite (female) (–): with 2 setae each side (total of 4) (0); with 3 setae each side (total of 6) (1); with 4 setae each side (total of 8) (2).
85. Apical abdominal ventrite 6 (female) (–): glabrous medially between apical setae (0); with setose patch of 4–5 setae medially (1); with pair of subapical setae medially (2).
86. Microsculpture on frons (–): granulate isodiametric sculpticells (0); evident to shallow isodiametric mesh (1); isodiametric to transverse mesh in transverse rows (2); indistinct transverse mesh or lines (3); absent, surface glossy (4). All terms for microsculptural configurations are derived from Lindroth (1974), though the term sculpticell was coined by Allen and Ball (1980).
87. Microsculpture of pronotal disc (–): isodiametric in transverse rows mixed with transverse mesh, 2–3× broad as long (0); transverse mesh, sculpticells 3–4× broad as long (1); mix of transverse mesh and transverse lines (2); reduced, surface glossy, with indistinct transverse mesh or lines (3).
88. Microsculpture of pronotal base (–): isodiametric between basal punctures (0); transversely stretched isodiametric between punctures (1); evident transverse mesh, sculpticells 2–3× broad as long (2); indistinct, elongate transverse mesh or unconnected lines (3).
89. Microsculpture of elytral disc (–): a mix of distinct isodiametric and transverse sculpticells (0); a regular transverse mesh, sculpticell breadth 2–3× length (1); a mix of transverse mesh 3–4× broad as long and transverse lines (2); reduced, surface glossy, indistinct mesh plus lines over part (3).
90. Microsculpture on abdominal lateral base: swirling isodiametric and transverse sculpticells (0); reduced, surface glossy with indistinct sculpticells (1).
91. Body coloration (–): dark, elytral margins concolorous or indistinctly, narrowly paler (0); ferruginous, elytra bicolored with outer 4–5 intervals much paler (1); ferruginous, elytra bicolored, outer 3–4 intervals and apex much paler (2).

See Table 2 for abbreviations used to label structures of the male genitalic and female reproductive tract illustrations.

92. Antecostal margin of male mediotergite IX (ring sclerite): angulate (0; Fig. 10C, E, H, J, O)); broadly rounded (1; Fig. 17F).
93. Distal terminus of male mediotergite IX antecostal margin: not extended (0; Fig. 10C, H, H, J, O); extended, the proximal angle with an elongate extension (1; Figs 10E, 17B).
94. Aedeagal ventral (right, except *M. storeyi*) paramere shape (+): elongate, paddle-like, apex broadly subparallel to rounded tip (0); quadrate-conchoid, dorsal and ventral margins subparallel to apex (1; Fig. 5C, lower paramere); elongate-conchoid, apex narrowed so shape is subtriangular (2; Fig. 5B, upper paramere); very elongate, moderately narrow, paramere > 0.85 lobe gape (3; Fig. 5A, lower paramere); very elongate, apical half narrowed to whiplike extension (4; Fig. 5D, lower paramere). State 0 of this character is diagnostic for taxa of the subtribe Moriomorphina, represented in this analysis by the ultimate adelphotaxon *Neonomius laevicollis* (Moore 1963). Note that males of *M. storeyi* are characterized by a bilaterally inverted aedeagal assembly, necessitating recognition of the ventral paramere in repose being the anatomically left paramere, and vice versa (Moore 1984).
95. Aedeagal ventral (right, except for *M. storeyi*) paramere (+): densely setose on apicoventral margin, apical setae not present (0); densely setose on apicoventral margin, apical setae not differentiated (1; Fig. 5C); with 8–21 setae on ventral margin, apical setae distinct (2; Fig. 5D); with 2–7 setae on ventral margin well separated from apical setae (3; Fig. 5A); glabrous (or a single seta) on ventral margin plus 2 apical setae (4; Fig. 5E).
96. Aedeagal ventral (right, except for *M. storeyi*) paramere: with dorsal surface glabrous or a single small seta subapically (0; Fig. 5A–B, E); with dorsal surface setose (4–18 setae present along apical half) (1; Fig. 5C, D).
97. Aedeagal dorsal (left, except *M. storeyi*) paramere shape (+): broad basally, apical half elongate, margins subparallel (0); broad basally, apex short, narrowly rounded, subangulate (1; Fig. 5C); broadly quadrate basally; apical extension narrowly attenuate (2; Fig. 11D);

Table 2. Key to abbreviations for structures of male genitalia, and female genitalia and reproductive tracts.

Abbreviation	Structure
aai	male aedeagal apical invagination
af	apical face of male aedeagal median lobe
afs	lateroapical fringe setae, female gc1
al	apical lobe of male aedeagal internal sac
ans	apical nematiform setae, female gc2
bc	female bursa copulatrix
bcd	female bursa copulatrix dorsal lobe
co	female common oviduct
des	dorsal ensiform seta, female gc2
dgd	defensive gland duct
dgr	defensive gland reservoir
dl	dorsal lobe of male aedeagal internal sac
dp	dorsal plate of male aedeagal internal sac
fl	flagellum of male aedeagal internal sac
fs	flagellar sheath of male aedeagal internal sac
fp	flagellar plate of male aedeagal internal sac
gc1	basal gonocoxite of female
gc2	apical gonocoxite of female
gp	gonopore of male aedeagal internal sac
hg	hindgut
hs	helminthoid sclerite of female
les	lateral ensiform setae, female gc2
la	ligular apophysis of female
lp	left paramere of male aedeagus
mac	dorsal macrospicules of male internal sac
mbs	mediobasal shagreening of female gc1
ms	medial setae, female gc 1
mtIX	antecostal margin of male mediotergite IX
ovo	ostial ventroapical operculum, male aedeagus
r	ramus of female gc1
rp	right paramere of male aedeagus
sd	female spermathecal duct
sg	female spermathecal gland
sp	female spermatheca
spi	spiracle
vss	ventral spicular sclerite of male internal sac

narrower basally, evenly narrowed to whip-shaped apex (3; Fig. 5A–B, D–E). State 0 of this character occurs in *Paratrichothorax brevistylus* (Baehr 2004, fig. 108d) and in *Neonomius laevicollis* (Moore 1963).

98. Aedeagal dorsal (left, except for *M. storeyi*) paramere (+): glabrous apically, though setae may be present on the ventral surface (0; Fig. 5C); 2–4 very short setae at apex (1); 2–4 (or 1) longer setae at apex (2; Fig. 5A–B, D–E); 2–4 apical setae plus 4 additional shorter subapical setae (3). State 3 has only been observed in males of *M. lissus*.
99. Aedeagal median lobe ostial opening: without ventroapical operculum (0; Fig.4A–E); with hinged ventroapical opercular flap (1; Fig. 4F–G).
100. Aedeagal internal sac: unilobed, short to long (0; Fig. 4F–G); bilobed, with distinct dorsal and apical lobes (1; Fig. 10L, Q)).
101. Aedeagal internal sac (–): with flagellum associated with gonopore (0; Fig. 4A–E); with circular flagellar plate associated with gonopore (1; Fig. 4F–G); without flagellum, only dorsal plate present (2; Fig. 21A, E–F, H, J, L).
102. Short to elongate flagellar condition (i.e. state 0 of #101) (+): thin, lightly sclerotized, may be short, sinuous, or long and whiplike (0; Fig. 4C–E); broad, porrect, spikelike (1); crescent-shaped remnant of flagellar sheath base (2; Fig. 10L, Q).
103. Apical flagellar plate (i.e. state 1 of #101): a donut-like roll, lightly sclerotized or spiculated, gonopore within convexity (0); a well-sclerotized and ridged plate, gonopore on convex side (1; Fig. 4F–G). A lightly sclerotized flagellar plate is observed in New Guinean males, such as in *M. andersoni*, *M. baehri*, and *M. gressitti* (Guéorguiev 2013, Liebherr 2017b).
104. Aedeagal sac dorsal plate: absent, flagellum and/or flagellar sheath only (0; Figs 4E, 10L, Q); present in addition to or instead of flagellum and flagellar sheath (1; Fig. 4C–D).
105. Aedeagal sac dorsal plate (i.e. state 1 #104): translucent, covered with microspicules (0; Fig. 10A, G); well sclerotized, smooth (1; Fig. 4C).
106. Aedeagal internal sac surface dorsad position of dorsal plate: unarmored (0); with patch of robust macrospicules (1; Fig. 17I, M).
107. Aedeagal internal sac ventral sclerite patch: absent, area basad flagellum and sheath unsclerotized (0); present as distinct sclerite basad flagellum and sheath (1). This ventral sclerotic patch is observed in species of the outgroups, *Dystrichothorax* and *Amblytelus*.
108. Aedeagal internal sac ventrobasal spicular sclerite: absent (0); present (1; Fig. 4F–G).
109. Aedeagal median lobe shaft: gracile, aedeagus relatively narrow dorsoventrally, parallel-sided (0; Fig. 4F–G); broad, aedeagus robust, broadest at midlength (1; Fig. 4A–E).
110. Aedeagal median lobe tip (–): extended narrowly beyond ostium (0; Figs 4F–G, 10I, L); narrow, not extended beyond ostium (1; Fig. 10N–R); broadly expanded dorsoventrally, extended beyond ostium (2; Fig. 10A, C–D); broadly expanded dorsoventrally, not extended beyond ostium (3; Fig. 4A–C).
111. Broad extension of aedeagal median lobe (i.e. states 2, 3 #110) (+): parallel-sided dorsoventrally to rounded tip (0; Fig. 10A, C–D); convexly spoon shaped, expanded both dorsally and ventrally (1; Figs 17A–B, E–F); downturned, tip at angle to shaft, apical face straight (2; Fig. 17I, M); apex expanded dorsally and ventrally, adze-shaped (3; Fig. 4A); broadly downturned in fishhook configuration, tip pointed (4). State 4 characterizes males of *M. lewisensis* and *M. inflatus* (Baehr 2003, figs 1D–F).
112. Aedeagal median lobe apical margin (+): smoothly convex to acuminate, no abrupt change in curvature along margin (0; Fig. 17I–N); with hitch to distinct invagination along apical margin (1; Fig. 21L); with distinct invagination along margin resulting in dentate margin (2, Figs 21A–K, 26).

113. Aedeagal median lobe apex: smoothly extended past ostial opening (0; Fig. 17A, E); with dorsoventral crease distad ostial opening resulting in an apical hook-like tip (1; Fig. 17C).
114. Female bursa copulatrix shape: elongate, columnar, length/width > 2.0–3.25 (0; Fig. 6A–C, F); short and columnar, length/width 1.0–2.0 (1; Fig. 6D–E).
115. Female bursa copulatrix surface (+): membranous, not wrinkled, transparent (0; Fig. 6D); thin, surface wrinkled and translucent (1; Fig. 6A–C, E); thick, surface wrinkled and not transparent (2; Fig. 6F).
116. Female bursal copulatrix apicoventral surface: membranous as remainder of bursa (0); sclerotized into plate-like structure (1). Bursal sclerites are observed in females of *M. kavanaughi* (Liebherr 2008a) and *M. oopteroides* (Liebherr and Marris 2009, fig. 18)
117. Female bursa copulatrix: of approximately equal diameter throughout length (0; Fig. 6A–D, F); with smaller apical portion, diameter there much less than basal part (1; Fig. 6E).
118. Spermathecal duct placement (+): on bursa near common oviduct/bursa juncture (0; Fig. 6A–E); apically on bursa copulatrix main lobe (1; Fig. 23D–E); dorsoapically on bursa copulatrix main lobe (2); basodorsally on bursa, dorsad common oviduct/bursa juncture (3; Fig. 6F). A dorsoapical position of the spermatheca (state 2) is observed in *M. amplipennis* (Liebherr and Marris 2009, fig. 6)
119. Spermathecal duct placement near common oviduct (i.e. state 0, #118): on right side of bursa laterad common oviduct (0; Fig. 6A–B); on ventral side of bursa distad common oviduct (1; Fig. 6E).
120. Female bursa copulatrix configuration (+): unipartite, without dorsal lobe (0; Fig. 6A–F); bipartite, spermathecal duct entering apex of dorsal lobe which is shorter than ventral lobe (1; Fig. 12D): bipartite, spermathecal duct entering dorsal lobe equal in length to ventral lobe (2; Fig. 12E).
121. Helminthoid sclerite at base of spermathecal duct (–): present as elongate sclerotized apodeme (0; Fig.6A–B); base of spermathecal duct sclerotized as rounded projection (1; Fig. 6C); base of spermathecal duct sclerotized as two parallel apodemes (2); absent (3; Fig. 6E). The helminthoid sclerite observed in females of *M. moorei* comprises state 2.
122. Ligular apophysis on common oviduct: absent (0; Fig. 6A–F); present (1; Fig. 12D–E). The ligular apophysis (Liebherr and Will 1998) is a sclerotic expansion with highly dissected surface on the common oviduct's ventral surface. This suggests a muscular attachment at this point along the oviduct.
123. Spermathecal duct: present, spermatheca stalked (0; Fig. 6A–F); absent, spermatheca appressed (1). A spermatheca appressed to the bursal surface is observed in females of *M. amplipennis* (Liebherr and Marris 2009, fig. 6)
124. Spermathecal duct (i.e. state 0 of #123): subequal to spermathecal length (0; Fig. 6C); 1.25–3.0× spermathecal length (1; Fig. 6E).
125. Spermathecal shape (+): fusiform or ovoid bulb on narrow duct (0; Fig. 6); filiform reservoir on equal-sized duct (1; Fig. 23D); appressed bulb (2).
126. Spermathecal gland duct: entering on spermathecal duct at spermathecal base (0; Fig. 6B–C, E); entering on spermathecal reservoir (1; Fig. 12E).
127. Ramus (gonocoxite VIII of Deuve [1993]): present as defined membranous fold (0; Figs 13, 24); present, heavily sclerotized (1). Heavily sclerotized rami occur sporadically throughout the *Mecyclothorax* lineage. Among the taxa studied here, they are observed in *M. peryphoides*, *M. eyrensis*, and *M. lissus*.
128. Lateroapical fringe of setae on gonocoxite 1 (+): composed of single seta (0); composed of 2 setae (1; Fig. 13A–B, D–F); composed of 2–5 setae (at least 3 setae unilaterally) (2; Fig. 13C, G).
129. Medial setae of gonocoxite 1 (–): absent along entire mesal margin (or only 1–2 small seta apically) (0; Fig. 13G); absent at apex but several subapically along margin (1; Figs 13A–F, 24); large seta at apical angle plus other setae along mesal margin (2). A large apical angle seta (state 3) is observed in females of many species in subgenus *Mecyclothorax*; e.g. *M. montivagus* (Liebherr 2015, fig. 129B).
130. Mediobasal surface of gonocoxite 1: smooth (0; Figs 13, 24A–B); extensively shagreened with overlapping cuticular scales (1; Fig. 24C–E).
131. Apical gonocoxite 2 (+): broadly subtriangular, apex rounded, mitten-shaped (0); narrowly subtriangular, basal width < 0.4× length (1); more broadly subtriangular, basal width about half length (2); with lateral apodeme basally, basal width 0.6–0.7× length (3; Fig. 13F); falciform with basolateral apodeme, basal width > 0.75 length (4; Fig. 13D–E).
132. Lateral ensiform setal count for apical gonocoxite 2 (+): 1 (0); 2–3 (at least 2 unilaterally) (1; Figs 13, 24); 3–5 (3 or more both sides) (2).
133. Lateral ensiform setae of apical gonocoxite 2: shorter, basal seta 0.25–0.40× gonocoxite length (0; Figs 13A–C, G, 24); longer, basal seta 0.40–0.50× gonocoxite length (1; Fig. 13D–F).
134. Lateral ensiform setae of gonocoxite 2: on lateral margin of gonocoxite (0; Figs 13, 24); on ventral surface of gonocoxite (1). Ventrally oriented ensiform setae occur in *Amblytelus* and the allied genera *Dystrichothorax*, *Epelyx*, and *Paratrichothorax* (Baehr 2004, figs 124–146)
135. Apical nematiform setae of gonocoxite 2: in fossa 1/4–1/5× length from apex (0; Figs 13, 24); in fossa 1/2–1/4× length from apex (1). The more basal position of the apical nematiform setae is a character defining subgenus *Qecyclothorax*; i.e., *M. storeyi* and allies.
136. Mesal surface of laterotergite IX: setose (0); spiculose (1). Spiculose laterotergites diagnose the genera *Amblytelus*, *Epelyx*, and *Dystrichothorax* (Baehr 2004, figs 124–145).

Cladistic methods. The character-state matrix was developed using Winclada (Nixon 2002) and is presented along with the results of the analysis as Suppl. material 1. The matrix was submitted to Nona (Goloboff 1999), with tree searches conducted using the ratchet (Nixon 1999), using 200, 1000, and 10,000 ratchet iterations under default values. Results inherent in the various most-parsimonious trees were summarized using strict consensus. The strict consensus (Fig. 7) presented character-state changes under fast optimization.

Results

Under all three numbers of ratchet iterations, eight equally parsimonious trees of 1203 steps were found (CI = 0.21, RI = 0.66), with those trees and the character-state changes summarized for presentation using the 1216-step strict consensus cladogram under fast optimization (Fig. 7), that optimization allowing all characters to be represented on the cladogram. Use of unambiguous optimization results a consensus tree of identical topology. There is strong support for the mutual monophyly of *Amblytelus* and related genera versus *Mecyclothorax*, with 25 state changes supporting the exemplar array of the former, and 17 state changes supporting *Mecyclothorax* monophyly. Baehr (2004) comprehensively summarized the many characters defining the *Amblytelus* related genera, with salient characters such as the large, convex eyes (characters 17, state 2, and 19 state 0), anteriorly margined pronotum (character 36, state 1) with broadly explanate lateral margins (character 38, state 2), apically carinate elytral interval 8 (character 58, state 3), and broadly triangular fourth metatarsomeres (Character 79, state 1), among others, defining monophyly of this lineage.

The converse monophyly of *Mecyclothorax* is supported in the resulting cladogram by many characters that reverse among the dense sampling of *Mecyclothorax* spp., however the presence of 4–5 setae medially on the apical abdominal ventrite (character 85, state 1) is an unreversed synapomorphy among the species analyzed here. The groundplan elytral striation for *Mecyclothorax* is more derived than observed among the "*Amblytelus*" genera, as striae 6 and 7, or 5 to 7 are reduced on the disc (character 65, states 2 to 5), versus all striae present or only the seventh reduced in the former. This strial reduction also affects the expression of striae on the elytral apex, with most *Mecyclothorax* taxa exhibiting reduction in striae 4–6 or 3–6 apically. The lone exception includes species of subgenus *Meonochilus* from New Zealand, a clade previously described as a distinct genus (Liebherr and Marris 2009), but falling within the phylogenetic network of species currently placed in *Mecyclothorax*. These species have all striae traceable on the elytral apex. Finally, just as *Amblytelus* and related genera exhibit a distinct carina laterad the seventh elytral interval (Fig. 2J), nearly all *Mecyclothorax* lack a carina at this position. The lone exceptions are *M. blackburni* (Fig. 2L) and *M. curtus*, members of the first divergent lineage within *Mecyclothorax*: the subgenus *Eucyclothorax*.

Classification of *Mecyclothorax* Sharp, 1903

Taxonomic treatment

The classification of *Mecyclothorax* subgenera is based on the results of the cladistic analysis (Fig. 7, Table 1). The various recognized subgenera are diagnosed below with type species designated as per The Code (I.C.Z.N. 1999). Synapomorphic and symplesiomorphic diagnostic characters are sequentially presented for each proposed subgeneric taxon. The species of subgenus *Phacothorax* Jeannel are subsequently revised, following all conventions of The Code.

Genus *Mecyclothorax* Sharp

Mecyclothorax Sharp, 1903: 243 (type species *Cyclothorax montivagus* Blackburn by Andrewes 1939).

Cyclothorax MacLeay, 1871: 104 (not *Cyclothorax* Frauenfeld, 1868; type species *Cyclothorax punctipennis* MacLeay by monotypy; synonymy Sloane 1903).

Thriscothorax Sharp, 1903: 257 (type species *Cyclothorax unctus* Blackburn by original designation; synonymy Britton 1948).

Atelothorax Sharp, 1903: 269 (type species *Atelothorax optatus* Sharp by monotypy; synonymy Britton 1948).

Metrothorax Sharp, 1903: 269 (type species *Metrothorax molops* Sharp by Lorenz 1998; synonymy Britton 1948).

Antagonaspis Enderlein, 1909: 488 (type species *Antagonaspis sculptopunctata* Enderlein by original designation; synonymy Jeannel 1940).

Phacothorax Jeannel, 1944: 84 (type species *Phacothorax fleutiauxi* Jeannel by original designation; synonymy Liebherr and Marris 2009; designated as subgenus herein).

Loeffleria Mandl, 1969: 54 (synonymy Baehr and Lorenz 1999; type species *Loeffleria globicollis* Mandl by monotypy).

Meonochilus Liebherr & Marris, 2009: 10 stat. n. (type species *Tarastethus amplipennis* Broun designated by Liebherr and Marris 2009: 10; designated as subgenus herein).

Eucyclothorax subgen. n. (type species C*yclothorax blackburni* Sloane hereby designated).

Qecyclothorax subgen. n. (type species *Mecyclothorax storeyi* Moore hereby designated).

Eucyclothorax subgen. n.

http://zoobank.org/03AF91A5-C31D-414B-852D-D6A40D71C718

Diagnosis. Species of this subgenus can be diagnosed by the synapomorphic presence of punctures on the prosternum (Fig. 2D–F), and the presence of a distinctly punctate prosternal anteapical groove, or the presence of punctures so deep and large that they obscure any groove (Fig. 2F). The pronotal front angles narrow and are not protruded (Fig. 8A) in all species except *M. curtus* and *M*. nsp. D, in which these angles are little protruded and more rounded (Fig. 2D). The paraglossae are generally

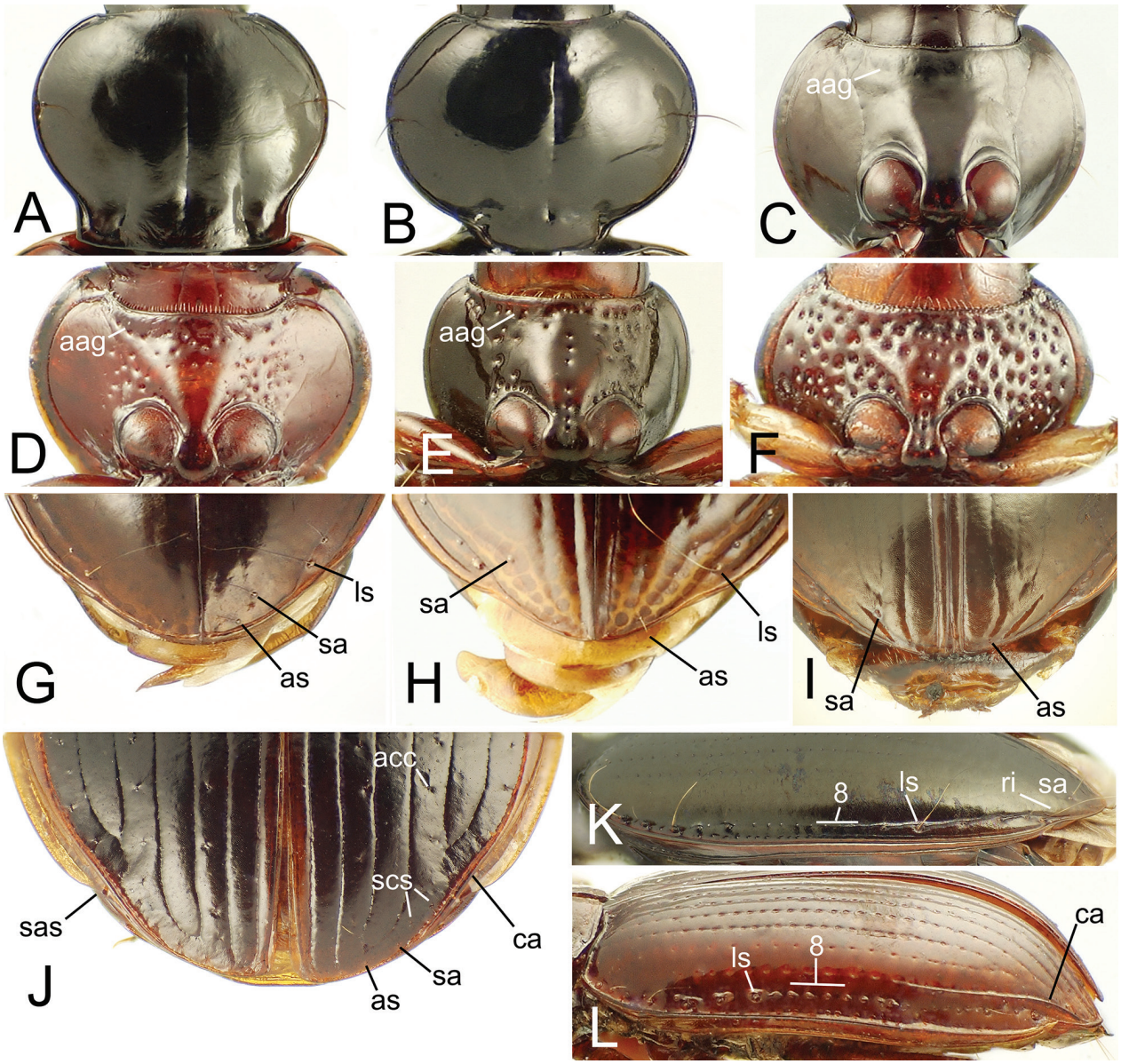

Figure 2. Thoracic structures of *Mecyclothorax* and *Amblytelus* spp. **A–B**. Pronotum, dorsal view: **A**, *M. laterorectus*; **B**, *M. mouensis*. **C–F**. Prosternum, ventral view: **C**, *M. fleutiauxi*; **D**, *M. curtus*; **E**, *M. blackburni*; **F**, *M. moorei*. **G–J**. Elytral apices, dorsal view: **G**, *M. fleutiauxi*; **H**, *M. laterorectus*; **I**, *M. lissus*; **J**, *A. curtus*. **K–L**. Elytral lateral margin showing eighth stria, lateral view: **K**, *M. ambiguus*; **L**, *M. blackburni*. Abbreviations include: **aag**, anteapical groove; **acc**, accessory elytral dorsal setae in interval 5; **as**, apical elytral seta; **ca**, carina laterad stria 7; **ls**, lateral elytral setae; **ri**, ridge mesad stria 8; **sa**, subapical elytral seta; **sas**, subapical sinuation of elytron; **scs**, supracarinal elytral setae; **8**, medial portion of stria 8.

elongate (Fig. 1D), extended twice as far from the anterior margin of the ligula than the distance from their base to the ligular margin; this is reversed in *M. punctatus* which has shorter paraglossae. The elytral striae are distinctly punctate (Fig. 8A), distinguishing *Eucyclothorax* spp. from species in *Qecyclothorax*, though not from other Australian members of subgenus *Mecyclothorax* such as *M. ambiguus* or *M. punctipennis*. Also, the eighth elytral stria is punctate at midlength in most species (Fig. 2L)–save *M. moorei* and *M. punctatus*–though this punctation is also seen in lesser development in some species of subgenus *Mecyclothorax* such as *M. punctipennis*. The surface of the basal abdominal ventrites is generally glossy without microsculpture, a synapomorphy, though this is reversed to a microsculptured surface in *M. lophoides* and *M*. sp. n. D. In the male genitalia the right paramere is elongate, with only 2–7 setae present on the ventral surface (Fig. 5A), and the internal sac bears a dorsal plate as well as a sinuous flagellum (Fig. 4C). Finally, the female reproductive tract has the spermathecal duct entering at the juncture of the common oviduct with the bursa (Fig. 6C), a symplesiomorphy shared with *Qecyclothorax* spp. (Fig. 6D), some *Amblytelus* spp. (Fig. 6A–B), *M. bellorum* of subgenus *Meonochilus* (Liebherr 2011, fig. 12). A

helminthoid sclerite is also symplesiomorphically present (Fig. 6C)

Member species. All Australian *Mecyclothorax* species have been examined, with the following species assignable to this subgenus represented in the analysis: *M. blackburni*, *M. curtus*, *M. eyrensis*, *M. lophoides*, *M. moorei*, *M. peryphoides*, and *M. punctatus* (Table 1; Moore et al. 1987, Baehr 2009). Baehr's (2016) southwestern Australian subspecies *M. punctatus peckorum* (Moore 1984, fig. 12) and *M. cordicollis* (Sloane) complement this list. An undescribed species from Queensland–sp. n. D–will be described in a subsequent publication.

Etymology. To indicate membership of species of this subgenus in *Mecyclothorax*, and to reflect the position of this taxon as the adelphotaxon to the remainder of *Mecyclothorax* sensu lato, the initial syllable "eu"–the Ancient Greek prefix *εύ*, meaning "proper" or "true"–is combined with the first name proposed for the genus, *Cyclothorax* (MacLeay 1871), resulting in the subgenus name *Eucyclothorax*. Based on the shared nominative masculine terminal syllable thorax, this epithet agrees in gender with the generic epithet.

Qecyclothorax subgen. n.

http://zoobank.org/4059AFC5-8924-40D4-B215-6B543F8E90BD

Diagnosis. These robust-bodied species (Fig. 8B) are geographically restricted to upland regions of Queensland, Australia, and have been recently revised by Baehr (2003). The pronotum of species in this subgenus is broad, with obtuse or obtusely rounded hind angles, and each elytron bears a single dorsal elytral seta just before midlength (Baehr 2003, fig. 3), a condition also observed in four species of subgenus *Meonochilus* (e.g. Fig. 8C). The mentum tooth is broadly rounded (Fig. 1E), though such a configuration is also observed in *M. blackburni* and *M. lophoides* of subgenus *Eucyclothorax*. The prothorax is depressed medially both between and anterad the procoxal cavities, a condition shared with most member species of *Eucyclothorax*, though prosternal punctures are never present here. The elytral striae are reduced, with striae 1–3 to 1–4 shallow, and striae 4– or 5–7 obsolete (Fig. 8B). Apically on the elytra the striae are reduced, with at most sutural and seventh stria present, and in several species only the sutural striae evident. The elytra are broadly convex, with the eighth interval not, or only slightly upraised (*M. lewisensis*) relative to the general curvature of the elytral surface. The suture between abdominal ventrites 1 and 2 is nearly straight, with the second ventrite hardly depressed relative to the first, whereas this suture is sinuous with the second ventrite depressed within the sinuosity in species of *Eucyclothorax* and *Meonochilus*. This condition varies among the New Caledonian *Phacothorax* spp. as well as across subgenus *Mecyclothorax*. The male aedeagal median lobe internal sac bears a flagellum (Fig. 4E), and the ventral paramere is elongate-conchoid in shape, broadly to narrowly subtriangular with ventral setae present (Fig. 5B; Baehr 2003, fig. 1). The female bursa copulatrix is relative short (Fig. 6D), with the spermathecal duct entering at the bursal-common oviduct juncture.

Member species. Baehr (2003) distinguishes the four species analyzed here (Fig. 7), recognizing seven subspecies.

Etymology. Given restriction of species in this subgenus to Queensland, the Queensland derived first syllable "qe" is combined with MacLeay's (1871) *Cyclothorax* to derive the subgeneric epithet. Just as in the original name of the Australian airline QANTAS–Queensland and Northern Territory Aerial Services Ltd.–*Qecyclothorax* obviates the unnecessary letter u while retaining the normal pronunciation of the letter Q. Based on the shared nominative masculine terminal syllable thorax, this epithet agrees in gender with the generic name.

subgenus *Meonochilus* Liebherr & Marris, 2009 [new status]

Diagnosis. Species of this subgenus share a robust, convex body shape with *Qecyclothorax* spp. (Fig. 8B–C), though in all *Meonochilus* spp. the elytral striae are well developed and punctate, with striae 1–7 deep at elytral midlength. The pronotal median base is depressed relative to the convex disc (Liebherr 2011, figs 9–10). The broad elytra are associated with a rounded humerus, a condition also observed among some New Caledonian *Phacothorax* and various species of subgenus *Mecyclothorax*. The head is transversely depressed behind the eyes, and the mentum is broad: over 3× broad as long. Opposed to New Zealand species of subgenus *Mecyclothorax* (as in Hawaii's *M. montivagus*, Fig. 1G), the ligula is rounded apically with the ligular setal sockets separated by only 2 diameters. The paraglossae extend beyond the ligular margin 1–2× the distance from their base to the ligula's margin (Fig. 1F). The male parameres also differ from those occurring among taxa of other *Mecyclothorax* subgenera, with the right paramere club-shaped and broadly setose apically (Fig. 5C), and the left paramere broadly conchoid.

Member species. The six species of this subgenus were revised by Liebherr (2011), and comprise the five species in this analysis (Fig. 7) plus *M. placens* (Broun). All species are restricted to North Island, New Zealand.

New taxonomic status. Liebherr and Marris (2009) proposed this clade as a distinct genus based on the great disparity between *Meonochilus* spp. and other New Zealand species currently assigned to subgenus *Mecyclothorax*. A subsequent cladistic analysis (Liebherr 2011) with taxon representation inadequate to display the phylogenetic structure within *Mecyclothorax* affirmed that generic status. The current analysis including a much more comprehensive sampling of *Mecyclothorax* spp. requires revision of that decision, with *Meonochilus* now treated as a subsidiary monophyletic subgenus of *Mecyclothorax* (Fig. 7). The member species include: 1, *Mecyclothorax* (*Meonochilus*) *amplipennis* (Broun) comb. n.; 2, *Mecy-*

clothorax (*Meonochilus*) *bellorum* (Liebherr) comb. n.; 3, *Mecyclothorax* (*Meonochilus*) *eplicatus* (Broun) comb. n. ; 4, *Mecyclothorax* (*Meonochilus*) *placens* (Broun) comb. n.; 5, *Mecyclothorax* (*Meonochilus*) *rectus* (Liebherr) comb. n.; 6, *Mecyclothorax* (*Meonochilus*) *spiculatus* (Liebherr) comb. n.

subgenus *Mecyclothorax* Sharp, 1903

Diagnosis. This subgenus holds most of the species-level diversity in the genus, and within those radiations character diversity is rampant, making setal configurations, body form, or mensural characters useless for diagnosis. The best means to diagnose this group is through male genitalic characters, as no species of this subgenus studied to date exhibit a flagellum on the internal sac. Instead, the gonopore is surrounded by either a donut-shaped, soft expansion, or this area of the sac bears a scoop-like flagellar plate, well sclerotized and even ridged, with the gonopore present in membrane lying on the convex surface of this plate (Fig. 4F, G). The male median lobe also exhibits an opercular flap: i.e. a sclerotized triangle articulated with membrane that lies at the distal end of the ostium (Fig. 4G). Male parameres are elongate, with the left paramere generally narrow basally with the apex extended as an attenuate whip (Fig. 5D). External characters differ greatly across the pectinate comb of taxa comprising the base of the radiation – *M. monteithi* to *M. globicollis* (Fig. 7) – though several external characters can assist in assignment of species to this subgenus. First, the labrum is emarginate apically, either distinctly as in *M. goweri* (Fig. 1A), or less so as in *M. montivagus* (Fig. 8D). The ligular margin is generally truncate with the ligular setae well separated (Fig. 1G), though as exceptions, the ligula is apically rounded in the Papuan taxa *M. brispex* and *M. andersoni* (Fig. 7, Liebherr 2017b). The prosternum exhibits a smooth to distinctly punctate anteapical groove, though never any other punctures. The parascutellar striole is present, and may be smooth or punctate, with up to 8 punctures along its length (Fig. 8D–E). The female reproductive tract is nearly exclusively characterized by the spermathecal duct entering the dorsal surface of the bursa directly dorsad the juncture of the common oviduct with the bursa copulatrix (Fig. 6F). However, based on the cladistic analysis (Fig. 7), entry of the spermathecal duct at the bursal-common oviduct juncture–as in subgenera *Eucyclothorax* and *Qecyclothorax*–atavistically and independently re-evolves in *M. brispex* and the Australian sister taxa *M. lateralis* and *M. minutus* (Fig. 6E).

Member species. The immense diversity of species comprising this subgenus is represented by 25 species in the cladistic analysis. The various species known from Norfolk Island (Moore 1985), Lord Howe Island (Moore 1992), Borneo (Baehr and Lorenz 1999), Java (Andrewes 1933, Louwerens 1949, 1953; 3 of 5 resident species analyzed); Papua New Guinea (8 species, Guéorguiev 2013, Liebherr 2008a, 2017b), St. Paul and Amsterdam Islands (Enderlein 1909, Jeannel 1940), and New Zealand (Liebherr and Marris 2009) all are members of this clade (Fig. 7). Examination of illustrations of male genitalia for other New Guinean species (Baehr 1992, 1995, 1998, 2002, 2008, 2014) indicates that the entire 22 species currently known from New Guinea belong to this subgenus. Phylogenetic placement of *M. montivagus* of Hawaii, and *M. marau* of Tahiti near *M. punctipennis* of Australia, the hypothesized colonist taxon for both the Hawaiian and Tahitian radiations (Liebherr 2013, 2015) indicates that these species appropriately act as surrogates for the entire 239 species of the Hawaiian *Mecyclothorax* radiation (Liebherr 2015) plus the 108 species comprising the Society Island radiation on Tahiti and Moorea (Liebherr 2012, 2013). The Australian *Mecyclothorax* fauna is shown to be biogeographically polyphyletic, with the Australian species *M. lateralis*, *M. minutus*, *M. ambiguus*, and *M. punctipennis* latecomers (Fig. 7) relative to member taxa of *Eucyclothorax* and *Qecyclothorax*, with the late-arriving branch of the Australian *Mecyclothorax* fauna having been derived from New Guinean roots. The two species recently described from Timor Leste (Baehr and Reid 2017) also appear to be members of this subgenus based on their gracile body form with cordate pronotum, largely impunctate ventral body surface, and lack of a flagellum in the male aedeagal median lobe.

subgenus *Phacothorax* Jeannel, 1944

Diagnosis. The species comprising this subgenus exhibit a remarkable diversity of body forms (Figs 9, 16, 20), but all species share a reduced or absent parascutellar striole (Jeannel 1944). The elytra either lack evident discal striae (Figs 9D–E, 16A, C), or the striae are shallow and smooth to only indistinctly punctate (Figs 9A–C, 16B–D, E, 20). The scutellum is narrow, less than twice as broad as long. As in the ground-plan for *Mecyclothorax*, the lateral elytral setae are arrayed in an anterior series of seven setae plus a posterior series of 6 setae. The vertex of the head is convex behind the eyes, and the ocular lobe meets the gena at a very obtuse angle without any groove marking the juncture. The prosternum, synapomorphously, either lacks an anteapical groove, or the groove is very broad, shallow and smooth (Fig. 2C). The abdomen bears a single seta each side of the apical ventrite in all males, and two setae each side in females complemented by a trapezoidal medial patch of 4–5 setae (for specimens of those genders observed among the various species). As Jeannel (1944, fig. 1) reported, the parameres are much like those of subgenus *Mecyclothorax* (Figs 5D–E, 11, 22). The male aedeagal median lobe internal sac may bear a well-developed flagellum, flagellar shield, and dorsal plate (e.g. Fig. 10D), or the flagellar apparatus may be secondarily reduced, as in *M. fleutiauxi* and *M. jeanneli*, where it is hypothesized that only the flagellar sheath remains (Fig. 10M, Q). As in males of the subgenera *Eucyclothorax* and *Qecyclothorax*, the male aedeagal

median lobe ostial opening is simple, without an ostial ventroapical operculum. The female reproductive tract exhibits extensive disparity in configuration, plesiomorphically exhibiting a helminthoid sclerite and spermathecal duct entering at the bursal-common oviduct juncture (Figs 12A–C, G, 23B), or in derived configurations at the apex of a single-lobed bursa copulatrix (Fig. 23A, D), or at the apex of a dorsal lobe in a bilobed bursal configuration (Fig. 12D–E). Finally, body coloration is uniformly somber, with head capsule piceous, pronotal disc piceous without contrasting margins, and slightly paler, rufopiceous elytra and concolorous sutural intervals. The legs are paler–brunneous, rufobrunneous, or flavobrunneous–generally without contrasting coloration on the femora (exceptions noted under appropriate species treatments).

Member species. There are 15 species assignable to subgenus *Phacothorax*, with all species restricted to New Caledonia.

Identification key to adults of *Mecyclothorax* subgenus *Phacothorax* of New Caledonia

1 Pronotal base broad, hind angles well defined, MPW/BPW = 1.30–1.40 (Figs 2A, 9A–C) 2
– Pronotal base narrow relative to maximal width, hind angles either broadly rounded, or if well-defined, MPW/BPW = 1.66–3.91 (Figs 2B, 9D–E, 16, 20)..... 4
2 Anterior and posterior supraorbital setae present; pronotal lateral seta present 3
– A single posterior supraorbital setae present; pronotal lateral seta absent..... 1. *M. laterobustus* Liebherr sp. n.
3 Sutural stria and striae 3–6 deep on disc, stria 2 shallower, nearly effaced between positions of dorsal elytral setae (Fig. 9B); male aedeagal median lobe broadly, smoothly rounded apically, flagellum broadly curved dorsally toward lobe apex (Fig. 10C–D)..... 2. *M. laterosinuatus* Liebherr sp. n.
– Sutural stria deep on disc, striae 2–6 nearly as deep, stria 2 smooth between positions of dorsal elytral setae (Fig. 9C); male aedeagal median lobe narrowly rounded to a downwardly oriented tip, flagellum curved ventral toward apex, a patch of large spicules apicad flagellum in uneverted condition (Fig. 10F–H) ..... 3. *M. laterorectus* Liebherr sp. n.
4 Head with only the posterior supraorbital seta present each side, the anterior supraorbital seta lacking (Fig. 1B) 5
– Head with two supraorbital setae each side (as in Fig. 1C) 6
5 Male aedeagal median lobe with apex prolonged beyond ostial opening to acuminate tip(Fig. 10I–M); female bursa copulatrix bilobed, but dorsal lobe much shorter than ventral lobe (Fig. 12D); distributed from Me Maoya to Ningua (Fig. 15) ..... 4. *M. fleutiauxi* (Jeannel)
– Male aedeagal median lobe briefly projected beyond ostial opening to a narrowly rounded tip (Fig. 10N–R); female bursa copulatrix bilobed with dorsal lobe as long as ventral lobe (Fig. 12E); distributed from Mt. Humboldt to Forêt Nord (Fig. 15)..... 5. *M. jeanneli* Liebherr sp. n.
6 Standardized body length larger, 4.7–5.9 mm..... 7
– Standardized body length smaller, 2.8–4.1 mm 9
7. Pronotum with only a single lateral seta each side at midlength; prosternum glabrous, metafemora with glabrous posterior margin..... 8
– Pronotum with single lateral seta on lateral reaches of disc at midlength, plus 13–14 accessory setae in the pronotal marginal bead, 4–5 setae anterad lateral seta, and 9 seta posterad; prosternum with sparse covering of elongate setae, metafemora with more than 10 fine, elongate setae along posterior margin ..... 6. *M. plurisetosus* Liebherr sp. n.
8 Elytral striae 1–8 fully developed, continuous and smooth from base to apex (Fig. 16B); pronotal disc glossy, microsculpture reduced; a deep fossa present at base of median longitudinal impression at median base, pronotal margin bead continuous across base..... 7. *M. megalovatulus* Liebherr sp. n.
– Elytral surface smooth, striae at most suggested by obsolete longitudinal depressions on disc, any evidence of striae 1–7 absent apically (Fig. 16C); pronotal disc subiridescent due to well-developed transverse mesh microsculpture; pronotal median longitudinal impression broadened basally at pedunculate pronotal base, no marginal or basal bead present on base ..... 8. *M. octavius* Liebherr sp. n.
9 Pronotal hind angles very obtuse to obsolete, rounded, lateral margin immediately anterad angle at most slightly concave (Figs 16D–E, 20A)..... 10
– Pronotal hind angles obtuse to nearly right, lateral margin immediately anterad angle distinctly concave, the lateral margin sinuate (Fig. 20B–H)..... 12
10 Elytral striae 1–4 evident on disc, shallow to deep, contrasted with obsolete to absent striae 5–7 (Figs 16E, 20A)..... 11
– Elytral striae 1–7 all evident on disc, striae 3–4 shallower than striae 1–2, but striae 5–7 deep, smooth and continuous at elytral midlength (Fig. 16D)..... 9. *M. laterovatulus* Liebherr sp. n.
11. Elytra orbicular–MEW/EL = 0.96–and very convex (Fig. 16E), interval 8 outwardly bulging dorsad deeply impressed stria 8, the outer elytral intervals thus nearly vertical to orientation of lateral marginal depression, interval 9 not visible in dorsal view ..... 10. *M. najtae* Deuve
– Elytra more ellipsoid–MEW/EL = 0.79–0.84–and moderately convex (Fig. 20A), interval 8 convex dorsad narrowly impressed stria 8, but interval 9 visible in dorsal view, lateral intervals obtusely angled to orientation of lateral marginal depression ..... 11. *M. manautei* Liebherr sp. n.

12 Pronotal hind angles obtuse with rounded apex, not protruded (Fig. 20C–H); elytral striae 1–4 present on disc, smoothly impressed to slightly punctate, though outer striae are shallower than sutural stria 13
– Pronotal hind angles protruded, nearly right (Fig. 20B); elytra with sutural stria traceable though shallow on disc, outer striae 2–7 obsolete, their positions evidenced by discontinuous series of extremely shallow depressions over portions of the elytral length ..... 12. *M. paniensis* Liebherr sp. n.
13 Elytral lateral marginal depression narrow outside anterior series of lateral elytral setae, the depression piceous to its margin to match coloration of elytral disc (Fig. 20D–H); male aedeagal median lobe apex downturned at tip, a small hitch or deep invagination nearly always present along apical face (Fig. 21A–D, F–L) [except *M. kanak* form Q of couplet 15, Fig. 21E] 14
– Elytral lateral marginal depression broad outside anterior series of lateral elytral setae, translucent brunneous outer reaches of explanate margin contrasted with piceous inner portion and elytral disc (Fig. 20C); male aedeagal median lobe apex subparallel dorsoventrally, the apical face somewhat flattened but without small hitch or distinct invagination (Fig. 17M–N) ..... 13. *M. mouensis* Moore & Liebherr sp. n.
14 Male aedeagal median lobe rounded apically, with only a very small hitch in the apical margin or no hitch at all (Fig. 21E, L, N) 15
– Male aedeagal median lobe with distinct invagination along apical face (Fig. 21A–D, F–K), though curvature and dorsoventral breadth of median lobe apex may vary (Fig. 26); female basal gonocoxite with narrow spiculate band along mediobasal margin (Fig. 24D) ..... 14. *M. kanak* Moore & Liebherr sp. n.
15. Male aedeagal median lobe slightly narrowed apically, with tip rounded and smooth, ostial opening asymmetrical apically, its ventroapical margin extended more toward tip than dorsoapical margin (Fig. 21E) [see Male genitalia section of *M. kanak* species description] ..... 14. *M. kanak* Moore & Liebherr sp. n., form Q
– Male aedeagal median lobe apex broadly downturned, tip broadly rounded, apical margin with or without a minute hitch, ostial opening broadly rounded, symmetrical apically relative to tip (Fig. 21L, N); female basal gonocoxite with broad spiculate band along mediobasal margin, the spicules flattened, blunt apically (Fig. 24E).. 15. *M. picdupinsensis* Liebherr sp. n.

1. *Mecyclothorax laterobustus* Liebherr, sp. n.

http://zoobank.org/F59062DE-95C1-48B7-A947-CAFE2EA6F98C
Figures 5E, 9A, 10A–B, 12A, 13A, 14

Diagnosis. These beetles are very robust, with a broad pronotum and broadly convex elytra (Fig. 9A). The pronotal base is broad, with MPW/BPW = 1.30–1.32, and the hind angles are projected, with the pronotal lateral margin concave just before the angle. Only the posterior supraorbital seta is present, and the pronotum is glabrous. Elytral striae 1–5 are well developed basally, with striae 3–5 deeper than those of individuals of the similar appearing *M. laterosinuatus* and *M. laterorectus* (Fig. 9B–C). Standardized body length 4.1–4.4 mm. Chaetotaxy –/+//–/–//+/2/+/+.

Description (n = 5). Head capsule broad, eyes moderately convex, ocular lobe meeting gena at very obtuse angle; 16 ommatidia along horizontal diameter of eye; ocular ratio 1.33–1.42, EyL/EyD = 2.34–3.0; frontal grooves deep, arcuately convergent and deepest just posterad clypeus, briefly and shallowly extended onto clypeus; mandibles moderately elongate, mandibular ratio 1.67; ligular anterior margin rounded to ligular seta, concave between setae, the two setae separated by two setal diameters; paraglossae thin, extended as far beyond ligular margin as their basal length to margin; antennae moderately elongate, antennomere 9 length 2.0× maximal breadth; antennomere 3 glabrous except for apical ring of setae. Pronotum moderately constricted basally, with obtuse-rounded hind angles and lateral margins briefly sinuate anterad angles (Fig. 9A); MPW/BPW = 1.30–1.32, MPW/PL = 1.19–1.22; front angles protruded anteriorly, but anterior margin narrowly approaching head capsule, APW/BPW = 0.69–0.71; basal margin broadly convex, beaded from just mesad deep, longitudinal laterobasal depression to and around obtuse-rounded hind angle; median longitudinal impression deep and narrow on disc, broader and shallower approaching base, absent anterad very shallow anterior transverse impression; proepisternum separated from prosternum by a very shallow groove anteriorly, but with a deep, slightly punctate groove ventrally; prosternal process deeply and narrowly depressed between procoxae, that depression extended 1/3 distance toward anterior prothoracic margin. Elytra broadly ovoid, humeri broad, humeral angle obtusely rounded laterad pronotal hind angles; MEW/EL = 0.87–0.93; basal groove evenly arcuate from scutellum to humeral angles, with depression at bases of sutural and elytral striae 4–5; sutural stria deep throughout length, stria 2 obsolete though traceable, stria 3 somewhat deeper, striae 4–5 deep in basal half, striae 6–7 obsolete; only sutural stria and stria 8 evident apically, elytra appressed and conjoined apically, sutural intervals narrower and upraised at apex. Pterothoracic mesepisternal anterior furrow with 6–7 deep punctures; mesosternal-mesepisternal suture complete (as in Fig. 3A); metepisternum maximum width/lateral length = 1.0; metepisternal-metepimeral suture incomplete, shallower and incomplete laterally. Abdomen with deep crescent-shaped depression along suture between first and second ventrite, second ventrite depressed within crescent; suture between second and third ventrites reduced though traceable laterally; ventrites 2–6 with broad, shallow, linear plaques near lateral margin. Microsculpture of frons a shallow transverse mesh, sculpticells twice as

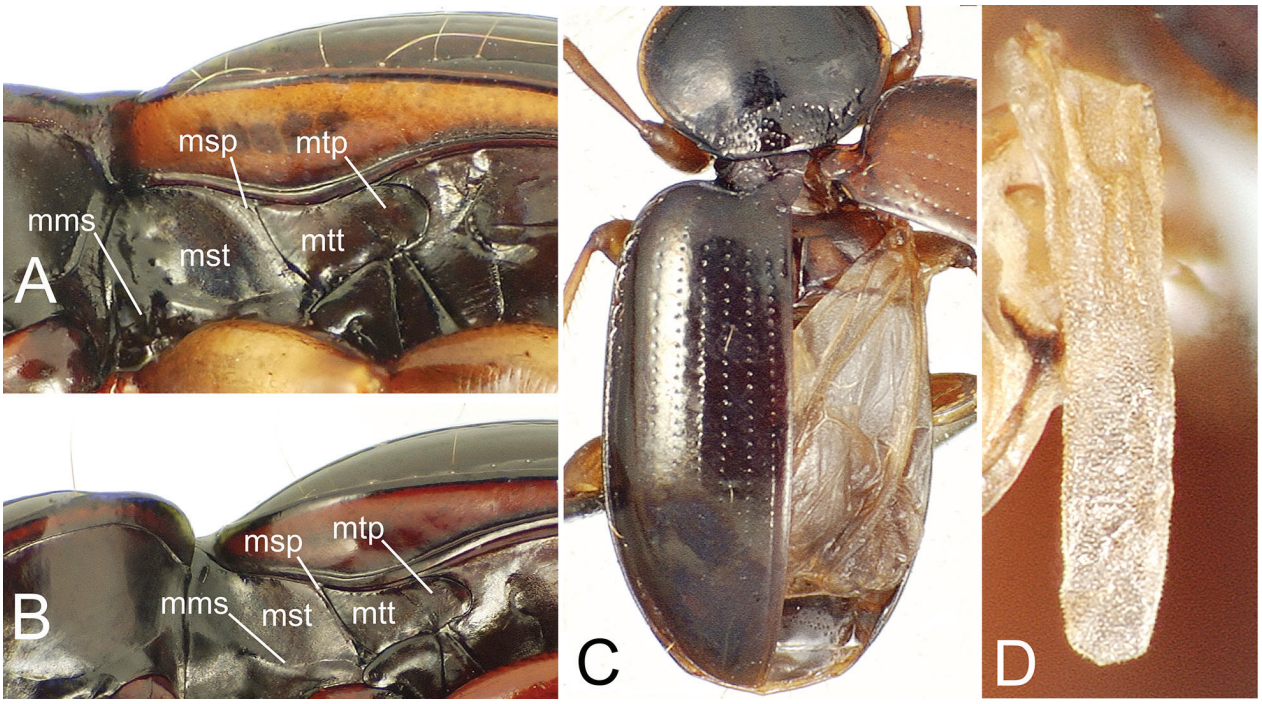

Figure 3. Thoracic structures of *Mecyclothorax* spp. **A–B**. Lateral view of elytral epipleuron and meso-and metapleurites: **A**, *M. laterorectus*; **B**, *M. fleutiauxi*. **C–D**. Metathoracic flight wing: **C**, *M. punctipennis*, showing fully developed flight wing folded under elytron; **D**, *M. lissus*, stenopterous wing rudiment that extends beyond metanotum, rudimentary wing venation present at base of strap. Abbreviations include: **mms**, mesepisternal-mesosternal suture; **msp**, mesepimeron; **mst**, mesepisternum; **mtp**, metepimeron; **mtt**, metepisternum.

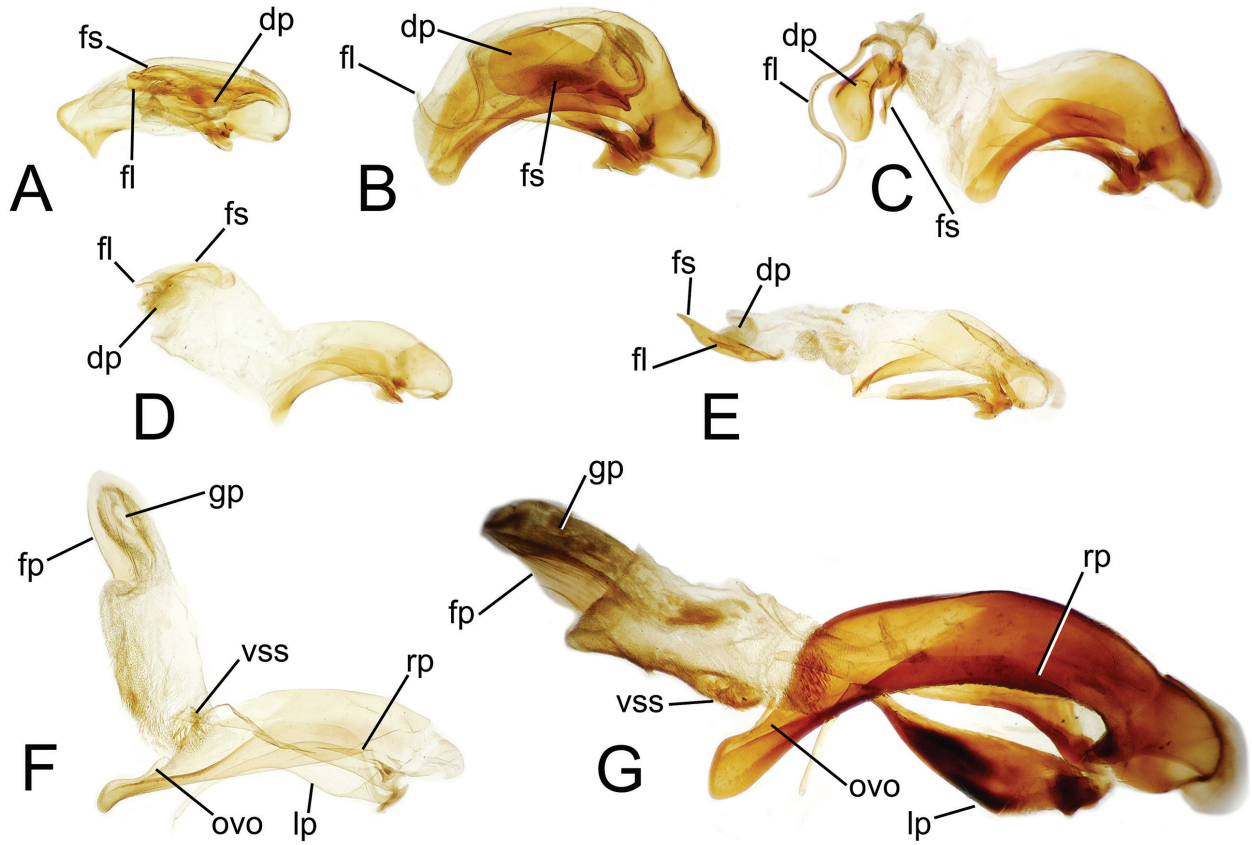

Figure 4. Male aedeagal median lobe and parameres of *Mecyclothorax* spp., right lateral view, internal sac everted in **C–G**: **A**, *M. blackburni*; **B–C**, *M. peryphoides*; **D**, *M. moorei*; **E**, *M. lewisensis*; **F**, *M. punctipennis*; **G**, *M. montivagus*. See Table 2 for abbreviations.

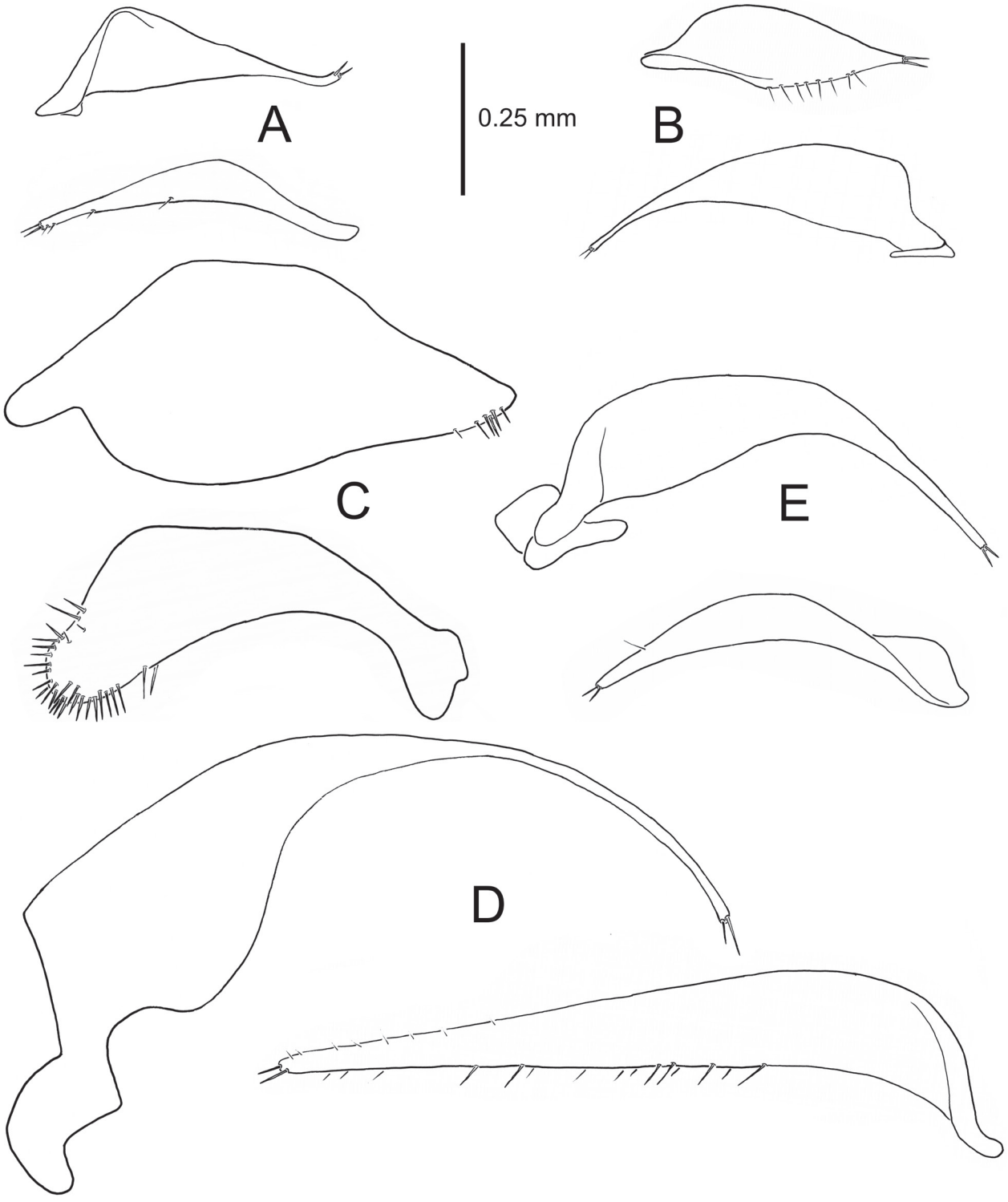

Figure 5. Paired left (above) and right (below) parameres of *Mecyclothorax* spp. (ectal view): **A**, *M. blackburni*; **B**, *M. storeyi*; **C**, *M. amplipennis*; **D**, *M. montivagus*; **E**, *M. laterobustus.* As the aedeagal assembly of *M. storeyi* males is inverted relative to other *Mecyclothorax* species (Moore 1984), the configuration of the upper, or right paramere of *M. storeyi* should be compared to the ventral, or left parameres of the other species, and vice versa.

broad as long, these mixed with isodiametric sculpticells on vertex; pronotal disc and base covered with elongate transverse mesh plus transverse lines, surface iridescent; elytral iridescent, disc with loose elongate transverse mesh, apex with very elongate transverse mesh, sculpticell breadth 3–4× length.

Male genitalia (n = 1). Antecostal margin of male mediotergite IX distally angulate, little extended (Fig. 10B);

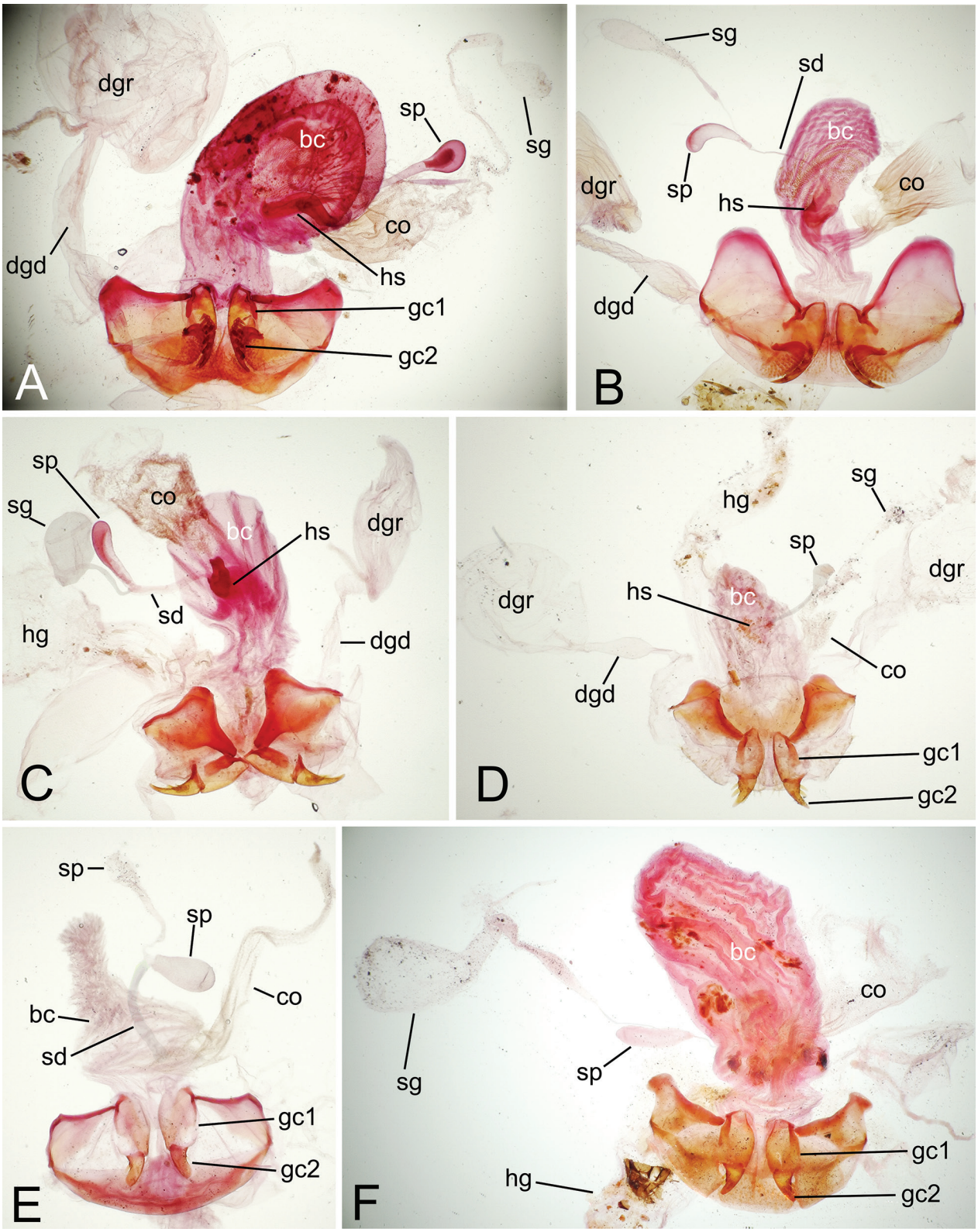

Figure 6. Female reproductive tract, gonocoxites and associated laterotergites, *Amblytelus* and *Mecyclothorax* spp: **A**, *A. matthewsi*; **B**, *A. brevis*; **C**, *M. blackburni*; **D**, *M. storeyi*; **E**, *M. minutus*; **F**, *M. rectangulus*. See Table 2 for abbreviations.

right paramere very elongate, moderately narrow, with a single seta on dorsal margin distant from two apical setae (Fig. 5E); left paramere narrow basally, evenly narrowed to a whip-shaped apex, two longer setae at apex; aedeagal median lobe shaft robust, broad dorsoventrally (Fig. 10A), median lobe apex broad, sides subparallel, with tip broadly rounded; aedeagal internal sac with flagellum, flagellar sheath, and sclerotized dorsal plate.

Female reproductive tract (n = 1). Bursa copulatrix elongate, length more than twice circumference, surface translucent, membranous (Fig. 12A); spermathecal duct entering near bursa-common oviduct juncture with duct oriented toward right side of bursa, duct longer than spermathecal reservoir; a rounded laminar helminthoid sclerite present at base of spermathecal duct; spermatheca fusiform on narrow duct, spermathecal gland duct entering at base of spermathecal reservoir; basal gonocoxite 1 with apical fringe of two setae near medial margin, a series of small setae lining medial margin (Fig. 13A); gonocoxite 2 moderately broad basally, basal width about half medial length; two gracile lateral ensiform setae of moderate length present.

Types – Holotype male (MNHN): NEW CALEDONIA / Ningua Res.camp / 12-13Nov 2001 / G.B.Monteith // QM Berlesate 1039 / 21°45'Sx166°09'E / Rainforest, 1100m / Sieved litter // QUEENSLAND / MUSEUM LOAN / Date: Nov. 2003 / No. LEN-1686 (green label) // HOLOTYPE / Mecyclothorax / laterobustus / J.K.Liebherr 2017 (black-bordered red label).

Paratypes (10 specimens). NEW CALEDONIA: Ningua Reserve, camp, 1100 m el., 21°45'S 166°09'E, rainforest, sieved litter, 12-13-xi-2001, lot 1039, Monteith (QMB, 4), near summit, rainforest, 1300 m el., 21°45'S 166°09'E, berlesate, sieved litter, 13-xi-2001, lot 1052, Monteith (QMB, 3); Plateau de Dogny, rainforest, 910 m el., 21°37'S, 165°53'E, berlesate sieved litter, 16-xi-2002, lot 1085, Burwell (QMB, 3).

Etymology. The very broad and robust body form of these beetles (Fig. 9A) suggests the compound, adjectival species epithet laterorobustus.

Distribution and habitat. This species is known from two localities, Ningua Reserve and Plateau de Dogny (Fig. 14), and specimens have been collected from 900–1300 m elevation. The three collecting events are all based on recovering specimens from sieved litter, consistent with an interpretation that these beetles occupy ground-level microhabitats.

2. *Mecyclothorax laterosinuatus* Liebherr, sp. n.

http://zoobank.org/BC6BAC70-3131-45CD-B8DE-0D72BB0D70A3
Figures 9B, 10C–E, 11A, 12B, 13B, 14

Diagnosis. These beetles are very similar in external appearance to those of *M. laterorectus* (Fig. 9B–C) below, sharing the moderately robust body form and cordate pronotum, though the pronotal base is slightly broader relative to the maximal pronotal width in this species: MPW/BPW = 1.28–1.33. This species also differs from *M. laterorectus* in the very shallow second elytral stria contrasted to the deeper sutural stria and striae 3–6. Like the preceding *M. laterobustus*, the pronotal hind angles protrude, with the pronotal lateral margin concave before the angle, but in this species and the following, the pronotal lateral seta is present. Also, this and the following species exhibit both anterior and posterior supraorbital setae. Standardized body length 3.7–4.3 mm. Chaetotaxy +/+//+/–//+/2/+/+.

Description (n = 5). Head capsule broad, eyes convex, ocular lobe meeting gena at obtuse angle very close to eye posterior margin; 12–14 ommatidia along horizontal diameter of eye; ocular ratio 1.43–1.50, ocular lobe ratio 0.84–0.89, EyL/EyD = 2.50–2.65; frontal grooves nearly straight from posterior terminus inside anterior supraorbital seta to deepest point just posterad clypeus, briefly and shallowly extended onto clypeus; mandibles moderately elongate, mandibular ratio 1.8; ligular anterior margin narrowly rounded to ligular seta, concave between setae, the two setae separated by two setal diameters; paraglossae thin, extended as far beyond ligular margin as their basal length to margin; antennae elongate, antennomere 9 length 2.25× maximal breadth; antennomere 3 glabrous except for apical ring of setae. Pronotum distinctly constricted basally, cordate, hind angles obtuse rounded, lateral pronotal margins subparallel anterad hind angles, then distinctly divergent anteriorly (Fig. 9B); MPW/BPW = 1.37–1.40, MPW/PL = 1.24–1.27; front angles protruded, obtusely angulate, APW/BPW = 0.75–0.78; basal margin slightly convex, nearly straight between broadly upraised hind margins posterad broad laterobasal depressions; laterobasal depression with longitudinal tubercle inside hind angle, and broad furrowlike longitudinal extension onto disc; median longitudinal impression fine and shallow on disc, with deep longitudinal pitlike depression anterad median base, absent anterad very broad and shallow anterior transverse impression; proepisternum separated anteriorly from prosternum by fine shallow groove, distinctly separated ventrally by smooth, deep groove; prosternal process deeply, narrowly between procoxae, that deep depression extended 1/3 distance toward anterior prothoracic margin. Elytra broadly ellipsoid, humeri extended laterally, humeral angle obtusely rounded outside pronotal hind angles; MEW/EL = 0.81–0.86; basal groove evenly arcuate from scutellum to humeral angles, with depressions at bases of sutural and elytral striae 3–5; sutural stria deep throughout length, stria 2 shallow, obsolete on disc, striae 3–5 deep, stria 6 shallow, and stria 7 obsolete in basal half; striae 1–2, 7 and 8 evident apically, elytra appressed and conjoined apically, sutural intervals narrower and upraised at apex. Pterothoracic mesepisternal anterior furrow with five broad depressions in one to two vertical rows; metepisternum maximum width/lateral length = 1.1; mesosternal-mesepisternal suture complete (as in Fig. 3A); metepisternal-metepimeral suture incomplete, shallower and incomplete laterally. Abdomen with deep crescent-shaped depression along suture between first and second ventrite, second ventrite depressed within crescent; suture between second and third ventrites reduced, incomplete laterally; ventrites 2–6 with broad, shallow, linear plaques near lateral margin. Microsculpture of frons an evident transverse mesh, transverse sculpticells mixed with isodiametric sculpticells on vertex; pronotal disc and base covered with elongate transverse mesh plus transverse lines,

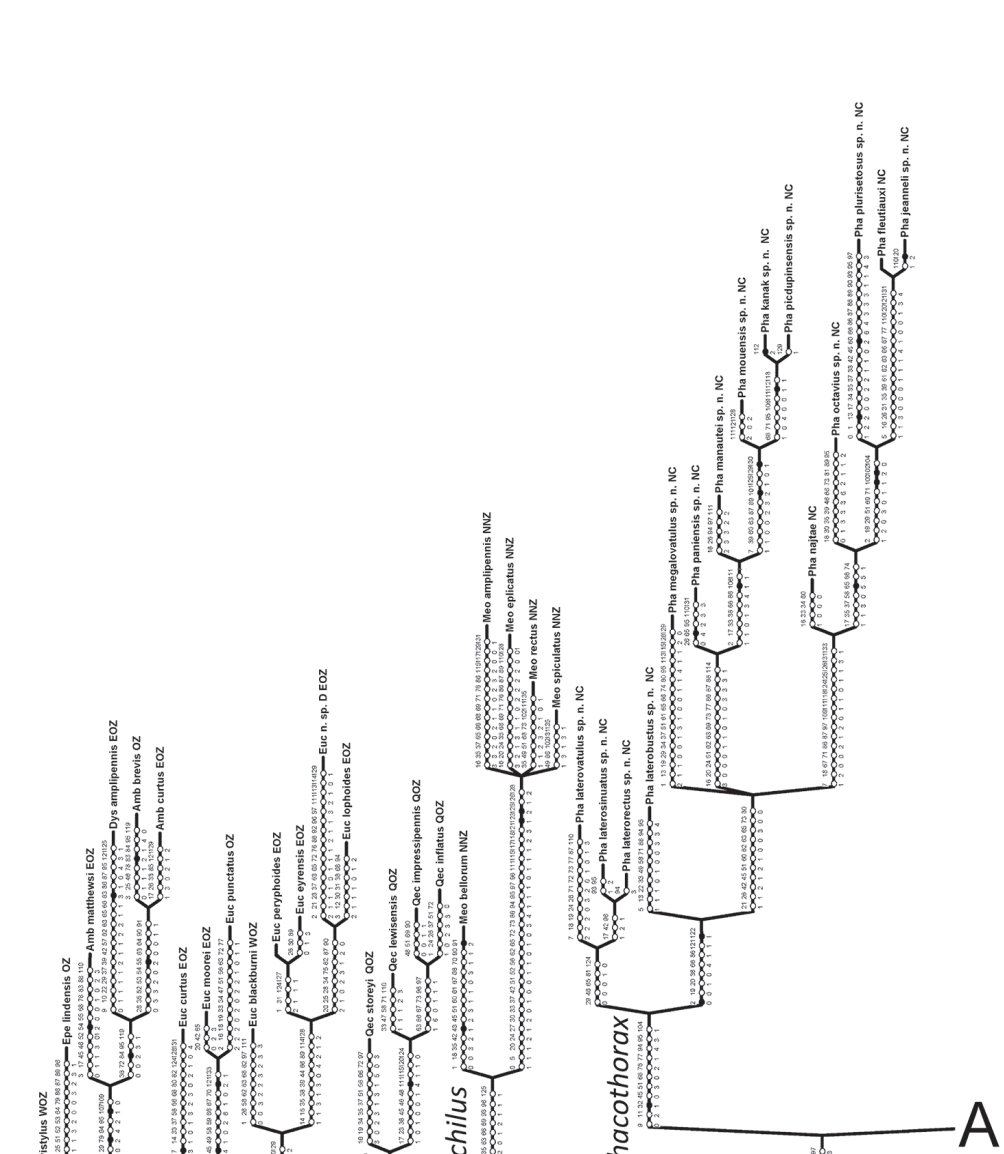

Figure 7. Strict consensus cladogram of 16 equally most-parsimonious trees derived from cladistic analysis of 65 moriomorphine taxa, including the secondary outgroup *Neonomius laevicollis*, six primary outgroup taxa in *Amblytelus* and allied genera, and 58 ingroup terminals; 57 *Mecyclothorax* species plus two genitalic forms of *M. andersoni*. Species terminals are labeled with species name and three-letter abbreviation of relevant generic or subgeneric name. Full listing of included taxa along with subgeneric assignments is presented in Table 2. Cladistic analysis is based on 137 characters (see character descriptions for nature of each character Areas occupied by the included taxa indicated by abbreviations following species epithets: **Bo**, Borneo; **EOZ**, eastern Australia, i.e. east of the Nullarbor Plain; **FP**, French Polynesia, Tahiti; **HI**, Hawaiian Islands, Maui; **Jv**, Java; **LH**, Lord Howe Island; **NC**, New Caledonia; **Nf**, Norfolk Island; **NNZ**, North Island of New Zealand; **NZ**, generally distributed across New Zealand; **OZ**, generally distributed across Australia; **PNG**, Papua New Guinea; **QOZ**, restricted to Queensland, Australia; **SNZ**, South Island of New Zealand plus Chatham Islands; **SP&A**, St. Paul and Amsterdam Islands; **WOZ**, western Australia, i.e. west of the Nullarbor Plain.

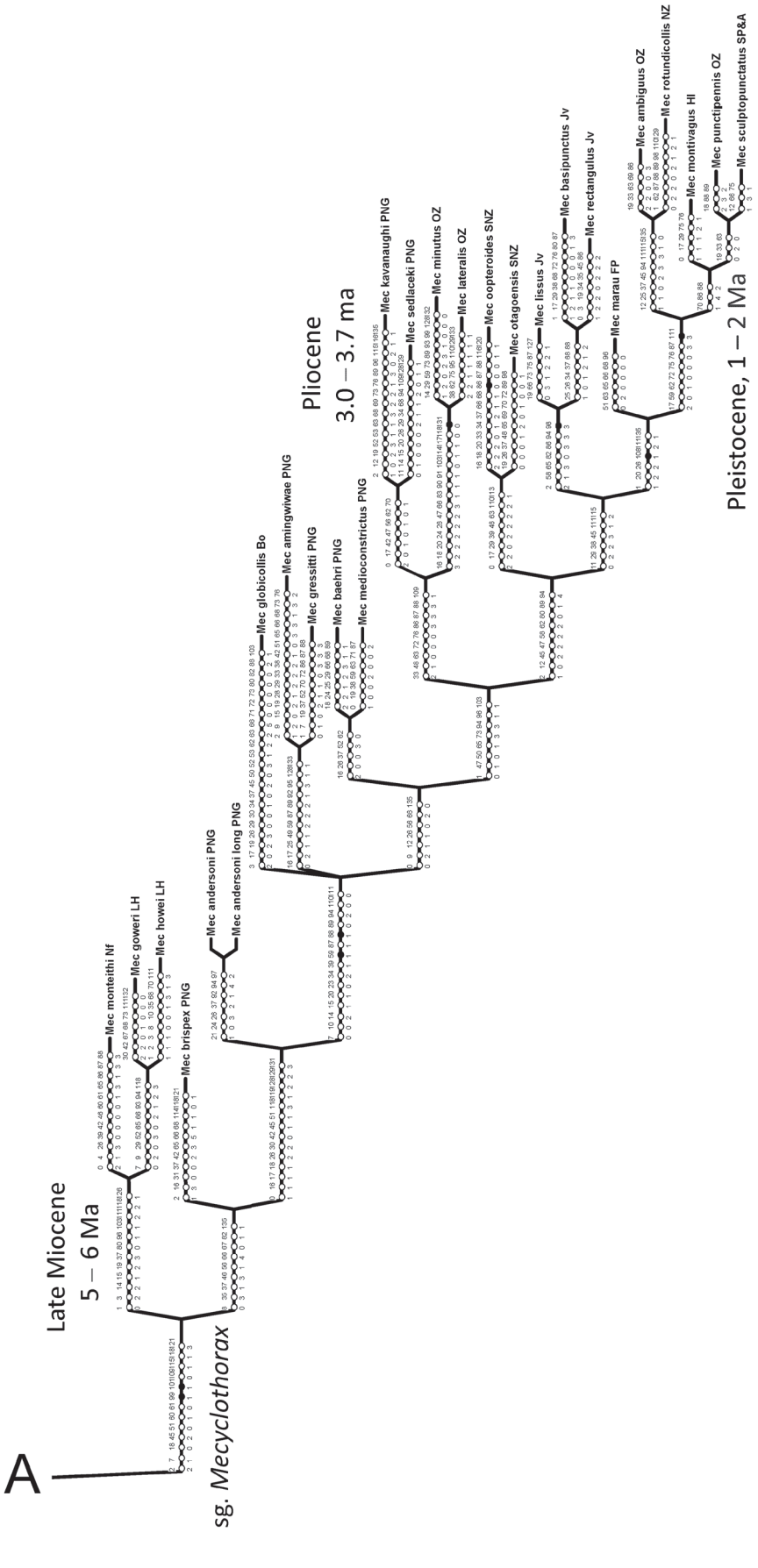

Figure 7. Continue.

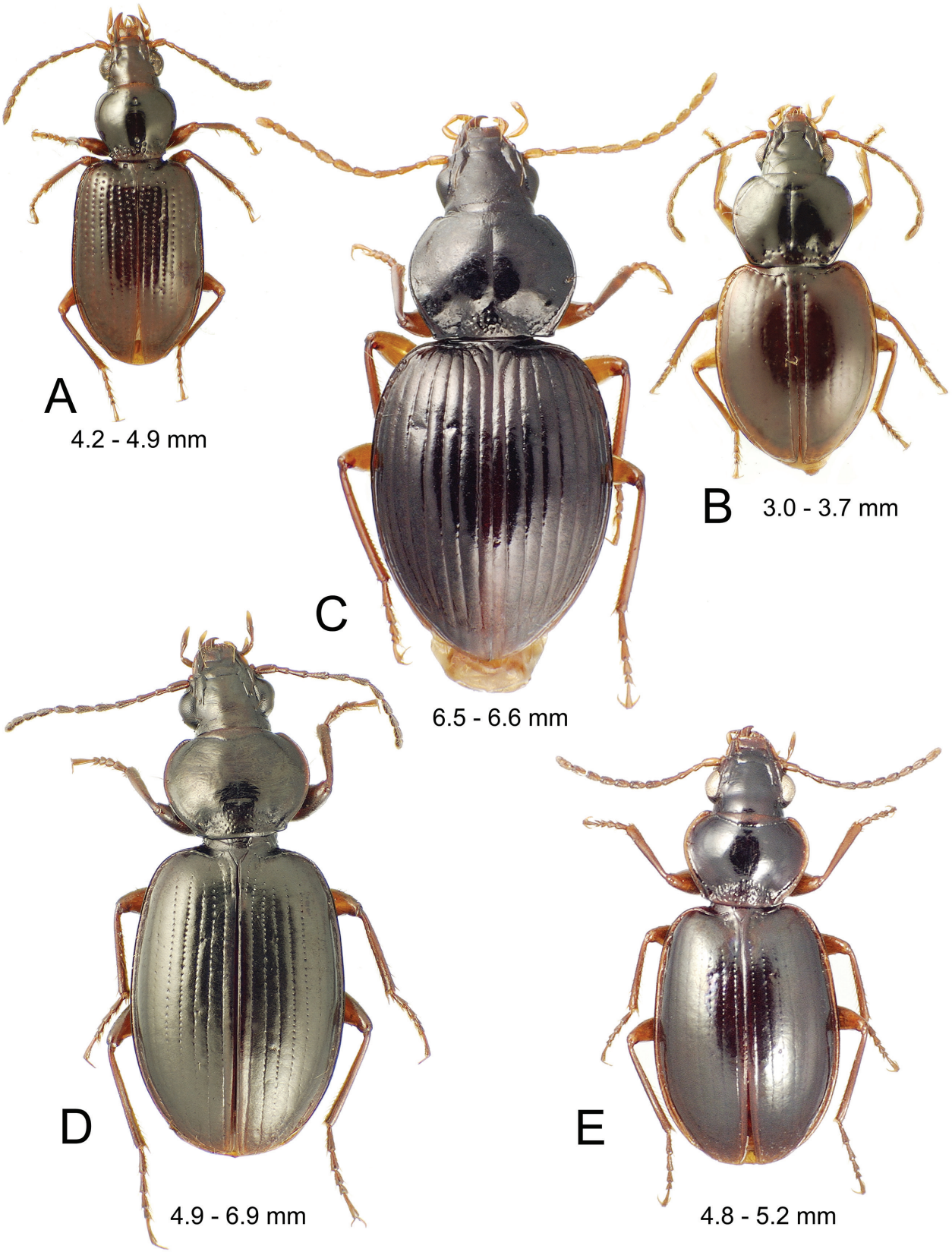

Figure 8. *Mecyclothorax* spp., dorsal view, with subgeneric assignments: **A**, *M.* (*Eucyclothorax*, subgen. n.) *blackburni* (type species); **B**, *M.* (*Qecyclothorax*, subgen. n.) *storeyi* (type species); **C**, *M.* (*Meonochilus*, status n.) *amplipennis* (type species); **D**, *M.* (*Mecyclothorax*) *montivagus* (type species); **E**, *M.* (*Mecyclothorax*) *lissus*.

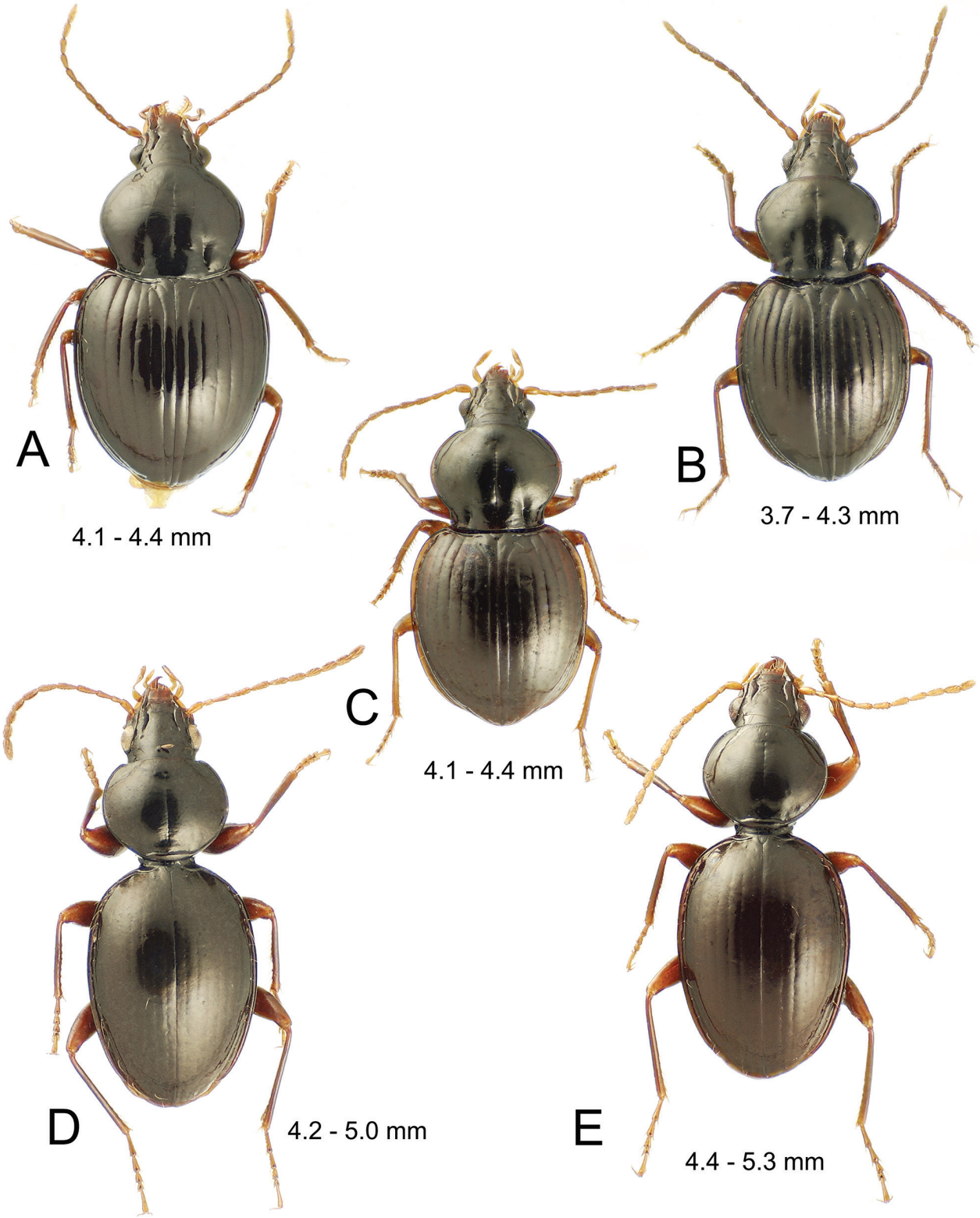

Figure 9. New Caledonian *Mecyclothorax* (*Phacothorax*) spp., dorsal view: **A**, *M. laterobustus*; **B**, *M. laterosinuatus*; **C**, *M. laterorectus*; **D**, *M. fleutiauxi*; **E**, *M. jeanneli*.

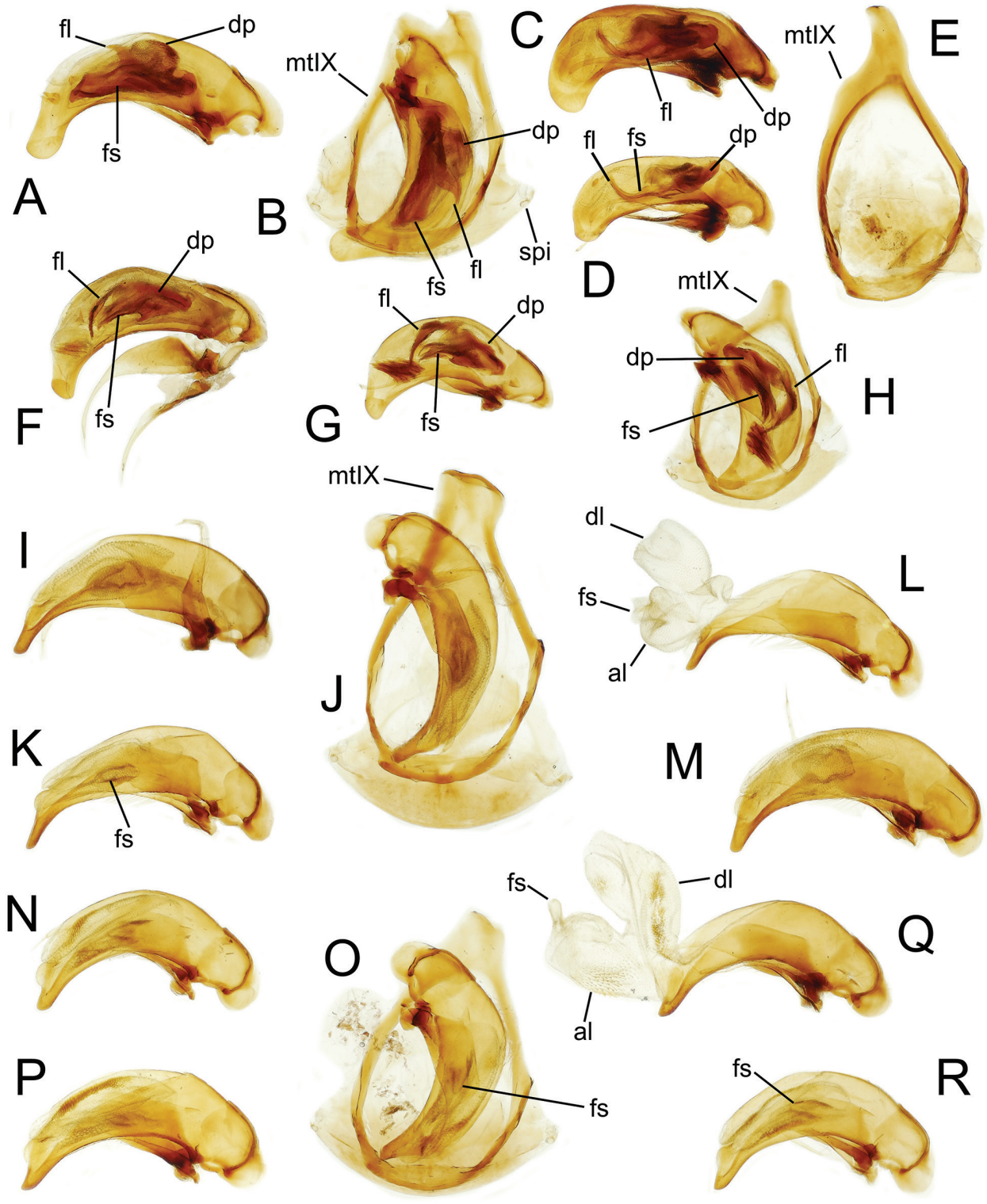

Figure 10. Male aedeagal median lobe and parameres, and ring sclerite–mediotergite plus antecostal margin, tergite IX–of *Mecyclothorax* (*Phacothorax*) spp.: **A–B**, *M. laterorobustus*, right view, dorsal view in situ (Ningua); **C**, *M. laterosinuatus*, right view (Col d'Amieu); **D**, *M. laterosinuatus*, right view (Touho TV tower); **E**, *M. laterosinuatus* ring, dorsal view; **F**, *M. laterorectus*, right view (Mt. Panié); **G–H**, *M. laterorectus*, right vew, dorsal view in situ (Mandjélia); **I–J**, *M. fleutiauxi*, right view, dorsal view in situ (Mt. Do); **K–L**, *M. fleutiauxi*, right view, sac inverted and everted (Me Maoya); **M**, *M. fleutiauxi*, right view (Ningua); **N–O**, *M. jeanneli*, right view, dorsal view in situ (Mt. Humboldt, 1350 m); **P**, *M. jeanneli*, right view (Mt. Humboldt, 1300 m); **Q**, *M. jeanneli*, right view, sac everted (Mt. Dzumac); **R**, *M. jeanneli*, right view (Rivière Bleue). See Table 2 for abbreviations.

surface iridescent; elytra iridescent, disc with loose elongate transverse mesh, apex with very elongate transverse mesh, sculpticell breadth 3–4× length. Femora rufobrunneous basally, with a broad flavous band in apical third.

Male genitalia (n = 5). Antecostal margin of abdominal mediotergite IX angulate distally, an elongate distal extension present (Fig. 10E); right paramere very elongate, apical half narrowed into a whiplike extension (Fig. 11A), with 10 setae on ventral surface complementing the two apical setae, dorsal surface with four small setae; left paramere narrow basally, evenly extended to whiplike apex, surfaces glabrous except for two apical setae; aedeagal median lobe robust, broad dorsoapically, apex broadly curved ventrally with tip rounded (Fig. 10C–D); aedeagal median lobe internal sac with flagellum, flagellar sheath, and dorsal plate, the former two structures curved dorsad apically. The median lobes of the two figured males–Col d'Amieu (Fig. 10C) and Touho TV Tower (Fig. 10D) – differ about 10% in length, whereas the males themselves are nearly identical in standardized body length; 4.0 versus 4.05 mm. As the internal sac structures do not appear to differ except in the basal shape of the dorsal plate (differing orientation inside median lobe?), these two populations are considered conspecific.

Female reproductive tract (n = 2). Bursa copulatrix elongate, length about twice circumference, surface translucent, membranous (Fig. 12B); spermathecal duct entering near bursa-common oviduct juncture with duct oriented toward right side of bursa, duct as long as spermathecal reservoir; an elongate laminar helminthoid sclerite present at base of spermathecal duct; spermatheca fusiform on narrow duct, spermathecal gland duct entering at base of spermathecal reservoir; ligular apophysis present near base of common oviduct; basal gonocoxite 1 with apical fringe of one to two short setae laterally on apical margin, smaller microsetae scattered along apical margin, and a series of small setae lining medial margin (Fig. 13B); gonocoxite 2 broad basally, basal width slightly more than half medial length; two short, gracile lateral ensiform setae present.

Types – Holotype male (MNHN): NEW CALEDONIA / Aoupinie top camp / 2-3Nov 2001 / G.B.Monteith // QM Berlesate 1060 / 21°11'Sx165°18'E / Rainforest, 850m / Sieved litter // QUEENSLAND / MUSEUM LOAN / DATE: Nov. 2003 / No. LEN-1686 (green label) // *New Caledonia Mecyclothorax* revision / measured specimen 2 / J.K. Liebherr 2016 // HOLOTYPE / Mecyclothorax / laterosinuatus / J.K.Liebherr 2017 (black-bordered red label).

Paratypes (83 specimens; BPBM, MNHW, PMGC, QMB): see Suppl. material 2.

Etymology. Like the preceding and immediately following species, beetles of this species exhibit a basally broad pronotum (Fig. 9A–C). In this species, the distinctly sinuate lateral pronotal margin leads to the compound adjectival species epithet laterosinuatus.

Distribution and habitat. This species is broadly distributed along mid-latitudinal Grand Terre, from Touho TV tower on the north to Mt. Rembai on the south (Fig. 14), with beetles found from 400 m elevation to the summits of the occupied uplands. Of the 76 known specimens, 67 have been collected from sieved litter, indicating occupation of the ground-level microhabitat. Exceptions with situational label data include a singleton found via headlamp search at night (Will, EMEC), and two beetles collected from two flight-intercept traps (Monteith, QMB; Théry, MNMH), no doubt after crawling into the collecting tray.

3. *Mecyclothorax laterorectus* Liebherr, sp. n.

http://zoobank.org/B689EE86-804C-491D-8790-A6E9CAA437D3
Figures 1C, 2A, 2H, 3A, 9C, 10F–H, 11B, 12C, 13C, 14

Diagnosis. This third of the species characterized by robust body and a cordate, broad-based pronotum with well-defined hind angles (Fig. 9A–C), can be diagnosed by the relatively narrower pronotal base: MPW/BPW = 1.37–1.40 (Fig. 2A). Like the immediately preceding *M. laterosinuatus* there are two supraorbital setae each side, and the pronotal lateral seta is present, but the discal elytral striae 3–5 are much shallower here, only slightly deeper than the shallow stria 2. The pronotal lateral margins are subparallel basally, with the pronotal hind angle obtuse, its apex not projected. Standardized body length 4.1–4.4 mm. Chaetotaxy +/+//+/–//+/2/+/+.

Description (n = 5). Head capsule broad, eyes very convex, popeyed, ocular lobe meeting gena at obtuse angle close to eye posterior margin; 14 ommatidia along horizontal diameter of eye; ocular ratio 1.37–1.45, ocular lobe ratio 0.81–0.90, EyL/EyD = 2.56–2.89; frontal grooves nearly straight from posterior terminus inside anterior supraorbital seta to deepest point just posterad clypeus, briefly and shallowly extended onto clypeus; mandibles moderately elongate, mandibular ratio 1.7; ligular anterior margin narrowly rounded to ligular seta, concave between setae, the two setae separated by one to two setal diameters; paraglossae thin, extended as far beyond ligular margin as their basal length to margin; antennae moderately elongate, antennomere 9 length 2.0× maximal breadth; antennomere 3 glabrous except for apical ring of setae. Pronotum distinctly constricted basally, cordate, hind angles protruded and nearly right, lateral margins distinctly, briefly sinuate anterad angles (Figs 2A, 9B); MPW/BPW = 1.37–1.40, MPW/PL = 1.19–1.25; front angles only slightly protruded, rounded, APW/BPW = 0.72–0.77; basal margin broadly convex, margin broadly upraised behind broad laterobasal depression, the depression extended longitudinally onto disc as a broad sinuous furrow; median longitudinal impression fine and shallow on disc, continued to basal margin (a shallow transverse impression inside basal margin), absent anterad very shallow anterior transverse impression; proepisternum incompletely separated anteriorly from prosternum, but by a deep, smooth groove ventrally; prosternal process broadly, shallowly depressed between procoxae, that depression extended 1/3 distance to anterior prothoracic margin. Elytra

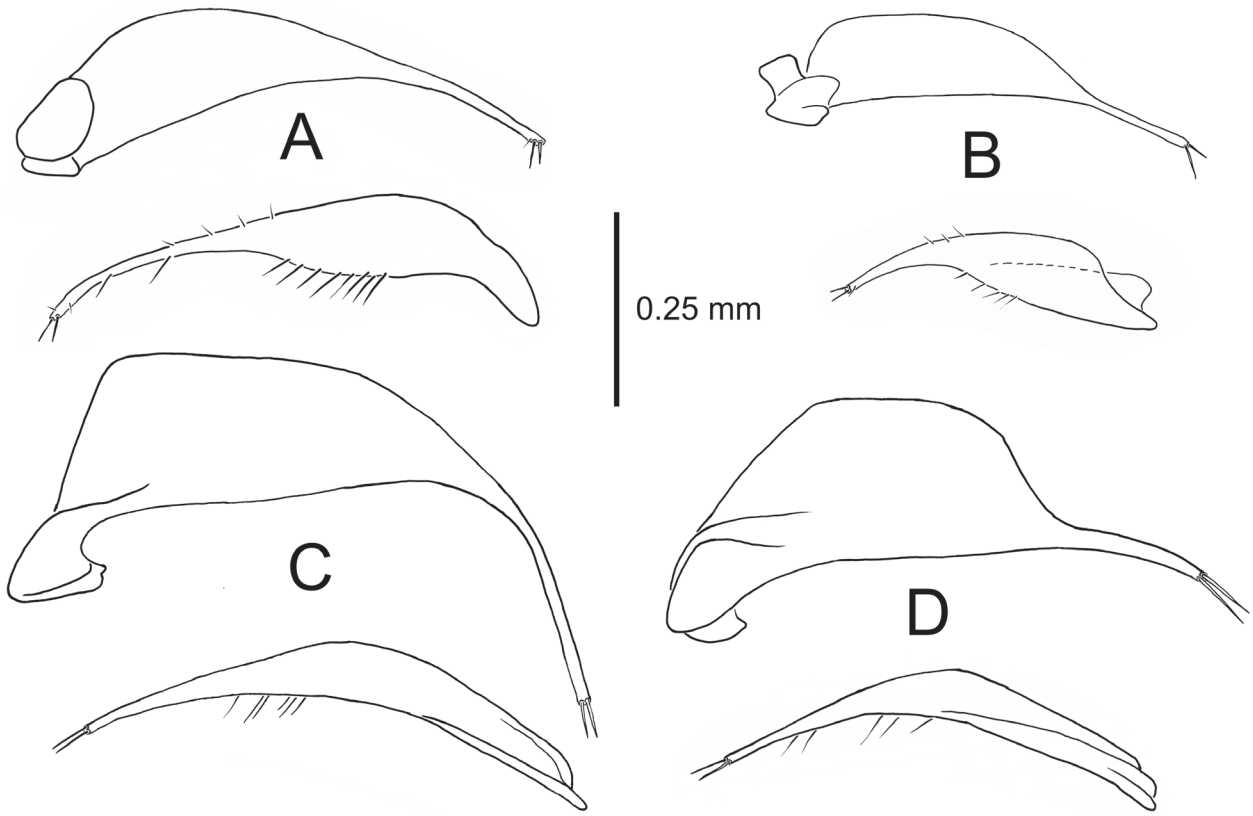

Figure 11. Paired left (above) and right (below) parameres of *Mecyclothorax* (*Phacothorax*) spp. (ectal view): **A**, *M. laterosinuatus*; **B**, *M. laterorectus*; **C**, *M. fleutiauxi*; **D**, *M. jeanneli.*

broadly ellipsoid to obovoid, humeri narrow, humeral angle obtusely rounded behind pronotal hind angles; MEW/EL = 0.82–0.86; basal groove evenly arcuate from scutellum to humeral angles, with depressions at bases of the sutural and elytral striae 4–5; sutural stria deep throughout length, striae 2–3 shallow but evident on disc, striae 4–7 deep in basal half; striae 1–2, 7 and 8 evident apically, elytra appressed and conjoined apically, sutural intervals narrower and upraised at apex. Pterothoracic mesepisternal anterior furrow with 5 broad depressions in 1–2 vertical rows; metepisternum maximum width/lateral length = 1.0; mesosternal-mesepisternal suture complete (as in Fig. 3A); metepisternal-metepimeral suture incomplete, shallower and incomplete laterally. Abdomen with deep crescent-shaped depression along suture between first and second ventrite, the second ventrite depressed within crescent; suture between second and third ventrites reduced, incomplete laterally; ventrites 2–6 with broad, shallow, linear plaques near lateral margin. Microsculpture of frons an evident transverse mesh, transverse sculpticells mixed with isodiametric sculpticells on vertex; pronotal disc and base covered with elongate transverse mesh plus transverse lines, surface of tubercle in laterobasal depression with less transverse sculpticells, surface iridescent; elytra iridescent, disc with loose elongate transverse mesh, apex with very elongate transverse mesh, sculpticell breadth 3–4× length. Femora rufobrunneous basally, with a broad flavous band in apical third.

Male genitalia (n = 3). Antecostal margin of abdominal mediotergite IX angulate, little extended distally (Fig. 10H); right paramere narrowly extended apically (Fig. 11B), with five setae on ventral margin and three on dorsal margin complementing two apical setae; left paramere narrow basally, evenly narrowed to a whiplike apex; aedeagal median lobe robust, broad dorsoventrally, apex distinctly curved ventrad to a narrowly rounded tip, its apical face slightly flattened; aedeagal median lobe internal sac with flagellum, flagellar sheath, and dorsal plate, flagellum and flagellar sheath curved ventrad apically (Fig. 10F–G), a patch of stout macrospicules present just inside ostial opening apicad flagellar structures. The median lobe apex is extended more in the specimen from Mt. Panié (Fig. 10F) than in the Mandjélia male (Fig. 10G). A third male from Mandjélia summit, 750–780 m elevation (MNHW) exhibits a lobe apex of intermediate extension. This continuous variation coupled with the extreme similarity of internal sac structures argues for conspecificity of these populations.

Female reproductive tract (n = 1). Bursa copulatrix elongate, length more than twice circumference, surface translucent, wrinkled, membranous (Fig. 12C); spermathecal duct entering near bursa-common oviduct juncture with duct oriented toward right side of bursa, duct as long as spermathecal reservoir; an elongate laminar helminthoid sclerite present near base of spermathecal duct; spermatheca fusiform on narrow duct, spermathecal gland

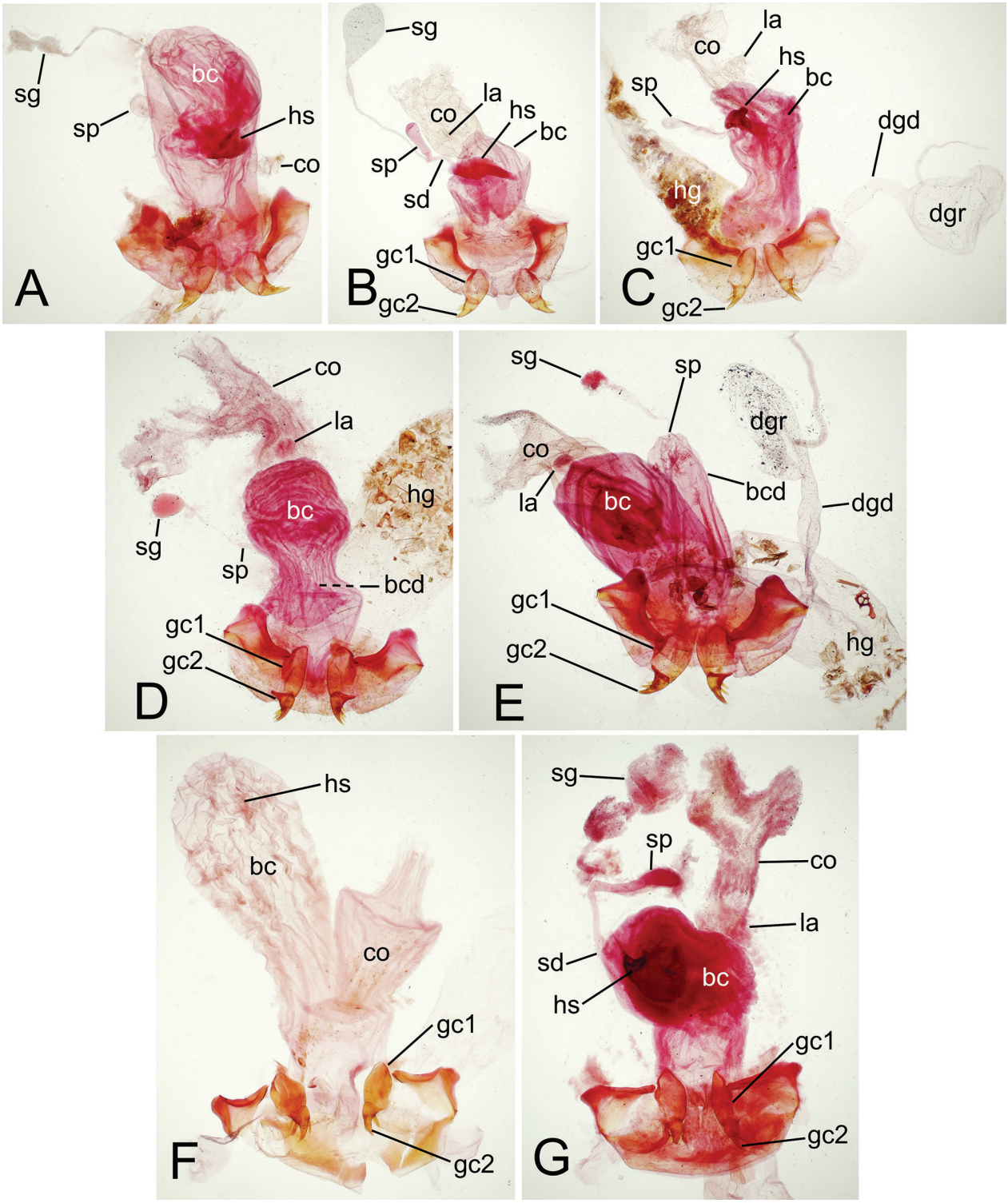

Figure 12. Female reproductive tract, gonocoxites and associated laterotergites, *Mecyclothorax* (*Phacothorax*) spp: **A**, *M. laterobustus*; **B**, *M. laterosinuatus*; **C**, *M. laterorectus*; **D**, *M. fleutiauxi*; **E**, *M. jeanneli*; **F**, *M. plurisetosus*; **G**, *M. megalovatulus*. See Table 2 for abbreviations.

duct entering at base of spermathecal reservoir; ligular apophysis present near base of common oviduct; basal gonocoxite 1 with apical fringe of two to three setae laterally on apical margin, middle seta of series largest, several small setae scattered along medial margin (Fig. 13C); gonocoxite 2 moderately narrow basally, medial length more than twice basal width; two broad lateral ensiform setae present, apical seta larger.

Types – Holotype male (MNHN): NEW CALEDONIA / Mt. Panié / 16 May 1984 / G. monteith & D. Cook // Q.M. BERLESATE No. 650 / 20.35S X 164.47E / Rainforest, 900 m / Litter // QUEENSLAND / MUSEUM

LOAN / DATE: Nov. 2003 / No. LEN-1686 (green label) // genitalia in polyethylene vial with glycerine // HOLOTYPE / Mecyclothorax / laterorectus / J.K.Liebherr 2017 (black-bordered red label).

Paratypes (21 specimens). NEW CALEDONIA: Hienghène [vicinity, code PA 63], 150 m el., 20°41'S 164°57'E, 02-ix-1970, Franz (NHMW, 4); Mandjélia, 700 m el., 20°24'S 164°32'E, 12-v-1984, rainforest, Q.M. berlesate 648, sieved litter, Monteith & Cook (QMB, 2), montane rainforest, 700-780 m el., 20°24'S 164°32'E, *Pandanus,* 20-xi-2008, Wanat (MNHW, 1), 750-780 m el., 20°24'S 164°32'E, 01-xi-2007, sieved litter, Wanat (MNHW, 5), summit, 750 m el., 20°24'S 164°32'E, hand collecting, 06-07-xi-2001, lot 8750, Burwell & /Monteith (QMB, 1), rainforest, sieved litter, 06-07-xi-2001, lot 1055, Monteith (QMB, 3), flight intercept trap, 29-xi-2003–11-i-2004, lot 11486, Monteith (QMB, 1), 780 m el., 20°24'S 164°32'E, berlesate, sieved litter, 12-xii-2004, lot 11941, Monteith (QMB, 2); Mt. Panié, rainforest, 900 m el., 20°33'S 164°45'E, Q.M. berlesate 650, litter, 16-v-1984, Monteith & Cook (QMB, 1); Roche d'Ouaïème, near Hienghène [PA 65], 500-700 m el., 20°37'S 164°52'E, 03-ix-1970, Franz (NHMW, 1).

Etymology. As in the preceding two species (Fig. 9A–C), the broad pronotal base leads to the use of latero- to modify the adjectival rectus, which denotes the right pronotal hind angles of these beetles.

Distribution and habitat. This species is distributed in the northern reaches of the Chaîne Centrale, from Mandjélia south to near Hienghène (Fig. 14). Elevations range 700–900 m for credible collecting localities where complete information was provided on the specimen label. Of the 22 specimens known, 14 were recovered from sieved litter. Other collecting situations include hand collecting (1, QMB), flight intercept trap (1, QMB), and association with *Pandanus* (Pandanaceae) screw palm (1, MNHW).

4. *Mecyclothorax fleutiauxi* (Jeannel)

Figures 1B, 1I, 2C, 2G, 3B, 9D, 10I–M, 11C, 12D, 13D, 15

Phacothorax fleutiauxi Jeannel 1944: 85.
Mecyclothorax fleutiauxi, Liebherr & Marris 2009: 10.

Diagnosis. Though markedly different from all other New Caledonian species, this and the following *M. jeanneli* (Fig. 9D–E) are indistinguishable externally. Both species are characterized by presence of only the single posterior supraorbital seta (Fig. 1B), and by the orbicular pronotum with a broadly margined base, and evenly ellipsoid elytra. The elytral striae are very shallow, though traceable to the fifth stria. That this and the following species are distinct is supported by characters of the male and female genitalia. In the males, the aedeagal median lobe has the apex elongate, variably extended beyond the apical margin of the ostium (Fig. 10I–M). The female reproductive tract in this species is characterized by presence of a short dorsal lobe of the bursa copulatrix, with the spermathecal duct joined to the lobe's apex (Fig. 12D). Standardized body length 4.2–5.0 mm. Chaetotaxy –/+//+/–//+/1–2/+–/+.

Description (n = 10). The description for *M. jeanneli* (below) serves to describe the external anatomy of this species, with the following exceptions: 18–20 ommatidia along horizontal diameter of eye; ocular ratio 1.43–1.52, ocular lobe ratio 0.89–0.94, EyL/EyD = 3.09–3.33; MPW/PL = 1.24–1.30; MEW/EL = 0.68–0.73; either one or two dorsal elytral setae associated with third interval; if one, the posterior seta is absent (in 2 of 10 specimens scored).

Male genitalia (n = 17). Antecostal margin of abdominal mediotergite IX robust distally, broadly angulate and truncate (Fig. 10J); right paramere very elongate, apical half narrowed to a whiplike extension (Fig. 11C), six setae along ventral margin well separated from apical pair of setae, dorsal surface glabrous; left paramere broad basally, distinctly narrowed to a whiplike extension; aedeagal median lobe moderately gracile, apical half evenly narrowed to extended tip that protrudes at least twice its dorsoventral dimension beyond the apex of the ostial opening (Fig. 10I–M); aedeagal internal sac bilobed, the dorsal lobe much larger than apical lobe (Fig. 10L), a small crescent-shaped structure with lightly sclerotized outer margin–interpreted as a reduced flagellar sheath–dorsad gonopore on apical lobe. Although there is variation in the amount of apical extension and apical curvature of the median lobe among males assigned to this species (Fig. 15), that variation occurs both within and between populational samples indicating that the variation is infraspecific.

Female reproductive tract (n = 5). Bursa copulatrix bilobate, an elongate ventral lobe with length more than twice circumference, and a short dorsal lobe that is about as long as broad and which bears the spermathecal duct at its apex (Fig. 12D); bursal walls moderately thick, wrinkled, semitranslucent; spermathecal duct that enters apex of bursal dorsal lobe about half the diameter of spermathecal reservoir, and about twice length of reservoir, spermathecal gland duct entering onto apex of spermathecal reservoir; well-developed ligular apophysis present on common oviduct as far distant from base of common oviduct as apex of ventral bursal lobe; basal gonocoxite 1 with apical fringe of two setae, a few microsetae near apicomedial margin of gonocoxite complementing very few medial setae (Fig. 13D); apical gonocoxite 2 falciform with an elongate laterobasal extension, basal width more than 0.75× length; two lateral ensiform setae elongate.

Type – Holotype male (MNHN): La Foa à Canala / fev. 1907 La Foa // TYPE (red label) // Phacothorax / Fleutiauxi / Jeannel (male dissected with genitalia separately mounted on card with label "Phacothorax / fleutiauxi ? Jeann."). So that the separated genitalia can remain unambiguously associated with the male holotype body, a black-bordered red holotype label has been added to that pin.

Additional taxonomic material (145 specimens; EMEC, MNHW, QMB): see Suppl. material 2.

Distribution and habitat. This species is recorded from middle latitudes of Grand Terre, from Aoupinié on the north to Ningua Reserve on the south (Fig. 15), its range a northerly parapatric disjunct to the range of its adelphotaxon, *M. jeanneli*. Species records indicate a broad altitudinal range among populations, from 485–1400 m elevation. Of 135 specimens with detailed ecological data, 127 have been collected via application of pyrethrin spray to tree trunks or downed logs, whereas none have been recovered from sieved litter. Thus this species is associated with epiphytic growth, bark, or loose bark on plants. That these beetles climb is shown by a record of one taken in an axil of a *Freycinetia* (Pandanaceae) plant (QMB).

5. *Mecyclothorax jeanneli* Liebherr, sp. n.

http://zoobank.org/834CBF6A-2041-4A93-B068-5CDE22913FB5
Figures 9E, 10N–R, 11D, 12E, 13E, 15

Diagnosis. The diagnosis for *M. fleutiauxi* serves to summarize external diagnostic characters for this species (Fig. 9D–E). Internally, the male aedeagal median lobe has a much shorter apex in beetles of this species, with the tip extended beyond the apical ostial margin only as much as the width of the median lobe at that point (Fig. 10N–R). The female reproductive tract differs in that the dorsal lobe of the bursa copulatrix is as long as the ventral or principal lobe (Fig. 12E), with the spermathecal duct again entering at its apex. Standardized body length 4.4–5.3 mm. Chaetotaxy –/+//+/–//+/1–2/+/+.

Description (n = 10). Head capsule narrowly elongate, with large, moderately convex eyes, ocular lobe meeting gena at obtuse angle, a broad shallow groove indicating juncture; 20 ommatidia along horizontal diameter of eye; ocular ratio 1.42–1.51, EyL/EyD = 2.8–3.4; frontal grooves sinuously canaliculate, deepest posterad frontoclypeal suture at a line between posterior margin of antennal fossae, briefly prolonged onto clypeus (as in Fig. 1B); mandibles elongate, mandibular ratio 1.9; ligular anterior margin angularly rounded to ligular seta, concave between setae, the two setae separated by two setal diameters (as in Fig. 1I); paraglossae thin, extended as far beyond ligular margin as half of basal length to margin; antennae moderately elongate, antennomere 9 length 2.05× maximal breadth; antennomere 3 glabrous except for apical ring of setae. Pronotum vase-shaped, lateral margins meeting base in a smooth convex curve, hind angles nonexistent (Fig. 9E); MPW/PL = 1.23–1.30; front angles protruded, obtusely rounded; basal margin bordered by broadly convex marginal bead that joins fine lateral marginal beads at very small, shallow laterobasal depressions; median longitudinal impression fine and shallow on disc, terminated anteriorly at a small depression at position of anterior transverse impression; anterior transverse impression broad, very shallow, traceable to front angles; proepisternum separated from prosternum by a broad shallow groove both anteriorly and ventrally; prosternum with shallow anteapical impression laterally, impression absent from ventral 2/3 of circumference; prosternal process broadly depressed between procoxae, that depression extended anteriorly where it broadens to a depressed anterior face extended nearly to prothoracic anterior margin. Elytra elongate, ovoid, humeri quickly sloping posterad outside humeral angles; MEW/EL = 0.70–0.75; basal groove very briefly recurved laterad scutellum, humeral angle tightly rounded; all striae broad and shallow on disc, intervening intervals only slightly convex; one to two dorsal elytral setae present in third interval, if one, the posterior seta is absent (in 3 of 10 specimens scored); shallow remnants of the sutural stria plus striae 2 and 7 traceable at apex; elytra appressed and conjoined apically, sutural intervals narrower and distinctly upraised at apex. Pterothoracic mesepisternal anterior surface smooth; mesosternal-mesepisternal suture incomplete, obsolete to absent anteriorly (as in Fig. 3B); metepisternum very foreshortened, maximum width/lateral length = 1.3; metepisternal-metepimeral suture complete. Abdomen with broad crescent-shaped depression along suture between first and second ventrite, second ventrite broadly depressed behind crescent; suture between second and third ventrites reduced though traceable laterally; ventrites 2–6 with broad, shallow, linear plaques near lateral margin. Microsculpture of frons distinct, a mix of isodiametric and transverse sculpticells; pronotal disc and base covered with elongate transverse mesh, sculpticells on disc 3–4× broad as long, those on base somewhat less broad, surface iridescent; elytra iridescent, disc covered with transverse-line microsculpture, apex with transverse lines loosely joined into a transverse mesh.

Male genitalia (n = 23). Antecostal margin of abdominal mediotergite IX robust distally, broadly angulate and obliquely truncate (Fig. 10O); right paramere very elongate, apical half narrowed to a whiplike extension (Fig. 11D), five setae along ventral margin well separated from apical pair of setae, dorsal surface glabrous; left paramere broadly quadrate basally, distinctly narrowed to a whiplike extension; aedeagal median lobe moderately gracile, apical half evenly narrowed to tip that protrudes less than its dorsoventral dimension beyond the apex of the ostial opening (Fig. 10N–R); aedeagal internal sac bilobed, the dorsal lobe subequal to the apical lobe (Fig. 10Q), a small crescent-shaped structure with lightly sclerotized outer margin–interpreted as a reduced flagellar sheath–dorsad gonopore on apical lobe. There is less variation among males with regard to extension of the median lobe apex (Fig. 15) – understandable due to the generally shorter extension–and this variation is not geographically associated. Thus the species geographic limits include all populations lying south and east of Mt. Humboldt (Fig. 15).

Female reproductive tract (n = 8). Bursa copulatrix bilobate, a broad ventral lobe complemented by narrower dorsal lobe of subequal length, dorsal lobe bearing spermathecal duct at apex (Fig. 12E); bursal walls moderately thick, wrinkled, semitranslucent; spermathecal duct that enters apex of bursal dorsal lobe slightly broader

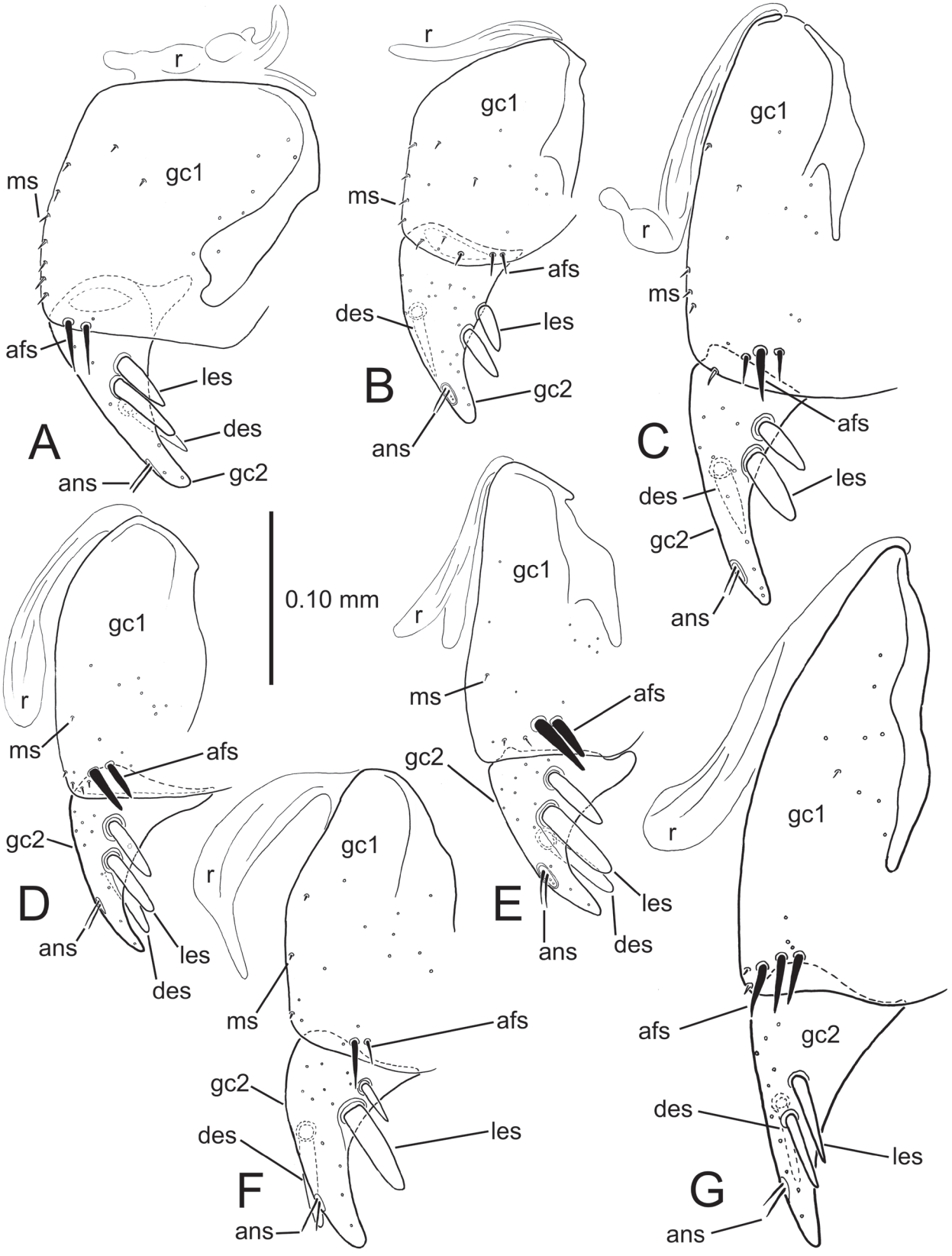

Figure 13. Left female gonocoxa, ventral view, *Mecyclothorax* (*Phacothorax*) spp.: **A**, *M. laterobustus*; **B**, *M. laterosinuatus*; **C**, *M. laterorectus*; **D**, *M. fleutiauxi*; **E**, *M. jeanneli* ; **F**, *M. plurisetosus*; **G**, *M. megalovatulus*. See Table 2 for abbreviations.

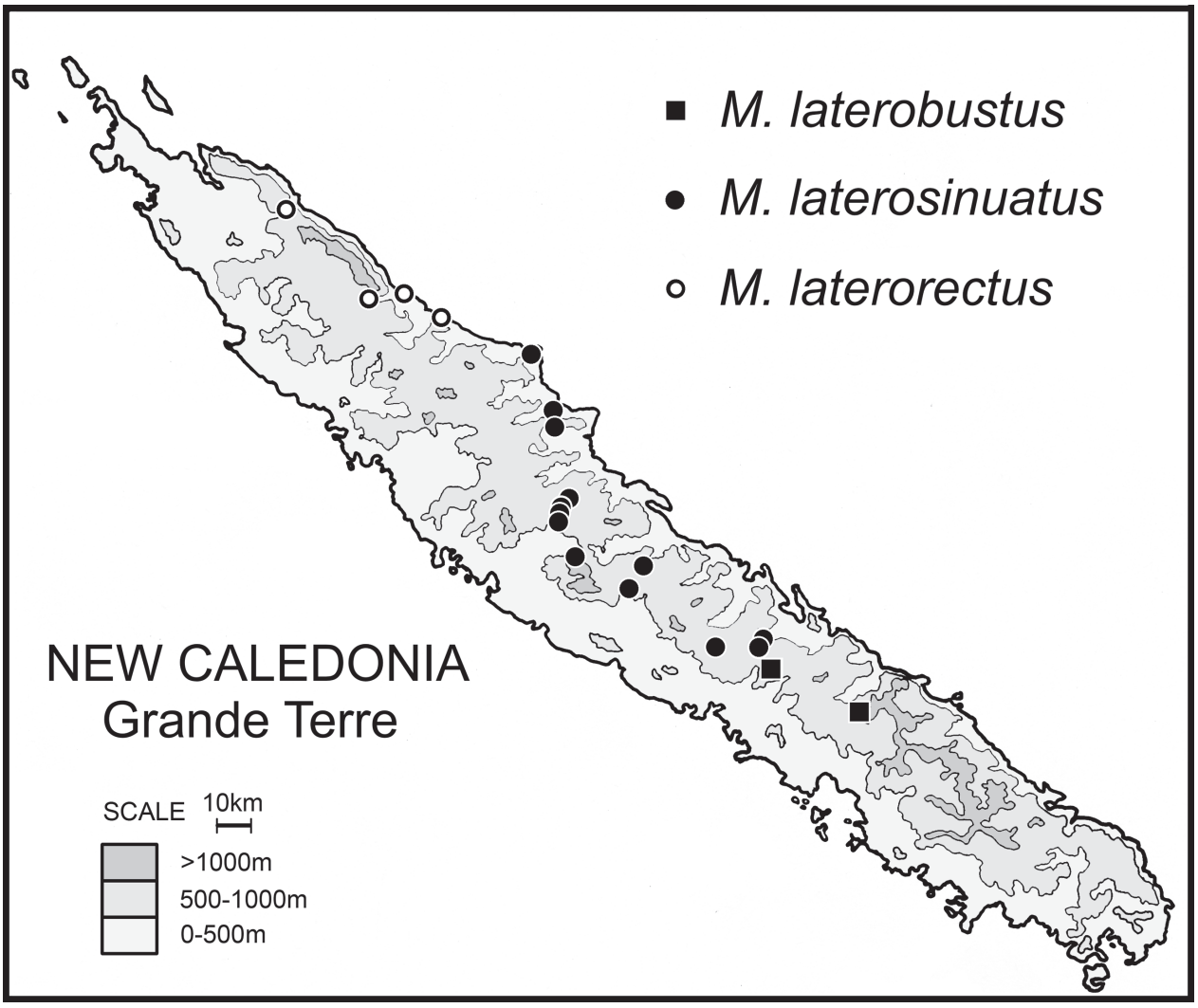

Figure 14. Geographical distributions of *Mecyclothorax* (*Phacothorax*) spp.

than spermathecal reservoir, and about twice length of reservoir, spermathecal gland duct entering onto apex of spermathecal reservoir; well-developed ligular apophysis present on common oviduct as far distant from base of common oviduct as apex of ventral bursal lobe; basal gonocoxite 1 with apical fringe of two setae, a few microsetae near apicomedial margin of gonocoxite complementing very few medial setae (Fig. 13E); apical gonocoxite 2 falciform with an elongate laterobasal extension, basal width more than 0.75× length; lateral ensiform setae elongate and broad.

Types – Holotype male (MNHN): NEW CALEDONIA.9944 / 22°11'Sx166°01'E [sic, crossed out and hand corrected to 31'E] / Mt Koghi, 750m / 29Nov2000.GB Monteith / Pyrethrum, trunks&logs // QUEENSLAND / MUSEUM LOAN / DATE: Nov. 2003 / No. LEN-1686 (green label) // HOLOTYPE / Mecyclothorax / jeanneli / J.K.Liebherr 2017 (black-bordered red label). The type locality longitude is incorrect on the label, and is corrected (Google Earth Pro 2017).

Paratypes (156 specimens; EMEC, HNHM, MNHW, NHMW, QMB): see Suppl. material 2.

Etymology. This species epithet is a patronym honoring Dr. René Jeannel, whose extensive body of literature dominates 20th Century carabidology. Dr. Jeannel's early and perspicacious appreciation of Wegenerian historical biogeography was ground breaking in Entomology (Jeannel 1942), and we have yet to test fully the biogeographic hypotheses he proposed in his many contributions. More close to home, the necessity of examining the male genitalia to determine *M. jeanneli* versus its sister species, *M. fleutiauxi*, reiterates Dr. Jeannel's pioneering research on the underlying homologies of insect genitalia (Jeannel 1955) and his extensive use of insect genitalia to diagnose species (e.g. Jeannel 1944).

Distribution and habitat. This species is distributed in the southern end of Grand Terre, from Mt. Humboldt on the north to Forêt Nord on the south (Fig. 15), allopatric to the northerly range of its adelphotaxon, *M. fleutiauxi*. These beetles are known from any even greater altitudinal range than *M. jeanneli*, with recorded elevations ranging 160–1600 m. As with *M. jeanneli*, the vast majority (150 of 156 specimens) have been collected on

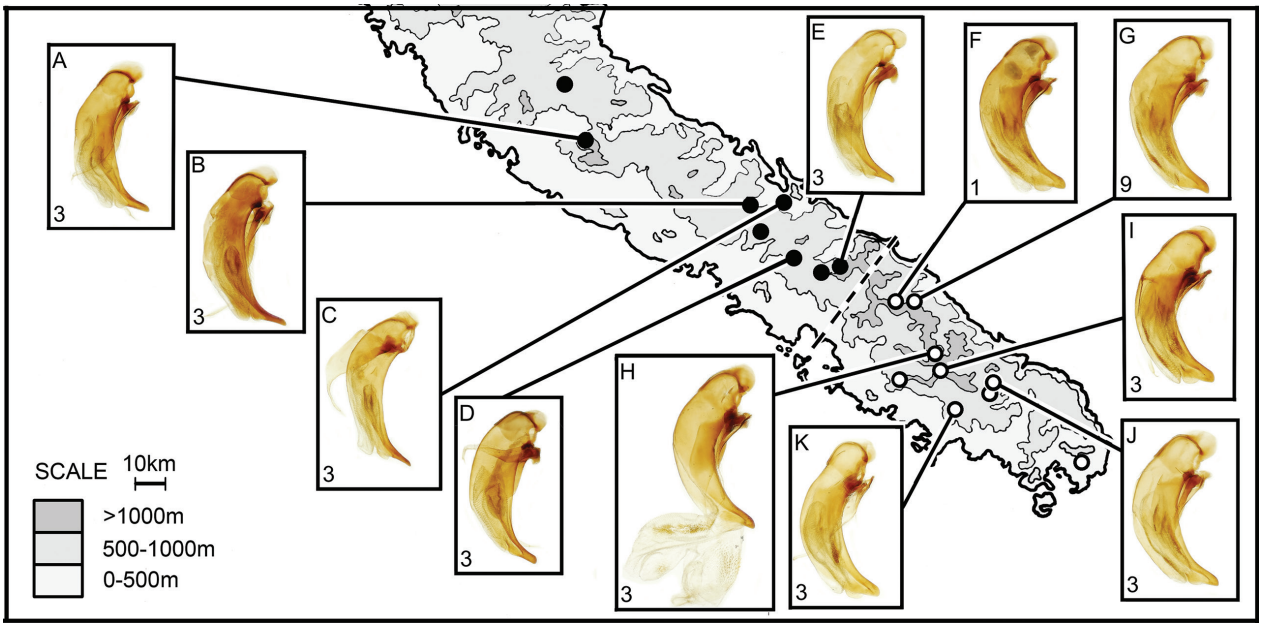

Figure 15. Recorded geographical distribution of *M. fleutiauxi* (including population samples **A–E** northwest of dashed boundary) and *M. jeanneli* (including population samples **F–K** southeast of dashed boundary): numbers of males sampled for each locality indicated in lower left of boxes. Sampled population localities for *M. fleutiauxi* include: **A**, Me Maoya; **B**, Rembai; **C**, Gelima; **D**, Mt. Do; **E**, Ningua. Sampled population localities for *M. jeanneli* include: **F**, Mt. Humboldt, 600 m; **G**, Mt. Humboldt, 1300–1600 m; **H**, Mt. Ouin; **I**, Mt. Dzumac; **J**, Rivière Bleue; **K**, Mts. Koghis.

tree trunks or downed logs, most via application of pyrethrin spray. A series of 31specimens was taken during one collecting event through spray application onto a moss-covered trunk (QMB). Thus, like *M. jeanneli*, this species is associated with emergent plant substrates, not the ground-level litter microhabitat.

6. *Mecyclothorax plurisetosus* Liebherr, sp. n.

http://zoobank.org/CE1562F9-33FE-440C-AE08-E6B1DFF160B0
Figures 12F, 13F, 16A, 17A–B, 18A, 19

Diagnosis. These beetles (Fig. 16A) share an orbicular pronotum and smooth ovoid elytra with the previous two species, *M. fleutiauxi* and *M. jeanneli* (Fig. 9D–E). This similarity in body form is indicative of phylogenetic relationship, as *M. plurisetosus* comprises the adelphotaxon to those species two (Fig. 7). However this species can be diagnosed from all others by the presence of extra setae on the pronotum. In addition to the large setae homologized with the lateral pronotal setae, there are 9–11 smaller setae in the marginal depression anterad the lateral seta, and 4–5 setae in the depression behind the lateral seta. The prosternum also bears a sparse pelage of elongate setae, with the anterior surfaces of the femora also so covered. The elytral striae are totally reduced in this species, and the cuticular microsculpture also totally absent from head capsule, pronotum, elytra, and ventrites. Standardized body length 4.7–5.1 mm. Chaetotaxy +/+//2+11/–5//+/2/+/+, signifying that the lateral pronotal seta has been doubled, with up to 11 microsetae lining the lateral marginal depression anterad those setae. Also, though the basal pronotal seta is absent, up to 5 microsetae lie along the lateral margin near the pronotal base. The two lateral pronotal setae are longer and stouter than the anterior 11 and posterior 5 microsetae, supporting homology of the double setae with the single lateral pronotal seta of the other species, and the autapomorphic status of the numerous and variable microsetae.

Description (n = 3). Head capsule trapezoidal, neck broad, with small, moderately convex eyes, ocular lobe meeting gena at obtuse angle very close to eye posterior margin; 18–19 ommatidia along horizontal diameter of eye; ocular ratio 1.28–1.42, ocular lobe ratio 0.88–0.91, EyL/EyD = 2.9–3.1; frontal grooves very deep, arcuately convergent at midlength, extended deeply onto clypeus; mandibles moderately elongate, mandibular ratio 1.8; ligular lateroanterior margin rounded to ligular seta, the two setae separated by one to two setal diameters; paraglossae thin, extended as far beyond ligular margin as half of basal length to margin; antennae very elongate, antennomere 9 length 3.4× maximal breadth; antennomere 3 with sparse fine setae near apex in addition to apical ring of longer setae. Pronotum transversely ovoid, median base depressed relative to disc, lateral margins evenly curved to meet narrow median peduncular collar, pronotal lateral margin obtusely concave at the juncture (Fig. 16A); MPW/BPW = 3.6–3.9, MPW/PL = 1.23–1.25; front angles protruded, obtusely rounded, the apex broad to match broad base of head, APW/BPW = 2.1–2.3; basal margin bordered by broadly convex marginal bead that joins lateral marginal bead at sinuate margin, three deep pits anterad median marginal bead; median longitudinal impression very finely incised on disc, terminated ante-

riorly at position of anterior transverse impression; anterior transverse impression very broad, very shallow, indistinctly traceable to front angles; proepisternum separated from prosternum by a narrow, shallow groove both anteriorly and ventrally; prosternum without anteapical impression, though anterior margin is irregularly punctate; prosternal process narrowly depressed between procoxae, that depression not extended anteriorly, but venter of prosternum is flattened toward front of prothorax (as in *M. fleutiauxi* and *M. jeanneli*). Elytra ovate, broadest in basal half and narrowed apically; MEW/EL = 0.81–0.85; basal groove very briefly extended laterad scutellum, the only indication of humeral angle being the basal groove's juncture with the broader lateral marginal depression; striae 1–7 absent, only striae 8 and 9 (i.e. the inner portion of the elytral lateral marginal depression) present; only an obsolete vestige of the sutural stria evident at apex; elytra appressed and conjoined at apex where the sutural margin is narrowly and distinctly upraised. Pterothoracic mesepisternal anterior surface smooth except for a broad deep pit ventrally near prosternum; mesosternal-mesepisternal suture incomplete, obsolete to absent anteriorly (as in Fig. 3B); metepisternum foreshortened, maximum width/lateral length = 1.0; metepisternal-metepimeral suture incomplete, obsolete laterally. Abdomen with only a shallow crescent-shaped depression along suture between first and second ventrite, second ventrite little depressed posterad crescent; suture between second and third ventrites reduced though traceable laterally; ventrites 2–6 with broad, shallow, linear plaques near lateral margin. Microsculpture of frons reduced, surface glossy; pronotal disc and base with shallow transverse mesh, sculpticell breadth 3–4× length; elytra glossy, only patchy indications of transverse microsculpture visible.

Male genitalia (n = 1). Antecostal margin of abdominal mediotergite IX angulate, an elongate "butterfly-net handle" extension distally (Fig. 17B); right paramere elongate, slightly convex dorsally near base, narrowly extended to apex (Fig. 18A), dorsal and ventral surfaces glabrous, two apical setae present; left paramere narrow basally, evenly constricted to a narrow, porrect apex, also glabrous except for two apical setae; aedeagal median love gracile, parallel-sided at midlength, the apex expanded dorsally to an acuminate point, and ventrally as a rounded projection (Fig. 17A); median lobe internal sac with evident crescent-shaped structure (Fig. 17A) homologous with flagellar sheath of above two species; folds of internal sac visible in the single uneverted type specimen interpreted as a bilobed sac as per the previous two species.

Female reproductive tract (n = 1). Bursa copulatrix unilobate, elongate, length about 3× circumference, walls thin, slightly wrinkled (Fig. 12F); the only evidence of spermathecal configuration is a lightly sclerotized helminthoid sclerite near apex of bursa, spermatheca lost in single dissected female; basal gonocoxite 1 with apical fringe of 2 setae, lateral seta smaller, a few medial setae scattered along median margin (Fig. 13F); apical gonocoxite 2 moderately broad basally, breadth less than half of length; two lateral ensiform setae, apical seta much longer and broader than basal seta.

Types – Holotype male (MNHN): NEW CALEDONIA 8716 / 21°11'Sx165°18'E.850m / Aoupinie, top camp, / 2-3Nov2001.C.Burwell& / GMonteith.pyr.trees,logs // QUEENSLAND / MUSEUM LOAN / DATE: Nov. 2003 / No. LEN-1686 (green label) // *New Caledonia Mecyclothorax* revision / measured specimen 3 / J.K. Liebherr 2016 // HOLOTYPE / Mecyclothorax / plurisetosus / J.K.Liebherr 2017 (black-bordered red label).

Paratypes (2 specimens): same locality and labeling as holotype (QMB, 1); Aoupinié summit, 1000 m el. [984 m; Google Earth Pro 2017], 21°11'S 165°16'E, pyrethrum trees & logs, 02-x-2004, lot 11665, Monteith (QMB, 1).

Etymology. The presence of accessory setae on the pronotal lateral margins (Fig. 16A), prosternum, legs, and ventral body surface supports application of the compound adjectival epithet plurisetosus.

Distribution and habitat. This species is known only from the upper elevations of Mt. Aoupinié (Fig. 19), either from the vicinity of the summit transmitting station, or along the approach road at 850 m elevation. The four specimens were all collected via the application of pyrethrin spray to standing trees or downed logs. As this species is the adelphotaxon to *M. fleutiauxi* + *M. jeanneli*, finding it in this arboreal microhabitat supports the phylogenetic retention of preferred microhabitat among this triplet of species.

7. *Mecyclothorax megalovatulus* Liebherr, sp. n.

http://zoobank.org/75E12733-B4D0-463E-957C-368853BD124C
Figures 12G, 13G, 16B, 17C–D, 18B, 19

Diagnosis. This and the following species, *M. octavius*, can be diagnosed by their large body size; in this species standardized body length = 5.4–5.8 mm. Individuals of this species have the elytral striae well developed, with striae 1–8 deep and continuous throughout their length (Fig. 16B) in contrast to the obsolete striae and smooth elytra of *M. octavius* (Fig. 16 C). The elytra are narrowly ellipsoid with very narrow humeri. The pronotal hind angles are obtuse but rounded at the apex of the angle, and the pronotal base is unmargined. Chaetotaxy +/+//+/–//+/2/+/+.

Description (n = 4). Head capsule trapezoidal, neck broad, eyes broad and little convex, ocular lobe meeting gena at very obtuse angle well behind eye posterior margin; 20 ommatidia along horizontal diameter of eye; ocular ratio 1.37–1.44, ocular lobe ratio 0.74–0.82, EyL/EyD = 2.81–2.86; frontal grooves narrow, well incised, sinuously convergent to just posterad clypeus, extended briefly onto clypeus; mandibles moderately elongate, mandibular ratio 1.83; ligular margin rounded to ligular seta, concave between the two setae, setae separated by one to two setal diameters; paraglossae thin, extended as far beyond ligular margin as half of basal length to margin;

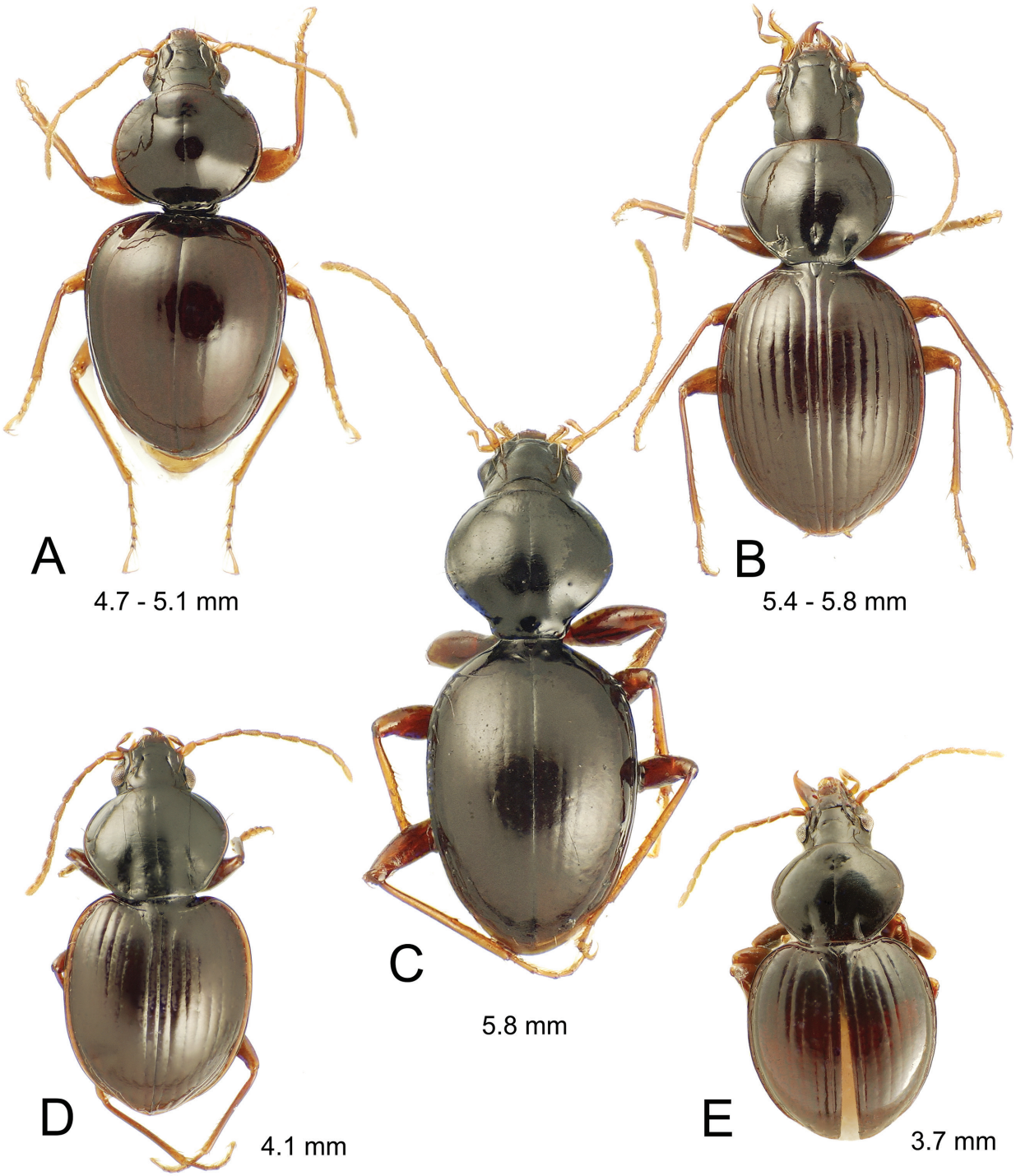

Figure 16. New Caledonian *Mecyclothorax* (*Phacothorax*) spp., dorsal view: **A**, *M. plurisetosus*; **B**, *M. megalovatulus*; **C**, *M. octavius*; **D**, *M. laterovatulus*; **E**, *M. najtae*.

antennae elongate, antennomere 9 length 2.9× maximal breadth; antennomere 3 glabrous except for apical ring of setae. Pronotum vase-shaped, narrow basally, lateral margins only slight concave anterad rounded hind angles, median base convex, not depressed relative to disc, without marginal bead (Fig. 16B); MPW/BPW = 2.56–2.83, MPW/PL = 1.21–1.28; front angles protruded, obtuse, pronotal apex distinctly broader than base, APW/BPW = 1.65–1.74; median longitudinal impression shallowly and very finely incised on disc, intermittently extended in front of evident anterior transverse impression, terminated posteriorly in deep ellipsoid pit situated medially between the anterior margins of laterobasal depressions; anterior transverse impression broad and shallow but easily traceable to front angles; laterobasal depressions flat, triangular, defined medially by a longitudinal crease laterad median base and

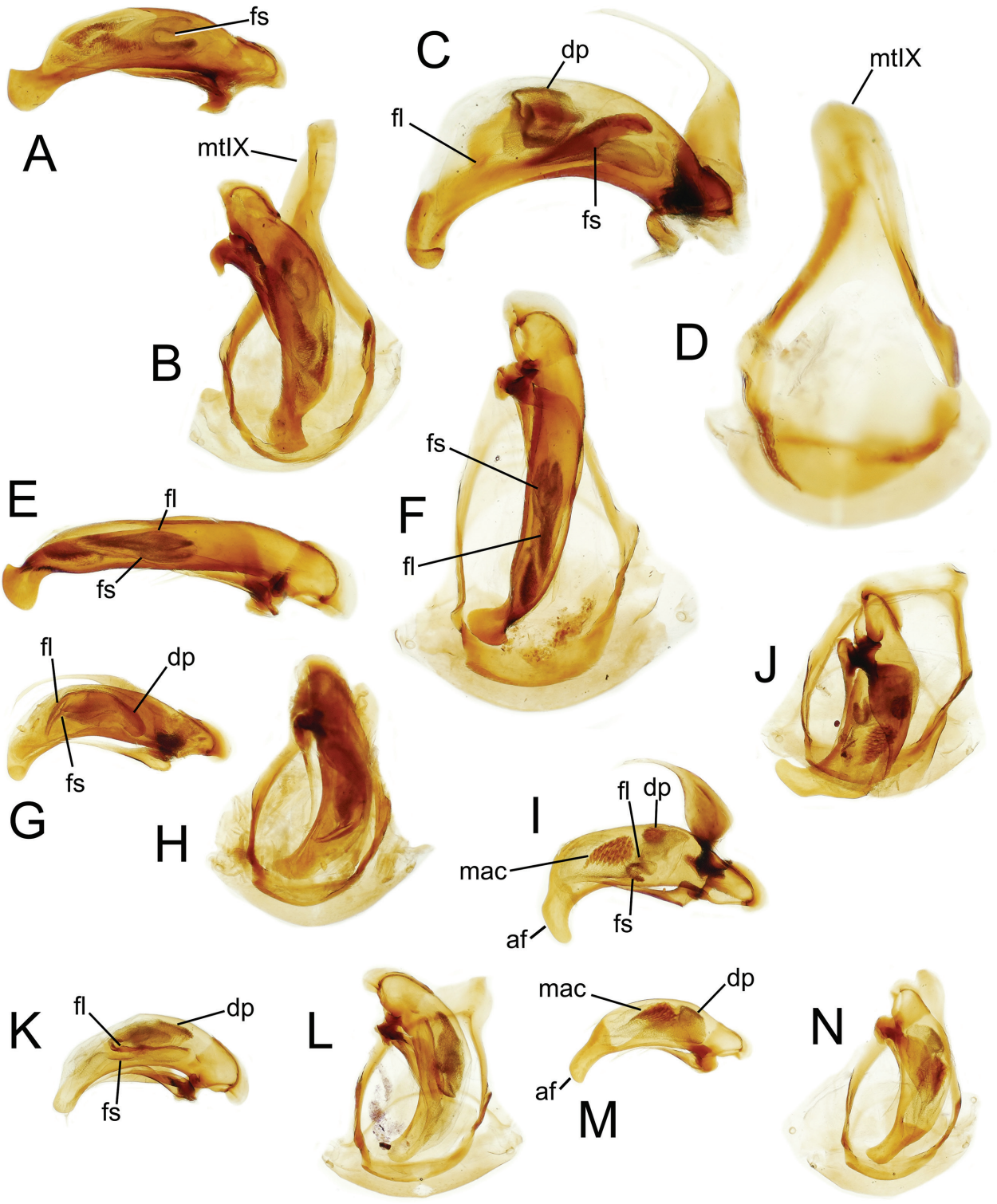

Figure 17. Male aedeagal median lobe and parameres, and ring sclerite–mediotergite plus antecostal margin, tergite IX–of *Mecyclothorax* (*Phacothorax*) spp.: **A–B**, *M. plurisetosus*, right view, dorsal view in situ (Aoupinié); **C–D**, *M. megalovatulus*, right view, dorsal view of righ sclerite (Mt. Panié); **E–F**, *M. octavius*, right view, dorsal view in situ (Me Maoya); **G–H**, *M. laterovatulus*, right view, dorsal view in situ (Aoupinié); **I–J**, *M. manautei*, right view, dorsal view in situ (Mt. Humboldt, 1400 m); **K–L**, *M. paniensis*, right view, dorsal view in situ (Mt. Panié); **M–N**, *M. mouensis*, right view, dorsal view in situ (Mt. Mou). See Table 2 for abbreviations.

anteriorly by a transverse crease bordering pronotal disc; proepisternum separated from prosternum by a shallow groove both anteriorly and ventrally; prosternum with well-defined anteapical impression laterally, the impression shallower though complete ventrally; prosternal process shallowly and broadly depressed between procoxae,

prosternum medially flattened anterad procoxae with an ovoid pitlike depression medially about 1/3 distance to anterior prosternal margin. Elytra ellipsoid, broadest about midlength, humeri distinctly sloping posterad humeral angle; MEW/EL = 0.74–0.81; basal groove briefly extended laterad scutellum, four-punctate at bases of abbreviated parascutellar striole, sutural and striae 3 and 4; intervals 3 and 8 more convex than the others at elytral apex, though all intervals are at least moderately convex; elytra appressed and conjoined at apex , sutural intervals slightly narrowed there. Pterothoracic mesepisternal anterior surface smooth except for a vertical furrow ventrally near prosternum; mesosternal-mesepisternal suture incomplete, obsolete to absent near anterior margin of mesothorax (as in Fig. 3B); metepisternum very short, maximum width/lateral length = 1.73, metepisternal-metepimeral suture incomplete, obsolete laterally. Abdomen with distinct, well-defined crescent-shaped depression along suture between first and second ventrite, second ventrite little depressed posterad crescent; suture between second and third ventrites reduced though traceable laterally; ventrites 2–6 with broad, shallow, linear plaques near lateral margin. Microsculpture of frons and vertex a well-defined, transversely-stretched isodiametric mesh; pronotal disc and base with shallow transverse mesh, sculpticell breadth 3–4× length, surface glossy, sculpticells arranged as a distinct transverse mesh in laterobasal depressions; elytral disc with shallow transverse lines, the surface glossy, subiridescent, the apex covered with indistinct transverse lines.

Male genitalia (n = 1). Antecostal margin of abdominal mediotergite IX angulate, broad and little distended (Fig. 17D); right paramere with broad base, apex elongate, narrowly extended and membranous, with two very short apical setae (Fig. 18B); left paramere broad basally, evenly narrowed in basal half to an elongate whiplike extension, two elongate setae apically; aedeagal median lobe robust, broad dorsoventrally, distinctly curved both dorsally and ventrally to a subparallel, extended apex, the tip of apex laterally curved into an apical hooklike crease (Fig. 17C); aedeagal internal sac with flagellum, flagellar sheath, and dorsal plate (Fig. 17C).

Female reproductive tract (n = 1). Bursa copulatrix elongate, length more than twice basal circumference, apical portion expanded laterally toward right, surface thick apically, wrinkled, densely stained relative to bursal base (Fig. 12G); spermathecal duct entering near bursa-common oviduct juncture with duct oriented toward right side of bursa, duct as long as spermathecal reservoir; a heavily sclerotized, triangular helminthoid sclerite present near base of spermathecal duct; spermatheca fusiform on narrow duct, spermathecal gland duct entering at base of spermathecal reservoir; ligular apophysis present near base of common oviduct; basal gonocoxite 1 with apical fringe of three setae situated near apicomedial angle, medial surface of gonocoxite 1 glabrous (Fig. 13G); gonocoxite 2 narrow basally, basal width about 2/3 medial length; two very gracile lateral ensiform setae present.

Types – Holotype male (MNHN): NEW CALEDONIA 8764 / 20°34'Sx164°46'E / Mt Panie refuge, 1300 m / 8-9Nov.2001.C.Burwell / Pyrethrum, trees & logs // QUEENSLAND / MUSEUM LOAN / DATE: Sept 2002 No. LE 02.43 (green label) // *New Caledonia Mecyclothorax* revision / measured specimen 3 / J.K. Liebherr 2016 ♂1 // genitalia in polyethylene vial with glycerine // HOLOTYPE / Mecyclothorax / megalovatulus / J.K.Liebherr 2017 (black-bordered red label).

Paratypes (3 specimens). NEW CALEDONIA: Mt. Panié, 1300-1600 m el., 20°35'S 164°46'E, 15-v-1984, Monteith & Cook (QMB, 1), refuge, 1300 m el., summit, 1600 m el., 20°34'S 164°46'E, rainforest, sieved litter, 9-xi-2001 lot 8769, Burwell (QMB, 1), track, 1500 m el., 20°34'S 164°46'E, pyrethrum trees & logs, 09-xi-2001, lot 8768, Burwell (QMB, 1).

Etymology. Large body size and ovoid pronotum and elytra (Fig. 16B) suggested the compound adjectival epithet megalovatulus.

Distribution and habitat. This species is only known from 1300–1600 m elevation on Mt. Panié, in the northern portion of the Chaîne Centrale (Fig. 19). Three of the six specimens have been recovered from sieved litter, whereas one was collected via pyrethrin spray application to trees and logs, supporting occupation of ground-level litter as well as plant-based, mossy microhabitats.

8. *Mecyclothorax octavius* Liebherr, sp. n.

http://zoobank.org/003616EF-AF92-4481-864C-A91512EC417E
Figures 16C, 17E–F, 18C, 19

Diagnosis. This species (Fig. 16C) exhibits superficial similarity to *M. fleutiauxi* and *M. jeanneli* (Fig. 9D–E), but differs in: 1, larger body size, standardized body length 5.8 mm; 2, presence of both anterior and posterior supraorbital setae; 3, an unmargined and depressed pronotal median base with sinuate lateral margins anterad the obtusely rounded hind angles; and 4, eyes of very small diameter, i.e. ocular lobe ratio = 0.71 versus ratios of 0.89–0.94 for individuals of the former two species. The male aedeagus is completely different, exhibiting a flagellum and flagellar sheath, and a dorsoventrally expanded apex (Fig. 17E). Chaetotaxy +/+//+/–//+/2/+/+.

Description (n = 1). Head capsule elongate, distinctly broader at the small, moderately convex eyes, ocular lobe gradually curving to meet gena well behind eye posterior margin; 20 ommatidia along horizontal diameter of eye; ocular ratio 1.45, ocular lobe ratio 0.71, EyL/EyD = 2.4; frontal grooves deep, sinuously convergent to just posterad clypeus, extended deeply onto clypeus; mandibles moderately elongate, mandibular ratio 1.8; ligular lateroanterior margin rounded to ligular seta, the two setae separated by one to two setal diameters; paraglossae thin, extended twice as far beyond ligular margin as their basal length to margin, apex observably spiculate (100×); antennae elongate, antennomere 9 length 2.3× maximal breadth; antennomere 3 with glabrous except for apical

ring of setae. Pronotum transverse, vase-shaped, median base depressed relative to broadly convex disc, lateral margins evenly curved until joined to long median peduncular collar, pronotal lateral margin obtusely concave at the juncture (Fig. 16C); MPW/BPW = 2.4, MPW/PL = 1.1; front angles narrowly protruded, obtuse, pronotal apex constricted, APW/BPW = 1.35; median base trapezoidally depressed relative to convex disc, 8–10 small punctures present each side, lateral marginal bead continued along anterior half of basal peduncle, terminated at base of peduncle, median base unmargined posteriorly; median longitudinal impression very finely incised on disc, extended briefly anterad broad and shallow anterior transverse impression; anterior transverse impression very broad, very shallow, indistinctly traceable to front angles; proepisternum separated from prosternum by a deep, sinuous groove both anteriorly and ventrally; prosternum with anteapical impression that is continuous ventrally; prosternal process narrowly and deeply depressed between procoxae, depression extended anteriorly half the distance to prothoracic anterior margin, the depression broadest at anterior terminus. Elytra ellipsoid, broadest just anterad midlength; MEW/EL = 0.72; basal groove absent from very narrowly pedunculate elytral base, the very narrow lateral marginal depressions converging on posterior margin of pronotum; striae 1–7 very shallow though traceable , stria 8 deep, diverging from stria 9 just posterad anterior series of lateral elytral setae; all striae except 8 absent from elytral apex; apical elytral setae positioned only slightly nearer to suture than subapical seta; elytra appressed and conjoined at apex, the upraised sutural margin forming an elongate isosceles triangle connected to the narrowly beaded elytral apical margin. Pterothoracic mesepisternal anterior surface with eight broad punctures, the largest anterior puncture separated from the remainder by a vertical ridge; mesosternal-mesepisternal suture incomplete, obsolete to absent anteriorly (as in Fig. 3B); metepisternum very short, maximum width/lateral length = 1.46 (difficult to measure due to fusion of metepisternum and metepimeron). Abdomen with first and second ventrites fused laterally, not suture visible; suture between second and third ventrites reduced though traceable laterally; ventrites 2–6 with broad, shallow, linear plaques near lateral margin. Microsculpture of frons reduced, an indistinct transverse mesh on a glossy surface, microsculpture on vertex an evident transverse mesh with some isodiametric sculpticells; pronotal disc and base with fine, elongate transverse mesh, sculpticell breadth 3–4× length, surface iridescent; elytra with evident transverse mesh, sculpticell breadth 2–3×length; elytral apex with elongate transverse mesh, sculpticell breadth 3–4× length where traceable.

Male genitalia (n = 1). Antecostal margin of abdominal mediotergite IX angulate, not extended (Fig. 17F); right paramere elongate, slightly expanded dorsally in basal half, narrowly extended apically (Fig. 18C), with 13 setae along the apical 2/3 of the ventral margin, those setae complementing two elongate apical setae; left paramere moderately broad basally, evenly narrowed to a moderately extended, narrow apex, two small setae present apically; aedeagal median lobe gracile, tubular, straight at midlength, with apex broadly expanded dorsoventrally, dorsally to am obtuse point, ventrally in a tightly rounded and projected margin; aedeagal median lobe internal sac with flagellum and flagellar sheath, apparently unilobate based on interpretation of uneverted unique type male (Fig. 17E), a diffuse spicular patch apicad flagellar apparatus, no structure present at position of dorsal plate.

Type –Holotype male (MNHN): NEW CALEDONIA / Me Maoya, summit / plateau.12Nov2002. / Monteith & Burwell // QM Berlesate 1080 / 21°22'Sx165°20'E / rainforest, 1400 m/ / sieved litter // QUEENSLAND / MUSEUM LOAN / DATE: Nov. 2003 / No. LEN-1686 (green label) // *New Caledonia Mecyclothorax* revision / measured specimen 1 / J.K. Liebherr 2016 ♂1 // genitalia in polyethylene vial with glycerine // HOLOTYPE / Mecyclothorax / megalovatulus / J.K.Liebherr 2017 (black-bordered red label) .

Etymology. Given that the body form comprises a pair of ovoids (Fig. 16C) suggesting the numeral eight, this species is given the epithet octavius. As a Latin personal name, denoting the eighth-born son, or a son born in the eighth month, the species name is to be treated as a noun.

Distribution and habitat. The single specimen of this species was collected from sieved litter collected at the 1400 m summit of Mt. Maoya (Fig. 19). This species is adelphotaxon to the species triplet *M. plurisetosus* (*M. fleutiauxi* + *M. jeanneli*), all of whom are most commonly found in arboreal microhabitats, supporting transformation of habitat preference to the arboreal realm in their common ancestor.

9. *Mecyclothorax laterovatulus* Liebherr, sp. n.

http://zoobank.org/A6065519-5F9F-4AE9-8BD3-F5A0A46CF137
Figures 16D, 17G–H, 18D, 19

Diagnosis. This and the following species *M. najtae* (Fig. 16D–E) are characterized by very obtuse pronotal hind angles that are rounded apically, pronotal lateral margins straight to only indistinctly concave before the very obtuse angles. The elytra are broader basally in beetles of this species, with the humeri extended anterad and the basal groove narrowly rounded near the base of stria 6, and elytral length is relatively longer than in *M. najtae*, with MEW/EL = 0.85. The outer elytral striae 5–7 are well impressed at midlength in this species, versus obsolete to entire absent laterally in *M. najtae*. The configuration of the male aedeagal internal sac–with elongate, curved flagellum and flagellar sheath and a dorsal plate (Fig. 17G) – indicates this species' true relatives (Fig. 7); *M. laterorectus* (Fig. 10F) and *M. laterosinuatus* (Fig. 10C–D). Chaetotaxy +/+//+/–//+/2/+/+.

Standardized body length 4.1 mm.

Description (n = 1). Head capsule broad, foreshortened, eyes small, moderately convex, ocular lobe meeting

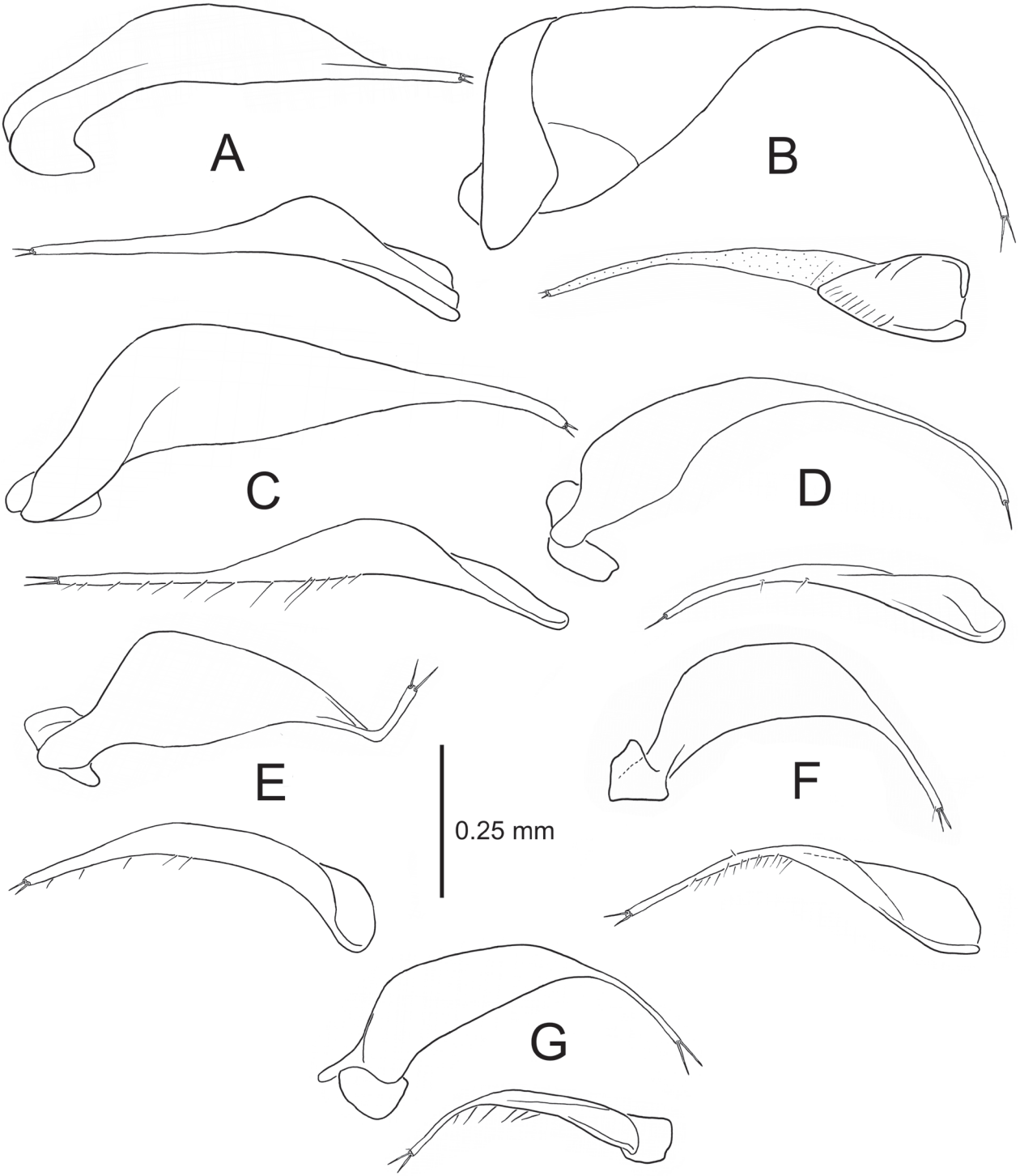

Figure 18. Paired left (above) and right (below) parameres of *Mecyclothorax* (*Phacothorax*) spp. (ectal view): **A**, *M. plurisetosus*; **B**, *M. megalovatulus*; **C**, *M. octavius*; **D**, *M. laterovatulus*; **E**, *M. manautei*; **F**, *M. paniensis*; **G**, *M. mouensis*.

gena at very obtuse angle; 15–16 ommatidia along horizontal diameter of eye; ocular ratio 1.39, ocular lobe ratio 0.89, EyL/EyD = 3.13; frontal grooves nearly straight from posterior terminus inside anterior supraorbital seta to deepest point just posterad clypeus, briefly and shallowly extended onto clypeus; mandibles moderately elongate, mandibular ratio 1.8; ligular anterior margin narrowly rounded to ligular seta, concave between setae, the two setae separated by one to two setal diameters; paraglossae thin, extended as far beyond ligular margin as their basal length to margin; antennae elongate, antennomere 9 length 2.5× maximal breadth; antennomere 3 glabrous except for apical ring of setae. Pronotum vase-shaped, hind angles broadly subangulate, lateral margins only slightly concave anterad angles (Fig. 16D); MPW/

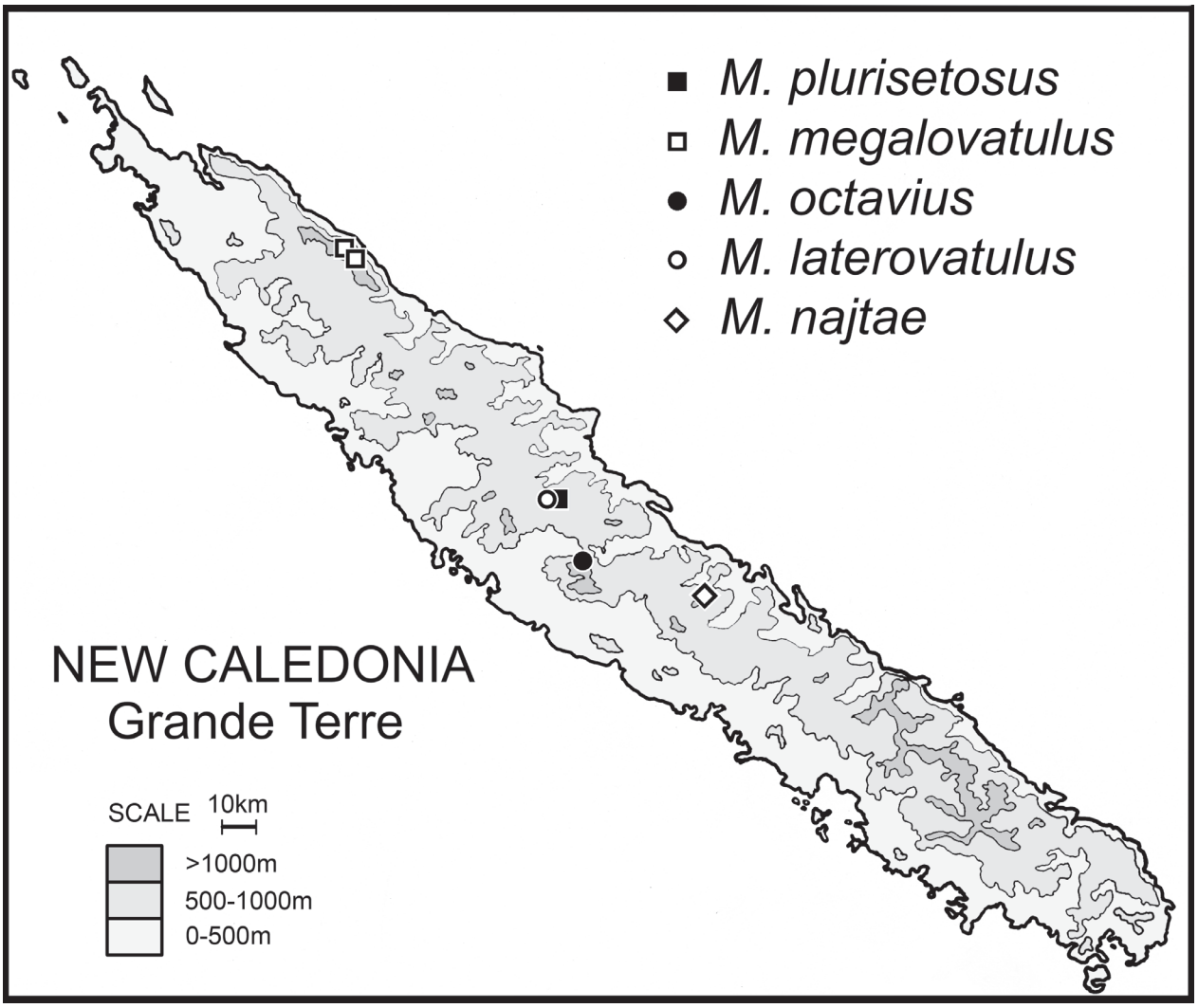

Figure 19. Geographical distributions of *Mecyclothorax* (*Phacothorax*) spp.

BPW = 1.66, MPW/PL = 1.24; front angles only slightly protruded, broadly obtuse, APW/BPW = 0.93; median base coplanar relative to disc, unmargined; laterobasal depression with longitudinal tubercle inside hind angle, defined medially by longitudinal border with median base; median longitudinal impression fine and shallow on disc, posteriorly terminated at deep lenticular pit anterad median base, terminated anteriorly at very broad and shallow anterior transverse impression; proepisternum separated anteriorly from prosternum by fine shallow groove, distinctly separated ventrally by smooth, deep groove; prosternal process deeply, narrowly depressed between procoxae, that depression extended 1/4 distance toward anterior prothoracic margin. Elytra broadly ellipsoid to hemiovoid, humeri extended laterally, humeral angle rounded outside pronotal hind angles; MEW/EL = 0.85; basal groove extended anterad from scutellum to humerus, with depressions at bases of sutural and elytral striae 4–5; sutural stria deep throughout length, striae 2 and 5–7 almost as well developed, striae 3–4 shallower though still evident; striae 1–2 and 7 evident apically, elytra appressed and conjoined apically, sutural intervals narrower and upraised at apex. Pterothoracic mesepisternal anterior furrow with five pitlike depressions in one vertical row; metepisternum maximum width/lateral length = 0.88; mesosternal-mesepisternal suture complete (as in Fig. 3A); metepisternal-metepimeral suture incomplete, shallower and incomplete laterally. Abdomen with deep crescent-shaped depression along suture between first and second ventrite, second ventrite depressed within crescent; suture between second and third ventrites reduced, incomplete laterally; ventrites 2–6 with broad, shallow, linear plaques near lateral margin. Microsculpture of frons and vertex an evident transversely stretched isodiametric mesh; pronotal disc and base covered with elongate transverse mesh, sculpticell breadth 3–4× length, surface iridescent, sculpticells in laterobasal depressions less transverse, breadth 2–3× length; elytra iridescent, disc with dense transverse lines loosely connected into a mesh, apex covered with transverse lines. Femora rufobrunneous, a piceous cloud in basal 2/3.

Male genitalia (n = 1). Antecostal margin of abdominal mediotergite IX angulate, not extended (Fig. 17H); right paramere narrow, narrowly extended apically (Fig.

18D), with two setae on the ventral margin complementing a single apical seta; left paramere narrow basally, extended as an elongate, whiplike extension with a single apical seta; aedeagal median lobe robust, broad dorsoventrally, apex evenly narrowed dorsally and ventrally to a narrowed rounded tip (Fig. 17G); aedeagal median lobe internal sac with dorsal plate, dorsally curved flagellum and flagellar sheath.

Type – Holotype male (MNHN): NEW CALEDONIA 11665 / 21°11'S 165°16'E. / Aoupinie, summit. 1000 m / 2Oct2004. G.Monteith / pyrethrum, trees&logs // QUEENSLAND / MUSEUM LOAN / DATE: July 2005 / No. LE 05.24 // *New Caledonia Mecyclothorax* revision / measured specimen 1 / J.K. Liebherr 2016 ♂1 // genitalia in polyethylene vial with glycerine // HOLOTYPE / Mecyclothorax / laterovatulus / J.K.Liebherr 2017 (black-bordered red label) /

Etymology. Though this species is separated in the dichotomous key and therefore in the species treatment sequence from its broad-bodied phylogenetic relatives (Fig. 9A-C), this species is given the compound adjectival epithet laterovatulus to signify the broad body and ovoid pronotum coupled with rounded pronotal hind angles (Fig. 16D), thereby making the species name reiterate the names of those other species; *M. laterobustus*, *M. laterorectus*, and *M. laterosinuatus*.

Distribution and habitat. The lone holotype of this species was collected on Aoupinié summit at 1000 m elevation via application of pyrethrin spray to trees and logs (Fig. 19). Based on restriction of its adelphotaxon, *M. laterorectus* + *M. laterosinuatus*, as well as the closely related *M. laterorobustus* (Fig. 7) to ground-level microhabitats, it is predicted that additional specimens of this species will be collected predominantly in ground level litter, or from mossy subcortical microhabitats.

10. *Mecyclothorax najtae* Deuve

Figures 16E, 19

Mecyclothorax najtae Deuve 1987: 144.

Diagnosis. This, the second of the small-bodied species with very obtuse pronotal hind angles and basally straight lateral pronotal margins (Fig. 16D–E) can be diagnosed by the unique elytral configuration with elytral length only slightly greater than breadth: MEW/EL = 0.96. This species is also characterized by extremely convex eyes, with the eye convexity ratio, EyL/EyD = 2.0. Standardized body length 3.7 mm. Chaetotaxy +/+//+/–//+/2/+/+.

Description (n = 1). As a complement to Deuve's (1987) description, we may add: 14 ommatidia along horizontal diameter of eye; ligular apex rounded, the two ligular setae separated by two setal diameters; paraglossae thin, extended beyond ligular margin 1/2 distance from their base to ligular margin; antennae moderately elongate, antennomere 9 length 2.25× maximal breadth. Pronotum transverse, hind angles very obtuse, the lateral margins only slightly concave anterad angles (Fig. 16E); MPW/BPW = 2.0, MPW/PL = 1.32; front angles only slightly protruded, broadly obtuse, pronotal apex and base subequal, APW/BPW = 1.05; proepisternum separated anteriorly from prosternum by fine shallow groove, distinctly separated ventrally by deep, indistinctly punctate groove; prosternal process deeply depressed between procoxae, that depression extended 1/2 distance toward anterior prothoracic margin. Abdomen with deep crescent-shaped depression along suture between first and second ventrite, second ventrite depressed within crescent; suture between second and third ventrites reduced, incomplete laterally; ventrites 2–6 with broad, shallow, linear plaques near lateral margin. Microsculpture of frons and vertex a shallow transversely stretched isodiametric mesh; pronotal disc covered with elongate transverse mesh, sculpticell breadth 2–3× length, surface subiridescent, sculpticells on median base and in laterobasal depressions less transverse, breadth 2× length; elytra iridescent, disc with dense transverse lines loosely connected into a mesh, apex covered with transverse lines.

Type – Holotype female (MNHN): HOLOTYPE (red label) // Nouvelle-Caledonie / Menazi 1020 m / 18.x84 Tillier"/"Bouchet // Mecyclothorax / najtae sp. n. / det. T. Deuve // *New Caledonia Mecyclothorax* revision / measured specimen 1 / J.K. Liebherr 2016. The specimen is mounted on two platens: 1, head, prothorax, and pterothorax separated from elytra; 2, abdominal ventrites. No female genitalic structures were available for study in this specimen.

Distribution and habitat. The type locality northwest of the summit of Menazi (Fig. 19) is situated at 21°26.83'S × 165°41.75'E. Deuve (1987) reported the microhabitat as humid *Auracaria* forest on peridotite; i.e. igneous, ultramafic rock.

11. *Mecyclothorax manautei* Liebherr, sp. n.

http://zoobank.org/0A0B84B4-7BC4-4925-B2DE-6AAF3582A1BF

Figures 17I–J, 18E, 20A, 23A, 24A, 25

Diagnosis. This species can be diagnosed by small body size–standardized body length 3.5–3.9 mm–and the transversely ovoid pronotum with evenly convex lateral margins basally, i.e., hind angles lacking (Fig. 20A). The elytral striae are much more reduced than in the prior two species–*M. laterovatulus* and *M. najtae*–with the sutural stria obsolete at midlength, and only striae 2–3 evident there, though very shallow. The eyes broadly cover the ocular lobe, ocular lobe ratio 0.88–0.89, and are very convex, i.e. "popeyed", with EyL/EyD = 2.2–2.4. Chaetotaxy +/+//+/–//+/2/+/+.

Description (n = 4). Head capsule quadrate, eyes very convex, popeyed, ocular lobe meeting gena at obtuse angle close to eye posterior margin; 14 ommatidia along horizontal diameter of eye; ocular ratio 1.48–1.52, ocular lobe ratio 0.88–0.89, EyL/EyD = 2.2–2.4; frontal grooves deep, slightly convergent to deepest portion just posterad clypeus, deeply extended onto clypeus; mandibles elongate, mandibular ratio 1.92; ligular anterior margin rounded to

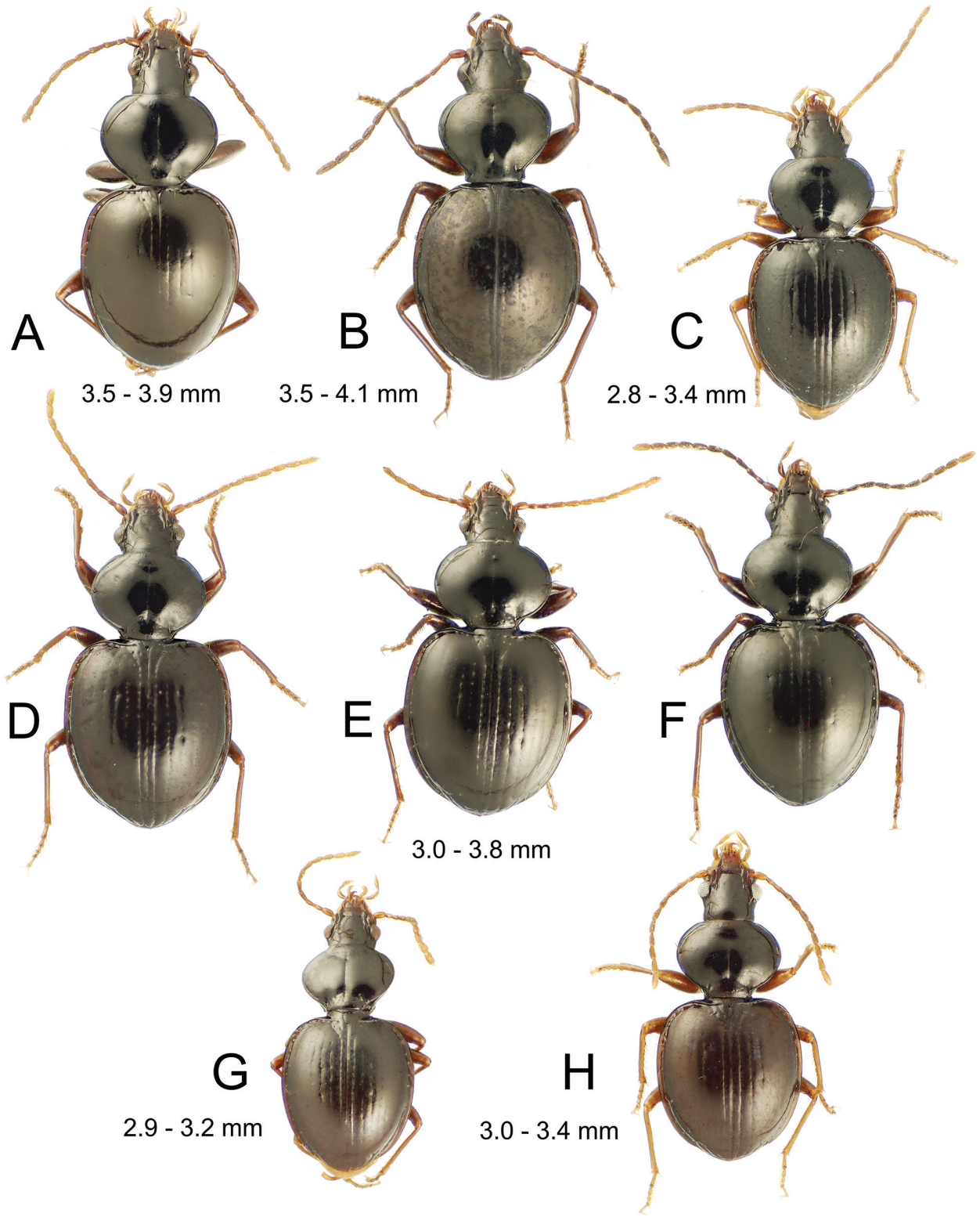

Figure 20. New Caledonian *Mecyclothorax* (*Phacothorax*) spp., dorsal view: **A**, *M. manautei*; **B**, *M. paniensis*; **C**, *M. mouensis*; **D**, *M. kanak* (Mt. Humboldt, 580 m); **E**, *M. kanak* (Mt. Humboldt, 630 m); **F**, *M. kanak* (Mt. Dzumac); **G**, *M. kanak* (Col de Yaté); **H**, *M. picdupinsensis*.

ligular seta, concave between setae, the two setae separated by one to two setal diameters; paraglossae thin, extended twice as far beyond ligular margin as their basal length to margin; antennae elongate, antennomere 9 length 2.25× maximal breadth; antennomere 3 glabrous except for apical ring of setae. Pronotum transversely ovoid, lateral margin evenly convex anterad base, hind angles absent though suggested by presence of short peduncular collar at base of

pronotum (Fig. 20A), MPW/BPW = 2.46–2.55, MPW/PL = 1.29–1.31; front angles slightly protruded, obtuse-rounded, APW/BPW = 1.39–1.48; median base unmargined basally, trapezoidally depressed relative to disc, the median longitudinal impression divided basally into two transverse impressions that isolate disc from base, each transverse basal impression terminated laterally in pitlike laterobasal depression; median longitudinal impression finely incised on disc, terminated anteriorly just anterad anterior transverse impression, a lenticular fovea at posterior juncture with basal transverse impressions; anterior transverse impression shallow, broad, but traceable to front angles; proepisternum separated from prosternum by a distinct groove both anteriorly and ventrally; smooth anteapical impression well developed laterally, continuous though shallower ventrally; prosternal process deeply and broadly depressed between procoxae, that depression extended 2/3 distance toward anterior prothoracic margin, the depression broadest at its anterior terminus. Elytra broadly ovoid, humeri sloped posteriorly laterad scutellum, humeral angle indicated only by slight change in curvature at juncture of narrow basal elytral groove and broader lateral marginal depression; MEW/EL = 0.79–0.94; all striae reduced on disc, stria 3 and 6 more evident, but intervening intervals at most slightly convex; only stria 8 evident apically, stria 2 present as very broad and shallow depression; elytra appressed and conjoined apically, the suture upraised at apex. Pterothoracic mesepisternal anterior furrow with 5 punctures in a curved line; mesosternal-mesepisternal suture complete (as in Fig. 3A); metepisternum maximum width/lateral length = 1.08; metepisternal-metepimeral suture complete. Abdomen with broad crescent-shaped depression along suture between first and second ventrite, second ventrite only slightly depressed within crescent; suture between second and third ventrites reduced though traceable laterally; ventrites 2–6 with broad, shallow, linear plaques near lateral margin. Microsculpture of frons reduced, surface glossy, indistinct transversely stretched sculpticells evident on vertex; pronotal disc glossy, transverse-line microsculpture visible over portions of surface depending on direction of light reflection, trapezoidal median base with only indistinct indications of transverse microsculpture; elytra iridescent, disc with elongate transverse mesh mixed with transverse lines, elytral apex covered with elongate transverse-mesh microsculpture.

Male genitalia (n = 1). Antecostal margin of abdominal mediotergite IX broadly angulate, not extended (Fig. 17J); right paramere narrow basally, evenly narrowed to apex, with 5 setae along ventral margin and two short apical setae (Fig. 18E); left paramere broad basally, narrowed to a dorsally twisted apex, parameral apex flexibly articulating with base, two elongate apical setae present; aedeagal median lobe robust, broad dorsoventrally, with apex distinctly down-curved relative to the expanded shaft and flattened into an apical face (Fig. 17I); male aedeagal internal sac with short flagellum and flagellar sheath present, a dorsal plate dorsad and basad flagellar complex, and a large dorsoapical field of macrospicules.

Female reproductive tract (n = 1). Bursa copulatrix length slightly greater than circumference, its surface thin, translucent, only slightly wrinkled (Fig. 23A); spermathecal duct entering near bursa-common oviduct juncture with duct oriented toward right side of bursa, duct length about 1.25× length of spermathecal reservoir; laminar helminthoid sclerite with rounded apex present at base of spermathecal duct; spermatheca fusiform on narrow duct, spermathecal gland duct entering at base of spermathecal reservoir; ligular apophysis present near base of common oviduct; basal gonocoxite 1 with apical fringe of two setae laterally–a smaller seta may be present medially–and several small setae near apex of medial margin (Fig. 24A); gonocoxite 2 moderately broad basally, basal width 0.6× medial length; two gracile lateral ensiform setae of moderate length present.

Types – Holotype male (MNHN): NEW CALEDONIA 11138 / 21°53'SX166°24'E.1400m. / Mt Humboldt, moss forest. / 6-7Nov2002. Monteith & / Burwell.pyreth,trees&logs // QUEENSLAND / MUSEUM LOAN / DATE: Nov. 2003 / No. LEN-1686 (green label) // *New Caledonia Mecyclothorax* revision / measured specimen 1 / J.K. Liebherr 2016 // HOLOTYPE / Mecyclothorax / manautei / J.K.Liebherr 2017 (black-bordered red label).

Paratypes (3 specimens). NEW CALEDONIA: Mt. Humboldt, moss forest, 1400 m el., 21°53'S 166°24'E, pyrethrum trees & logs, 06-07-xi-2002, lot 11138, Monteith/Burwell (QMB, 2), beyond summit, 1500 m el., 21°53'S 166°25'E, 07-xi-2002, lot 11122, Burwell (QMB, 1).

Etymology. This species epithet is a patronym honoring Joseph Manauté, Directeur du Parc Provincial de la Rivière Bleue chez Province Sud, who provided helicopter support for the Queensland Museum expedition to Mt. Humboldt, allowing Geoff Monteith and Chris Burwell to collect the type series of this species as well as other interesting and important taxa (Reid and Smith 2004).

Distribution and habitat. The species is known only from elevations 1400–1500 on Mt. Humboldt (Fig. 25). The four specimens were all collected via application of pyrethrin spray to tree trunks and downed logs.

12. *Mecyclothorax paniensis* Liebherr, sp. n.

http://zoobank.org/E2C4B0A1-CF5D-4890-AF6B-EA86F9D0F9CF
Figures 17K–L, 18F, 20B, 23B, 24B, 25

Diagnosis. These beetles can be diagnosed by the parallel lateral margins at the base of the pronotum, resulting in very slightly obtuse hind angles that protrude laterally (Fig. 20B). The elytral striae are much reduced, with the sutural striae only evident basally where it comprises a series of shallow, disconnected, elongate depressions. The elytra are broadly ovoid, with the humeri very reduced, with the elytral basal groove angulate posterad the protruded pronotal hind angles. Standardized body length 3.5–4.1 mm. Chaetotaxy +/+//+/–//+/2/+/+.

Description (n = 5). Head capsule elongate, eyes small, convex, ocular lobe-genal juncture evenly curved,

a very shallow groove indicating limit of ocular lobe; 14 ommatidia along horizontal diameter of eye; ocular ratio 1.35–1.42, ocular lobe ratio 0.77–0.82, EyL/EyD = 2.0–2.49; frontal grooves narrowly incised, straight and convergent to deepest portion at frontoclypeal suture, deeply extended onto clypeus; mandibles moderately elongate, mandibular ratio 1.71; ligular anterior margin narrowly rounded, the two ligular setae separated by one to two setal diameters; paraglossae thin, extended twice as far beyond ligular margin as their basal length to margin; antennae elongate, antennomere 9 length 2.62× maximal breadth; antennomere 3 glabrous except for apical ring of setae. Pronotum distinctly cordate, lateral margins slightly convergent anterad protruded, obtusely-angulate hind angles, the lateral margin immediately divergent anterad subparallel lateral margins at pronotal base (Fig. 20B), MPW/BPW = 1.83–1.88, MPW/PL = 1.13–1.26; front angles slightly protruded, obtuse, APW/BPW = 1.11–1.16; median base unmargined basally, trapezoidally depressed relative to disc, the median longitudinal impression divided basally into two transverse impressions that isolate disc from base, each transverse basal impression terminated laterally in a longitudinally arcuate laterobasal depression; median longitudinal impression finely incised on disc, terminated anteriorly just anterad anterior transverse impression, a lenticular fovea at posterior juncture with basal transverse impressions; anterior transverse impression shallow, broad, intermittently traceable to front angles; proepisternum separated from prosternum by a shallow groove anteriorly, and deep, distinct groove ventrally; smooth anteapical impression well developed laterally, continuous though shallower ventrally; prosternal process broadly depressed between procoxae, that depression extended 1/2 distance toward anterior prothoracic margin, the depression broadest at its anterior terminus. Elytra broadly ovoid, humeri extended laterally before sloping posteriorly laterad distinct, obtuse humeral angle; MEW/EL = 0.80–0.88; all striae reduced on disc, sutural and fourth stria most evident, but intervening intervals flat; sutural stria distinctly impressed apically to complement deep stria 8; elytra appressed and conjoined apically, the sutural margin upraised at apex. Pterothoracic mesepisternal anterior furrow with 2–3 irregular pits in deepest portion of furrow; mesosternal-mesepisternal suture complete (as in Fig. 3A); metepisternum slightly longer than broad, maximum width/lateral length = 0.92; metepisternal-metepimeral suture complete. Abdomen with broad crescent-shaped depression along suture between first and second ventrite, second ventrite only slightly depressed within crescent; suture between second and third ventrites reduced though traceable laterally; ventrites 2–6 with broad, shallow, linear to circular plaques near lateral margin. Microsculpture of frons reduced, surface glossy, indistinct transverse mesh visible over portions of vertex; pronotal disc glossy but with transverse sculpticells, breadth 4× length, and transverse lines over surface, trapezoidal median base with transverse sculpticells, breadth 3× length visible in areas of no reflection; elytra distinctly iridescent, disc covered with transverse lines, elytral apex covered with elongate transverse sculpticells and lines.

Male genitalia (n = 1). Antecostal margin broadly angulate, not extended (Fig. 17L); right paramere narrow basally, apical half narrowed into a narrow whiplike extension, its ventral surface bearing 15 setae near midlength distant from elongate pair of apical setae (Fig. 18F); left paramere narrow basally, evenly narrowed to a whiplike apex, two apical setae present; aedeagal median lobe robust, broad dorsoventrally, the ventral and dorsal margins evenly curved to a broadly rounded apex that extends moderately beyond ostial opening (Fig. 17K); aedeagal median lobe internal sac with elongate flagellum and flagellar sheath plus dorsal plate.

Female reproductive tract (n = 1). Bursa copulatrix length slightly greater than circumference, its surface thin, translucent, not wrinkled (Fig. 23B); spermathecal duct entering near bursa-common oviduct juncture with duct oriented toward right side of bursa, duct length twice length of spermathecal reservoir; knoblike helminthoid sclerite present at base of spermathecal duct; spermatheca fusiform on narrow duct, spermathecal gland duct entering at base of spermathecal reservoir; ligular apophysis present on common oviduct; basal gonocoxite 1 with apical fringe of two setae laterally and several smaller setae medially, a series of small setae lining medial margin (Fig. 24B); gonocoxite 2 moderately broad basally, basal width half medial length; two gracile lateral ensiform setae of moderate length present, the apical seta slightly broader.

Types – Holotype male (MNHN): NEW CALEDONIA / Mt Panie summit / Nov 2001 / C. Burwell // QM Berlesate 1058 / 20°34’Sx164°46’E / Rainforest, 1600m / Sieved litter // QUEENSLAND / MUSEUM LOAN / DATE: Sept 2002 No. LE 02.43 (green label) // HOLOTYPE / Mecyclothorax / paniensis / J.K.Liebherr 2017 (black-bordered red label).

Paratypes (11 specimens). NEW CALEDONIA: Mt. Panié, 20°34’S 164°46’E, 08-x-1977, J. Balogh (HNHM, 1), 1300-1600 m, 15-v-1984, Monteith & Cook (QMB, 1), E trail, 1350–1629 m el., 20°35.3’S 164°46.2’E, rainforest, 24-xi-2010, Wanat & Ruta (MNHW, 3), refuge, 1300 m el., 20°34’S 164°46’E, rainforest, sieved litter, 8–9–xi–2001, lot 1056, Burwell (QMB, 2), summit, 1600 m el., 20°34’S 164°46’E, rainforest, sieved litter, xi-2001, lot 1058, Burwell (QMB, 2), summit, 1600, 20°35’S 164°46’E, 18-xi-2000, 9939, Bouchard, Burwell & Monteith (QMB, 2).

Etymology. The adjectival ending -ensis is elided with the type locality Mt. Panié to obtain the species epithet paniensis, an adjective in the genitive case.

Distribution and habitat. This species’ distribution is restricted to Mt. Panié (Fig. 25). Collecting localities are in the higher reaches of the mountain, 1300–1629 m elevation, with recorded microhabitats or collecting situations including rainforest and sieved litter. As such it appears beetles of this species occupy the ground-level litter layer.

13. *Mecyclothorax mouensis* Moore & Liebherr, sp. n.

http://zoobank.org/572EF2F8-5BF7-4663-8F53-74100E27DF5E
Figures 2B, 17M–N, 18G, 20C, 23C, 24C, 25

Diagnosis. This species, along with *M. kanak* and *M. picdupinsensis*, comprises a triplet of cryptic sibling species best determined using the male aedeagal median lobe. To that end, this species is characterized by a median lobe with the apex dorsally and ventrally subparallel beyond the ostial opening, and with the lobe's apical face narrowly flattened (Fig. 17M). All three species share broadly hemiovoid elytra, with this species exhibiting a broadly rounded basal groove across the humerus. Individuals of this species can be best diagnosed externally from those of the following two species by the broader elytral lateral marginal depression outside the anterior series of lateral elytral setae (Fig. 20C). The anterior lateral elytral setae are situated in the lateral depression in beetles of this species, whereas they lie on the upraised lateral reaches of the elytral disc in *M. kanak* and *M. picdupinsensis*. Also the sutural stria is deep and smooth on the disc and striae 2–3 are evident and traceable to nearly obsolete in *M. mouensis*. This differs from the sutural stria in beetles of the following two species where the sutural stria is crenulate to indistinctly punctate on the disc. Standardized body length 2.8–3.4 mm. Chaetotaxy +/+//+/–//+/2/+/+.

Description (n = 5). Head capsule elongate, eyes small, very convex, ocular lobe-genal juncture evenly curved, a very shallow groove indicating limit of ocular lobe; 11 ommatidia along horizontal diameter of eye; ocular ratio 1.43–1.48, ocular lobe ratio 0.73–0.77, EyL/EyD = 2.17–2.38; frontal grooves narrowly incised, sinuously convergent to pit at frontoclypeal suture, briefly extended onto clypeus; mandibles moderately elongate, mandibular ratio 1.73; ligula narrowed to a moderately broad, slightly convex anterior margin, the two ligular setae separated by one setal diameter; paraglossae thin, extended twice as far beyond ligular margin as their basal length to margin, apex visibly spiculate (100×); antennae moderately elongate, antennomere 9 length 2.0× maximal breadth; antennomere 3 glabrous except for apical ring of setae. Pronotum very transverse, distinctly cordate, lateral margins sinuately concave anterad obtuse-rounded hind angles (Figs 2B, 20C), MPW/BPW = 2.43–2.82, MPW/PL = 1.35–1.39; front angles slightly protruded, obtuse, APW/BPW = 1.42–1.50; median base unmargined basally, trapezoidally depressed relative to disc, the median longitudinal impression divided basally into two transverse impressions that isolate disc from base, each transverse basal impression terminated laterally in a short laterally arcuate laterobasal depression; median longitudinal impression finely incised on disc, terminated anteriorly at anterior transverse impression, a narrow fovea at posterior juncture with basal transverse impressions; anterior transverse impression shallow, broad, traceable to front angles; proepisternum separated from prosternum by a shallow groove anteriorly, and deep, distinct groove ventrally; smooth anteapical impression well developed laterally, continuous though shallower ventrally; prosternal process broadly, shallowly depressed between procoxae, the shallow depression extended 1/2 distance toward anterior prothoracic margin. Elytra broadly hemiovoid, humeri well-extended laterally before lateral margins curve posteriorly; basal elytral groove posteriorly curved laterad obtuse humeral angle; MEW/EL = 0.85–0.91; sutural stria well developed in basal 2/3, striae 2–3 traceable on disc near positions of dorsal elytral setae, stria 4 indicated by an series of intermittent longitudinal depressions; only stria 8 evident on elytral apex; elytra appressed and conjoined apically, the sutural margin upraised at apex. Pterothoracic mesepisternal anterior furrow with five to six depressions in one to two irregular rows; mesosternal-mesepisternal suture complete (as in Fig. 3a); metepisternum length and breadth subequal; metepisternal-metepimeral suture complete though fine laterally. Abdomen with elongate crescent-shaped depression along suture between first and second ventrite, second ventrite only slightly depressed within crescent; suture between second and third ventrites reduced though traceable laterally; ventrites 3–6 with broad, shallow, linear plaques near lateral margin. Microsculpture of frons reduced, surface glossy, indistinct transverse mesh–sculpticell breadth 2× length–visible over portions of vertex; pronotal disc glossy but with transverse sculpticells visible outside areas of reflection, trapezoidal median base glossy with indistinct transverse mesh anterad laterobasal depression; elytra opalescent, disc covered with very finely separated transverse lines, elytral apex covered with elongate transverse sculpticells and lines.

Male genitalia (n = 8). Antecostal margin of mediotergite IX angulate, not extended (Fig. 17N); right paramere narrow, with basal cuff articulating with elongate, whiplike apical extension (Fig. 18G), six setae along ventral margin to complement to longer apical setae; left paramere narrow basally, evenly narrowed to whiplike apex; aedeagal median lobe robust, broadest medially basad apex of ostial opening, apex subparallel dorsoventrally beyond ostium, with apical face somewhat flattened (Fig. 17M); aedeagal median lobe internal sac with broad, basal dorsal plate and a large field of macrospicules apicad the plate, but flagellum and flagellar sheath not present.

Female reproductive tract (n = 1). Bursa copulatrix length subequal to circumference, its surface thin, translucent, slightly wrinkled (Fig. 23C); spermathecal duct entering near bursa-common oviduct juncture with duct oriented toward right side of bursa; elongate laminar helminthoid sclerite present at base of spermathecal duct; spermatheca of only slightly greater circumference than spermathecal duct, spermathecal gland duct entering at base of spermathecal reservoir; ligular apophysis present on common oviduct; basal gonocoxite 1 with apical fringe of two setae laterally, a very small setae may be present immediately mesad, and several smaller setae along medial margin (Fig. 24C); medial margin bearing a dense field of microtrichia basally, this field about 3–4

microtrichia broad and appearing like the hooklike surface of a Velcro® closure; gonocoxite 2 moderately broad basally, basal width 0.6× medial length; two gracile lateral ensiform setae of moderate length present.

Types – Holotype male (MNHN): NEW CALEDONIA / Mt Mou summit / 24 May 1984 / G. Monteith & D. Cook // Q.M. Berlesate 659 / 22.04S X 166.21E / Rainforest, 1200 n / Litter // QUEENSLAND / MUSEUM LOAN / DATE: Nov. 2003 / No. LEN-1686 (green label) // HOLOTYPE / Mecyclothorax / mouensis / B.P. Moore & J.K. / Liebherr 2017 (black-bordered red label).

Paratypes (33 specimens). NEW CALEDONIA: Mts. Koghis, [code PA 58], 22°11'S 166°31'E, 30-viii-1970, Franz (NHMW, 3), ~5 km N Noumea, 550 m el., 22 10.5'S, 166 30.3'E, forest litter, 25-xi-2009, Schuh (NHMW, 1), forest, 520 m el., 22°10.7'S 166°30.3'E, sifted litter, 25-x-2008, Wanat (MNHW, 9), La Roussette, 600 m el., 22°10.8'S 166°30.7'E, sifted litter, 27-x-2008, Wanat (MNHW, 4), track entrance, 500 m el., 22°11'S 166°31'E, berlesate, 06-v-2005, lot 12264, Monteith (QMB, 4), 500 m el., 22°10'S 166°31'E, 26-viii-1978, S. & J. Peck (CNC, 1), 400-500 m el., 22°11'S 166°31'E, primary forest, 18–19-x-1998, Löbl (MBC, 1; MHNG, 6); Mt. Mou, summit, 1200 m el., 22°04'S, 166°21'E, rainforest litter, 24-v-1984, Monteith & Cook (QMB, 2), top camp, 1150 m el., 22°04'S, 166°21'E, berlesate, sieved litter, 27-xii-2004, lot 12013, Monteith (QMB, 2). Non-type female specimen: Forêt Cachée, 250 m el., 22°11.5'S 166°47.2'E, sifted litter, 26-x-2008, Wanat (MNHW, 1).

Etymology. As in the species above, this species epithet elides the type locality, Mt. Mou, with the genitive, adjectival ending -ensis. As Dr. Barry P. Moore had both diagnosed this species from the following *M. kanak* through the use of male genitalic characters, and had chosen a holotype specimen, he is given senior author status for this species.

Distribution and habitat. This species is restricted to the southern portion of Grande Terre, from Mt. Mou on the west, Mts. Koghis north of Noumea, and with a easternmost record from Forêt Cachée based on a single non-type female specimen (Fig. 25). Collection localities range 250–1200 m elevation. Given that 24 of the 35 specimens are labeled from Berlese samples or sieved litter, and another 7 specimens (1, S. & J. Peck, CNC; 6, Löbl, MHNG) were collected by coleopterists studying the microcoleopteran litter fauna, it can be concluded that this species occupies the ground-level litter layer.

14. *Mecyclothorax kanak* Moore & Liebherr, sp. n.

http://zoobank.org/062E8A3B-6762-429F-B2D7-669FB5A2AE14
Figures 1H, 20D–G, 21A–K, 22A, 23D–E, 24D, 26

Diagnosis. This second of the species triplet also including *M. mouensis* and *M. picdupinsensis* can be diagnosed externally by characters listed in the *M. mouensis* diagnosis. This species and the following *M. picdupinsensis* are adelphotaxa based on possession of the synapomorphous hitch on the apical surface of the male aedeagal median lobe (Fig. 7, character 112, state 1). This species can be diagnosed from *M. picdupinsensis* by the hitch configuration being a well-developed apical invagination (Fig. 21A–D, F–K), the level of invagination, curvature and length of the apex varying among populations assigned to this species (Fig. 26). In these instances the apical invagination is much more developed than in the sister species below (Fig. 21L–N). Much like the externally-cryptic species pair *M. fleutiauxi* and *M. jeanneli* (Fig. 9D–E), these two species are indistinguishable based on external characters. They are treated as distinct species because just as in the *M. fleutiauxi* + *M. jeanneli* pair, female reproductive tract characters also differ between the two taxa. In *M. kanak* females, the bursa copulatrix is more parallel-sided in ventral view, with the apex narrowed (Fig. 23D–E). Also, the basal gonocoxites bear a narrow, spiculate mediobasal band of fine, setose spicules (Fig. 24D), versus basal gonocoxites with a broader spiculate mediobasal band of spatulate spicules in *M. picdupensis* (Fig. 24E). Standardized body length 3.0–3.8 mm (Fig. 20D–F) for all population samples except that from Col de Yaté, for which the three specimens range 2.9–3.2 mm length (Fig. 20G). Chaetotaxy +/+//+/–//+/2/+/+.

Description (n = 24). Head capsule elongate, eyes small, very convex, ocular lobe-genal juncture evenly curved, a very shallow groove indicating limit of ocular lobe; 12–14 ommatidia along horizontal diameter of eye; ocular ratio 1.41–1.54, ocular lobe ratio 0.74–0.81, EyL/EyD = 2.16–2.45; frontal grooves narrowly incised, sinuously convergent to pit at frontoclypeal suture, extended onto clypeus; mandibles moderately elongate, mandibular ratio 1.60; ligula narrowed to a moderately broad, slightly convex anterior margin, the two ligular setae separated by 1–2 setal diameters; paraglossae thin, extended twice as far beyond ligular margin as their basal length to margin, apex visibly spiculate (100×); antennae moderately elongate, antennomere 9 length 2.1× maximal breadth; antennomere 3 glabrous except for apical ring of setae. Pronotum very transverse, distinctly cordate, lateral margins sinuately concave anterad obtuse-rounded hind angles (Fig. 20D–G), MPW/BPW = 2.31–2.64, MPW/PL = 1.27–1.37; front angles slightly protruded, obtuse, APW/BPW = 1.27–1.48; median base unmargined basally, trapezoidally depressed relative to disc, the median longitudinal impression divided basally into two transverse impressions that isolate disc from base, each transverse basal impression terminated laterally in a short linear laterobasal depression; median longitudinal impression finely incised on disc, terminated anteriorly just anterad anterior transverse impression, a narrow fovea at posterior juncture with basal transverse impressions; anterior transverse impression shallow, broad, traceable to front angles; proepisternum separated from prosternum by a shallow groove anteriorly, and deep, distinct groove ventrally; smooth anteapical impression well developed laterally, continuous though shallower ventrally; prosternal pro-

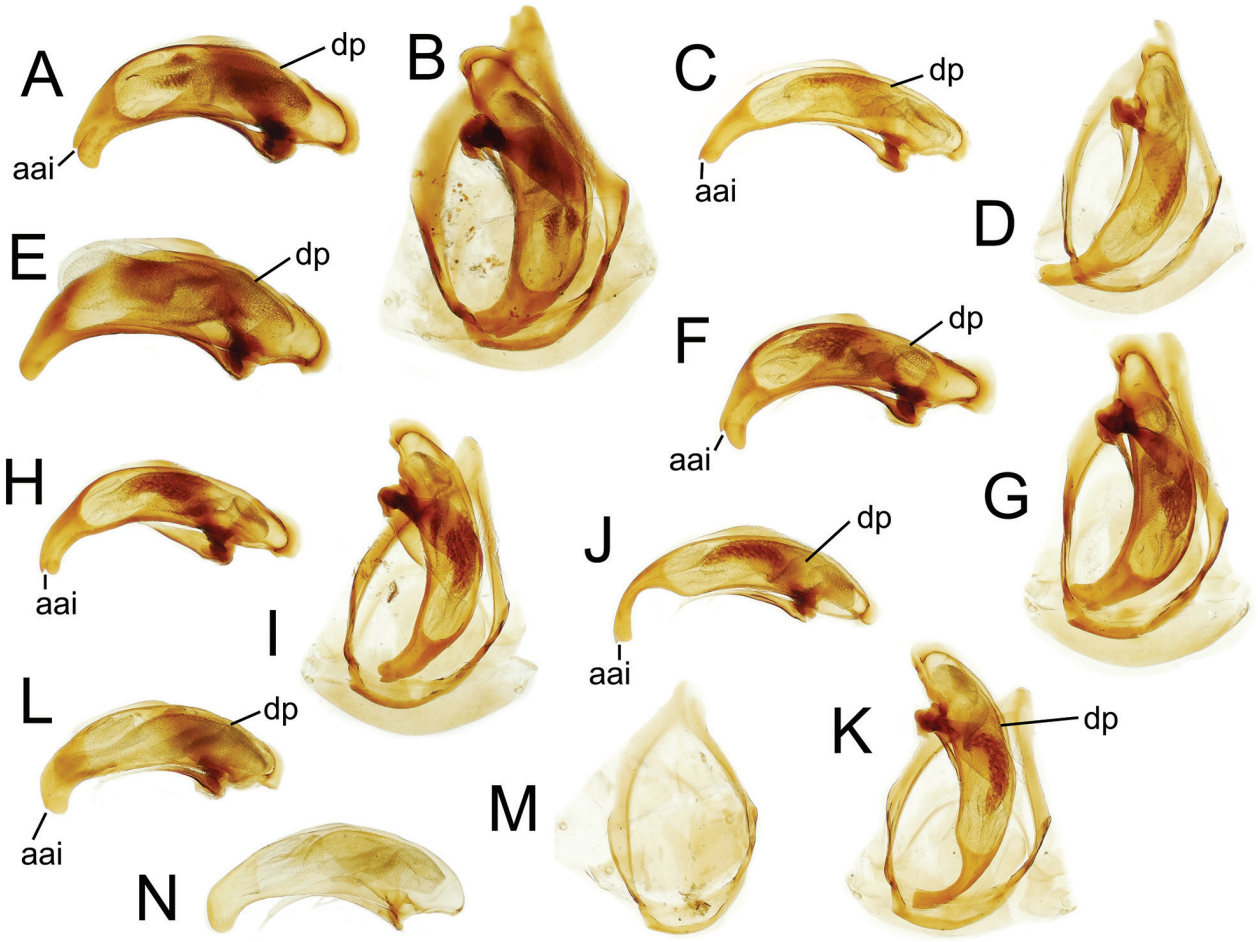

Figure 21. Male aedeagal median lobe and parameres, and ring sclerite–mediotergite plus antecostal margin, tergite IX–of *Mecyclothorax* (*Phacothorax*) spp.: **A–B**, *M. kanak*, right view, dorsal view in situ (Mt. Humboldt, 630 m); **C–D**, *M. kanak*, right view, dorsal view in situ (Mt. Humboldt, 1400 m); **E**, *M. kanak*, form Q, right view (Mt. Humboldt, 1300 m); **F–G**, *M. kanak*, right view, dorsal view in situ (Mt. Dzumac); **H–I**, *M. kanak*, right view, dorsal view in situ (Rivière Bleue); **J–K**, *M. kanak*, right view, dorsal view in situ (Col de Yaté); **L–N**, *M. picdupinsensis*, right views, dorsal view of ring sclerite. See Table 2 for abbreviations.

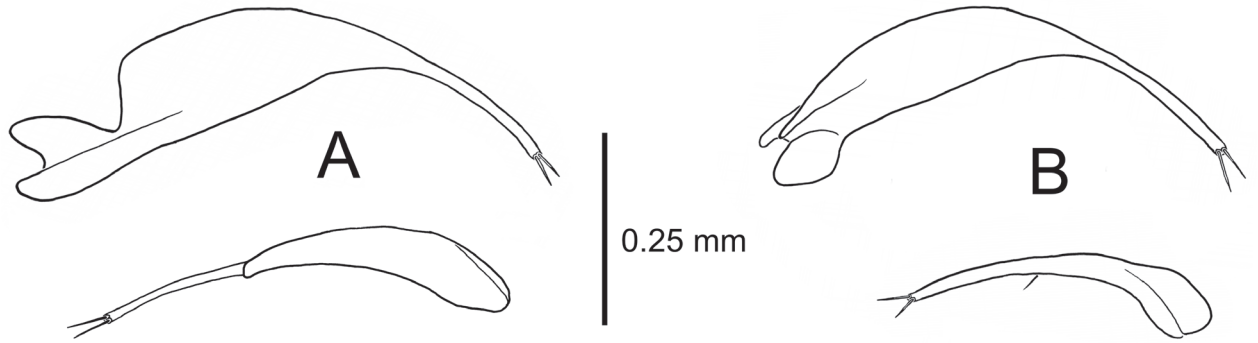

Figure 22. Paired left (above) and right (below) parameres of *Mecyclothorax* (*Phacothorax*) spp. (ectal view): **A**, *M. kanak*; **B**, *M. picdupinsensis*.

cess broadly, shallowly depressed between procoxae, the shallow depression extended 1/3 distance toward anterior prothoracic margin. Elytra broadly hemiovoid, humeri well-extended laterally before lateral margins curve posteriorly; basal elytral groove posteriorly curved laterad obtuse humeral angle, with three punctate depressions at the base of sutural and striae 5 and 5; MEW/EL = 0.81–0.93; sutural stria well developed in basal 2/3, striae 2–3 traceable on disc near positions of dorsal elytral setae, all three irregularly depressed with intermittent crenulations or elongate punctures along their length; stria 4 indicated by an intermittent series of shallow longitudinal depressions;

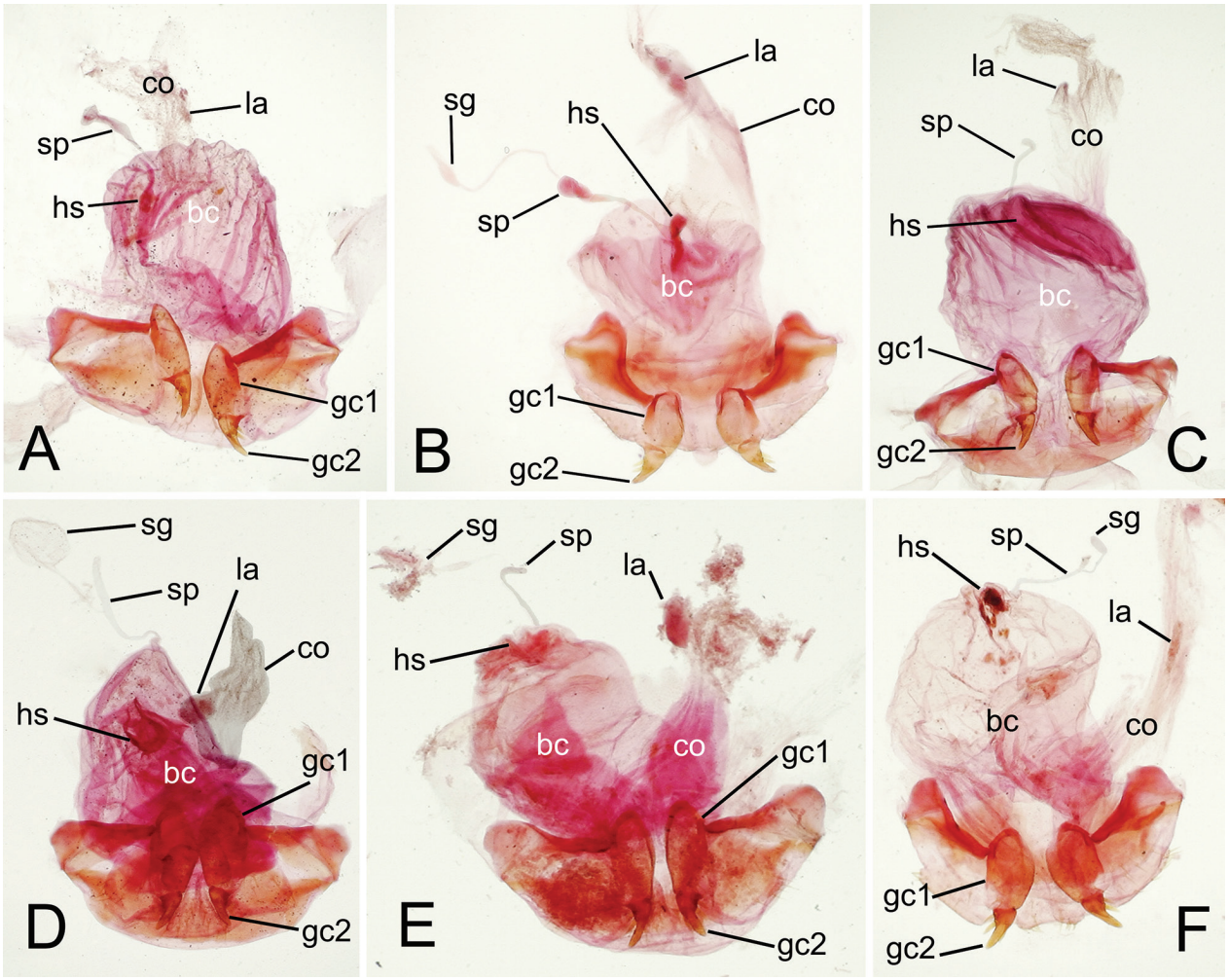

Figure 23. Female reproductive tract, gonocoxites and associated laterotergites, *Mecyclothorax* (*Phacothorax*) spp: **A**, *M. manautei*; **B**, *M. paniensis*; **C**, *M. mouensis*; **D**, *M. kanak* (Mt. Dzumac; common oviduct artificially darkened to show configuration); **E**, *M. kanak* (Pic du Grand Kaori); **F**, *M. picdupinsensis*. See Table 2 for abbreviations.

striae 1 and 2 shallow and traceable, and stria 8 evident on elytral apex; elytra appressed and conjoined apically, the sutural margin upraised at apex. Pterothoracic mesepisternal anterior furrow with 5 depressions in 1–2 irregular rows; mesosternal-mesepisternal suture complete (as in Fig. 3A); metepisternum foreshortened, lateral length/maximum width = 1.1–1.25; metepisternal-metepimeral suture complete though fine laterally. Abdomen with very elongate, shallowly curved crescent-like depression along suture between first and second ventrite, second ventrite only slightly depressed within crescent; suture between second and third ventrites reduced though traceable laterally; ventrites 3–6 with broad, shallow, linear plaques near lateral margin. Microsculpture of frons reduced, surface glossy, indistinct transverse mesh–sculpticell breadth 2× length–visible over portions of vertex; pronotal disc glossy but with transverse sculpticells visible outside areas of reflection, trapezoidal median base glossy with indistinct transverse mesh anterad laterobasal depression; elytra opalescent, disc covered with very finely separated transverse lines, elytral apex covered with elongate transverse sculpticells and lines.

Male genitalia (n = 25). Antecostal margin of abdominal mediotergite IX angulate, not extended (Fig. 21B, D, G, I); right paramere narrow, extended as a very narrow whiplike extension which flexibly articulates with the base, both ventral and dorsal margins glabrous, with two apical setae (Fig. 22A); left paramere moderately broad basally, evenly narrowed to a whiplike apex, two longer apical setae present; aedeagal median lobe variously robust, broader relative to length in specimens with a shorter aedeagal apex (Fig. 21A, F), and narrower relative to length in males with more gracile median lobes (Fig. 21C, H, J); median lobe apex variously bifurcate–except for the infraspecific variant, form Q discussed below (Fig. 21E)–with an apical aedeagal invagination laterally splitting the tip, that invagination continued laterally on the median lobe toward the ostial opening (Fig. 21A, C, F, H, J); aedeagal apex variously extended and curved, from short and broad, and briefly extended beyond the ostial opening (Fig. 21A, F), to more elongate broadly extended and slightly downturned (Fig. 21H), to more elongate and narrowly extended (Fig. 21C), to very narrowly extended and distinctly curved (Fig. 21J); median lobe internal sac

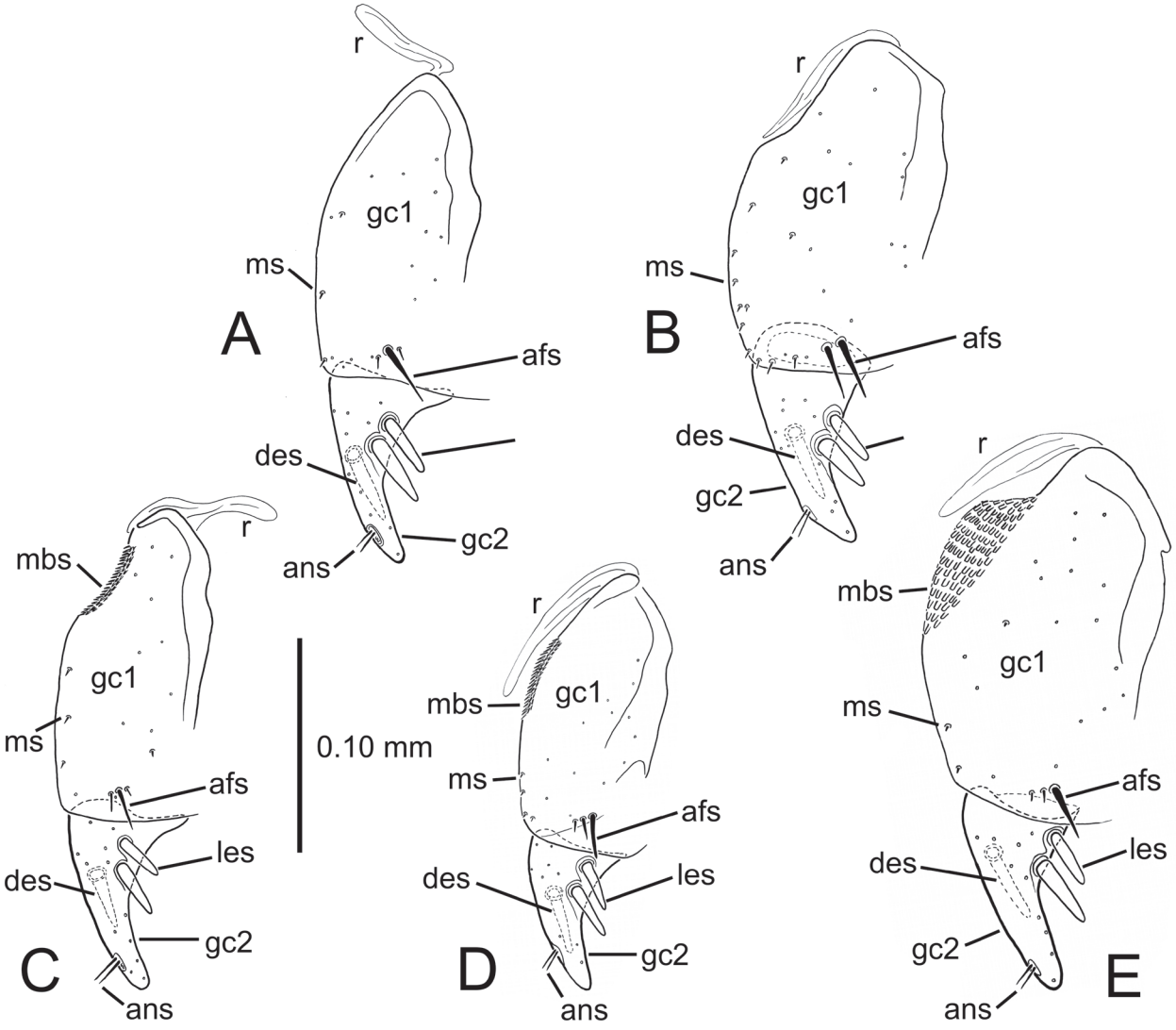

Figure 24. Left female gonocoxa of *Mecyclothorax* (*Phacothorax*) spp., ventral view: **A**, *M. manautei*; **B**, *M. paniensis*; **C**, *M. mouensis*; **D**, *M. kanak*; **E**, *M. picdupinsensis*. See Table 2 for abbreviations.

with translucent dorsal plate, most visible in well-sclerotized specimens (Fig. 21A, E, J), and a longitudinal apical field of microspicules (Fig. 21A, J).

One of a series of nine males from Mt. Humboldt, 1300 m el., 6–7-xi-2002, Monteith & Wright, lot 1076 (QMB) exhibits a broad aedeagus with a rounded tip, the ostial opening more asymmetrical apically (Fig. 21E), herein dubbed form Q. The other eight males of this particular collecting series all exhibit aedeagal apices similar to those from Mt. Humboldt, 1400 m (Fig. 21C). There are no external differences discernible among the males of this series, and no other examined male from Mt. Humboldt or anywhere else across the distributional range exhibits the "form Q" aedeagal configuration. Therefore this form is considered an infraspecific variant without nomenclatural status, with its evolutionary basis requiring further study.

The geographic pattern of aedeagal configuration shows that populations in the southern end of the range include males with a longer, narrower, and more curved aedeagal apex (Fig. 26, populations G, H, I). The extreme of this trend is observed in two males from Col de Yaté (Fig. 26, population G). The beetles comprising the Col de Yaté sample also tend to be smaller, though the size range of the three specimens of this population sample overlap the ranges of other populations, precluding diagnosis by size. Given the trend toward longer, narrower aedeagal apices in the south, and the demonstrated variation in aedeagal apices among other population samples (e.g. Fig. 26, population samples C, F), this variation is considered infraspecific.

Female reproductive tract (n = 4). Bursa copulatrix length 1.1–1.4× circumference, its surface thin, translucent, slightly to not wrinkled (Fig. 23D–E); spermathecal duct entering at apex of bursa separate from bursa-common oviduct juncture; rounded helminthoid sclerite on bursal wall between, and separate from both, bursal-common oviduct juncture and spermatheca; spermatheca of

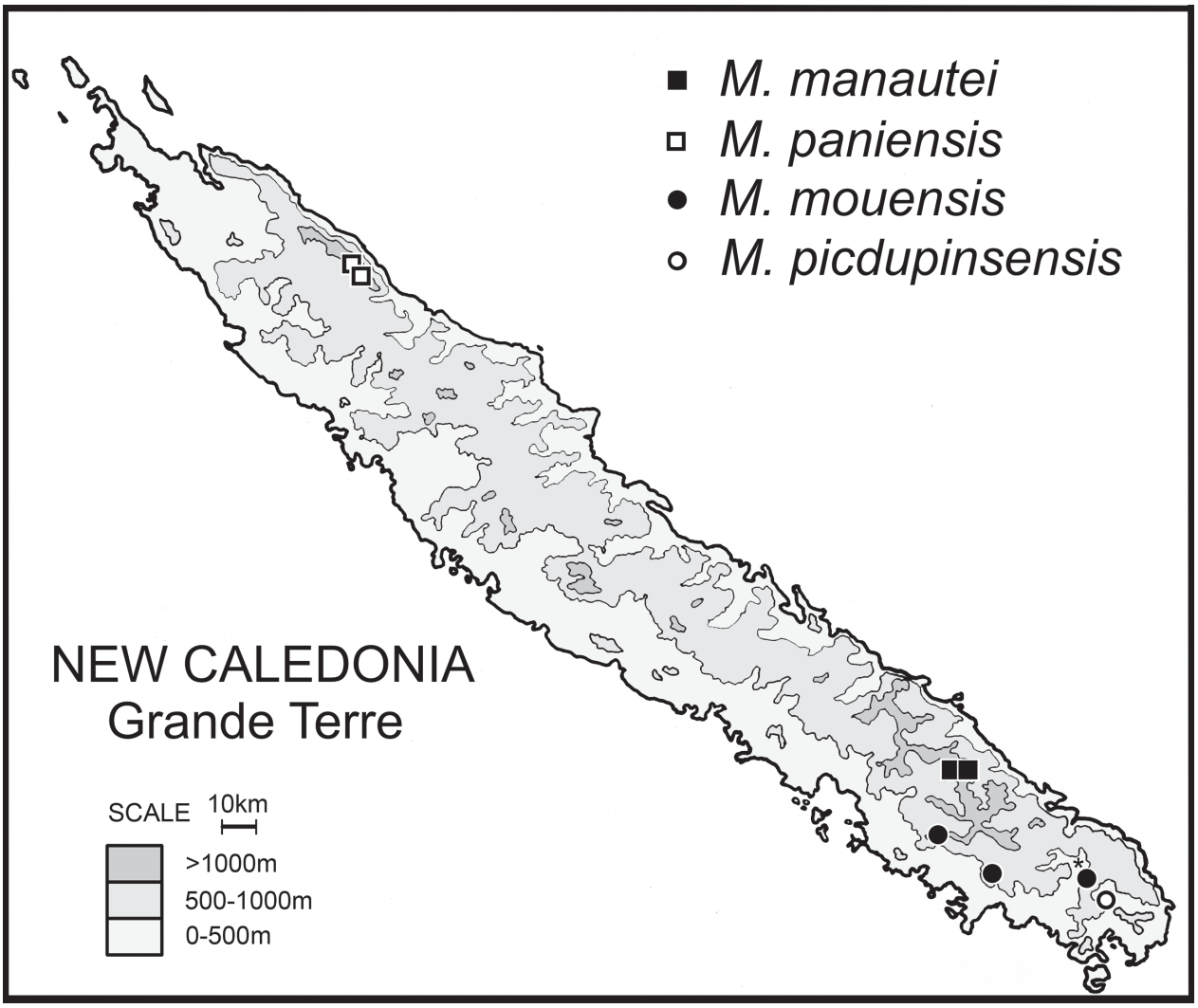

Figure 25. Geographical distributions of *Mecyclothorax* (*Phacothorax*) spp. (asterisked locality attributed to *M. mouensis* based on non-type female specimen).

only slightly greater circumference than spermathecal duct, reservoir about 1/2 length of spermathecal duct, spermathecal gland duct entering at base of spermathecal reservoir (Fig. 23E); ligular apophysis present on common oviduct; basal gonocoxite 1 with apical fringe of two to unilaterally three setae laterally, a very small setae may be present immediately mesad, and several smaller setae occur along apex of medial margin (Fig. 24D); medial margin bearing a dense field of spiculate microtrichia basally, this field about 3–4 microtrichia broad and appearing like the hooklike surface of a Velcro® closure; gonocoxite 2 moderately broad basally, basal width 1/2 medial length; two gracile lateral ensiform setae of moderate length present.

Types – Holotype male (MNHN): NEW CALEDONIA / Mt Dzumac / 28 May 1987 / R.Raven // Q.M. Berlesate No. 800 / 22.03'S. 166.28'E. / Rainforest 900m / Litter // QUEENSLAND / MUSEUM LOAN / DATE: Nov. 2003 / No. LEN-1686 (green label) // HOLOTYPE / Mecyclothorax / kanak / B.P. Moore & J.K. / Liebherr 2017 (black-bordered red label).

Paratypes (181 specimens; CUIC, EMEC, MBC, MHNG, MNHW, NHMW, PMGC, QMB): see Suppl. material 2.

Etymology. This species is named to honor the Kanak people of New Caledonia. As the species epithet kanak is not derived from Latin, it is to be treated as indeclinable (I.C.Z.N. 1999, Article 31.2.3). Dr. B. P. Moore diagnosed this species from the preceding sibling species *M. mouensis*, and as such it is appropriate that he receive senior authorship for the species.

Distribution and habitat. This species is densely and abundantly distributed across the southern reaches of Grande Terre, with records from Mt. Humboldt south to Forêt Nord (Fig. 26). Collecting localities range from 70 m elevation along the Tontouta River, to 1500 m on the slopes of Mt. Humboldt. Professor Alexander von Humboldt (Wulf 2015) would no doubt be very interested to learn that this species occurs from 580–1500 m elevation on his namesake mountain, inhabiting lowland rain forest, montane rain forest, and high-altitude maquis (Mueller-Dombois and Fosberg 1998), where this species was

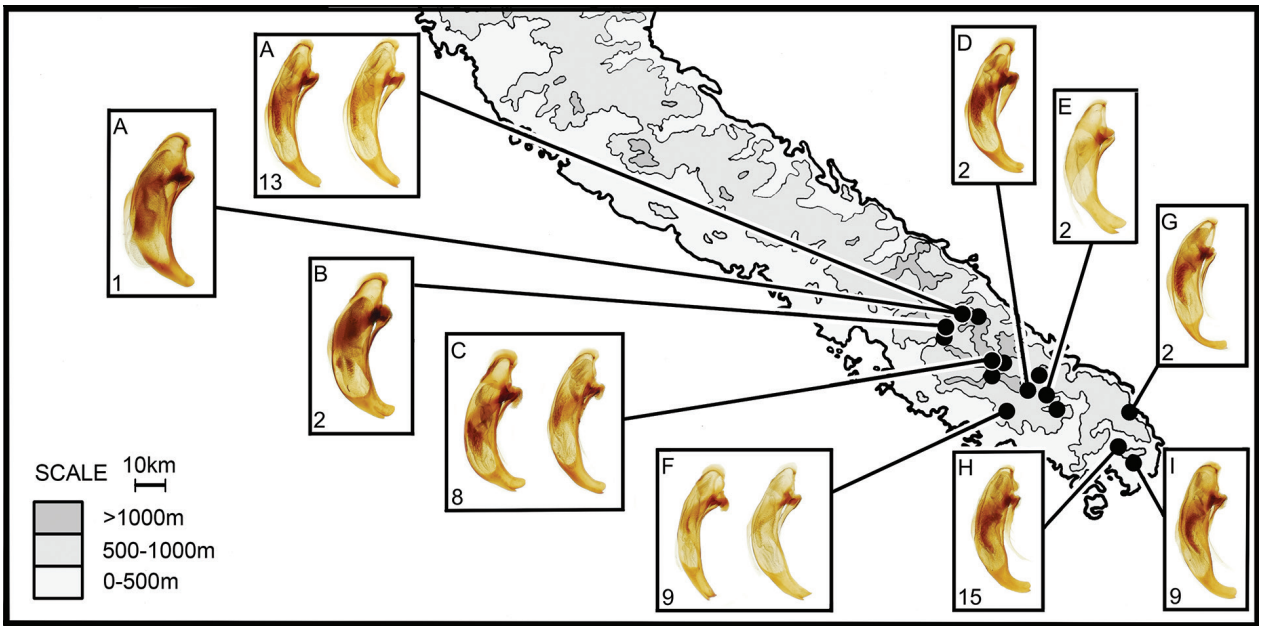

Figure 26. Recorded geographical distribution of *M. kanak* (including population samples A–I for which representative male aedeagi are figured): numbers of males sampled for each locality indicated in lower left of boxes. Sampled population localities include: **A**, Mt. Humboldt, 1300–1400 m; **B**, Mt. Humboldt, 600 m; **C**, Mt. Dzumac; **D**, Rivière Bleue, 800 m; **E**, Rivière Bleue, 400 m; **F**, Mts. Koghis; **G**, Col de Yaté; **H**, Pic du Grand Kaori; **I**, Forêt Nord.

collected from sifted litter under *Callitris neocaledonica* Dümmer (1, Wanat, MNHW). Of the 177 specimens examined, 133 were labeled as collected in sieved litter or by Berlese extraction. A further 34 specimens (Löbl, MHNG) can also be assigned as the products of these methods. This leaves the remaining 6% of specimens to be divided between such collecting methods as headlamp search at night, "at light", flight intercept trap, and no data. Thus this species can be characterized as a fastidious denizen of the ground-level litter layer.

15. *Mecyclothorax picdupinsensis* Liebherr, sp. n.

http://zoobank.org/469A110B-37CD-48A9-B118-E78BED4D6367
Figures 20H, 21L–N, 22B, 23F, 24E, 25

Diagnosis. This final member of the species triplet also including *M. mouensis* and M. *kanak* can be diagnosed from the former by characters listed in the *M. kanak* species diagnosis. As stated above, this species cannot be diagnosed from *M. kanak* based on external characters. The basis for species recognition lies both in the form of the male aedeagal median lobe apex–i.e., broadly rounded with a minute hitch present (Fig. 21L)–and female gonocoxae with a broad mediobasal patch covered with quadrate cuticular scales (Fig. 24E). Also, based on specimens at hand, the female bursa copulatrix is shorter and broader in this species, and the helminthoid sclerite is more narrowly extended as a laminar structure that is heavily melanized (Fig. 23F). Standardized body length 3.0-3.4 mm. Chaetotaxy +/+//+/–//+/2/+/+.

Description (n = 5). The description of *M. kanak* can serve to describe this species, with substitution of the following ranges of ratios of the measured specimens: ocular ratio 1.44–1.52; ocular lobe ratio 0.71–0.80; EyL/EyD = 2.08–2.38; MPW/BPW = 2.30–2.44; MPW/PL = 1.33–1.38; APW/BPW = 1.32–1.36; MEW/EL = 0.85–0.89.

Male genitalia (n = 2). Antecostal margin of abdominal mediotergite IX angulate, not extended (Fig. 21M); right paramere narrow, evenly narrowed from narrow base to whiplike apex, with one seta near midlength on ventral margin complementing two long apical setae (Fig. 22B); left paramere narrow basally, evenly narrowed to whiplike apex, two longer apical setae present; aedeagal median lobe robust, broad dorsoventrally, evenly curved dorsally and ventrally to a broadly downturned apex which bears a variously developed apical invagination, present as a small tubercle or change of angle of the apical margin (Fig. 21L); aedeagal median lobe internal sac with sclerotized region in position of dorsal plate, internal sac folded longitudinally toward apex (Fig. 21L, N).

Female reproductive tract (n = 1). Bursa copulatrix length subequal to circumference, its surface thin, translucent (Fig. 23F); spermathecal duct entering at apex of bursa separate from bursa-common oviduct juncture; rounded laminar helminthoid sclerite extended from bursal wall between, and separate from both, bursal-common oviduct juncture and spermatheca; spermatheca of only slightly greater circumference than spermathecal duct, reservoir about 1/2 length of spermathecal duct, spermathecal gland duct entering at base of spermathecal reservoir (Fig. 23F); ligular apophysis present on common oviduct; basal gonocoxite 1 with apical fringe of two setae laterally, a very small setae may be present immediately mesad, and several smaller setae occur near apex of medial margin (Fig. 24E); medial margin bearing a dense field of mi-

crotrichia basally, this field about 8 microtrichia maximal breadth, with the macrotrichia appearing like flattened scales; gonocoxite 2 moderately narrow basally, basal width 0.4× medial length; two gracile lateral ensiform setae of moderate length present, the apical seta broader.

Types – Holotype male (MNHN): NEW CALEDONIA 11787 / 22°15'Sx166°49'E, 280m / Pic du Pin, site 1,rainfor. / 26Nov2004, berlesate / G.Monteith,P.Grimbacher // QUEENSLAND / MUSEUM LOAN / DATE: July 2005 / No. LE 05.24 // *New Caledonia Mecyclothorax* revision / measured specimen 1 // HOLOTYPE / Mecyclothorax / picdupinsensis / J.K.Liebherr 2017 (black-bordered red label) /

Paratypes (11 specimens). NEW CALEDONIA: Pic du Pin[code PA 48], 22°15'S 166°49'E, 28-vi-1970, Franz (NHMW, 3), base, 280 m el., 22°14.9'S 166°49.7'E, sifted rainforest, litter, 26-xii-2006, Wanat & Dobosz (MNHW, 1), 22°15'S 166°49'E, sifted litter, 22-x-2008, Wanat (MNHW, 1), site 1, rainforest, 280 m el., 22°15'S 166°49'E, berlesate, 26-xi-2004, lot 11787, Monteith & Grimbacher (QMB, 5), 21-xii-2004, lot 12045, Monteith (QMB, 1).

Etymology. This species name represents the genitive adjectival form of the type locality, Pic du Pin; picdupinsensis. This final species name includes reference to the New Caledonian Pine, *Araucaria columnaris* J. R. Forster and W. J. Hooker, and partially recapitulates the final species named in Liebherr (2016); *Cyphocoleus iledespinsensis* Liebherr.

Distribution and habitat. This species is restricted to the vicinity of Pic du Pin, southern Grande Terre (Fig. 25), with all collecting localities recorded at 280 m elevation. Nine of the 12 specimens were collected from sieved litter, whereas three specimens (NHMW) are associated with the collecting note: "Total stehendes Stammen von *Aruacaria biramulata* (Herbert Franz field notebook: Jäch, pers. comm.)": Thus this species may climb the lower reaches and boles of larger trees in addition to occupying the ground-level litter layer.

Discussion

Phacothorax historical biogeography and ecology

The question regarding time of origin of the New Caledonian *Phacothorax* radiation is answered by the results of the cladistic analysis. As sister taxa (Fig. 7), subgenera *Phacothorax* and *Mecyclothorax* are of the same age. The earliest divergent lineage within subgenus *Mecyclothorax* comprises the two species precinctive to Lord Howe Island–*M. goweri* and *M. howei*–and the single species, *M. monteithi*, precinctive to Norfolk Island. Of these two islands, Lord Howe is the older, having been formed and become subaerial 5–6 Ma (Woodroffe et al. 2006, Kennedy et al. 2011), whereas the younger Norfolk Island developed 2.3–3.0 Ma (Jones and McDougall 1973). Thus the cladistic relationships at the base of subgenus *Mecyclothorax* (Fig. 7) support initial colonization of Lord Howe Island from New Guinea + Australia by the common ancestor of *M. goweri* + *M. howei* + *M. monteithi*, with subsequent colonization of Norfolk Island by the ancestor of *M. monteithi* after 3 Ma. Speciation of *M. goweri* and *M. howei* followed colonization of Norfolk Island by the propagule resulting in the present-day *M. monteithi*.

Given an age of origin for New Caledonian *Phacothorax* of 5–6 Ma, this lineage colonized New Caledonia over water. Subgenus *Phacothorax* is bracketed on the cladogram by subgenus *Mecyclothorax* with early divergent taxa in New Guinea, and subgenus *Meonochilus* of New Zealand. Any biogeographic relationship of *Phacothorax* and *Meonochilus* is likely based on overwater dispersal. Zealandic relationships tying together New Caledonia and New Zealand have been demonstrated for stick insects (Buckley et al. 2010), but the connections between the two areas are dated 24–46 Ma, and thus represent an earlier time when the Norfolk and Reinga Ridges were subaerial and could provide means for terrestrial dispersal (Herzer et al. 1997). Any post-Zealandic biogeographic hypothesis connecting these areas must implicate dispersalist expansion of distributions over water. Given the earliest divergence in Australia of the sister group to *Mecyclothorax* sensu lato (consisting of *Amblytelus* and associated genera, Fig. 7), plus Australian distributions of the subgenera *Eucyclothorax* and *Qecyclothorax*, independent colonization of New Zealand and New Caledonia from Australia by the ancestors of *Meonochilus* and *Phacothorax* represents the most parsimonious biogeographic hypothesis with regard to minimizing overwater dispersal events. Thus an Australian origin for the New Caledonian *Phacothorax* is proposed here.

The distributional ranges of the 15 New Caledonian *Mecyclothorax* spp. include a significant proportion of narrowly endemic species. Species richness is concentrated in relatively few localities for this taxonomic data set (Fig. 27A): **1**, Mt. Panié; **2**, Aoupinié; **3**, Me Maoya; **4**, Mt. Humboldt; **5**, Mts. Koghis. Of these localities, Mt. Panié and Me Maoya are each known to house three species, with that diversity represented in only 18 and 19 specimens respectively. Aoupinié is documented as the most diverse site with four species, based on collections totaling 58 specimens. Samples at all three of these sites differ in elevation by 300–700 m, indicating the great effort by collectors to sample different life zones on these mountains. Yet the more common species in each instance span these elevational transects, and the rarest–being known from only one specimen or a single collecting series–are restricted to a single elevation, meaning that we have a long way to go to determine how diversity is distributed elevationally at the richer sites in New Caledonia. Four of the most diverse sites–all except Me Maoya–are known to be hotspots housing many narrowly endemic plant species (Wulff et al. 2013), supporting the integration of invertebrate data into the comparatively more advanced conservation priority schemes based on New Caledonian plant species. Of the four sites held in common with Wulff et al.'s (2013) plant conservation prioritization protocol,

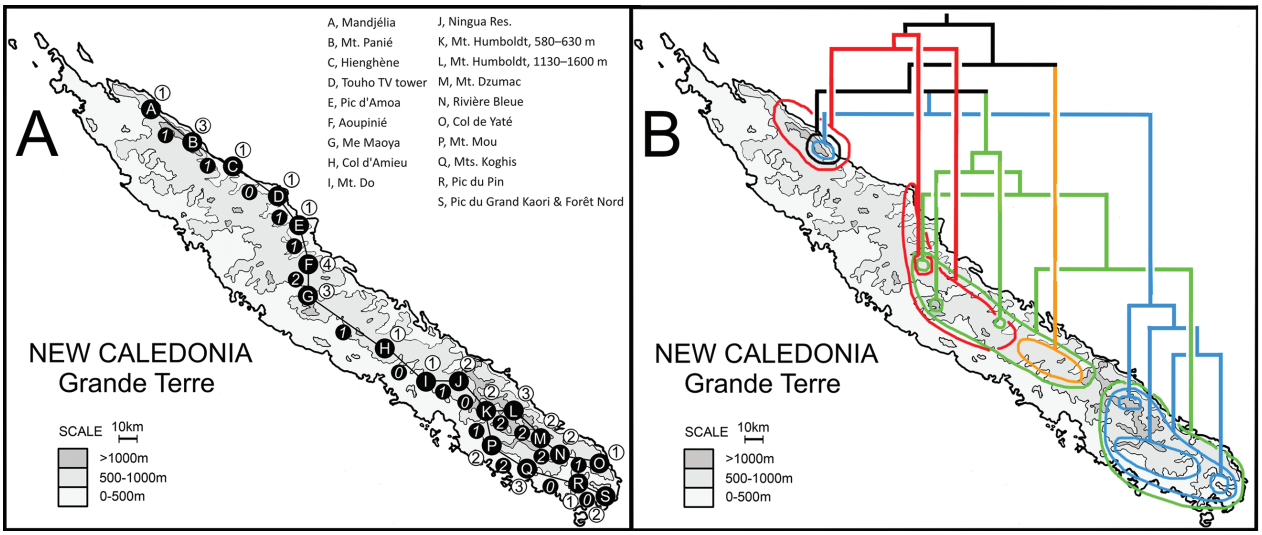

Figure 27. Distributional attributes of New Caledonian subgenus *Phacothorax* spp.: **A**, recorded species richness (open circles) at principal collecting localities represented in this revision (A–S), and species shared between adjacent localities (filled circles and italicized numerals) – see text regarding parallel networks of collection localities in southern end of Grand Terre; **B**, chorologically oriented cladogram of subgenus *Phacothorax* spp. (Fig. 7) with species terminals corresponding to areas of distribution, and the five monophyletic or monobasic constituent lineages spectrally colored red, orange, green, blue, and black (after Sharma & Giribet 2009).

Mt. Panié and Aoupinié each house two narrowly endemic *Mecyclothorax* spp.: *M. paniensis* and *M. megalovatulus* for the former, and *M. laterovatulus* and *M. plurisetosus* for the latter. These two sites are also among the most unique in the Northern Province based on endemic plant species composition (Ibanez et al. 2017).

The pattern of speciational diversification for New Caledonian *Mecyclothorax* indicates earlier diversification on the older, continental northern portion of Grand Terre, outside the areas of recently deposited ultramafic rocks. The most morphologically similar and therefore difficult to diagnose cryptic species comprise the clade of four species subtended by *M. manautei*; also including *M. kanak*, *M. mouensis*, and *M. picdupinsensis* (Figs 7; 27B, southerly blue-outlined distributions). These occur in the mountains from Mt. Humboldt south, an area exclusively dominated by ultramafic soils (Grandcolas et al. 2008, fig. 1). The adelphotaxon to this four-species clade is *M. paniensis* (Fig. 7), distributed only on Mt. Panié (Fig. 27B) far to the north in an area of older non-ultramafic continental rocks. The pattern of initial diversification in the north with more recent diversification in the ultramafic south is concordant with the taxon-area relationships exhibited both by *Augustonicus* cockroaches (Murienne et al. 2005) and by harvestman of the family Troglosironidae (Sharma and Giribet 2009). However, the timing of diversification of New Caledonian *Mecyclothorax* spp. is contemporaneous only with that of *Augustonicus*, as both cockroaches and *Mecyclothorax* beetles have radiated during the Pliocene. Conversely, divergence dating estimates for the *Trogolosiro* harvestman place the origin of that radiation in the Eocene, 49 Ma, with diversification on the ultramafic substrates dated to 6.7 Ma (the "Apex" clade of *T. longifossa* and *T. urbanus*, Sharma & Giribet 2009, fig. 6), a time contemporaneous with the origin of the entire New Caledonian *Mecyclothorax* radiation.

New Caledonian species of subgenus *Phacothorax* appear phylogenetically fickle with regard to occupation of ultramafic soils. In addition to the juxtaposition of *M. paniensis* on continental rocks versus its four-species adelphotaxon on ultramafic soils, the sister species *M. jeanneli* and *M. fleutiauxi*, though as closely related as possible phylogenetically, exhibit a stark dichotomy with regard to occupation of ultramafic soils; the former distributed strictly on such soils, the latter mostly not (Fig. 27B, Grandcolas et al. 2008, fig. 1). Thus soil type does not appear to correlate significantly among closely related species, with the single exception of the four species clade, *M. manautei*, *M. kanak*, *M. mouensis*, and *M. picdupinsensis*.

The ecological situations within which species of subgenus *Phacothorax* have been collected include both semi-arboreal and ground-level microhabitats. The former situations are represented by specimens collecting through the application of pyrethrin insecticide to the mossy surfaces of tree trunks and downed logs (G. Monteith pers. comm.). The area of application spanned the lower trunk or log upwards to where the insecticide fog stopped being effective: less than 4 m or so. Occupation of ground-level situations are guaranteed for specimens collecting by sieving leaf litter with or without subsequent Berlese extraction. Using these criteria, 8 of the 14 species for which data are available have been collected only in sieved litter: *M. laterobustus*, *M. laterorectus*, *M. laterosinuatus*, *M. megalovatulus*, *M. mouensis*, *M. octavius*, *M. paniensis*, and *M. picdupinsensis*. Four species have been collected only through pyrethrin fogging: *M. fleutiauxi*, *M. jeanneli*, *M. manautei*, and *M. plurisetosus*. Two species have been collected using both methods:

the very abundantly collected *M. kanak*, and *M. megalovatulus*. Occupation of ground-level microhabitats is the groundplan ecological condition for this radiation, with this behavior symplesiomorphically shared with the other basal lineages of *Mecyclothorax*: subgenera *Eucyclothorax*, *Qecyclothorax*, and *Meonochilus* (see below). The strict utilization of semiarboreal microhabitats by *M. plurisetosus*, *M. fleutiauxi*, and *M. jeanneli* is ecologically synapomorphous, as these three species constitute a triplet of species terminating one of the clades of the radiation (Fig. 7).

Mecyclothorax historical biogeography

The sister-group relationship between *Amblytelus* and allied genera (Baehr 2004) and *Mecyclothorax* (Liebherr 2011) establishes the basis for estimating the time of origin of the *Mecyclothorax* radiation. The earliest diverging lineage among the *Mecyclothorax* adelphotaxon (Fig. 7) comprises *Paratrichothorax brevistylus*, a species restricted to the southern coast of Western Australia. A second hypothesized early offshoot of the *Amblytelus* line not included in this analysis, *Trichamblytelus ovalipennis* Baehr, is also restricted to the coastal forests of southwestern Australia (Baehr 2004). This area was isolated during the Late Eocene to Early Oligocene by climatic cooling and marine incursions across southern Australia (Ladiges et al. 2011). Thus the time of origin of the sister group to *Mecyclothorax*, and therefore to *Mecyclothorax*, is hypothesized to be Late Eocene to Early Oligocene.

The initial divergence event within *Mecyclothorax* involved separation of the taxa newly proposed as subgenus *Eucyclothorax* (Fig. 7) from the remainder of the *Mecyclothorax* radiation. These taxa retain plesiomorphies including presence of a flagellar structure in the male aedeagal internal sac (Fig. 4A–C), and a female reproductive tract with the spermathecal duct entering the bursa ventrally in association with a sclerotized helminthoid sclerite (Fig. 6C). Individuals of these species autapomorphically present increased punctation on the body surface (Fig. 2D–F, L). The species are predominantly distributed in the east, although *M. blackburni* (Fig. 8A) is distributed across much of the more arid south and west and *M. punctatus peckorum* Baehr is restricted to southwestern Australia. Individuals of all of these species inhabit ground-level microhabitats, a plesiomorphic ecological association that differs from the derived occupation of semiarboreal, subcorticular habitats frequented by taxa in the sister group, including *Paratrichothorax brevistylus* and species of *Amblytelus* and *Districhothorax* (Baehr 2004).

Species now classified in subgenus *Qecyclothorax* constitute evolutionary products of the next divergence event along the *Mecyclothorax* line (Fig. 7). These species are all restricted to high-elevation mountain tops in Queensland, where, like *Eucyclothorax* spp., the individuals also inhabit ground-level microhabitats (Baehr 2003). Like those of subgenus *Eucyclothorax*, these species also retain the plesiomorphic presence of a male aedeagal flagellum (Fig. 4D–E) and a female reproductive tract with ventral entry of the spermathecal duct (Fig. 6D). Their external anatomy is remarkably canalized: a broad body and convex elytra with reduced striation being the norm for the clade (Fig. 8B). Populations on different, neighboring mountaintops are principally characterized by male aedeagal differences, leading Baehr (2003) to recognize such variation as infraspecific.

The third lineage to diverge from the main *Mecyclothorax* stem, those species in subgenus *Meonochilus* (Fig. 7), is distributed on North Island, New Zealand (Liebherr 2011). As in the subgenera *Eucyclothorax* and *Qecyclothorax*, the groundplan for this subgenus includes a male aedeagal flagellum and a female reproductive tract with a ventrally entering spermathecal duct, however this state synapomorphously transforms among species of this radiation. The groundplan female tract observed in females of *M. bellorum* has transformed in the other five species, four included in this analysis (Fig. 7), to a tract with the spermathecal duct entering the dorsal surface of the bursa near its distal end. All species exhibit vestigial flight wings, with the bodies characterized by the presence of heavy cuticle (least so in the most generalized *M. bellorum*). The elytra are broad, foreshortened and convexly domed, though the elytral striae are deeply impressed and distinctly punctate (Liebherr 2011, figs 9, 10). The North Island distributions of the constituent species are highly skewed to endemism in the northern peninsular extension of the Reinga Ridge–Northland–with three of the six species restricted to this administrative division. Only *M. amplipennis* (Fig. 8C) is distributed in the southern half of North Island. As in the first two subgenera–*Eucyclothorax* and *Qecyclothorax*–individuals of all species are restricted to ground-level microhabitats.

The nominate subgenus *Mecyclothorax* is by far the most diverse subgeneric taxon recognized here. Males for all species of this clade for which males are known, exhibit a modification of the male aedeagal internal sac whereby the apex of the sac bears either a roll of thickened cuticle, or a hardened, scooplike sclerite that is associated with the gonopore (Fig. 4F–G). Besides the earliest-divergent lineage that colonized the Lord Howe and Norfolk Islands, this clade exhibits its earliest diversification in New Guinea (Fig. 7). Comprehensive character analysis was possible only for species from Papua New Guinea (Liebherr 2017b), though this sampling viewed in light of the descriptions by Baehr (1992, 1995, 1998, 2002, 2008) supports an interpretation that the entire New Guinean *Mecyclothorax* fauna is assignable to this subgenus. The core of the subgenus *Mecyclothorax* radiation has produced propagules that have colonized the Greater Sunda Islands of Borneo and Java. The Australian *Mecyclothorax* fauna has diverse roots, even after taking into account the Australian *Eucyclothorax* and *Qecyclothorax* spp. removed to those subgenera. The Australian sister-species pair *M. minutus* + *M. lateralis* comprise the adelphotaxon to New Guinea's *M. sedlaceki* + *M. kavanaughi* among species sampled for the cladistic analysis. Given that *M. kavanaughi* is hypothesized to have evolved after the geo-

logical suturing of its home Finisterre Range to mainland New Guinea 3.0–3.7 Ma (Liebherr 2008a), the ancestor of these Australian taxa has been in residence since at least that time. Two other Australian *Mecyclothorax* species are highly interdigitated biogeographically with taxa that have colonized other areas over water. *Mecyclothorax ambiguus* and *M. punctipennis*, abundant species of Australian carabid beetles within their ranges (Moore 1984), are related respectively to *M. rotundicollis* of New Zealand, and *M. punctipennis* of Hawaii. *Mecyclothorax punctipennis* was also the source taxon for the propagule that colonized St. Paul and Amsterdam Islands, resulting in the very similar but distinct species *M. sculptopunctatus*. Liebherr (2013) proposed that *M. punctipennis* is also the species that produced a propagule that colonized Tahiti in the Society Islands, with *M. striatopunctatus* Perrault as the most generalized taxon in that radiation. Individuals of *M. striatopunctatus* were not available for this analysis, being returned to the Paris Museum when all types were deposited (Liebherr 2013), and so the less generalized *M. marau* was used as a surrogate. This substitution results in the French Polynesian representative species being placed as adelphotaxon to the five species associated with *M. ambiguus* and *M. punctipennis*. However, given the subaerial geological history of Tahiti and the Hawaiian Island of Maui where *M. punctipennis* resides as the most generalized Hawaiian species (Britton 1948, Liebherr 2015), all evolution in this nexus of the cladogram (Fig. 7) has taken place within the last 1–2 Myr, the time of subaerial appearance of Tahiti Nui and Maui (1.4 and 1.8 Ma respectively; Hildenbrand et al. 2004, Sherrod et al. 2007).

Mecyclothorax and flight wing loss

The species included to represent diversity of subgenus *Mecyclothorax* are a small subset of all known species. Only one of the 108 French Polynesian *Mecyclothorax* (Liebherr 2012, 2013) and one of the 239 Hawaiian *Mecyclothorax* (Liebherr 2015) are included. For New Guinea, 8 of the 22 species are represented. All 369 *Mecyclothorax* species known to date from these geographical areas lack functional flight wings, and nearly all have the wings reduced to vestigial flaps shorter than the apical margin of the metanotum. Based on taxa in this analysis, only three species within subgenus *Mecyclothorax* exhibit fully functional flight wings; *M. ambiguus*, *M. punctipennis*, and *M. rotundicollis* (Fig. 7; character 75, state 0). Two species, *M. lateralis* and *M. sculptopunctatus* include individuals studied for this revision that have brachypterous flight wings the alar surface reduced so that little of the wing extends beyond the wing fold (character 75, state 1). And two other species, *M. lissus* of Java and *M. montivagus* of Hawaii, exhibit flight wings reduced to stenopterous straps that extend beyond the apex of the metanotum, though the alar surface is very narrow and the medial and cubital wing veins are greatly reduced (character 75, state 2). In the initially diverging subgenus *Eucyclothorax*, two of the nine species are known from macropterous individuals–*M. blackburni* and *M. eyrensis*–and two exhibit dimorphic wing polymorphism with the flight wings either fully developed or completely vestigialized; *M. peryphoides* and *M. lophoides* (Fig. 7). The other four species of *Eucyclothorax* are all monomorphically vestigially winged. These four examples of wing presence in *Eucyclothorax* and three examples of wing presence in subgenus *Mecyclothorax* stand in stark contrast to the hundreds of species that exhibit flight wing loss, in many instances that loss associated with thickening of the cuticle, and remarkable changes in body shape (Figs 8B–C, 9, 16, 20). The metathoracic flight wing character was coded as an unordered four-state character so as not to unduly distort the cladistic analysis. This is especially important as the wing-dimorphic taxa polymorphically exhibit the end states 0 and 3 along the character transformation series. Although this cladistic analysis is based on the principal of parsimony–i.e. minimizing the number of character-state changes in either direction on the cladogram–this reduction character should be interpreted under Dollo Parsimony (Farris 1977); i.e., the evolutionary transformation, in this case the loss of flight wings, cannot be reversed in the cladistic hypothesis.

The interpretation of carabid beetle flight wing loss under Dollo Parsimony is consistent with flight wing polymorphism in carabid beetles and the observed transformation over ecological time from populations comprising predominantly macropterous individuals to those within which nearly all individuals lack wings. Such a change was documented over only two seasons in a population of *Trechus obtusus* colonizing a newly available polder in the Netherlands (den Boer 1970). This phenomenon was observed again in Hawaii, when samples of *T. obtusus* taken after colonization of Maui in 1998 by this European species contained only macropterous individuals (Liebherr and Takumi 2002), but samples subsequently taken four years later at the same site contained 33% brachypterous individuals (Liebherr and Krushelnycky 2007). Wing polymorphism is determined by few genes in those carabid beetles studied, with a single gene determining wing development in the European *Pterostichus anthracinus* (Illiger) (Lindroth 1946) and *P. melanarius* (Illiger) (Aukema et al. 1996). A somewhat more complex hereditary basis involving either two genes or three alleles of one gene is posited for *Bembidion lampros* (Herbst), where several different brachypterous forms complement the macropterous form (Langor and Larson 1983). In these three instances, the macropterous allele is recessive to the brachypterous, necessitating the presence of either a homozygous or heterozygous brachypterous individual within a propagule in order to introduce the short-winged allele to a new locale. If that new location offers ecological stability, selection will favor brachypterous individuals due to physiological advantage (Darlington 1936, Southwood 1977), or disfavor flighted individuals due to increased mortality (Darwin 1859, Short and Liebherr 2007), or both (Kavanaugh 1985). The end point

of these strong selective forces, assuming the habitat is stable enough to preclude extinction of the populations or species, is functional elimination of the recessive macropterous allele from the population, and the cascade of evolutionary changes to the metathoracic flight apparatus–foreshortening of the segment, sclerite fusion–and modification of the elytra, now converted to dorsal protective shells without the need to open during flight.

Given the preponderance of brachypterous lineages branching off the *Mecyclothorax* radiation, with isolated radiations occupying New Zealand, New Caledonia, New Guinea, and Polynesia, it is tempting to suggest that the many independent origins of island lineages during the evolution of *Mecyclothorax* may have been accomplished by 100% brachypterous propagules. Such a conclusion is contrary to the evidence for at least some of the radiations. The Hawaiian *Mecyclothorax* include the most generalized species, *M. montivagus*, individuals of which retain stenopterous wing stubs 3.3× long as broad with rudimentary Sc, R, M, and Cu veins present, indicating this species' recently evolved brachypterous condition. Similarly, species of the generalized *M. striatopunctatus* group in Tahiti–e.g. *M. curtisi* Liebherr (2013)–exhibit stenopterous wing rudiments 4× long as wide, with the alar surface including rudimentary Sc, R, and M veins. The cladistic relationships among the four macropterous or wing-polymorphic species in subgenus *Eucyclothorax* ambiguously optimize the base of that clade as either macropterous or brachypterous. It is among the subgenera *Qecyclothorax*, *Meonochilus*, and *Phacothorax*, that all evidence of macroptery has been evolutionarily erased. One could argue that flight wings have re-evolved with a small subset of species in subgenus *Mecyclothorax* à la Whiting et al. (2003). However that would require reversals in a suite of characters associated with metathoracic reduction, and elytral configuration including fusion along the sutural margin. An interpretation of independent, repetitive wing loss, as repeatedly observed within wing-polymorphic populations during ecological time (den Boer 1970), is preferred as an explanation for the observed pattern of brachyptery (Trueman et al. 2004).

Mecyclothorax genitalic evolution

Isolation of closely related carabid beetle species is mediated by physical incompatibility between the male aedeagal intromittent organ and the female bursa copulatrix (Nagata et al. 2009, Kubota et al. 2013). Specific structures of the male aedeagal internal sac may interact with specific structures or lobes in the bursa to emplace or remove male spermatophores (Jeannel 1941, fig. 30), positioning the mating male's spermatophore near the spermathecal duct (Okuzaki and Sota 2014). Correlation of male and female reproductive parts is documented here for the adelphotaxa *M. fleutiauxi* and *M. jeanneli*. Females of both species exhibit a bilobed bursa copulatrix, with a dorsal lobe complementing the plesiomorphically present ventral lobe. In females of *M. fleutiauxi*, the dorsal lobe is much shorter than the ventral lobe (Fig. 12D), and the spermathecal duct enters at its apex. In *M. jeanneli* females the spermathecal duct also enters the apex of the bursal dorsal lobe, but the lobe itself is as long as the ventral lobe (Fig. 12E). The aedeagal internal sac is also bilobed in these two species, with an apical lobe that bears the reduced flagellar sheath at its apex and a dorsal lobe that extends from the sac near the base of the ostial opening (Fig. 10L versus Q). The dorsal lobe is of similar length for the two species, however the apical lobe is much shorter in males of *M. fleutiauxi* (Fig. 10L), being about half the length of the dorsal lobe. In contrast, the apical and dorsal lobes are of approximately equal length in *M. jeanneli* males. Given the male above, head to head mating posture of carabid beetles that necessitates inversion of the male's aedeagus from its anatomical position (Deuve 1993), the male's apical lobe would enter the female's bursal dorsal lobe –the lobe joining the spermathecal duct–during intromission, and the male's dorsal lobe would inflate to fill at least part of the female's ventral lobe; the lobe joining the common oviduct. The male gonopore is associated with the flagellum, in these instances represented by the reduced flagellar sheath, and so in both species, the apex of the male apical lobe would be proximate to the base of the spermathecal duct at the apex of the female dorsal lobe. Given the lack of any known zone of parapatry between these two species (Fig. 15), it is not known how these two species may interact when individuals are present at the same site. The frontier between these two species is correlated with a faunal break isolating the southern five species restricted to ultramafic substrates (Fig. 27B). Thus given present knowledge, an initial hypothesis is proposed wherein these correlated structures of *M. fleutiauxi* and *M. jeanneli* evolved in allopatry.

Occurrence of either bilobed male aedeagal internal sacs or bilobed female bursae has been documented repeatedly for species in subgenus *Mecyclothorax*. Males of *M. bilobatus* Liebherr from Haleakalā, Maui have bilobed internals sacs, with the large scoop-like flagellar plate characteristic of the subgenus located at the apex of the apical lobe (Liebherr 2015, figs 150E–F), however this species is characterized by a single-lobed female bursa (Liebherr 2015, fig. 145D). The converse presence of bilobed female bursae and single-lobed male aedeagal sacs has evolved independently four times among various species in Hawaii and New Zealand: **1**, *M. oculatus* Sharp of Molokai (Liebherr 2007, fig. 125); **2**, *M. flavipes* Liebherr of Lanai (Liebherr 2009a, fig. 4A); **3**, *M. simiolus* (Blackburn) of Oahu (Liebherr 2009b, fig. 14C); and **4**, *M. oopteroides* Liebherr & Marris from New Zealand (Liebherr and Marris 2009, fig. 18). Details among these instances of bilobed bursae vary, including differential lengths of dorsal versus ventral lobes, and possible presence of sclerotization on the dorsal lobe. These details strongly support an underlying developmental pathway that triggers a bilobed bursa, though other genes are differentially associated with that genetic program resulting in different configurations of the bilobed condition.

However, the association of male and female "bilobism" observed for the New Caledonian *M. fleutiauxi* and *M. jeanneli* is unique among *Mecyclothorax* species studied to date.

Infraspecific variation of the male genitalia can be documented for several species of New Caledonian *Phacothorax* recognized in this revision. Males of *M. laterosinuatus* exhibit uniform flagellar structures associated with the internal sac (Fig. 10C, D), however the aedeagal median lobe differs about 10% in length for males of nearly the same external body dimensions. As no other external characters diagnose these males, they were considered conspecific, though of course more specimens or molecular sequence data could provide the means to assign these populations to more than one species. The aedeagal tip in males of *M. fleutiauxi* varies in length and dorsoventral breadth among individuals available for study (Fig. 15A–E), though individuals within population samples exhibit relatively consistent aedeagal conformations. Much more dramatic aedeagal variation is presented by members of *M. kanak*, a comparatively widespread species across southern Grand Terre (Fig. 26A–I). No external anatomical characters allowed differential diagnosis of the individuals studied from these population samples. Moreover, while all but one of the males exhibited the diagnostic invaginated "hitch" at the apex of the median lobe, other attributes of the aedeagal apex–e.g., dorsoventral breadth, apical curvature, length of the dorsal projection relative to the ventral tip, and whether the ventral tip was rounded or acuminate–varied somewhat within some of the population samples (e.g., Mt. Dzumac, Mts. Koghis, Fig. 26C, F). In several instances, aedeagal configuration differs dramatically among samples separated by 10–20 kilometres; e.g. Mt. Humboldt low elevation versus high elevation sites (Fig. 26A–B), and Col de Yaté versus Pic du Grand Kaori (Fig. 26G–H). The general pattern of geographic variation that can be advanced involves the occurrence of longer and more curved apical portions of the median lobe toward the southern limits of Grand Terre. The endpoint for this trend would be the two males known from Col de Yaté, where the apical portion of the lobe beyond the ostial opening is extremely narrow and distinctly curved. What the relatively smaller, though non-diagnostic body size exhibited by the three known specimens from Col de Yaté signifies must await more data. Among all the examined *M. kanak* males, one stands out due to its lack of the "hitch" in the median lobe apical margin (Fig. 26, sample A, Mt. Humboldt 1300–1400 m elevation). This male is one of nine other syntopic males, with the complementary eight exhibiting the diagnostic apical invagination (Fig. 26). That this specimen represents a hybrid between *M. kanak* and *M. manautei* (the only other sympatric, small bodied species) can be discounted because the aedeagus of *M. manautei* males exhibits extensive internal sac spination and a broad, asymmetrical apex (Fig. 17I), traits not present in this non-conforming male. At present this male's aedeagal configuration can only be interpreted to represent an extreme in aedeagal morphology observed within this species.

The amount and manner of variation in the *M. kanak* male aedeagus is much greater than that observed within species of the very speciose *Mecyclothorax* radiation from Haleakalā, Maui (Liebherr 2015). Among the more widespread species of that 116-species radiation–e.g. species with distributions spanning either the 20–30 km breadth of Haleakalā's windward forest, or elevations ranging 1200–2800 m–aedeagal conformation is remarkably stable and thus extremely useful for species diagnosis; e.g. *M. consanguineus* Liebherr (Liebherr 2015, figs 34–35), *M. cordithorax* Liebherr (ibid, figs 88–89), and *M. montivagus* (Blackburn) (ibid, figs 131–132). These widespread, morphologically consistent species occur within a diverse species swarm where up to 39 *Mecyclothorax* spp. have been recorded from a 1′ × 1′ quadrat (Fig. 28A). The 63 such latitude × longitude quadrats occupied by *Mecyclothorax* on Haleakalā house an average of nine species. With such extensive species packing, even given the diversity of microhabitats from which these beetles have been recorded, and the extensive variation in body size represented among the various species, more uniform genitalia within species would allow more precise species recognition during male-female encounters (Nagata et al. 2009, Okuzaki and Sota 2014). The very low levels of sympatry in New Caledonia, where maximally four *Mecyclothorax* species occur at any locality (average of 1.9 species per locality; Fig. 27A), are associated with more extensive infraspecific male genitalic variation. A useful intermediate comparison may be made using the *Mecyclothorax* fauna of Hawaii Island (Liebherr 2008b), an island housing 30 species of *Mecyclothorax*. Taking the larger area of that island into consideration (10,432 km^2 versus 1450 km^2 for Haleakalā), a calculation of sympatry level using 5′ × 5′ latitude × longitude quadrats results in an average of 4.2 species per occupied quadrat, with a maximal quadrat diversity of 12 species (Fig. 28B). In this fauna, based on multiple dissections of specimens, two species have been shown to exhibit extensively variable male genitalia. *Mecyclothorax deverilli* (Blackburn) (Liebherr 2008b, figs 67–78) and *M. konanus* Sharp (ibid, figs 153–165). Patterns of variation in both species represent a mosaic of forms not associated strongly with geographic distance. In fact, variation among males of *M. konanus* is rampant as much within collecting series as it is among samples separated by up to 70 km straight-line distance, as demonstrated by a parsimony network based on 12 aedeagal attributes joining 84 specimens (Liebherr 2008b, fig. 181). Although data are preliminary, male aedeagal morphology is also infraspecifically variable among New Guinea *Mecyclothorax* (Liebherr 2017b), with *M. andersoni* exhibiting variation in the median lobe apex similar to that observed in *M. kanak*. The New Guinean fauna is very poorly known, however based on current knowledge sympatry levels are very low with a maximum of two species known from any locality. As male genitalic morphology in carabid beetles has been shown

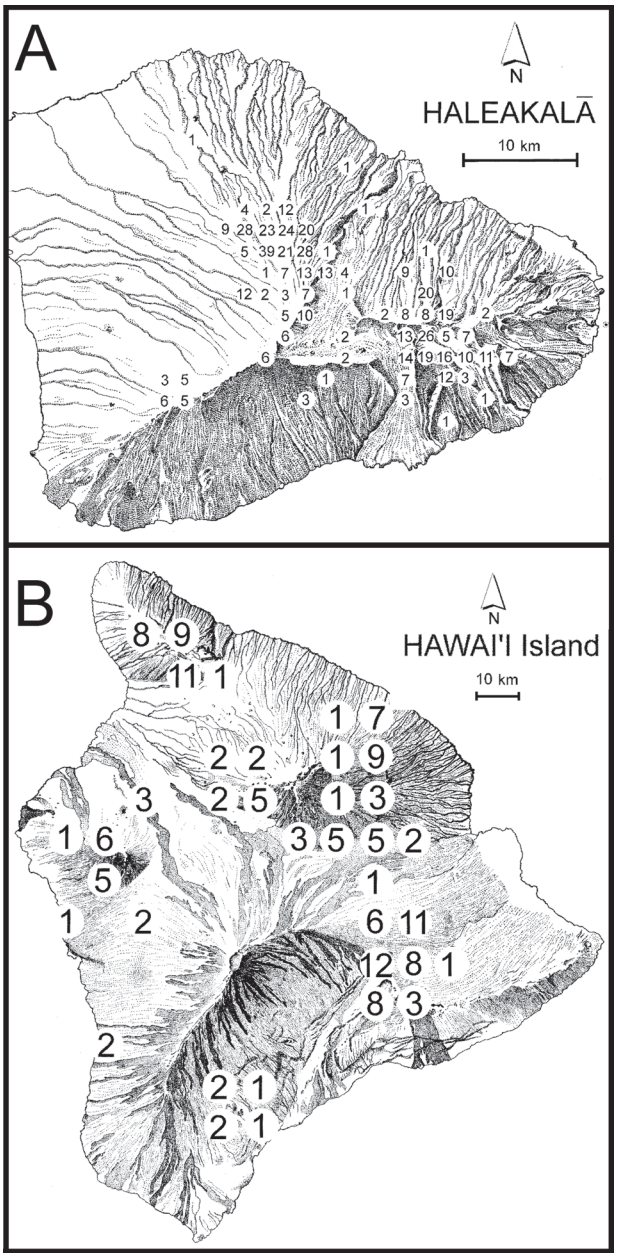

Figure 28. Number of *Mecyclothorax* spp. present in latitude × longitude quadrats for two Hawaiian Islands: **A**, Haleakalā volcano, Maui (area 1450 km^2) with species recorded within 1′ × 1′ cells; **B**, Hawai`i Island (10,432 km$^2$) with species recorded within 5′ × 5′ cells. A total of 116 species of *Mecyclothorax* are known to occur on Haleakalā (Liebherr 2015), and 30 species are known from Hawai`i Island (Liebherr 2008b).

to be controlled by relatively few genes (Sasabe et al. 2007), large amounts of infraspecific genitalic variation in depauperate *Mecyclothorax* faunas support the presence of abundant genetic variability in and among populations of these flightless species (Liebherr 1988, Ikeda et al. 2012). Thus the patterns of variation observed among these anatomically variable species supports the existence of genetic variation sufficient for subsequent diversification and adaptation as observed in the hyperdiverse island radiations.

Acknowledgements

This study was made possible through the kind loan offer of significant numbers of New Caledonian *Mecyclothorax* specimens made by Dr. Geoff Monteith, Queensland Museum. Receipt of additional specimens from other curators resulted in access to specimens from nine institutional and two personal collections. I thank the following curators and collection managers (institutional coden presented in Material and Methods follows parenthetically): James Boone (BPBM); Yves Bousquet (CNC); Jason Dombroskie, Cornell University Insect Collection (CUIC); Peter Oboyski and Kipling W. Will (EMEC); Győző Szél, Hungarian Natural History Museum, Budapest (HNHM); Giuluo Cuccodoro, Muséum d'Histoire naturelle, Genève (MHNG); Thierry Deuve and Azadeh Taghavian (MNHN); Pawel Jałoszyński (MNHW); Manfred Jäch (NHMW); Susan Wright (QMB); Martin Baehr personal collection (MBC); Pier M. Giachino personal collection (PMGC). Additional specimens were used for the cladistic analysis of *Mecyclothorax* and allied genera, with the following curators and collection managers thanked for access to that material: Robert L. Davidson, Carnegie Museum of Natural History, Pittsburgh; Borislav Guéorguiev, National Museum of Natural History, Sofia; Peter Hudson, South Australian Museum, Adelaide; Beulah Garner, The Natural History Museum, London; Kate Lemann, Australian National Insect Collection, Canberra; John Marris, Lincoln University Entomological Research Collection, Canterbury, New Zealand; Catriona McPhee, Museums Victoria, Melbourne; Philip D. Perkins, Museum of Comparative Zoology, Harvard University, Cambridge; Roberto Poggi, Museo Civico di Storia Naturale "G. Doria", Genova; Chris Reid, Australian Museum, Sydney; Danny Shpeley, Strickland Entomological Museum, University of Alberta, Edmonton. I thank Manfred Jäch for providing a copy the pertinent pages of Herbert Franz's field notebook that detail the itinerary and stops during his 1970 New Caledonian expedition. Photographic equipment essential to this research project was underwritten by National Science Foundation award DEB-0315504. I thank Borislav Guéorguiev and Kipling W. Will for their comprehensive critical editorial reviews, which substantially improved the manuscript.

References

Allen RT, Ball GE (1980) Synopsis of Mexican taxa of the *Loxandrus* series (Coleoptera: Carabidae: Pterostichini). Transactions of the American Entomological Society 105: 481–576.

Andrewes HE (1933) On some new species of Carabidae, chiefly from Java. Treubia 14: 273–286.

Andrewes HE (1939) Papers on Oriental Carabidae.–XXXV. On the types of some Indian genera. Annals and Magazine of Natural History 3(series 11): 128–139.

Aukema B, Spee AJ, van Dijk TS (1996) Wing dimorphism and development in Pterostichus melanarius (Coleoptera: Carabidae). Entomologische berichten (Amsterdam) 56: 93–100.

Baehr M (1992) A new *Mecyclothorax* Sharp from New Guinea (Insecta, Coleoptera, Carabidae, Psydrinae). Spixiana 15: 249–252.

Baehr M (1995) The genus *Mecyclothorax* Sharp, 1903 in New Guinea (Coleoptera, Carabidae, Psydrinae). Mitteilungen der Münchner Entomologische Gesellschaft 85: 3–19.

Baehr M (1998) A further new species of the genus *Mecyclothorax* Sharp from western New Guinea. Spixiana 21: 21–24.

Baehr M (2002) Two new species of the genus *Mecyclothorax* Sharp from Papua New Guinea (Insecta, Coleoptera, Carabidae, Psydrinae). Revue Suisse de Zoologie 109: 695–704. https://doi.org/10.5962/bhl.part.79563

Baehr M (2003) Psydrine ground beetles (Coleoptera: Carabidae: Psydrinae), excluding Amblytelini, of eastern Queensland rainforests. Memoirs of the Queensland Museum 49: 65–109.

Baehr M (2004) The Amblytelini. A tribe of corticolous ground beetles from Australia. Taxonomy, phylogeny, biogeography. (Coleotera: Carabidae: Psydrinae). Coleoptera 8: 286 pp.

Baehr M (2008) Two new species of the genus *Mecyclothorax* Sharp from New Guinea (Coleoptera: Carabidae: Psydrinae). Tijdschrift voor Entomologie 151: 133–140. https://doi.org/10.1163/22119434-900000258

Baehr M (2009) A new species of the genus *Mecyclothorax* Sharp from New South Wales (Insecta: Carabidae: Psydrinae). Records of the Australian Museum 61: 89–92. https://doi.org/10.3853/j.0067-1975.61.2009.1519

Baehr M (2014) A new species of the genus *Mecyclothorax* Sharp from New Guinea (Coleoptera, Carabidae, Psydrini, Mecyclothoracina). Spixiana 37: 123–129.

Baehr M (2016) A new subspecies of *Mecyclothorax punctatus* (Sloane) from south-western Australia. Spixiana 39: 93–97.

Baehr M, Lorenz W (1999) A reevaluation of *Loeffleria globicollis* Mandl from Borneo (Insecta, Coleoptera, Carabidae, Psydrinae). Spixiana 22: 263–267.

Baehr M, Reid CAM (2017) On a collection of Carabidae from Timor Leste, with descriptions of nine new species (Insecta: Coleoptera: Carabidae). Records of the Australian Museum 69: 421–450. https://doi.org/10.3853/j.2201-4349.69.2017.1660

Britton EB (1948) A revision of the Hawaiian species of *Mecyclothorax* (Coleoptera: Carabidae). Occasional Papers of the Bernice P. Bishop Museum 19: 107–166.

Buckley TR, Attanayake D, Nylander JAA, Bradler S (2010) The phylogenetic placement and biogeographical origins of the New Zealand stick insects (Phasmatodea). Systematic Entomology 35: 207–225. https://doi.org/10.1111/j.1365-3113.2009.00505.x

Csiki E (1931) Carabidae: Harpalinae V., Coleopterorum Catalogus. In Junk W, Schenkling S (Eds) Dr W Junk Publishers, Berlin 115: 739–1022.

Darlington PJ Jr (1936) Variation and atrophy of flying wings of some carabid beetles. Annals of the Entomological Society of America 24: 136–179. https://doi.org/10.1093/aesa/29.1.136

Darlington PJ Jr (1952) The carabid beetles of New Guinea part 2. the Agonini. Bulletin of the Museum of Comparative Zoology 107: 89–252 + 4 pls.

Darwin C (1859) On the Origin of Species. John Murray, London.

den Boer PJ (1970) On the significance of dispersal power for populations of carabid-beetles (Coleoptera: Carabidae). Oecologia 4: 1–28. https://doi.org/10.1007/BF00390612

Deuve T (1987) Descriptions de deux carabiques nouveaux de Nouvelle-Caledonie et de Thaïlande (Coleoptera, Caraboidea, Psydridae, Trechidae). Revue française d'Entomologie (NS) 9: 143–146.

Deuve T (1993) L'abdomen et les genitalia des femelles de Coléoptères Adephaga. Mémoires du Muséum national d'Histoire naturelle Serie A Zoologie 155: 1–184.

Enderlein G (1909) 9. Des Insektenfauna der Insel Neu-Amsterdam. In Enderlein G (ed). Die Insekten des Antarktischen Gebietes, 10. Druck und Verlag von Georg Reimer, Berlin: pp. 486–492.

Farris JS (1977) Phylogenetic Analysis Under Dollo's Law. Systematic Zoology 26: 77–88. https://doi.org/10.2307/2412867

Frauenfeld GR von (1868) Zoologische Miscellen, XV. Verhandlungen der kaiserlich-königlichen zoologisch-botanischen Gesellschaft in Wien 18(6 Mai): 885–899.

Goloboff PA (1999) NONA (NO NAME). Tucumán, Argentina, Published by the author. http://www.softpedia.com/get/Science-CAD/NONA.shtml [accessed 6-ix-2016]

Google Earth Pro (2017) Earth version 7.1.8.3036, https://earth.google.com/ [Accessed 2-ix-2017]

Grandcolas P, Murienne J, Robillard T, Desutter-Grandcolas L, Jourdan H, Guilbert E, Deharveng L (2008) New Caledonia: a very old Darwinian island? Philosophical Transactions of the Royal Society B 363: 3309–3317. https://doi.org/10.1098/rstb.2008.0122

Guéorguiev B (2013) Taxonomic, nomenclatural, and faunistic records for species in tribes Melaenini, Moriomorphini, Pterostichini, Licinini, and Sphodrini (Coleoptera: Carabidae). Zootaxa 3709: 52–70. https://doi.org/10.11646/zootaxa.3709.1.2

Hennig W (1966) *Phylogenetic Systematics*. University of Illinois Press, Champaign-Urbana.

Herzer RH, Charponiere GCH, Edwards AR, Hollis CJ, Pelletier B, Raine JI, Scott GH, Stagpoole V, Strong CP, Symonds P, Wilson GJ, Zhu H (1997) Seismic stratigraphy and structural history of the Reinga Basin and its margins, southern Norfolk Ridge system. New Zealand Journal of Geology and Geophysics 40: 425–451. https://doi.org/10.1080/00288306.1997.9514774

Hildenbrand A, Gillot P-Y, Le Roy I (2004) Volcano-tectonic and geochemical evolution of an oceanic intra-plate volcano: Tahiti-Nui (French Polynesia). Earth and Plaetary Science Letters 217: 349–365. https://doi.org/10.1016/S0012-821X(03)00599-5

Ibanez T, Blanchard E, Hequet V, Keppel G, Laidlaw M, Pouteau R, Vandrot H, Birnbaum P (2017) High endemism and stem density distinguish New Caledonian from other high-diversity rainforests in the Southwest Pacific. Annals of Botany, mcx107. https://doi.org/10.1093/aob/mcx107

Ikeda H, Nishikawa M, Sota T (2012) Loss of flight promotes beetle diversification. Nature Communications 3: 648. https://doi.org/10.1038/ncomms1659

International Commission on Zoological Nomenclature (1999) *International Code of Zoological Nomenclature*. London, England, The International Trust for Zoological Nomenclature. http://iczn.org/iczn/index.jsp [accessed 12 September 2017]

Jeannel R (1940) Coléoptères. In Jeannel R (ed). Croisière de Bougainville aux Iles Australes Françaises. Mémoires de Muséum National d'Histoire Naturelle, Paris 14(N.S.): 63–201.

Jeannel R (1941) Coléoptères Carabiques, première partie. Faune de France 39: 1–571.

Jeannel R (1942) La Genèse des Faunes Terrestres: Éléments de Biogéographie. Presses Universitaires de France, Paris.

Jeannel R (1944) Un carabique nouveau de la Nouvelle-Calédonie. Revue Française d'Entomologie 10: 84–86.

Jeannel R (1955) L'Édéage, initiation aux recherches sur la systématique des Coléoptères. Publications du Muséum national d'Histoire naturelle No. 16: 155 pp.

Jones JG, McDougall I (1973) Geological history of Norfolk and Philip Islands, southwest Pacific Ocean. Journal of the Geological Society of Australia 20: 239–254. https://doi.org/10.1080/14400957308527916

Kavanaugh DH (1985) On wing atrophy in carabid beetles (Coleoptera: Carabidae) with special reference to *Nebria*. In Ball GE (ed). Taxonomy, Phylogeny and Zoogeography of Beetles and Ants, Dr W Junk Publishers, Dordrecht: 408–431.

Kennedy DM, Brooke BP, Woodroffe CD, Jones BG, Waikari C, Nichol S (2011) The geomorphology of the flanks of Lord Howe Island volcano, Tasman Sea, Australia. Deep-Sea Research II 58: 899–908. https://doi.org/10.1016/j.dsr2.2010.10.046

Kubota K, Miyazaki K, Ebihara S, Takami Y (2013) Mechanical reproductive isolation via divergent genital morphology between *Carabus insulicola* and *C. esakii* with implications in species coexistence. Population Ecology 55: 35–42. https://doi.org/10.1007/s10144-012-0335-4

Ladiges PY, Cantrill D (2007) New Caledonia–Australian connections: biogeographic patterns and geology. Australian Systematic Botany 20: 383–389. https://doi.org/10.1071/SB07018

Ladiges P, Parra-O C, Gibbs A, Udovicic F, Nelson G, Bayly M (2011) Historical biogeographical patterns in continental Australia: congruence among areas of endemism of two major clades of eucalypts. Cladistics 27: 29–41. https://doi.org/10.1111/j.1096-0031.2010.00315.x

Langor DW, Larson DJ (1983) Alary polymorphism and life history of a colonizing ground beetle, *Bembidion lampros* Herbst (Coleoptera: Carabidae The Coleopterists Bulletin 37: 365–377.

Liebherr JK (1988) Geme flow in ground beetles (Coleoptera: Carabidae) of different habitat preference and flight-wing development. Evolution 42: 129–137. https://doi.org/10.1111/j.1558-5646.1988.tb04113.x

Liebherr JK (2007["2006"]) Taxonomic revision of the *Mecyclothorax* beetles (Coleoptera: Carabidae, Psydrini) of Molokai, Hawaii and recognition of areas of endemism on Kamakou volcano. Journal of the New York Entomological Society 114: 179–281. https://doi.org/10.1664/0028-7199(2007)114[179:TROTMB]2.0.CO;2

Liebherr JK (2008a) *Mecyclothorax kavanaughi* sp. n. (Coleoptera: Carabidae) from the Finisterre Range, Papua New Guinea. Tijdschrift voor Entomologie 151: 147–154. https://doi.org/10.1163/22119434-900000260

Liebherr JK (2008b) Taxonomic revision of *Mecyclothorax* Sharp (Coleoptera, Carabidae) of Hawaii Island: abundant genitalic variation in a nascent island radiation. Deutsche Entomologische Zeitshrift 55: 19–78. https://doi.org/10.1002/mmnd.200800004

Liebherr JK (2009a) Native and alien Carabidae (Coleoptera) share Lanai, an ecologically devastated island. The Coleopterists Bulletin 63: 383–411. https://doi.org/10.1649/1176.1

Liebherr JK (2009b) Taxonomic revision of the *Mecyclothorax* beetles (Coleoptera: Carabidae) of Oahu: epithets as epitaphs for an endangered fauna? Systematic Entomology 34: 649–687. https://doi.org/10.1111/j.1365-3113.2009.00477.x

Liebherr JK (2011) Cladistic assessment of subtribal affinities within the tribe Moriomorphini with description of *Rossjoycea glacialis*, gen. n. and sp. n. from the South Island, and revision of *Meonochilus* Liebherr and Marris from the North Island, New Zealand (Coleoptera, Carabidae ZooKeys 147: 277–335. https://doi.org/10.3897/zookeys.147.1898

Liebherr JK (2012) The first precinctive Carabidae from Moorea, Society Islands: new *Mecyclothorax* spp. (Coleoptera) from the summit of Mont Tohiea. ZooKeys 224: 37–80. https://doi.org/10.3897/zookeys.224.3675

Liebherr JK (2013) The *Mecyclothorax* beetles (Coleoptera, Carabidae, Moriomorphini) of Tahiti, Society Islands. ZooKeys 322: 1–170. https://doi.org/10.3897/zookeys.322.5492

Liebherr JK (2015) The *Mecyclothorax* beetles (Coleoptera, Carabidae, Moriomorphini) of Haleakalā, Maui: Keystone of a hyperdiverse Hawaiian radiation. ZooKeys 544: 1–407. https://doi.org/10.3897/zookeys.544.6074

Liebherr JK (2016) *Cyphocoleus* Chaudoir (Coleoptera, Carabidae, Odacanthini): descriptive taxonomy, phylogenetic relationships, and the Cenozoic history of New Caledonia. Deutsche Entomologische Zeitschrift 63: 211–270. https://doi.org/10.3897/dez.63.10241

Liebherr JK (2017a) *Bryanites graeffi* sp. n. (Coleoptera, Carabidae): museum rediscovery of a relict species from Samoa. Zoosystematics and Evolution 93: 1–11. https://doi.org/10.3897/zse.93.10802

Liebherr JK (2017b) Review of *Mecyclothorax* Sharp (Coleoptera: Carabidae: Moriomorphini) from Papua New Guinea with descriptions of five new species. The Coleopterists Bulletin 71: 679–703.

Liebherr JK, Krushelnycky PD (2007) Unfortunate encounters? Novel interactions of native *Mecyclothorax*, alien *Trechus obtusus* (Coleoptera: Carabidae), and Argentine ant (*Linepithema humile*, Hymenoptera: Formicidae) across a Hawaiian landscape. Journal of Insect Conservation 11: 61–73. https://doi.org/10.1007/s10841-006-9019-8

Liebherr JK, Marris JWM (2009) Revision of the New Zealand species of *Mecyclothorax* Sharp (Coleoptera: Carabidae: Psydrinae, Mecyclothoracini) and the consequent removal of several species to *Meonochilus* gen. n. (Psydrinae: Meonini New Zealand Entomologist 32: 5–22.

Liebherr JK, Takumi R (2002) Introduction and distributional expansion of *Trechus obtusus* (Coleoptera: Carabidae) in Maui, Hawaii. Pacific Science 56: 365–375.v https://doi.org/10.1353/psc.2002.0035

Liebherr JK, Will KW (1998) Inferring phylogenetic relationships within Carabidae (Insecta, Coleoptera) from characters of the female reproductive tract. In Ball GE, Casale A, Vigna Taglianti V (eds Atti Museo Regionale di Scienze Naturali, Museo Regionale di Scienze Naturali, Torino: 107–170.

Lindroth CH (1946) Inheritance of wing dimorphism in *Pterostichus anthracinus* Ill. Hereditas 32: 37–40. https://doi.org/10.1111/j.1601-5223.1946.tb02769.x

Lindroth CH (1974) On the elytral microsculpture of carabid beetles (Col.). Carabidae Entomologica Scandanavica 5: 251–264. https://doi.org/10.1163/187631274X00290

Lorenz W (1998) Nomina Carabidarum, A Directory of the Scientific Names of Ground Beetles. Published by the author, Tutzing.

Lorenz W (2005) Systematic List of Extant Ground Beetles of the World (Insecta Coleoptera "Geadephaga": Trachypachidae and Carabidae incl. Paussinae, Cicindelinae, Rhysodinae), 2nd Ed. Published by the author, Tutzing.

Louwerens CJ (1949) Some notes on the Carabidae, collected by Mr. P. H. van Doesburg in the Malay Archipelago with descriptions of new species. Tijdschrift voor Entomologie 90: 45–53.

Louwerens CJ (1953) Carabidae (Col.) from the Sunda Islands. Verhandlungen der Naturforschenden Gesellschaft in Basel 64: 303–327.

MacLeay W (1871) Notes on a collection of insects from Gayndah. Transactions of the Entomological Society of New South Wales 2(2): 79–205.

Mandl K (1969) Zwei neue *Heptodonta*-Arten und eine neue Carabidae-Gattung (Col.) aus Nord-Borneo. Zeitschrift der Arbeitsgemeinschaft Österreiches Entomologen 21: 51–54.

Moore BP (1963) Studies on Australian Carabidae (Coleoptera)–3. the Psydrinae. Transactions of the Royal Entomological Society, London 115: 277–290. https://doi.org/10.1111/j.1365-2311.1963.tb00810.x

Moore BP (1984) Taxonomic notes on some Australasian *Mecyclothorax* Sharp (Coleoptera: Carabidae: Psydrinae) and descriptions of new species. Journal of the Australian Entomological Society 23: 161–166. https://doi.org/10.1111/j.1440-6055.1984.tb01935.x

Moore BP (1985) The Carabidae of Norfolk Island. In Ball GE (ed Taxonomy, Phylogeny and Zoogeography of Beetles and Ants, Dr W Junk Publishers, Dordrecht: 237–256.

Moore BP (1992) The Carabidae of Lord Howe Island. In Noonan GR, Ball GE, Stork NE (Eds) The Biogeography of Ground Beetles of Mountains and Islands, Intercept Ltd., Andover, Hampshire, UK.

Moore BP, Weir TA, Pyke JE (1987) Coleoptera: Adephaga: Rhysodidae and Carabidae. In: Walton DW (Ed.) Zoological Catalogue of Australia Vol 4, Australian Government Printing Service, Canberra: 17–320.

Mueller-Dombois D, Fosberg FR (1998) Vegetation of the Tropical Pacific Islands. Springer Verlag, New York, Inc. https://doi.org/10.1007/978-1-4419-8686-3

Murienne J, Grandcolas P, Piulachs MD, Bellés X, D'Haese C, Legendre F, Pellens R, Guilbert E (2005) Evolution on a shaky piece of Gondwana: is local endemism recent in New Caledonia? Cladistics 21: 2–7. https://doi.org/10.1111/j.1096-0031.2004.00042.x

Nagata N, Kubota K, Takami Y, Sota T (2009) Historical divergence of mechanical isolation agents in the ground beetle *Carabus arrowianus* as revealed by phylogeographical analyses. Molecular Ecology 18: 1408–1421. https://doi.org/10.1111/j.1365-294X.2009.04117.x

Nattier R, Pellens R, Robillard T, Jourdan H, Legendre F, Caesar M, Nel A, Grandcolas P (2017) Updating the phylogenetic dating of New Caledonian biodiversity with a meta-analysis of the available evidence. Scientific Reports 7(3705). https://doi.org/10.1038/s41598-017-02964-x

Nelson G, Platnick N (1981) Systematics and Biogeography, Cladistics and Vicariance. Columbia University Press, New York.

Nixon KC (1999) The parsimony ratchet, a new method for rapid parsimony analysis. Cladistics 15: 407–414. https://doi.org/10.1111/j.1096-0031.1999.tb00277.x

Nixon KC (2002) WinClada. Ithaca, NY, Published by the author. http://www.softpedia.com/get/Science-CAD/WinClada.shtml [accessed 16-ix-2016]

Okuzaki Y, Sota T (2014) How the length of genital parts affects copulation performance in a carabid beetle: implications for correlated evolution between the sexes. Journal of Evolutionary Biology 27: 565–574. https://doi.org/10.1111/jeb.12323

Perrault GG (1984) La faune des Carabidae de Tahiti VI. révision du genre *Mecyclothorax* (Sharp) (Psydrini 1. le groupe de *M. muriauxi* Perrault (Coleoptera Nouvelle Revue d'Entomologie (NS) 1: 19–31.

Reid CAM, Smith KI (2004) A new genus and first record of Chrysomelinae from New Caledonia (Coleoptera: Chrysomelidae Memoirs of the Queensland Museum 49: 705–711.

Sasabe M, Takami Y, Sota T (2007) The genetic basis of interspecific differences in genital morphology of closely related carabid beetles. Heredity 98: 385–391 https://doi.org/10.1038/sj.hdy.6800952

Sharma P, Giribet G (2009) A relict in New Caledonia: phylogenetic relationships of the family Troglosironidae (Opiliones: Cyphophthalmi Cladistics 25: 279–294. https://doi.org/10.1111/j.1096-0031.2009.00252.x

Sharp D (1903) Coleoptera II. Caraboidea. In Sharp D (ed Fauna Hawaiiensis 3. The University Press, Cambridge: pp. 175–292 + pls. VI–VII.

Sherrod DR, Sinton JM, Watkins SE, Brunt KM (2007) Geological Map of the State of Hawai`i. US Geological Survey Open-File Report 2007-1089, Version 1.0 (22 May 2007). http://pubs.usgs.gov/of/2007/1089/ [accessed 5 July 2013]

Short AEZ, Liebherr JK (2007) Systematics and biology of the endemci water scavenger beetles of Hawaii (Coleoptera: Hydrophilidae, Hydrophilini Systematic Entomology 32: 601–624. https://doi.org/10.1111/j.1365-3113.2007.00403.x

Sloane TG (1903) Studies in Australian Entomology No. XII. New Carabidae (Panagaeini, Bembidiini, Pogonini, Platysmatini, Platynini, Lebiini, with revisional lists of genera and species, some notes on synonymy, &c. Proceedings of the Linnean Society of New South Wales 28: 566–642.

Southwood TRE (1977) Habitat, the templet for ecological strategies? Journal of Animal Ecology 46: 337–365. https://doi.org/10.2307/3817

Trueman JWH, Pfeil BE, Kelchner SA, Yeates DK (2004) Did stick insects *really* regain their wings? Systematic Entomology 29: 138–139. https://doi.org/10.1111/j.0307-6970.2004.00251.x

Whiting MF, Bradler S, Maxwell T (2003) Loss and recovery of wings in stick insects. Nature 412: 264–267. https://doi.org/10.1038/nature01313

Will KW (2011) Taxonomic review of the Pterostichini and Loxandrini fauna of New Caledonia (Coleoptera, Carabidae) ZooKeys 147: 337–397. https://doi.org/10.3897/zookeys.147.1943

Woodroffe CD, Kennedy DM, Brooke BP, Dickson ME (2006) Geomorphological evolution of Lord Howe Island and carbonate production at the latitudinal limit to reef growth. Journal of Coastal Research 22: 188–201. https://doi.org/10.2112/05A-0014.1

Wulf A (2015) The Invention of Nature, Alexander von Humboldt's New World. Alfred A. Knopf, New York.

Wulff AS, Hollingsworth PM, Ahrends A, Jaffré T, Veillon J-M, L'Huillier L, Fogliani B (2013) Conservation priorities in a biodiversity hotspot: analysis of narrow endemic plant species in New Caledonia. PLOS One 8: E73371. https://doi.org/10.1371/journal.pone.0073371

Supplementary material 1

Data file for cladistic analysis of Mecyclothorax Sharp.

Author: James K. Liebherr

Data type: NONA format data file

Link: https://doi.org/10.3897/dez.65.21000.suppl1

Supplementary material 2

Date-locality data for Mecyclothorax (Phacothorax) species represented by more than 50 specimens.

Author: James K. Liebherr

Data type: specimen records

Link: https://doi.org/10.3897/dez.65.21000.suppl2

Dtsch. Entomol. Z. 65 (1) 2018, 65–74 | DOI 10.3897/dez.65.23593

PENSOFT

museum für naturkunde

Mouthpart dimorphism in male and female wasps of *Vespula vulgaris* and *Vespula germanica* (Vespidae, Hymenoptera)

Baranek Bianca[1], Kuba Kenneth[1], Bauder Julia A.-S.[1], Krenn Harald W.[1]

1 *Department of Integrative Zoology, University of Vienna, Althanstraße 14, 1090 Vienna, Austria*

http://zoobank.org/6245AADD-F20E-4B75-81AF-5BB98A79D200

Corresponding author: *Krenn Harald W* (harald.krenn@univie.ac.at)

Received 12 January 2018
Accepted 16 February 2018
Published 13 March 2018

Academic editor:
Dominique Zimmermann

Abstract

Social wasps perform a variety of tasks with their mouthparts. Female workers use them to feed on carbohydrate-rich fluids, to build nests by collecting wood fibers and forming paper, to hunt and manipulate insect prey for feeding larvae as well as for brood care. Since male wasps neither feed on insects nor participate in nest building, sex-specific differences in mouthpart morphology are expected. Despite these different applications, general mouthpart morphology of male and female wasps from the genus *Vespula* was similar. However, males possessed significantly shorter mandibles with fewer teeth than females. Furthermore, the adductor muscles of the mandibles were distinctly smaller in males than in females. Male wasps showed a higher number of sensilla on the mandibles and the labial palpi. Mouthpart dimorphism and functional morphology of fluid uptake are discussed.

Key Words

mandible
sensilla
morphology
feeding
social insects
sexual dimorphism

Introduction

Insect mouthparts are composed of a set of homologous organs that are derived from appendages of head segments adapted to various tasks in context of feeding, defence and nesting. The mouthparts are composed of an unpaired labrum plate in front of the mouth, paired mandibles and paired maxillae as well as an unpaired labium extending from the last head segment (Snodgrass 1935, Seifert 1995). In general, the mandibulate mouthparts of Hymenoptera are characterized by the labio-maxillary complex which is formed by components of the labium and the maxillae (Duncan 1939, Krenn et al. 2005). This unique functional unit of the mouthparts as well as the four-segmented labial palpus are regarded as autapomorphies of the Hymenoptera (Krenn 2007). Adaptations of the labio-maxillary complex for nectar feeding evolved several times independently in many Hymenoptera (Jervis 1998, Jervis and Vilhelmsen 2000). Especially in social wasps, the mouthparts are functionally versatile allowing their use in various kinds of tasks that are reflected by the well-developed biting mandibles and the labio-maxillary complex which is used to take up nectar and other kinds of fluids (Schremmer 1962).

Social wasps collect two main kinds of food. Adult wasps nourish themselves with liquid carbohydrates obtained from honeydew, ripe fruits, flower nectar and sometimes tree sap (Matsuura and Yamane 1990). Female wasps are involved in brood care, nest building and hunting prey, while male wasps do not forage (Schremmer 1962, Spradbery 1973). Females prey mainly on other insects, bite off the wings, legs, and head of the captured prey and convert the remaining parts into a meatball, which is fed to the larvae in the nest (Berland 1928, Schremmer 1962). In addition to supplying themselves and their brood with food, female wasps use their mouth-

parts for cutting and scraping off plant fibers during nest building, for picking up soil and stones when colonizing underground cavities, as well as for the uptake of water. Hence the mandibles and labio-maxillary complex can be compared to a set of microtools for different kinds of tasks. By contrast, male wasps are not involved in brood care and feed on nectar obtained from flowers with freely accessible nectaries (Schremmer 1962, Matsuura and Yamane 1990).

The mouthparts of some *Vespula* species were previously examined in detail (Kirmayer 1909, Duncan 1939, Spradbery 1973). They consist of the large biting mandibles and the labio-maxillary complex (Fig. 1). Each maxilla consists of the slender cardo and the flat stipes with the small lacinia, the lateral galea and the 6-segmented maxillary palpus. The labium can be divided into the submentum, forming the lateral connection to the cardines, the roof-shaped mentum and the prementum bearing the 4-segmented labial palpi as well as the median ligula, composed of the united glossae and paired paraglossae (Duncan 1939, Seifert 1995). The labrum (termed as epipharynx in Seifert 1995) is situated under the frontal rim of the clypeus (termed as labrum in Seifert 1995).

Wasps from the genus *Vespula* are widely distributed in the Northern hemisphere (Greene 1991, Kimsey and Carpenter 2012). During the last decades, researchers focused mainly on behavioural studies of these social wasps (e.g., Matsuura and Yamane 1990, Mauss 2007). The principle composition of the mouthparts is well studied and was found to be very similar in female workers and queens (Kirmayer 1909, Duncan 1939, Spradbery 1973). However, the mouthparts of male wasps were not studied in detail.

The present study used various morphological methods including scanning electron microscopy and micro CT to investigate the micromorphology of the mouthparts in two species of the genus *Vespula*. Detailed examination of the cuticle structures including the sensilla allowed conclusions on the functional morphology of the various parts. Special emphasis is laid on the differences between females (workers and queens) and male wasps. Fundamental sex-specific differences in mouthpart morphology can be expected because of characteristic differences in behaviour of each sex.

Methods

Specimen sampling

8 individuals (2 queens, 4 female workers, 2 males) of *Vespula germanica* (Fabricius, 1793) and 7 individuals (3 queens, 4 female workers) of *Vespula vulgaris* (Linnaeus, 1758) were used for light microscopy. Eighteen individuals of *V. germanica* were measured including nine female workers and nine males. 4 individuals of *V. germanica* (1 queen, 1 female worker, 2 males) and 8 individuals of *V. vulgaris* (5 female workers, 3 males) were used for scanning electron microscopy. 1 female worker and 1 male individual of *V. germanica* were used for micro CT to compare the musculature of the mandibles in different sexes.

Light microscopy (LM)

The mouthpart components were extracted from the head using a pair of scissors, forceps and dissecting needles. The disaggregated mouthparts were rinsed with deionized water for 10 minutes and were subsequently transferred into 30 % lactic acid. The musculature dissolved after 120 hours on the vibrating unit at room temperature. The mouthparts were rinsed for 10 minutes, transferred to 30 % ethanol for several minutes and put into a drop of polyvinyl-lactophenol on a hollow microscopic slide which was covered with coverslip. The slides were dried in a fume hood for several days before examination with a light microscope (Nikon Laborphot 2) and a stereomicroscope (Nikon SMZ 10). Micrographs were taken using a light microscope (Nikon Eclipse E 800) with an attached camera (Nikon DS-Fi2 U3) and NIS-elements software.

Morphometry

The heads were placed in a small watch glass filled with sand, arranged under the stereomicroscope (Nikon SMZ 10) and imaged with an attached Samsung Digimax V50 camera. Length measurements of the mandibles and other parts of the head were conducted in both sexes (N=18). For the comparison of mandible size to head size three different measurements were performed using ImageJ (US National Institutes of Health, Bethesda, USA): (1) Mandible length measured from the anterior articulation to the tip of the third tooth; (2) Length from the basis of the scapus of one antenna to the distal ridge of the clypeus; (3) Length of the head from the vertex to the distal ridge of the clypeus (Fig. 1A). Data were analysed using a Mann-Whitney U-Test (SPSS Statistics 23.0, IBM Corporation, New York, USA). The significance level was set at $p = 0.05$.

Scanning electron microscopy (SEM)

Wasp heads and mouthparts were dehydrated in an ascending ethanol series, subsequently submerged in 100% acetone for 90 minutes and transferred to hexamethyldisilazane for 60 minutes. The samples were taken out and left to air-dry under the fume hood overnight. Samples were mounted on aluminium stubs using carbon foils and conductive silver and were subsequently sputtered with gold using a JEOL JFC-2300HR Sputter Coater for 120 seconds. SEM micrographs were taken using a Philips XL 30 ESEM and JEOL IT 300 with an acceleration voltage of 20 kV.

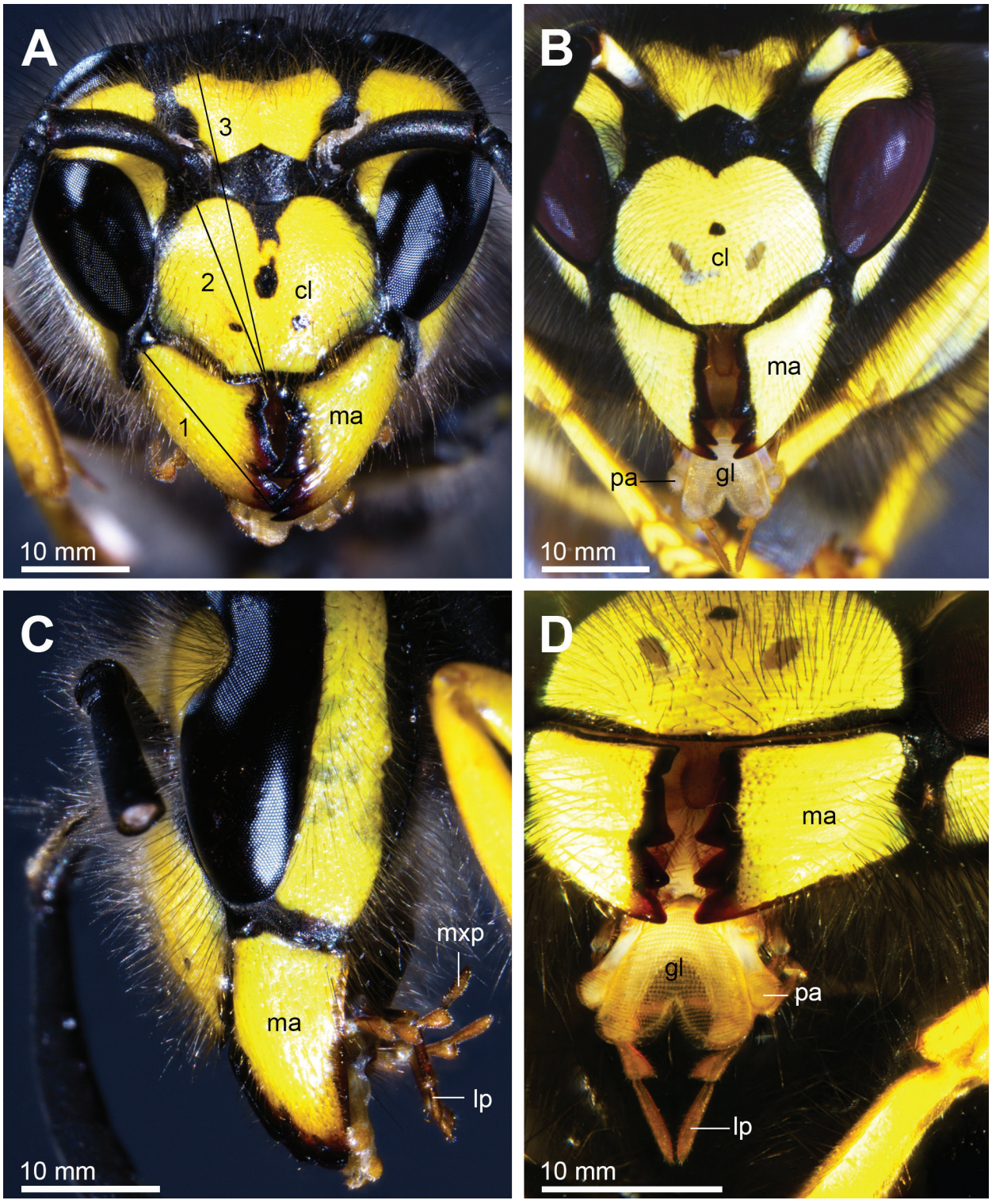

Figure 1. Head of *Vespula germanica* (LM). **A.** Female worker in frontal view; 1, 2, 3 measuments taken to compare head size. **B.** Male in frontal view. **C.** Female worker in lateral view. **D.** Male in ventral view; **cl** – clypeus, **gl** – glossa, **lp** – labial palpus, **ma** – mandible, **mxp** – maxillary palpus, **pa** – paraglossa.

Microcomputed tomography (Micro CT)

Wasps were fixed in Dubosq-Brazil solution (alcoholic Bouin solution), stored in 70 % ethanol and stained with 1 % Iodine in ethanol (Metscher 2009). An Xradia MicroXCT system was used for scanning. The photo stacks (.tiff files) were prepared using Xradia software. The stacks were reconstructed using Amira 6.0 and 6.1 (FEI comp., Hillsborow, USA). The musculature of the mandibles was reconstructed for each individual. Photoshop CC (Adobe Systems Inc., San Jose, California, USA) was used for composing the plates and contrast enhancing of the pictures.

Results

No differences in head and mouthpart morphology were found between *V. vulgaris* and *V. germanica* (Fig. 1). The heads of male wasps were slightly larger (males: 3.23 ± 0.38 mm, N = 9; females: 3.08 ± 0.21 mm, N = 9), but no significant differences between sexes were found (Z = - 0.97, p = 0.33, N = 18). Female workers had significantly longer mandibles than males (males: 1.88 ± 0.11 mm, N = 9; females: 2.07 ± 0.13 mm, N = 9; Z = - 2.87, p = 0.003, N = 18). The distance between the scapus and the distal ridge of the clypeus was similar in males and females (males: 1.85 ± 0.16 mm, N = 9; females: 1.79 ± 0.13 mm, N = 9; Z = - 0.88, p = 0.38, N = 18).

The mouthparts of both sexes in *V. vulgaris* and *V. germanica* are characterized by large toothed mandibles and the labio-maxillary complex which is folded posteriorly under the head behind the mandibles (Fig. 1C). The labrum can only be observed when the mandibles are open. The proximal part of the labrum is entirely concealed behind the clypeus; the distal part of the labrum is well equipped with sensilla trichodea (Fig. 2B).

The dentate mandibles are heavily sclerotized and shaped like a gouge in both sexes (Fig. 2C, D). The mandibles have sharp distal margins; they are slightly convex on their lateral sides and concave on the medial sides. In repose, one mandible is folded over the other (Fig. 2A). The right mandible folds over the left in 11 (including 5 males) out of 18 wasps, whereas 7 wasps (including 4 males) fold the left mandible over their right one. The cutting edge of the incisive part bears three frontal teeth and a curved proximal cutting edge (Fig. 2C, D). In female workers and queens, two additional teeth and edges with stout bristles are present on the median side of the mandible that is not visible from frontal side (Fig. 2C). In comparison to the incisive part the molar region of the mandible is rather small in females and reduced in male wasps (Fig. 2C, D).

The mandibles bear bristle-shaped sensilla and sensilla campaniformia towards the teeth on the frontal side (Fig. 2). The mandibles of males are almost entirely covered with long sensilla trichodea (Fig. 2B). Their sensory bristles are rough and some are as long as the mandible. Mandibles of female workers show a lower number of sensilla. Their bristles are smooth and shorter, measuring

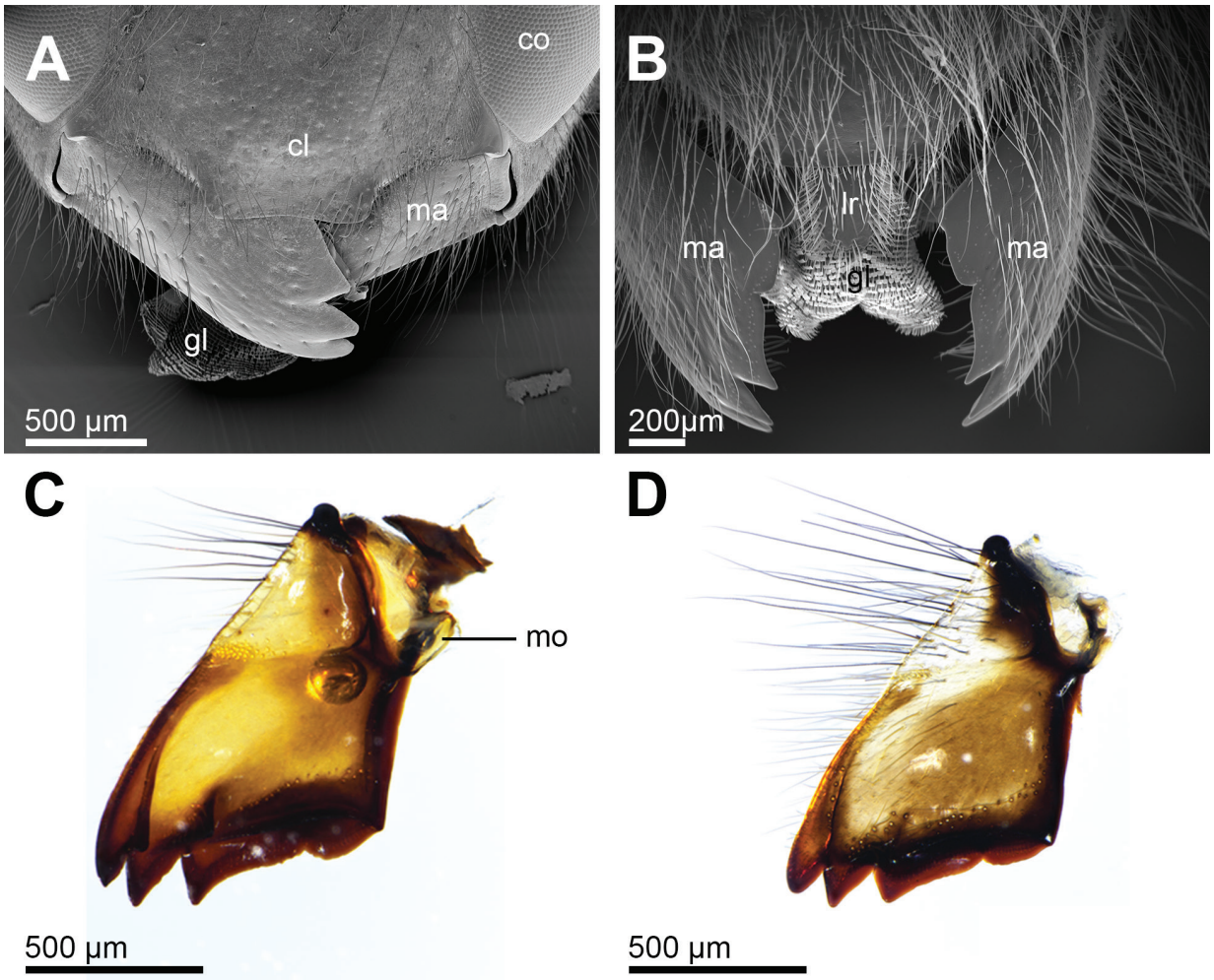

Figure 2. Mandibles and labrum (SEM, LM). **A.** Mandibles (**ma**) overlapping in repose in front of the clypeus (**cl**); **co** – compound eye, **gl** – glossa. **B.** Open mandibles (**ma**), labrum (**lr**) and glossa (**gl**) underneath (male wasp). **C.** Mandible of female (LM), short bristles and mola (**mo**). **D.** Mandible of male (LM), long bristles and inconspicuous inner teeth.

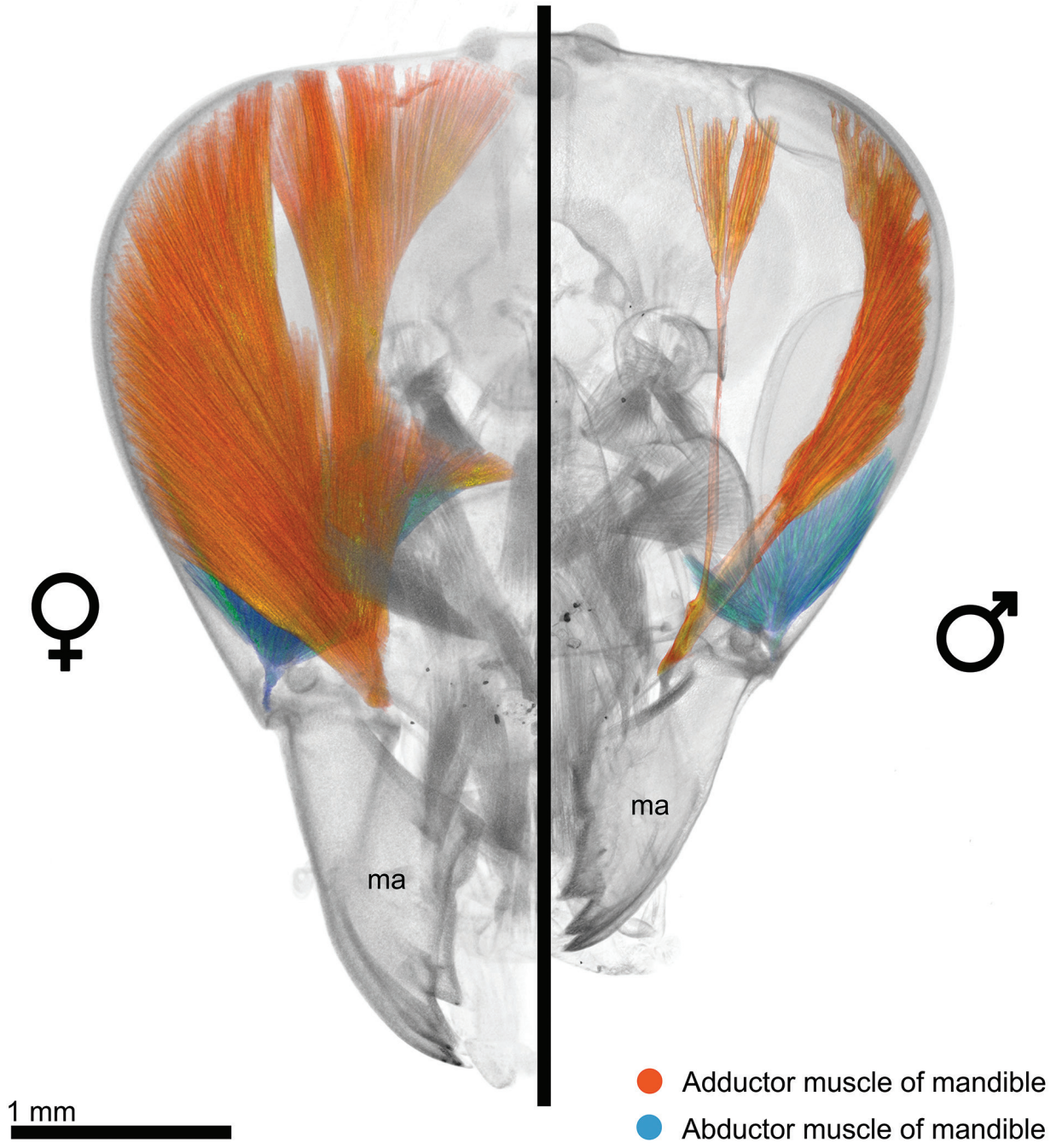

Figure 3. Head anatomy of a female worker (left) and a male individual (right) of *V. germanica* (micro CT). Adductor of the mandible (red) is much bigger in females than in males; abductor muscle (blue) is slightly bigger in females; **ma** – mandible.

only half of the mandible length (Fig. 2C) in contrast to males (Fig. 2D).

The comparison of the head anatomy in female workers and males showed that the muscles of the mandibles were remarkably smaller in males (Fig 3). Despite both portions of the adductor of the mandible (Musculus craniomandibularis internus) had the same origin and attachment sites, the volume of both was much smaller in males than in females. Especially the median portion of the adductor muscle was very small in males. The volume of the abductor muscle (Musculus craniomandibularis externus) was slightly smaller in male wasps than in workers (Fig. 3).

The labio-maxillary complex of both sexes is retracted in an oval depression on the posterior part of the head capsule in repose (Fig. 4). The components of this functional unit are firmly connected to ensure that the complex extends and retracts as a unit. In the extended position, the ligula (i.e., glossa plus paraglossae) is longer than the mandibles (Fig. 1B, D). In retracted position, the glossa and paraglossae are folded backwards under the head (Figs 1C, 4A).

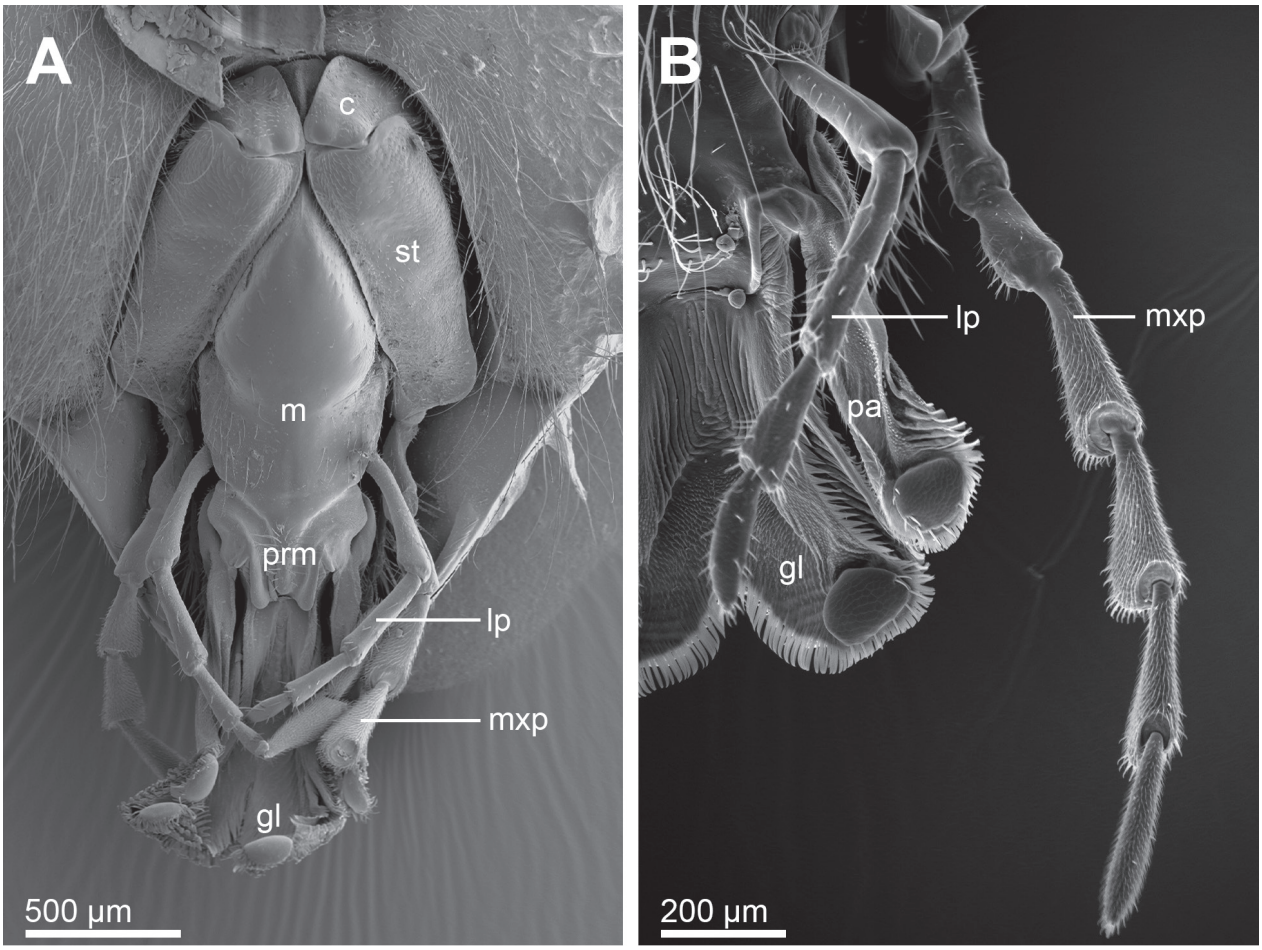

Figure 4. Labio-maxillary complex (SEM), head in posterior view. **A**. Maxilla and labium in resting position, ligula (**gl** – glossa and paraglossa) folded, female worker; **c** – cardo, **lp** – labial palpus, **m** – mentum, **mxp** – maxillary palpus, **prm** – prementum, **st** – stipes. **B.** Extended ligula, labial palpus (**lp)** and maxillary palpus (**mxp**), male; **gl** – glossa, **pa** – paraglossa.

The cardo is a roughly triangular sclerite that connects the rest of the labio-maxillary complex with the head. The flat stipes is medially uplifted with the median side next to the labium (Fig. 4A). A few bristle-shaped sensilla are distributed over the lateral surface of the stipes. Lacinia and galea are weakly sclerotized and bear a high number of sensory bristles in both sexes (Fig. 5A). The lacinia is a short lobe positioned medially and covered by the larger flat galea from the lateral and ventral sides. The lacinia shows long bristle-shaped sensilla on the ridge that borders the galea. The galea is subdivided and bears a high number of long bristle-shaped sensilla on the edge and shorter ones over the entire outer surface; sensilla campaniformia occur medially (Fig. 5C).

All six segments of the maxillary palpus vary with respect to length and distribution of sensory bristles (Fig. 4B). The first two segments are cylindrical in shape and possess a few bristle-shaped sensilla. Segments three to six are club-shaped and have smaller diameters proximally than distally. In comparison to segments one and two, the number of bristle-shaped sensilla increases distinctly in segments three to six including an increasing number of sensilla basiconica (Fig. 5B). The maxillary palpi bear a much higher number of sensilla than the labial palpi, although the types of sensilla are the same (Fig. 4B).

The basal sclerites of the labium are embraced laterally by the well sclerotized two stipites and cardines (Fig. 4A). The mentum is heavily sclerotized and has the shape of a trough, whereas the prementum and the submentum are less sclerotized. The prementum is beset with a small number of bristle-shaped sensilla on the median surface (Fig. 4A). At its distal end the prementum bears the four-lobed ligula composed of the central bilobed glossa as well as the two slimmer and shorter paraglossae laterally on each sides (Figs 1D, 6A). The whole complex of the glossae and paraglossae is folded up behind the mandibles in resting position or extended in the feeding position in males and females (Figs 1B, D; 4). While the ventral cuticle is more or less smooth, the dorsal surface of the glossae and paraglossae is covered with numerous spatula-shaped microtrichia (Fig. 6A–C). Each microtrichium is relatively thin at the base but broadens towards its tip, which is curved backwards and appears hook-shaped (Fig. 6B, C). These spatula-shaped microtrichia are arranged in 25–30 rows and form a large cuticular surface. The microtrichia on the paraglossae are similar but their basis is almost as broad as the tip.

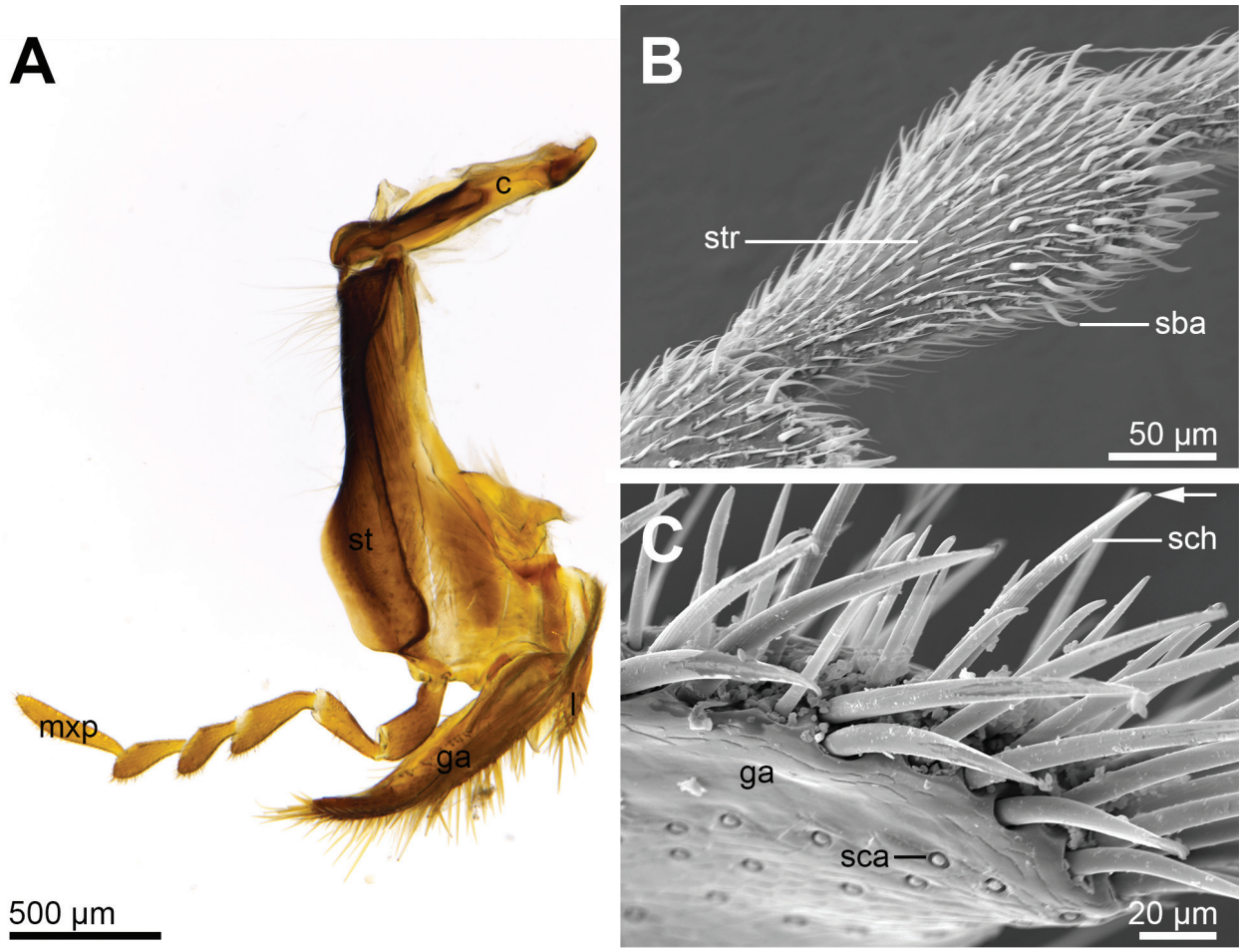

Figure 5. A. Maxilla (LM); **c** – cardo, **ga** – galea, **l** – lacinia, **mxp** – maxillary palpus, **st** – stipes. **B.** Fifth segment of maxillary palpus equipped with various sensilla (SEM); **sba** – sensillum basiconicum, **str** – sensillum trichodeum. **C.** Sensilla at the distal edge of galea (**ga**) (SEM); arrow indicates terminal pore; **sca** – sensillum campaniformium, **sch** – sensillum chaeticum.

Ventrally the glossae and paraglossae each bear an apical brownish cuticular thickening, termed the acroglossal button (Duncan 1939), which has a smooth surface in both sexes (Figs 4B, 5A). On the distal and lateral sides of the acroglossal buttons, a single row of sensilla basiconica is situated (Fig. 6C). In addition, a row of long, flat cuticle structures are present. These microtrichia extend from the edges of the glossae and paraglossae (Fig. 6A–C). The distal rim of the glossae and the tips of the paraglossae bear one row of sensilla basiconica (Fig. 6B). These sensilla basiconica which are positioned close to the acroglossal button have a small socket and a terminal pore whereas the sensilla basiconica found on the acroglossal button lack a socket and a terminal pore (Fig. 6C).

The two labial palpi insert at the prementum where it borders the mentum (Fig. 4). Each palpus consists of four segments bearing some bristle-shaped sensilla and few sensilla basiconica (Fig. 4B). Both the second and the third segment additionally have a large thorn-shaped bristle in females (Fig. 6D), which is less conspicuous in males. Female wasps have one sensillum basiconicum both on the second and third segment of the labial palpus whereas male wasps have 6 to 8 sensilla basiconica at the end of the third segment.

Discussion

Mouthpart dimorphism in female and male wasps

Mouthparts of social wasps are complex in form and function and show particular adaptations to both biting and fluid feeding. Our results confirm those of Spradbery (1973) who reported that the mouthpart morphology is similar in female workers and queens. The comparison of female workers and male *Vespula* individuals showed that the mandibles were significantly smaller in male wasps. In female wasps the mandibles are stout and heavily sclerotized since they primarily serve as cutting tools. They are applied to cut plant fibers from wood surfaces and also function as weapons for snatching prey (Duncan 1939). The mandibles are also used for scraping earth loose and picking up stones and debris in with the context of nest building (Spradbery 1973, Matsuura and Yamane 1990, Mauss 2007). Additionally, the mandibles are used by emerging wasps to cut through the cocoon of the pupae (Schremmer 1962). For all those tasks the mandibles bear three frontal teeth and a cutting edge. In repose, one mandible is folded over the other, which indicates a scissor-like function in action in both sexes.

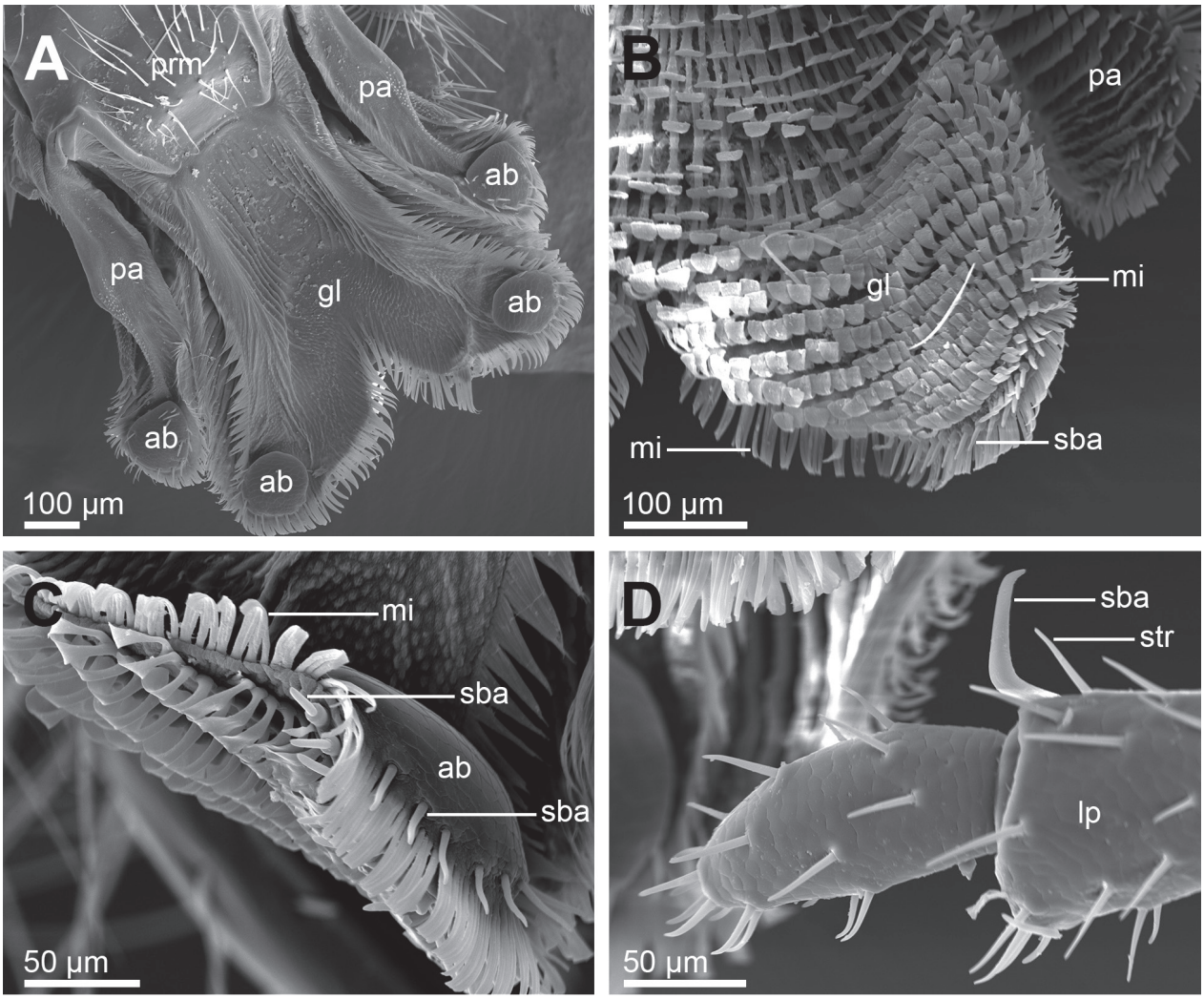

Figure 6. Labium (SEM). **A.** Extended ligula (**gl** – glossa, **pa** – paraglossa) in posterior view, acrosomal buttons (**ab**) at the apex; **prm** – prementum. **B.** Apex of glossa (**gl**), spatula shaped microtrichia (**mi**) of the dorsal side; **pa** – paraglossa, **sba** – sensillum basiconicum. **C.** Distal edge of the paraglossa with rows of microtrichia (**mi**) and sensilla basiconica (**sba**); **ab** – acrosomal button. **D.** Third segment of labial palpus (**lp**), female with thorn-shaped sensillum basiconicum (**sba**) and sensilla trichodea (**str**).

However, our results showed that the smaller size of the mandibles in male wasps is associated with inconspicuous median teeth and mola as well as reduced musculature in *Vespula*. Micro CT investigations showed that especially the adductor muscles are conspicuously smaller in males. From this dimorphism of head anatomy, it can be expected that the biting force is smaller in males than in females. The different morphology is explained by the fact that male wasps do not use their mandibles for larval provisioning (Spradbery 1973, Matsuura and Yamane 1990). In male wasps, the mandibles are only used to bite open the pupae during emerging (Schremmer 1962).

The labio-maxillary complex is capable of operating completely independent from the mandibles (Jervis 1998). In adult wasps of both sexes the labio-maxillary complex is extensible and almost solely concerned with the uptake of liquid food. The lobe-shaped distal parts of the labium act like a tongue where the surface of the glossa and paraglossa is used for fluid uptake. Both components are characterized by the dense endowment with microtrichia on the dorsal/frontal side. The high number of spatula-shaped microtrichia forms a large surface on the ligula. The particular shape of the microtrichia creates a space underneath and between the cuticular structures. Under the assumption that the cuticle is wettable, it can be supposed that this arrangement and the specific micromorphology of the structures are crucial to upload fluids and the ligula serves as an adhesive device (López-Cubillos and Sarmiento 2013). Schremmer (1962) suggested that these structures are no sensory bristles but chitin emergences, enabling the wasps to lap up liquids. Alternatively, the microtrichia of the glossa and paraglossae were interpreted to serve as a rasping device (Duncan 1939). This function should be considered in addition, since wasps feed from soft ripe fruits by rasping over the surface to gain more fruit juice.

Fluid feeding in wasps

Adult Vespinae of both sexes feed exclusively on liquid food such as the juice of ripe fruits, honeydew or nectar since larger particles of food are prevented from travel-

ling down the narrow esophagus (Spradbery 1973). Since wasps are not equipped with a closed tubular proboscis, feeding of fluid has to be accomplished in a different way than suction. A short food canal for the uptake of liquid food is temporally formed by parts of the labio-maxillary complex and the labrum/epipharynx. The labium constitutes the bottom, the stipites including the laciniae and galeae form the sides and the labrum/epipharynx composes the roof of this short temporary food tube (Duncan 1939) which was termed "Wespenrüssel" (Kirmayer 1909) or "wasp proboscis". The glossae and paraglossae produce lapping motions, similar to the "licking cycle" in honey bees (Snodgrass 1956, Wu et al. 2015). In the extended position of the ligula, liquid adheres to the spatula-shaped microtrichia that is thus transported into the food canal when the glossae and paraglossae are retracted towards the mouth (Seifert 1995).

Imagines of *V. germanica* and *V. vulgaris* may feed only on flowers with easily accessible nectar (Schremmer 1962, Mauss 2007). Likewise, many adult Hymenoptera feed on flowers with freely accessible nectar using rather short feeding organs (e.g., Osten 1982, Jervis 1998, Jervis and Vilhelmsen 2000, Mauss 2007). The fluids adhering to the mouthpart structures are brought into the food canal by retraction of the distal parts of the labium. The liquids are conveyed further by suction force from the muscular cibarial or pharyngeal pumps (Krenn et al. 2005). Likewise in ants, insects devoid of elongated mouthparts, employ the labium for the uptake of liquid food by capillarity (Paul et al. 2003). Like in social wasps, the distal components of the labium are prime organs for the uptake of liquid food by capillarity. By contrast, many representatives of pollen wasps (Masarinae) are able to feed from concealed nectaries in spurred and resupinate flowers using their elongated labio-maxillary complex (Gess and Gess 1989, Gess 1996, Mauss and Müller 2000, Mauss et al. 2010). These pollen wasps possess an elongate suctorial proboscis which is composed primarily of the particularly long glossa. The cuticle structures of the glossa form a closed food tube and a specialized apex for nectar uptake (Krenn et al. 2002).

Sensilla equipment of mouthparts

Compared to the female workers, male wasps have a higher number of long bristle-shaped sensilla on the mandibles, whereas the sensilla equipment of the labio-maxillary complex is nearly identical except for the higher number of sensilla basiconica and the lack of the thorn-shaped sensillum on the labial palpi of males. The reason for the higher numbers of mandibular sensilla of male wasps is unknown. Although it can be expected that the sensilla on the palpi mainly provide information about food, the differences in sensilla equipment cannot be interpreted since the external morphology of sensilla gives only rough estimates about their sensory functions (Zacharuk 1985).

Various types of sensilla are located on the labio-maxillary complex that could give information about food uptake and transport as well as position of the mouthpart components. Both the lacinia and the galea serve as lateral parts of the passageway through which food may be ingested (Kirmayer 1909). SEM analyses of the sensilla located on the galea revealed sensilla with a terminal pore in addition to thin sensory bristles and sensilla campaniformia. The observed porus at the sensillum tip of galeal sensilla suggests a chemosensitive function rather than a bare tactile one (Zacharuk 1985). Likewise, the sensilla of galea and lacinia could provide information about the status of extension of the labio-maxillary complex. In addition, the lobes of the lacinia and galea serve a secondary function as cleaning organs for the antennae, maxillary and labial palpi and the forelegs (Spradbery 1973), where sensilla are expected to play a role in behavioral control.

In spite of the similar putative function of the palpi in feeding, the coverage with sensilla is much higher on the maxillary palpi than on the labial palps. In addition to many sensory bristles having a putative tactile function, the labial palpi just show one to three sensilla basiconica whereas the number of sensilla basiconica is much higher on the maxillary palpi. This distribution of sensilla would suggest that the maxillary palpi are rather used for testing the consistence of food substances. Detailed analysis of the movements of both maxillary palpi and labial palpi during feeding could provide insight into the possible different tasks.

It can be expected that the sensilla at the distal edges of the ligula and the acroglossal buttons detect sugar. The acroglossal buttons are developed in this typical form only in Vespidae (Duncan 1939). The thickenings of the cuticle located on the ventral/posterior side of both the glossae and paraglossae were assumed to have a protective function (Kirmayer 1909). However, the fact that the acroglossal buttons are beset with sensilla basiconica suggests that they serve to taste food. Sensilla basiconica could either be mechanosensitive, both mechano- and chemosensitive, thermosensitive, hygrosensitive, olfactory or combinations of these functions (Zacharuk 1985). Either one of these possible functions would make sense at this specific location. Instead, we suggest that the wasps taste composition and quality of liquids with the sensilla basiconica on the acroglossal buttons before they lap up the fluids. These sensilla basiconica, which lay close to the acroglossal buttons, show a socket and a terminal pore. This porus suggests that the sensillum could react chemosensitively and could be helpful in tasting substances (Altner 1977). The arrangement of sensilla is in line with other nectar feeding insects, i.e. butterflies, flies or bees that exhibit sugar detecting sensilla at the apex of the proboscis where nectar adheres to the mouthpart surface (Galić 1971, Krenn 1998, Krenn et al. 2005, Bauder et al. 2013, Krenn and Bauder 2017, Düster et al. 2018).

Acknowledgements

We thank Volker Mauss (Staatliches Museum für Naturkunde, Stuttgart, Germany) for providing male *Vespula* wasps. We are grateful to Daniela Gruber of the electron microscopy laboratory (CIUS) and Brain Metscher

(Department of Theoretical Biology) at the Faculty of Life Scienes (University of Vienna, Austria) as well as to Stephan Handschuh (VetCORE, University of Veterinary Medicine, Vienna) who helped with the µCT imaging.

References

Altner H (1977) Insektensensillen: Bau- und Funktionsprinzipien. Verhandlungen der Deutschen Zoologischen Gesellschaft IV. Morphologie und funktionelle Anatomie: 139–153.

Bauder JAS, Handschuh S, Metscher BD, Krenn HW (2013) Functional morphology of the feeding apparatus and evolution of proboscis length in metalmark butterflies (Lepidoptera: Riodinidae). Biological Journal of the Linnean Society 110(2): 291–304. https://doi.org/10.1111/bij.12134

Berland L (1928) Hyménoptères vespiformes. 2. Eumenidae, Vespidae, Masaridae, Bethylidae, Dryinidae, Embolemidae. Faune de France, 19. Lechevalier, Paris, 208 pp.

Duncan DC (1939) A contribution to the biology of north american vespine wasps. Stanford University Publications, University Series, Biological Sciences, 8 (1), Oxford University Press, Oxford, 1–257.

Düster JV, Gruber MH, Karolyi F, Plant JD, Krenn HW (2018) Drinking with a very long proboscis: Functional morphology of orchid bee mouthparts (Euglossini, Apidae, Hymenoptera). Arthropod Structure & Development 47: 25–35. https://doi.org/10.1016/j.asd.2017.12.004

Galić M (1971) Die Sinnesorgane an der Glossa, dem Epipharynx und dem Hypopharynx der Arbeiterin von *Apis mellifica* L. (Insecta, Hymenoptera). Zeitschrift für Morphologie der Tiere 70: 201–228. https://doi.org/10.1007/BF00302025

Gess SK (1996) The pollen wasps - Ecology and natural history of the Masarinae. Harvard University Press, Cambridge, Massachusetts, 340 pp. https://doi.org/10.4159/harvard.9780674281684

Gess SK, Gess FW (1989) Flower visiting by masarid wasps in southern Africa (Hymenoptera: Vespoidea: Masaridae). Annals of the Cape Provincial Museums (Natural History) 18: 95–134.

Greene A (1991) *Dolichovespula* and *Vespula*. In: Ross KG, Matthews RW (Eds) The social biology of wasps. Comstock, Ithaca, 263–305.

Jervis M (1998) Functional and evolutionary aspects of mouthpart structure in parasitoid wasps. Biological Journal of the Linnean Society 63: 461–493. https://doi.org/10.1111/j.1095-8312.1998.tb00326.x

Jervis M, Vilhelmsen L (2000) Mouthpart evolution in adults of the basal, „symphytan", hymenopteran lineages. Biological Journal of the Linnean Society 70: 121–146.

Kimsey LS, Carpenter JM (2012) The Vespinae of North America (Vespidae, Hymenoptera). Journal of Hymenoptera Research 28: 37–65. https://doi.org/10.3897/jhr.28.3514

Kirmayer R (1909) Bau und Entwicklung der Mundteile bei *Vespa vulgaris*. Gegenbaurs Morphologisches Jahrbuch. Zeitschrift für Anatomie und Entwicklungsgeschichte 39: 1–30.

Krenn HW (1998) Proboscis sensilla in *Vanessa cardui* (Nymphalidae, Lepidoptera): functional morphology and significance in flower-probing. Zoomorphology 118: 23–30. https://doi.org/10.1007/s004350050053

Krenn HW (2007) Evidence from mouthpart structure on interordinal relationships in Endopterygota? Arthropod Systematics & Phylogeny 65(1): 7–14.

Krenn HW, Mauss V, Plant J (2002) Evolution of the suctorial proboscis in pollen wasps (Masarinae, Vespidae). Arthropod Structure and Development 31: 103–120. https://doi.org/10.1016/S1467-8039(02)00025-7

Krenn HW, Plant JD, Szucsich NU (2005) Mouthparts of flower-visiting insects. Arthropod Structure and Development 34: 1–40. https://doi.org/10.1016/j.asd.2004.10.002

Krenn HW, Bauder JAS (2017) Morphological fine tuning of the feeding apparatus to proboscis length in Hesperiidae (Lepidoptera). Journal of Morphology 279(3): 396–408. https://doi.org/10.1002/jmor.20780

López-Cubillos S, Sarmiento CE (2013) A mandible arresting system in neotropical social wasps (Vespidae, Polistinae): structural diversity within homogeneous functionality. Naturwissenschaften 100(5): 429–435. https://doi.org/10.1007/s00114-013-1041-6

Matsuura M, Yamane S (1990) Biology of the vespine wasps. Springer, Berlin, 323 pp. https://doi.org/10.1007/978-3-642-75230-8

Mauss V, Müller A (2000) A study of the bionomy of the Spanish pollen wasp *Ceramius hispanicus* Dusmet (Hymenoptera, Vespidae, Masarinae): Nesting, mating, and flower association. Journal of Hymenoptera Research 9: 1–17.

Mauss V (2007) Evolution verschiedener Lebensformtypen innerhalb basaler Teilgruppen der Faltenwespen (Hymenoptera, Vespidae). Denisia 20, zugleich Kataloge der oberösterreichischen Landesmuseen Neue Serie 66: 701–722.

Mauss V, Müller A, Yildirim E (2010) First contribution to the bionomics of the pollen wasp *Ceramius palestinensis* (Giordani Soika, 1957) (Hymenoptera: Vespidae: Masarinae) in Turkey. Entomological Science 13: 42–59. https://doi.org/10.1111/j.1479-8298.2010.00370.x

Metscher BD (2009) MicroCT for comparative morphology: simple staining methods allow high-contrast 3D imaging of diverse non-mineralized animal tissues. BMC Physiology 9(1): 11. https://doi.org/10.1186/1472-6793-9-11

Osten T (1982) Vergleichend-funktionsmorphologische Untersuchungen der Kopfkapsel und der Mundwerkzeuge ausgewählter „Scolioidea" (Hymenoptera, Aculeata). Stuttgarter Beiträge zur Naturkunde Serie A (Biologie) 354: 1–60.

Paul J, Roces F, Hölldobler B (2003) How do ants stick out their tongues? Journal of Morphology 254: 39–52. https://doi.org/10.1002/jmor.10011

Schremmer F (1962) Wespen und Hornissen. Die einheimischen sozialen Faltenwespen. A. Ziemsen Verlag, Wittenberg Lutherstadt: 104 pp.

Seifert G (1995) Entomologisches Praktikum. 3. Auflage. G. Thieme Verlag, Stuttgart, New York: 332 pp.

Snodgrass RE (1935) Principles of Insect Morphology. McGraw Hill, New York, 667 pp.

Snodgrass RE (1956) Anatomy of the honey bee. Comstock Pub. Assoc. Ithaca, New York, 352 pp.

Spradbery JP (1973) An account of the biology and natural history of social and solitary wasps. University of Washington Press, Seattle: 408 pp.

Wu J, Zhu R, Yan S, Yang Y (2015) Erection pattern and section-wise wettability of a honeybee's glossal hairs in nectar feeding. Journal of Experimental Biology 218: 664–667. https://doi.org/10.1242/jeb.111013

Zacharuk RY (1985) Antennae and sensilla. In Kerkut GA, Gilbert LI (Eds), Comprehensive insect physiology, biochemistry and pharmacology, Vol. 6, Pergamon, Oxford, 1–69.

Dtsch. Entomol. Z. 65 (1) 2018, 75–80 | DOI 10.3897/dez.65.23538

PENSOFT

museum für naturkunde

Vansoniella chirindensis gen. n., sp. n. – an unusual taxon with translucent wings from Zimbabwe (Lepidoptera, Limacodidae)

Wolfram Mey[1]

1 *Museum für Naturkunde, Invalidenstr. 43, 10115 Berlin, Germany*

http://zoobank.org/E8E8E866-686F-4F99-BCE5-B3648CF6EEE0

Corresponding author: *Wolfram Mey* (mey@mfn-berlin.de)

Received 10 January 2018
Accepted 9 March 2018
Published 16 March 2018

Academic editor:
Dominique Zimmermann

Abstract

The genus *Vansoniella* **gen. n.** is established to accommodate the species *V. chirindensis* **sp. n.**, collected in Zimbabwe by Van Son in 1937. The new species differs externally from other African taxa by translucent fore- and hindwings in the male sex. The wing venation is highly derived and the male genitalia are also structurally different from other genera. The genus occupies an isolated position within the family.

Key Words

Afrotropical Region
Limacodidae
taxonomy
wing dimorphism
southern Africa
Zimbabwe

Introduction

Over the years, the curator of the Lepidoptera collection of the Ditsong Museum of Natural History of South Africa, Pretoria (TMSA), M. Krüger, has set aside some strange moth specimens that could not readily be assigned to any of the South African families. The present specimen resembled some smaller species of Cossidae (e.g. *Stygiodes* Bruand, 1853) and was brought to my attention by M. Krüger. After dissections of the male genitalia, the individuals turned out to belong to the family Limacodidae. The family is currently divided into two subfamilies, Limacodinae and Chrysopolominae (De Prins and De Prins 2018). The latter was originally established as a family of its own, a view which is upheld by Kurshakov and Zolotuhin (2013, 2016) who provide a number of strong arguments. A molecular analysis of the family is not available to date leaving the rank of the two groups unresolved.

The examined specimen belongs to Limacodinae and was remarkable by its sparse scaling of the wings which gave them a translucent appearance. This character is not known to occur in any of the described genera of Limacodidae from Africa. In an attempt to find and identify related species, the Neotropical, Oriental and Australian parts of the rich Limacodidae collection of the Museum für Naturkunde, Berlin, were searched for similar species exhibiting translucent wings. Also, monographic treatments of the family were consulted (e.g. Viette 1980, Holloway 1986). Indeed, a number of species with this unusual character were found. A closer examination and comparison of antennae, wing venation and genitalia revealed these species to differ clearly from the African individual. The external resemblance did not indicate a relationship, and instead resulted from an independent, analogous development. The several specialized traits observed in the African species seemed not to be shared with any other genera.

The first species of Limacodidae described from Africa south of the Sahara was *Bombyx cloeckneria* Stoll, 1781. The species was collected from the Cape of Good Hope (Stoll 1781) and is now placed in *Caffricola* Hampson, 1919. Today, the Afrotropical Region is known to contain a very rich and diverse fauna of Limacodidae with many endemic genera. Heppner (1991) has reported 275 described species from south of the Sahara, but since then new descriptions (Krüger 2004; Mey 2011; Kurshakov and Zolotuhin 2013, 2016; Basquin 2016) have shifted the number to over 300.

The African fauna of Limacodidae was comprehensively treated by Hering (1928), who later added an identification key to the genera (Hering 1955). The South African species were revised by Janse (1964). He established 21 new genera and provided a dichotomous key to the African genera too. Though the latter is incomplete by omitting about a dozen genera from the tropical zone of the continent, it includes nearly all South African taxa and, thus, is of great help in the determination of species at least from this part of Africa. However, both keys did not work in the determination of the present species. The taxon is obviously not included in the keys. This result is not necessarily evidence for an unnamed taxon. Sexual dimorphism of the wings is a frequent feature of adult moths and occurs in many Lepidoptera families. In the past, males and females were often described as separate species until recognized as being the same taxon. Wing dimorphism seems to be an exceptional case in Limacodidae (Solovyev 2014). Neither Hering (1955) nor Janse (1964) mentioned or illustrated a single dimorphic species. However, it cannot be ruled out, that the male specimen has a dimorphic female, which was perhaps already described.

Translucent wings have evolved independently in species of different families, e.g. Cossidae, Metarbelidae, Sesiidae, Megalopygidae, Sphingidae. In Cossidae, Megalopygidae and also in Limacodidae this character is mostly restricted to the male sex, while the females exhibit the usual, dense scaling on the wings. The wing venation, however, does not need to be affected by this dimorphism and appears to be largely the same in both sexes. Some dimorphic species with both sexes available in the collection were examined for this feature. A corresponding venation was observed in the following species:

Doratifera oxleyi (Newman, 1855) (Australia) – Limacodidae
Phobetron pithecium (J.E. Smith, 1797) (USA) – Limacodidae
Laphridia francesca (Swinhoe, 1902) (Java) – Limacodidae
Podalia bolivari (Heylaerts, 1884) (Colombia) – Megalopygidae.
Stygioides colchicus (Herrich-Schäffer, 1851) (Turkey) – Cossidae

In contrast, the wing venation of both the fore- and hindwings differs between sexes in the strongly dimorphic *Eulophonotus myrmeleon* Felder, 1874 (South Africa) – Cossidae.

The differences are due to a reduction of veins in the male, whereas the female has retained the conventional vein configuration (Mey 2016).

There are three genera in the review of Janse (1964), which are known only from females. A closer inspection of the wing venation and number of tibial spurs provided the following results: The wing venation does not correspond with the venation of the species in question. The species of *Prolatoia* Holland, 1893 and *Zorostola* Janse, 1964 have two pairs of spurs on the hind tibia. *Zoradella* Jordan, 1924 has only the terminal spur pair like the unknown species but the venation is very apomorphic with stalked cubital veins Cu1a+b in the forewings and a very short fork of RR+M1 in the hindwings. This is not a conservative venational pattern, but a highly derived character that can be expected to occur in the male too, according to the observations of other cases of dimorphic species.

The three genera can be excluded as representing the potential female. In conclusion, none of the described genera are suited to accommodate the species with the translucent wings. Since this character as well as the unique genitalia is considerably broadening the morphological diversity of Limacodidae, the establishment of a new genus seems to be justified, even with only a single specimen at hand. It seems to be a rare species, and we cannot expect fresh material to become available in the near future.

Material and methods

Dissection of genitalia was performed according to the procedure described in Robinson (1976). The genitalia were embedded in Euparal. Chlorazol Black was used for staining. Prior to embedding the cleared genitalia on microscope slide, they were drawn using a camera lucida attached to a Leica MZ12 compound microscope. Photographic documentation of the imago and genitalia was done with a Leica Z 16 APOA Microscope in combination with a Leica DFC490 camera and Leica Application Suite programme, version 4.5.0 on a Windows PC.

Holotype label data are quoted verbatim: quotation marks (“) signify data on a single label, a forward slash (/) indicates the end of a line of print. Supplementary or qualifying information is provided in square parentheses.

The terminology used in the description of the species follows Janse (1964) with the exception of aedoeagus, which is replaced by phallus.

Taxonomic account

Vansoniella gen. n.

http://zoobank.org05CAAB8A-F861-4501-9BC9-C6A0C2B6BD98

Type species. *V. chirindensis* sp. n.

Gender. feminine.

Systematic position. Limacodidae, Limacodinae.

Etymology. The genus name was chosen to the memory of George van Son (1898–1967), former curator of Lepidoptera at the Transvaal Museum in Pretoria and collector of the type species.

Description. see description of *V. chirindensis* sp. n.

Diagnosis. Small species with translucent wings resulting from sparse scaling and minute scales in upright position. Antenna bipectinate towards tip; epiphysis absent, spurs 0.2.2.; forewing with R3+4+5 on common stalk, areole absent; hindwing with RR+M1 as long fork, M3+Cu1a shortly stalked. Male genitalia beak-like uncus and hook-like gnathos; vinculum slender, long saccus present; valva triangular, with rounded hump on median side close to vinculum; juxta with pair of long, digitate processes and basal apophyses; apex of phallus with curved thorn and short, subapical spine.

Vansoniella chirindensis sp. n.

http://zoobank.org/4F04E05C-E89A-4696-9C16-A0BB4A09D860

Material examined. Holotype ♂, [Zimbabwe], "Chirinda For-/est, S. Rhod. XII/ -1937 G. van Son" [printed on white card], [20°24'S 32°41'E], genitalia slide Mey 85/17 (deposited in TMSA)

Etymology. The specific epithet is derived from the collecting site of the holotype, Chirinda on Mount Selinda.

Description. Adult male (Figs 7, 8): Length of forewing 7 mm, wing span 16 mm. Vertex of head with tuft of dark brown, shining, piliform scales projecting frontad between scapes; frons with appressed, downwardly directed, yellow scales; ocelli and chaetosemae absent; labial palpi short, porrect, with terminal segment not protruding beyond frontal scaling; scape and pedicellus short; antenna yellow-brown, bipectinate from base to tip, 52 pairs of rami, sparsely scaled dorsally and with numerous, short cilia on ventral sides. Thorax and tegulae dorsally with long, dark brown, shining scales; tibia of forelegs shorter than femur, epiphysis absent, tarsal segments of all legs without ventral spines, metatarsus with broad arolium and short pulvilli (Fig. 4), dorsal side of all legs with tufts of long scales, spurs 0.2.2.; forewings densely scaled on veins and in costal and anal fields, wing membrane with small, broad, short scales in upright position and widely spaced, multi-dentate at apex; scales on hindwing membrane smaller and mostly bi-dentate at apex; scales usually brown but yellow on bases of cubital and medial veins; fringes orange-brown with metallic shine. Forewing venation (Fig. 6) without areole, R2+3+4+5 stalked from upper corner of cell, A1+2 without distinct basal loop; hindwing with frenular bristle, R+M1 and M3+Cu1a shortly stalked, anal field densely covered by long, dark brown scales. Abdomen dark brown, tergum VIII with short, quadrangular plate on apical margin.

Male genitalia (Figs 1–3, 5): Tegumen and vinculum largely separate structures, interconnected in one point; lateral arms of vinculum slender, saccus large and broad; tegumen dorsally excised, separated from beak-like uncus by a small, membranous band; gnathos hook-like, preapical dorsal margin with minute den-

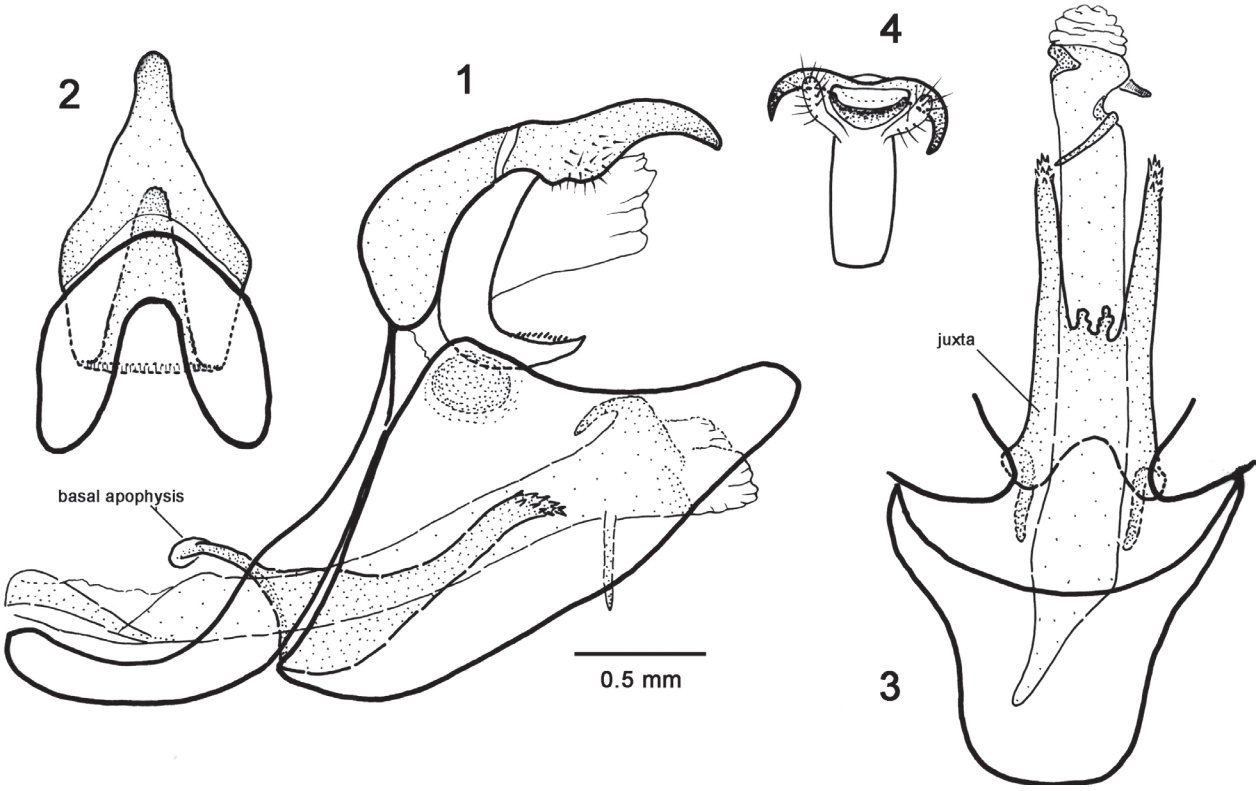

Figures 1–4. *Vansoniella chirindensis* sp. n., male genitalia, **1.** lateral, **2.** dorsal, **3.** ventral, **4.** ventral view of pretarsus

Figure 5. *Vansoniella chirindensis* sp. n., male genitalia slide Mey 85/17, caudal view

ticles; valva triangular, apex rounded, costal margin concave, inner side with a rounded hump on the basal dorsal corner close to vinculum; juxta large, covering the ventral and lateral sides of the phallus base and produced apically into a pair of finger-like processes bearing small dents on the tips, base of juxta with long and slightly curved apophyses, reaching into segment VIII; phallus tubular, longer than valva, apex with curved, dorsal process and short, subapical spine, directed ventrad; vesica without cornuti.

Female: unknown.

Distribution. The new species is known from the type locality only. The Chirinda Forest is an isolated patch of mountain forest on Mt. Selinda from about 1000 m to 1250 m elevation in East Zimbabwe (Fig. 9). The species may occur also in the Chimanimani Mts. north of the Chirinda Forest.

Remarks. Janse (1964) was not able to examine himself all species known at that time. But he included the information provided by other authors in his revisionary work (e.g. West 1937). In addition, after 1964 a number of further species of Limacodidae was described from Africa (Carcasson 1965, Pinhey 1968, Rougeot 1977, Viette 1980). They are fully scaled and not related to *Vansoniella* gen. n., with the exception of males of *Latoia pumilus* (Hering, 1957) and *L. heringi* (Viette, 1965) from Madagascar which exhibit some resemblance by the presence of hyaline patches on the forewings, but other characters as antennal structure and wing venation indicate that this resemblance is due to convergence.

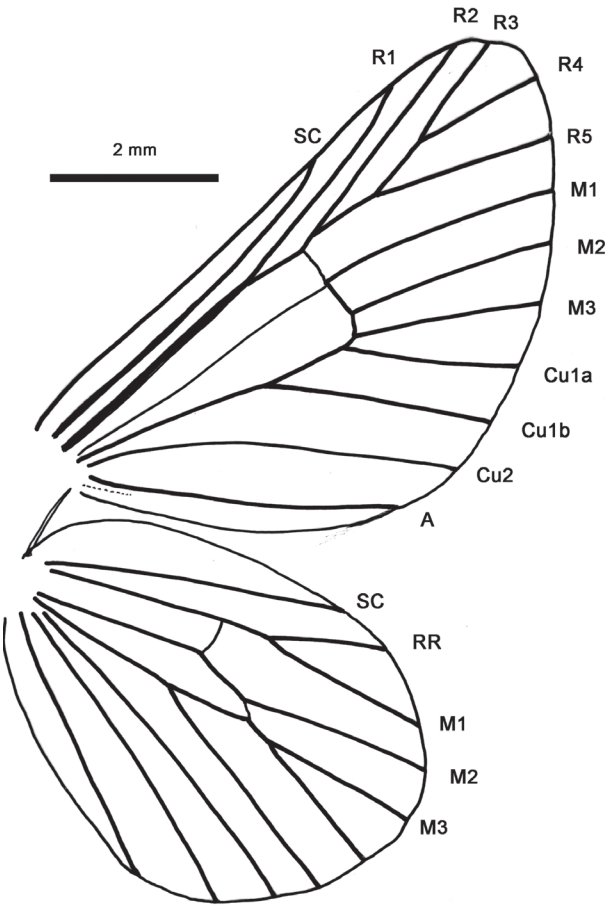

Figure 6. *Vansoniella chirindensis* sp. n., male wing venation

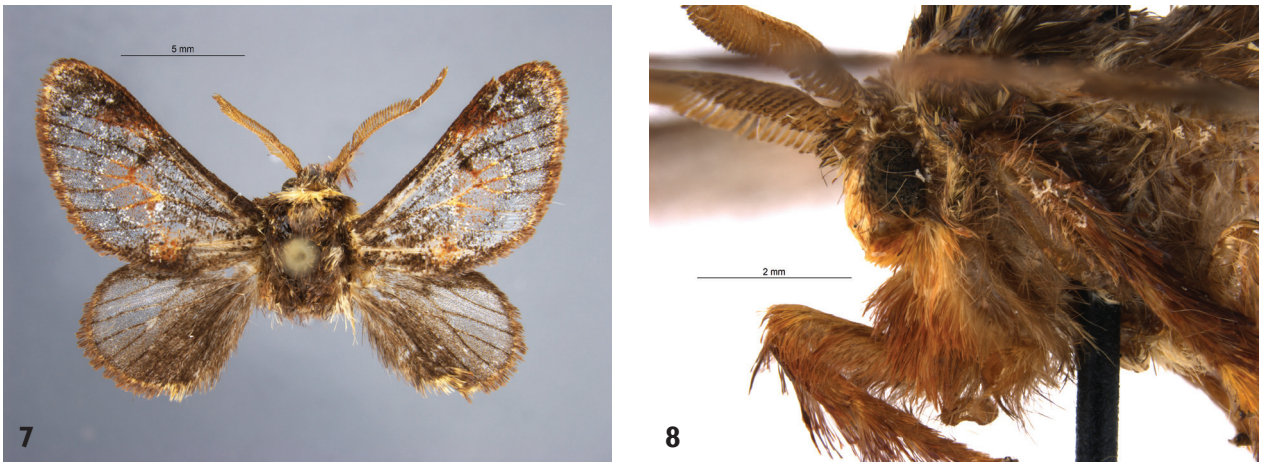

Figures 7–8. *Vansoniella chirindensis* sp. n., male holotype, **7.** dorsal view, **8.** lateral view of head and labial palpi.

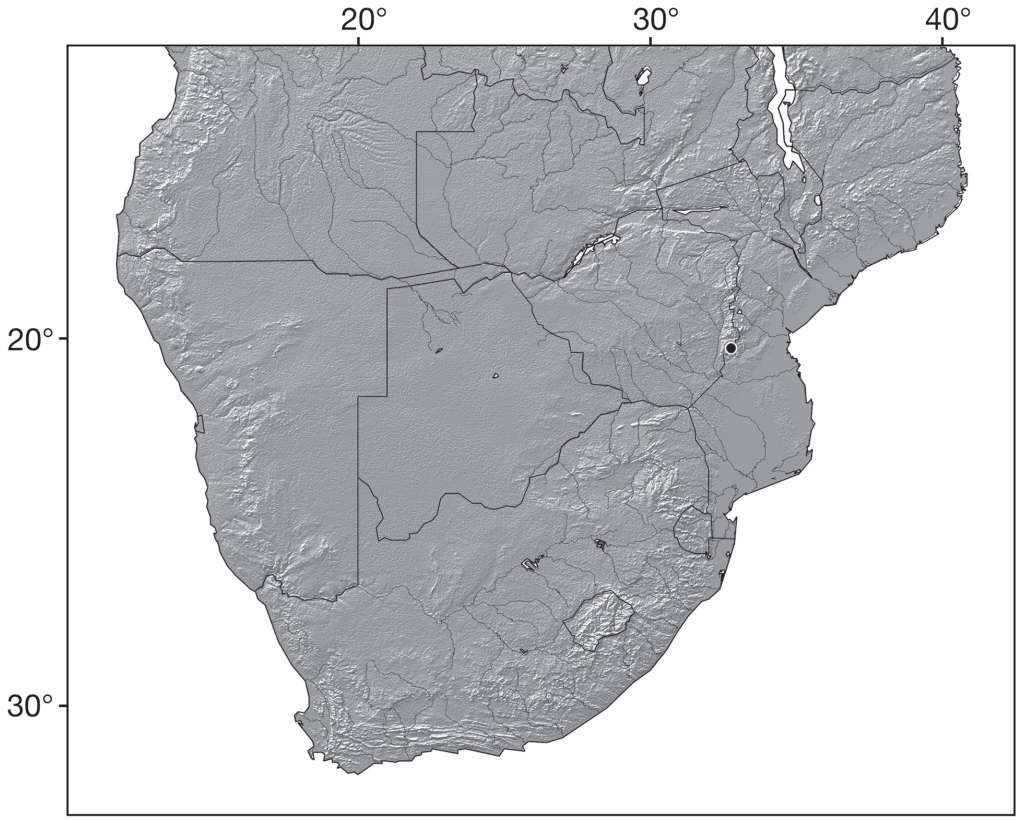

Figure 9. Map of southern Africa showing the type locality of *V. chirindensis* sp. n. in Zimbabwe (20°24'S 32°41'E).

Discussion

The forewing venation of the new genus is similar to *Afrobirthama* Hering, 1955, with R2+3+4+5 on a short stalk and the evenly spaced M veins at their bases. Also, the long fork of RR+M1 in the hindwings is like in *Afrobirthama*. The basally fused M3 and Cu1a is a remarkable character of *Vansoniella* gen. n. and does not occur in the former genus. Also, the genitalia, the antenna and the spur formula are quite different.

The terminal structures of the phallus are not shared by any of the African genera. The digital processes of the juxta of *Vansoniella* gen. n. are also present in *Jordaniana* Hering, 1955 and *Macroplectra* Hampson, 1892. The latter genus even bears the basal apophyses of the juxta, but other genital and external characters are completely different.

The few genera of Limacodidae with transparent wings in the Oriental- and Australasian Region can be distinguished externally by wing venation and antennal

structure. Their genitalia are also quite distinct. The genera do not form a monophyletic entity. In consequence, transparency of wings is to be considered a character which can originate in different evolutionary lines and at different times. It is, thus, of minor value in searching for the sistergroup of *Vansoniella* gen. n., which could comprise species with fully scaled wings. At present time, *Vansoniella* gen. n. is regarded as a derived genus with an isolated position within Limacodidae.

Acknowledgements

I am grateful to Martin Krüger for the loan of specimens from the collection under his curatorship at the Ditsong Museum of Natural History of South Africa, Pretoria. My thanks go to Alexey V. Solovyev (Uljanowsk) for fruitful discussions on the taxonomy of Limacodiae over the years. He and W. Speidel were prepared to review the manuscript. My colleague Jason Dunlop (Berlin) corrected the English text. The financial support of the Museum für Naturkunde, Berlin for the publication of this article is thankfully acknowledged.

References

Basquin P (2016) Découverte d'un nouveau *Chrysopoloma* dans l'ouest africain (Lepidoptera, Limacodidae, Chrysopolominae). Saturnafrica 24: 1–3. [pl. A]

Carcasson RH (1965) New Lepidoptera from East Africa. Journal of the East African Natural History Society 25(2): 131–160.

De Prins J, De Prins W (2018) Afromoths, on line database of Afrotropical moth species (Lepidoptera). http://www.afromoths.net

Heppner JB (1991) Faunal regions and the diversity of Lepidoptera. Tropical Lepidoptera 2(Suppl. 1): 1–85.

Hering EM (1928) Limacodidae (Cochliopodidae, Cochlidionidae). In: Seitz A (Ed.) Die Gross-Schmetterlinge der Erde 14. A. Kernen, Stuttgart, 448–476.

Hering EM (1955) Synopsis der afrikanischen Gattungen der Cochlidiidae (Lepidoptera). Transactions of the Royal Entomological Society of London 107: 209–225. https://doi.org/10.1111/j.1365-2311.1955.tb00474.x

Holloway JD (1986) The moths of Borneo, part 1: Key to the families; families Cossidae, Metarbelidae, Ratardidae, Dudgeoneidae, Epipyropidae and Limacodidae. Malayan nature Journal 40: 1–166.

Janse AJT (1964) Limacodidae. The Moths of South Africa 7: 1–136. [pl. 1–44]

Kurshakov PA, Zolotuhin VV (2013) A review of the genus *Strigivenifera* Hering 1937 (Lepidoptera, Chrysopolomidae) with a description of ten new species. Zoologicheskyi Zhurnal 92(7): 808–824. https://doi.org/10.7868/S0044513413070106

Kurshakov PA, Zolotuhin VV (2016) A new genus and a new species of archaic Chrysopolomidae (Lepidoptera) from Angola. Entomofauna 37(2): 33–40.

Krüger M (2004) Description d'un nouveau *Taeda* de l'Afrique du Sud (Lepidoptera Limacodidae). Lambillionea 104(4): 725–726.

Mey W (2011) Basic pattern of Lepidoptera diversity in southwestern Africa. Esperiana Memoir 6: 1–315.

Pinhey ECG (1968) Some new African Lepidoptera. Annals of the Transvaal Museum 25(9):153–176.

Robinson G (1976) The preparation of slides of Lepidoptera genitalia with special reference to the Microlepidoptera. Entomologist`s Gazette 27: 127–132.

Rougeot PC (1977) Lepidoptera. Missions entomologiques en Ethiopie 1973–1975. Fascicule 1. Mémoires du Muséum national d'Histoire naturelle (A)105: 1–150. [pls. 1–20]

Solovyev AV (2014) *Parasa* Moore auct.: phylogenetic review of the complex from the Palearctic and Indomalayan Regions (Lepidoptera, Limacodidae). Proceedings of the Museum Witt Munich 1, 239 pp.

Stoll C (1781) De uitlandsche Kapellen voorkomende in de drie waereld-deelen Asia, Africa en America, by een verzameld en beschreeven door den Heer Pieter Cramer. S.J. Baalde, Amsterdam, B. Wild, Utrecht, 4(25–34): 1–252. [pls. 289–396. pl. 348, fig. A]

Viette P (1980) Insects Lépidoptères Limacodidae. Faune de Madagascar 53: 1–162.

West RJ (1937) Descriptions of new species of Limacodidae. Annals and Magazine of Natural History (10)20: 77–87. https://doi.org/10.1080/00222933708655316

Dtsch. Entomol. Z. 65 (1) 2018, 81–98 | DOI 10.3897/dez.65.25747

PENSOFT

museum für naturkunde

Review of the genus *Tricerophora* Janse, 1958 (Lepidoptera, Gelechiidae) with description of six new species

Oleksiy V. Bidzilya[1], Wolfram Mey[2]

1 *Institute for Evolutionary Ecology of the National Academy of Sciences of Ukraine, 37 Academician Lebedev str., 03143, Kiev, Ukraine*

2 *Museum für Naturkunde, Leibniz Institute at Humboldt Universität, Invalidenstrasse 43, D-10115, Berlin, Germany*

http://zoobank.org/4FE56A19-4D03-4C35-B4E5-CB1E7469B4CC

Corresponding author: *Oleksiy V. Bidzilya* (olexbid@gmail.com)

Received 12 April 2018
Accepted 4 June 2018
Published 12 June 2018

Academic editor:
Dominique Zimmermann

Abstract

An improved diagnosis of the genus *Tricerophora* is provided, and its position within Gelechiidae is briefly discussed. A new generic synonym is established: *Leucophylla* Janse, 1960, **syn. n.** of *Tricerophora* Janse, 1958. Six new species are described: *T. pundamilia* **sp. n.** (RSA), *T. rukinga* **sp. n.** (Kenya), *T. nigrinervis* **sp. n.** (RSA, Namibia), *T. brumale* **sp. n.** (Namibia), *T. acutivalva* **sp. n.** (Iran), *T. minimorum* **sp. n.** (Namibia). The following new combinations are proposed: *Tricerophora nigribasis* (Janse, 1960), **comb. n.**, *Tricerophora objecta* (Meyrick, 1921), **comb. n.** A key to the species is given based on external characters and the genitalia of both sexes. Adults and genitalia of all species are illustrated.

Key Words

Gelechiinae
Leucophylla
new species
new synonym
Afrotropical region
Namibia
South Africa
Kenya
Palaearctic region
Iran

Introduction

Since their descriptions, the gelechiid genera *Tricerophora* Janse, 1958 and *Leucophylla* Janse, 1960, were considered as monotypic taxa restricted to southern Africa (Namibia, RSA, Mozambique, Zimbabwe). Recent field work in southern (Mey 2011) and eastern Africa (D.J.L. Agassiz in 2010 and 2012) yielded new material of these groups, which turned out to be more species-rich than previously thought. The examination of this fresh material resulted in the discovery of six additional species collected in RSA, Namibia, Kenya and South Iran. The study of the type species of *Tricerophora* and *Leucophylla* revealed a high similarity that does not justify the recognition of two different genera and led us to accept only a single genus with *Tricerophora* as the oldest available name. We also found that *Telphusa objecta* Meyrick, 1921 belongs to *Tricerophora* too. With the discovery of additional new species we are now able to provide an improved and more detailed diagnosis of the genus *Tricerophora*. On this basis we provide some suggestions about the phylogenetic relationship of the genus and its possible sister group, and discuss briefly the position of *Tricerophora* within the family Gelechiidae.

Material and methods

The present paper is based on material from the following collections:

Museum für Naturkunde, Berlin, Germany (MfN), Ditsong National Museum of Natural History of South Africa (formerly Transvaal Museum), Pretoria, South Africa (TMSA), Staatliches Museum für Naturkunde Karlsruhe, Germany (SMNK), Landesmuseum für Kärnten, Klagenfurt, Austria (LMK), Muséum d'histoire Naturelle, Geneva, Switzerland (MHNG) and the research collection of David Agassiz, London, UK (DA) (later transferred to BMNH).

The genitalia slides were prepared according to the "unrolling technique" described in Pitkin (1986) and Huemer (1988). The genitalia were embedded in Euparal. Chlorazol Black and mercurochrome were used for staining. Photographic documentation of the imago was done with Olympus E-410 digital camera attached to microscope Olympus SZX12. Slide-mounted genitalia were photographed with a Canon EOS 600D digital camera mounted on Olympus U-CTR30-2 combined with Carl Zeiss microscope. Holotype label data are quoted verbatim: quotation marks (") signify data on a single label, the end of a line of print is indicated by comma (,) and a straight slash (|) separates labels. Supplementary or qualifying information is provided in square parentheses.

The descriptive terminology of genitalia structures generally follows Huemer and Karsholt (1999) and Kristensen (2003).

Taxonomic account

Check-list of the genus *Tricerophora*

T. commaculata (Meyrick, 1921)	Mozambique, Zimbabwe, RSA
T. nigribasis (Janse, 1960), comb. n.	Namibia, RSA
T. sp. A	RSA
T. pundamilia sp. n.	RSA
T. rukinga sp. n.	Kenya
T. objecta (Meyrick, 1921), comb. n.	D.R. Congo, Zimbabwe
T. brumale sp. n.	Namibia
T. nigrinervis sp. n.	Namibia, RSA
T. acutivalva sp. n.	Iran
T. minimorum sp. n.	Namibia

***Tricerophora* Janse, 1958**

Moths of South Africa 6 (1): 64

Type species: *Telphusa commaculata* Meyrick, 1921

Leucophylla Janse, 1960, **syn. n.**

Moths of South Africa 6 (2): 202

Type species: *Leucophylla nigribasis* Janse, 1960

Diagnosis. Most of *Tricerophora* species are defined by white forewings with black pattern along longitudinal axis without transverse fasciae and dark spots in cell and fold that are common in many other genera of Gelechiidae. Thiotrichinae genus *Polyhymno* Chamners, 1874 has somewhat similar wing pattern to *Tricerophora*, but species of *Polyhymno* are usually smaller in size and pattern along longitudinal axis is brown rather than black in *Tricerophora*.

The tegumen with a strongly sclerotized posterior belt and lateral processes as well as very narrow, long uncus are considered to be presumed autapomorphies of *Tricerophora.*

The female genitalia are characterized by laterally sclerotized segment VIII, well developed antrum, entirely sclerotized ductus bursae in most species, and usually long, serrated arms of the signum.

Species of *Tricerophora* shares the male abdominal segment VIII separated into free tergum and sternum and the presence of a sub-rhomboid or hexagonal signum in females with members of the subfamily Gelechiinae (Huemer & Karsholt 1998: 19). The diagnosis of Gelechiinae was recently improved and clarified on the basis of DNA sequence data for one mitochondrial gene and seven nuclear genes (Karsholt et al 2013). It confirmed the subdivision of subfamily into three tribes - Litini, Gelechiini and Gnorimoschemini based on above mentioned construction of male abdominal segment VIII that is considered as the only synapomorphy of Gelechiinae. *Tricerophora* along with most of related genera has not been considered in the recent classification of Gelechiidae (Karsholt et al. 2013). However, we suggest, that within this subfamily the male genitalia of *Tricerophora* display some similarity to those of the genus *Trychnopalpa* Janse, 1958 by the shape of the uncus (Janse 1960: 203) and the posteriorely modified tegumen. The latter genus can be separated from *Tricerophora* by a quite different gnathos and the presence of well developed, paired process on the posterior margin of the vinculum. Both genera differ additionally in the shape of the phallus, which is shorter and devoid of cornuti in the vesica in *Trychnopalpa*. The genus *Agnippe* Chambers, 1872 shares with species of *Tricerophora* a long, flat gnathos, a long and narrow uncus, cornuti in the vesica but differs by the structure of the gnathos which is separated on dorsal and ventral parts, by the absence of posterior belt-shaped sclerite of tegumen and by the presence of a sclerotized plate in the vesica (Bidzilya and Li 2010). The evenly sclerotized and unmodified sternum VIII and well developed antrum in the female genitalia indicate an affinity of *Tricerophora* with some genera of the tribe Gelechiini like *Mirificarma* Gozmány, 1955, *Chionodes* Hübner, [1825] and *Aroga* Busck, 1914. The female genitalia of *Agnippe* are similar to those of *Tricerophora* too, except for the corpus bursae with long accessory and spines inside that is characteristic for *Agnippe*. However, a somewhat similar but much shorter accessory is observed in *T. nigrinervis* which also points to a close relationship of both genera.

The tribal assignment of *Tricerophora* is rather questionable and difficult to determine. The tendency of form-

ing an accessory bursae in the female genitalia is observed both in genera of Litini (*Parastenolechia* Kanazwa, 1985; *Parachronistis* Meyrick, 1925) and Gelechiini (*Agnippe*). However, the long antrum, the well developed culcitula and the valva, divided into long cucullus and short sacculus are characteristic for Gelechiini (Ponomarenko 2005; Huemer and Karsholt 2010). So, we tentatively place *Tricerophora* into Gelechiini, until the systematic position of this genus will be clarified in future by using molecular methods.

The genus *Leucophylla* Janse, 1960 was established as monotypic for *L. nigribasis* Janse, 1960. Janse (1960) assumed a relationship of *Leucophyla* to *Trychnopalpa* by sharing the same form of the uncus in the male genitalia and a similar signum in the female genitalia. He mentioned that both genera differ in the scale cover of the labial palpi, wing venation and the shape of the phallus. The male genitalia of *Leucophylla* match well of those of *T. commaculata*, the type-species of the genus *Tricerophora*. Also, the female genitalia fit to *T. commaculata* except for the indistinctly formed ostium. However, the examination of the new species of *Tricerophora* shows that this character is rather variable: the ostium may be well developed or indistinct in species whose male genitalia undoubtedly match that of *Tricerophora*. Hence, the following synonymy is proposed here: *Leucophylla* Janse, 1960, syn. n. of *Tricerophora* Janse, 1958.

Description. Adult. Head smoothly scaled, ocelli absent, light, usually off-white or grey, labial palpus strongly up-curved, far protruding over the head, segment 2 with tuft of long scales at base, underside with short brush of scales; segment 3 about as long as segment 2, narrow, pointed. Scape without pecten, male flagellomeres finely ciliated underside.

Thorax white, often mottled with grey or brown, yellowish-white in *T. minimorum*; tegulae the same color as thorax; forewing elongated, moderately narrow, wingspan 7.0–18.0 mm, ground color white to light grey with black pattern along veins, or forewing grey with basal touch at base of costal margin and diffuse black spots under costa (*T. nigribasis*); in *T. minimorum* the forewing is uniformly yellowish-white; hindwing grey, narrow with small subapical excavation, cilia grey.

Abdomen: Male tergum VIII longer than broad, tongue-shaped or triangular, with long haired coremata at base, sternum VIII broader than long, posterior margin broadly rounded. Female segment VII 1.5 times as long as rest of abdominal segments, trapezoidal, weakly narrowed posteriorly.

Male genitalia. Posterior margin of tegumen strongly sclerotized forming a belt-shaped sclerite terminated laterally in narrow short processes (reduced in *T. rukinga*), medially with a stout, long, narrow uncus with a pointed tip; gnathos flat, weakly sclerotized, elongated; culcitula well developed, membranous; tegumen sub-rectangular, about twice as long as broad, anterior margin with deep, triangular emargination; valva elongated, narrow or moderately broad, straight, of even width or curved inwards at 1/3, densely covered with hairs after halfway; sacculus short and slender in most species, merged with valva in *T. acutivalva* or stout, broad, with inwardly curved tip in *T. rukinga*, displaced medially in *T. commaculata*, posterior margin with weakly sclerotized, medial lobe; saccus long and narrow, sub-triangular in *T. rukinga* and *T. acutivalva*; phallus tubular, weakly swollen on base (except for *T. rukinga*), with lateral sclerotized filaments, vesica with one or two (*T. nigrinervis*) cornuti.

Female genitalia. Segment VIII slightly longer than broad, weakly sclerotized; sternum VIII simple, evenly sclerotized, usually more or less covered with microtrichia, with narrow lateral sclerites extending from the base of apophysis anterioris to the posterior margin of sternum, anterior margin strongly sclerotized, projecting medially into well developed tubular or funnel-shaped antrum; ostium rounded, ovate or funnel-shaped, strongly edged with several transverse rings, placed near posterior margin of sternite VIII, or indistinct; apophysis anterioris narrow, straight, about as long as length of segment VIII or longer, apophysis posterioris three-five times as long as apophysis anterioris; ductus bursae varies considerably in length and width, with long sclerotized portion that is connected with antrum or separated (*T. nigribasis*), sometimes entirely sclerotized (*T. rukinga*), with numerous short teeth (*T.* sp. A) or with serrated folds projecting into the corpus bursae (*T. nigrinervis*); corpus bursae rounded or sub-ovate, with posterolateral, partially sclerotized accessory in *T. nigrinervis*; signum a sub-hexagonal plate with short lateral arms, deep medial ridge and long usually serrated laterally anterior and posterior arms.

Biology. Host plant unknown. Adults have been collected from August to December, in February-March and in June in southern Africa up to 1740 m elevation (Brandberg Massive in Namibia), in November in Kenya, in August in DR Congo and in early June in South Iran.

Distribution. Afrotropical Region **(**RSA, Namibia, Mozambique, Zimbabwe, Kenya, DR Congo) and Palaearctic Region (South Iran).

Key to adults based on external characters

(Note: *T. commaculata*, *T. pundamilia* sp. n. and *T. rukinga* sp. n. can hardly be distinguished from each other without examination of genitalia)

1 Wingspan 7.0 mm, forewing uniformly yellowish-white ..... *T. minimorum* sp. n.
– Wingspan 11.1–18.0 mm, forewing mainly light grey or blackish-white 2
2 Forewing light grey with black blotch on base and diffuse black spot in the middle of costa and in cell ..... *T. nigribasis*
– Forewing blackish-white 3

3 Wingspan 13.2–18.0 mm, predominantly black 4
– Wingspan 11.0–12.0 mm, predominantly white 5
4. Forewing with paired white triangular spot in the middle of the costal and dorsal margin ..... *T. objecta*
– Forewing without paired white triangular spot in the middle of the costal and dorsal margin ..... *T. commaculta*, *T. pundamilia* sp. n., *T. rukinga* sp. n.
5 Head and thorax snow-white, forewing with three broad black-lined veins ..... *T. nigrinervis* sp. n.
– Head and thorax mottled with brown, forewing less contrasting..... 6
6 Forewing narrowed in distal half, black irroration indistinct ..... *T. acutivalva* sp. n.
– Forewing not narrowed in distal half, black irroration present ..... *T. brumale* sp. n.

Key to males based on genitalia

(Note: *T.* sp. A. is not included in the key due to its unclear taxonomic state; the male of *T. pundamilia* sp. n. is unknown)

1 Valva inwardly broadened on base and curved inwardly before middle..... *T. commaculata*
– Valva straight, on base of even width 2
2 Sacculus merged with valva..... *T. acutivalva* sp. n.
– Sacculus separated from valva 3
3 Sacculus broader than valva, with inwardly curved tip, uncus longer than tegumen, gnathos trifid apically .. *T. rukinga* sp. n.
– Sacculus narrower than valva, straight, uncus shorter than tegumen, gnathos rounded or truncate apically..... 4
4 Posteromedial lobe of vinculum about half length of valva, phallus with two cornuti ..... *T. nigrinervis* sp. n.
– Posteromedial lobe of vinculum shorter than half length of valva, phallus with single cornutus..... 5
5 Gnathos of even width..... *T. nigribasis*
– Gnathos broadened apically 6
6 Gnathos sub-triangular, truncated posteriorly ..... *T. brumale* sp. n.
– Gnathos clavate, rounded posteriorly..... *T. minimorum* sp. n.

Key to the females based on genitalia

1 Sternum VIII extremely anteriorly prolonged with a large, medial membranous window ..... *T. objecta*
– Sternum VIII without anterior projection 2
2 Ostium distinct 3
– Ostium indistinct..... 5
3 Ostium funnel-shaped, ductus bursae membranous, as long as antrum ..... *T. commaculata*
– Ostium rounded, ductus bursae shorter than antrum, sclerotized 4
4 Ostium sub-ovate, with two transverse sclerotized belts, ductus bursae with teeth..... *T. pundamilia* sp. n.
– Ostium bursae rounded, with one transverse sclerotized belt, ductus bursae without teeth..... *T. rukinga* sp. n.
5 Antrum shorter than half length of the apophysis anterioris 6
– Antrum longer than half length of the apophysis anterioris..... 7
6 Antrum broad, tubular, ductus bursae entirely sclerotized..... *T. brumale* sp. n.
– Antrum narrow, funnel-shaped, ductus bursa sclerotized in proximal half ..... *T. minimorum* sp. n.
7 Ductus bursae with several strongly serrated folds projecting into the corpus bursae ..... *T. nigrinervis* sp. n.
– Ductus bursa without folds..... 8
8 Ductus bursae sclerotized in medial portion, anterior arm of signum truncate..... *T. nigribasis*
– Ductus bursae sclerotized in distal half, anterior arm of signum narrowed apically ..... *T. acutivalva* sp. n.

Review of species

***Tricerophora commaculata* (Meyrick, 1921)**

Telphusa commuculata Meyrick, 1921 – Annals of the Transvaal Museum 8 (2): 69

Type material examined. Holotype of *T. commaculata,* ♀: [Mozambique] "Magude, 11.1910, C.J. Swierstra" | "Telphusa commaculata Meyr., Type Mo. 2517." | "g. 5544" | "994" (TMSA). Paratypes: 2 ♂, Inyack Isl., ix.1910 (Breijer) (gen. slide 5282, 8617) (TMSA).

Other material examined. 1 ex. (abdomen missing), [Mozambique] Lour. Marques, xi.3.21, P.E.A. (Hardenberg); 1 ♂, 1 ex. (abdomen missing), [South Africa], Pretoria N., ix. 1949 (G. v. Son) (gen. slide 8408); 1 ♀, Pretoria N., x.1948 (G. van Son) (gen. slide 8406); 2 ♂, Zoutpan, Pta, 4–10. ii.1929 (G.v.Son) (gen. slide 5152; 606/14, O. Bidzilya); 1 ♂, Lower Sabi, 26.iii.1952 (Janse & Vari); 1 ex. (abdomen missing), Lower Sabi, 26.iii.1962 (Janse & Vari) (all TMSA); 1 ♂, Zimbabwe, Bulawayo, Matopo Nat. Park, 28–30.xi.1993 (Mey & Ebert) (gen. slide 322/07, O. Bidzilya) (MfN).

Diagnosis. The species is defined by black forewings with white area along dorsal margin and diffuse white

spots on 1/3 and 2/3 on costal margin. Externally is nearly indistinguishable from *T. rukinga* sp. n. and *T. pundamilia* sp. n. The valva, broadened medially on base, wrinkled and curved inwardly before middle, and the medially displaced sacculus are characteristic for the male genitalia. The female genitalia are distinct by the tubular antrum sub-equal in length with sternum VIII and the apophysis anterioris, together with the funnel-shaped ostium and long arms of the signum.

Description. Adult (Figs 1–4): Wingspan 15.0–18.0 mm. Head, thorax and tegula white to light grey; segment 2 of labial palpus with short tufts of scales at base, underside with brush of scales, outer surface black at base, three brown rings from middle to apex of segment, inner surface off-white; segment 3 narrow, pointed, light grey irregularly mottled with black; forewing narrow, prolonged, ground colour grey-whitish, densely mottled with brown and black-tipped scales, costal margin with black touch at base and in middle, broad black medial fascia from base to apex, fringe grey black-tipped; hindwing narrow, grey, apex short, weakly pointed.

Male genitalia (Fig. 21): Posterolateral processes of tegumen short, pointed; uncus long, evenly curved; gnathos half the length of uncus, gradually broadened towards rounded top; tegumen a little more than twice as long as broad; valva moderately broad, weakly extending beyond the top of uncus, distinctly curved inwards and wrinkled at 1/3, inwardly broadened on base, hairy after half length, apex pointed; sacculus displaced medially, about 1/4 length of valva, with outwardly curved tip; vinculum three times as broad as long and length 1/4 of valva, posteromedial lobe narrow, pointed apically, about 1/4–1/5 length of valva; saccus broad,weakly narrowed towards rounded apex; phallus weakly swollen on base, distal portion weakly sclerotized, cornutus weakly curved, finely serrated.

Female genitalia (Fig. 29): Sternum VIII 1.5 times as long as broad, lateral sclerites broadened in basal half; ostium funnel-shaped, strongly edged, weakly wrinkled; apophysis anterioris about as long as a length of segment VIII; antrum sub-equal in length in apophysis anterioris, tubular; ductus bursae as long as antrum, weakly broadened towards corpus bursae, with short colliculum; corpus bursae sub-ovate; signum with long serrated arms, the anterior one slightly longer than the posterior one, placed in lateral broadening of the corpus bursae.

Distribution. RSA, Mozambique, Zimbabwe.

Biology. Adults have been collected from September to November and in February-March.

Notes. *T. commaculata* was described on the basis of one female holotype collected in Magude (Mozambique) and two male paratypes from Inyack Island (Mozambique). Additional specimens associated by Janse with *T. commaculata* are from Lourenço Marques (Mozambique), Pretoria, Zoutpan and Kruger National Park (RSA). The holotype matches externally both to paratypes and other specimens except for the head and labial palpi that are white in holotype rather than greyish-white. However, the female genitalia of the holotype (gen. slide 5544) do not match the female from Pretoria (gen. slide 8406) that is figured in the original description (Janse 1960, Pl. 57 g, h). The males including ones from Pretoria and Zoutpan, are similar externally to the female from Pretoria and identical in the genitalia to each other. It is remains unclear if these males are conspecific with the female holotype from Magude or with the female from Pretoria. We provisionally follow Janse and consider the males being *T. commaculata* until additional material becomes available.

Tricerophora nigribasis (Janse, 1960), comb. n.

Leucophylla nigribasis Janse, 1960 – Moths of South Africa 6 (2): 203

Tricerophora sp. 1 – Bidzilya 2007: 99, figs 32, 36; pl. 7, fig. 2

Type material examined. Holotype of *L. nigribasis*, ♂: [RSA] "Pentonville, 60 m, N.W Vaalwater, 27.ix.1953, Harvey & Rorke" | "*Leucophylla nigribasis* J., ♂, HOLOTYPE No: 3729." | "g. 8455" (TMSA). Paratypes: 1 ♀, same data as for holotype (gen. slide 8456); 1 ♂, same data as for holotype (gen. slide 599/14, O. Bidzilya); 1 ♀, [Namibia] Abachaus, S.W.A., Oct. 43 (Hobohm); 1 ♀, Abachaus, S.W.A., xi' 45 (Hobohm) (gen. slide 600/14, O. Bidzilya) (all TMSA).

Material examined. 1 ♂, 2 ♀, [Namibia], Brandberg, Mason Shelter, 1740 m, 5, 7.iii.2002 (Mey) (gen. slide 117/05♂; 197/12♀, O. Bidzilya); 1 ♀, Brandberg, Hungarob-valley, 17.iii.2001, 1200 m (gen. slide 105/05, O. Bidzilya) (all MfN).

Diagnosis. The species is easy recognized by light grey forewing with prominent black touch on base of costal margin, distinct black streak in fold and diffuse black spots under costal margin. The male genitalia are defined by parallel-sided gnathos which is sub-equal in length with uncus, in combination with short, slender saccus, slender valva and phallus with basally broadened cornutus. *T. nigrinervis* sp. n. differs from other congeners by the longer posteromedial lobe of vinculum, longer valva, sacculus and phallus. The comparatively long ductus bursae with a long medially sclerotized portion separated from antrum is diagnostic for *T. nigribasis*.

Description. Adult (Figs 5–6): Wingspan 14.0–18.0 mm. Head, thorax and tegulae white, slightly mottled with brown; segment 2 of labial palpus light grey, base black, brush of raised scales underside, segment 3 slender, acute. Forewing light-grey, black-tipped scales forming indistinct touch at the base of cell, mainly concentrated in subapical area, black spot in the middle and black point in the cell corner, costal margin with obvious black touch at base, diffuse black spots in middle and in 3/4, cilia grey, black-tipped; hindwing and cilia grey.

Male genitalia (Fig. 22): Posterolateral processes of tegumen short, pointed; uncus long, evenly curved; gna-

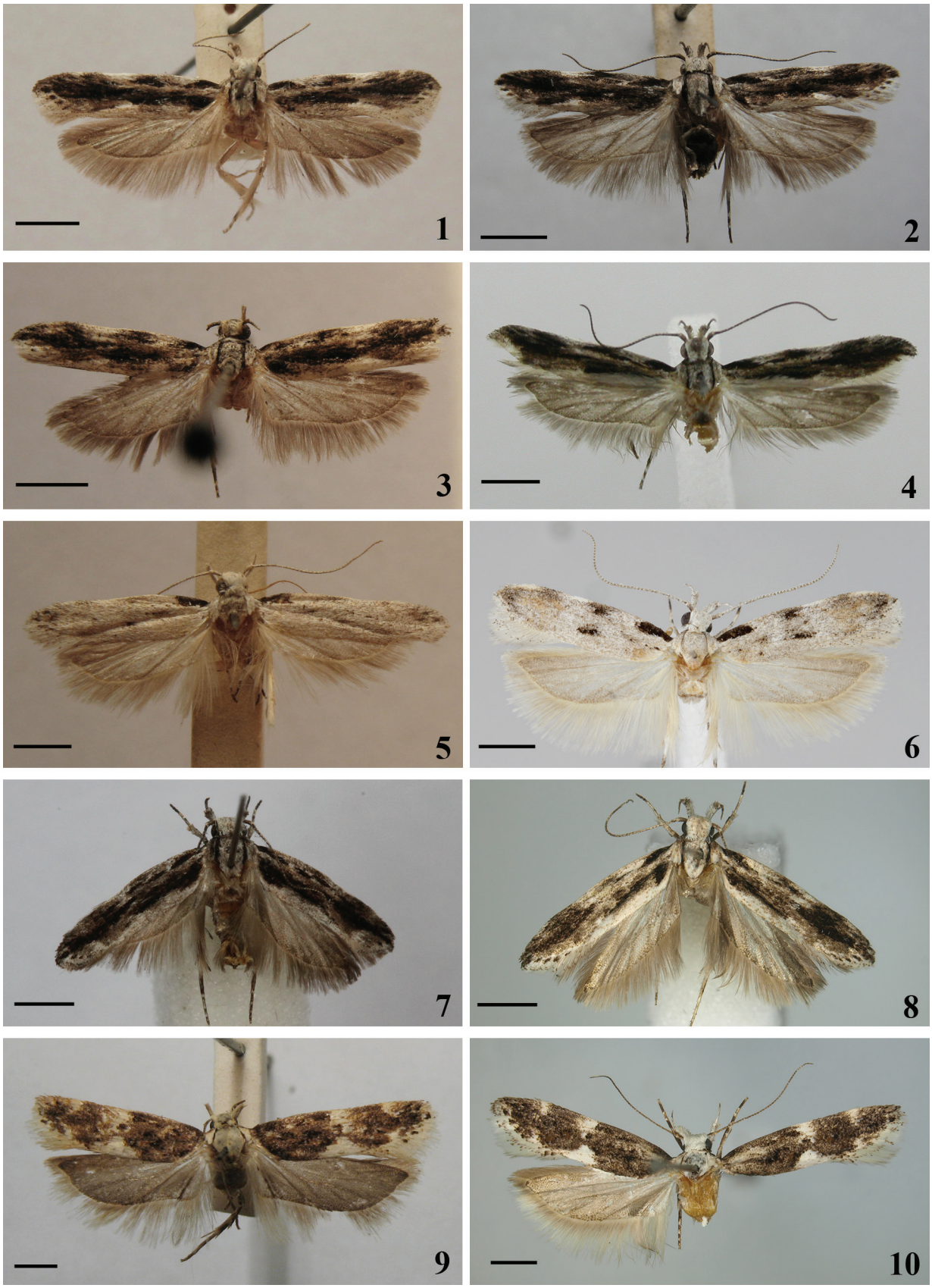

Figures 1–10. Adult of *Tricerophora* spp. **1–4.** *T. commaculata*. **1.** HT, ♀, Magude (gen. slide 5544). **2.** PT, ♂, Inyack Isl. (gen. slide 8617). **3.** ♀, Pretoria (gen. slide 8406). **4.** Zimbabwe, ♂ (gen. slide 322/07, O. Bidzilya). **5–6.** *T. nigribasis*. **5.** HT, ♂, Pentonville (gen. slide 8455). **6.** ♂, Brandberg (gen. slide 117/05, O. Bidzilya). **7–8.** *T. rukinga* sp. n. 7. HT, ♂, Rukinga (gen. slide 324/14, O. Bidzilya (= 1542, DJLA)). **8.** PT, ♀, Rukinga (gen. slide 325/14, O. Bidzilya (= 1543, DJLA)). **9–10.** *T. objecta*. **9.** HT, ♀, Harare. **10.** ♀, Kenya, Tschinkolobwe (gen. slide 103/18, O. Bidzilya). Scale bar = 2 mm.

thos slightly shorter than uncus, of even width, tip rounded; tegumen two times as long as broad; valva nearly straight, narrow, of even width except for weakly broadened distal 1/4, rarely haired, slightly extending beyond the tip of uncus, apex pointed; sacculus about 1/6 length of valva; vinculum 1.5 times as broad as long, slightly more than two times shorter than valva, posteromedial lobe extending to about 1/6 length of the valva, medially with broad triangular emargination; saccus gradually narrowed in middle; phallus weakly swollen on base, cornutus straight, broadened at base.

Female genitalia (Fig. 33): Sternum VIII slightly broader than long, weakly sclerotized, covered with microtrichia and finely wrinkled in basal 2/3; ostium indistinct; apophysis anterioris as long as a length of segment VIII; antrum broad on base, then tubular, 2/3 length of apophysis anterioris; colliculum broad; ductus bursae three times as long as apophysis anterioris, narrow, weakly broadened towards corpus bursae, sclerotized in medial portion; corpus bursae egg-shaped, arms of signum of equal length, anterior one truncate, posterior one weakly narrowed apically, laterally serrated.

Distribution. RSA, Namibia.

Biology. Adults have been collected in September-November and March up to 1740 m elevation at the Brandberg (Namibia).

Notes. *Leucophila nigribasis* was described from two males (including the holotype) and one female collected in Pentonville (South Africa, Limpopo) and five females from Abachaus (Namibia). Janse (1960: 203) noted that females from Abachaus are smaller (14 mm instead of 18 mm) and darker than the specimens from Pentonville. However, the female genitalia are identical indicating their conspecifity. One male and three females from the Brandberg match externally to the female paratypes from Abachaus having the forewing densely irrorated with grey and a wingspan of 14.1–15.2 mm. The male genitalia (gen. slide 117/05, O. Bidzilya) are identical with the holotype and paratype from Pentonville. However, the genitalia of two females (gen. slide 105/05; 197/12, O. Bidzilya) differ considerably (Fig. 34) from female paratypes from Pentonville and Abachaus. The females from Brandberg may represent a further, undescribed species, whose male is unknown.

Tricerophora sp. A

Material. 1 ♂, [RSA] Wylies Poort, 3 m, North, 16.vi.1954 (Janse) (gen. slide 331/14, O. Bidzilya) (TMSA)

Notes. The male genitalia of this single specimen (Fig. 23) differ significantly from the other species of *Tricerophora*. However, taking into account the extreme similarity in habitus among this species (Fig. 12), *T. commaculata* and *T. pundamilia* sp. n. we can not rule out that this specimen might be the opposite sex of one of the following species (see also remarks to *T. commaculata*). Therefore we refrain from naming the species to avoid confusion in future.

Tricerophora pundamilia sp. n.

http://zoobank.org/B6A0D54C-A6B7-4D56-87A5-A49E295F8AB7

Type material. Holotype ♀, [RSA] "Punda Milia, K.N.P. Survey, 1–5.xii.1964, Vari & Potgieter" | "gen. slide 61/15, O. Bidzilya" (TMSA)

Diagnosis. The new species is characterized externally by predominately black forewing with white pattern along dorsal margin and white diffuse spots on 1/3 and 2/3 of costal margin. *T. commaculata* is very similar, but differs in the white head without black irroration and the dorsal margin of the forewing mottled with black. A sub-ovate ostium with two transverse sclerotized belts and sclerotized anterior margin in combination with very short ductus bursae that bears teeth are characteristic for the female genitalia.

Description. Adult (Fig. 11): Wingspan 17.0 mm. Head and thorax covered with white black-tipped scales, labial palpus white, segment 2 with black base and rare brown scales on outer surface, brush of scales underside, segment 3 acute, white mottled with black. Scape brown, flagellum white with brown rings, underside pubescent in male. Tegulae blackish-grey. Forewing covered by weakly raised, black-tipped scales, diffuse white spots on 1/4 and 1/2 of costal margin, subcostal vein with black interrupted streak from base to 1/2 length, distinct black pattern around fold and in mid width from 2/3 towards apex, white patch mottled in with brown from 1/5 of dorsal margin to termen, cilia white, black-tipped. Hindwing and cilia grey.

Male genitalia. Unknown.

Female genitalia (Fig. 30): Sternum VIII about as longer as broad, weakly narrowed distally, membranous, densely covered with fine microtrichia, anterior margin with triangular medial sclerites; ostium sub-ovate, weakly broadened posteriorly, anterior margin strongly edged, with two transverse sclerotized belts; apophysis anterioris about as long as a length of segment VIII; antrum broad, as long as apophysis anterioris, narrowed in distal part towards very short, entirely sclerotized ductus bursae that bears numerous teeth before entrance to corpus bursae; corpus bursae sub-ovate, weakly broadened anteriorly; signum with well serrated arms, the anterior one slightly longer than the posterior.

Etymology. The species is named after Punda Milia in Kruger National Park, the type locality of the new species.

Distribution. RSA.

Biology. The holotype has been collected in early December.

Tricerophora rukinga sp. n.

http://zoobank.org/D524CC4E-C3DC-4B74-A530-70C39B4EF1CC

Type material. Holotype ♂, "KENYA: Coast, Rukinga Estate 500 m, S 3°42'22" E 38°46'34", 14.xi.2012, Agassiz, Beavan & Heckford" | "gen. slide 324/14 (=1542 DJLA), O. Bidzilya" (DA). Paratypes. 1 ♂, 1 ♀,

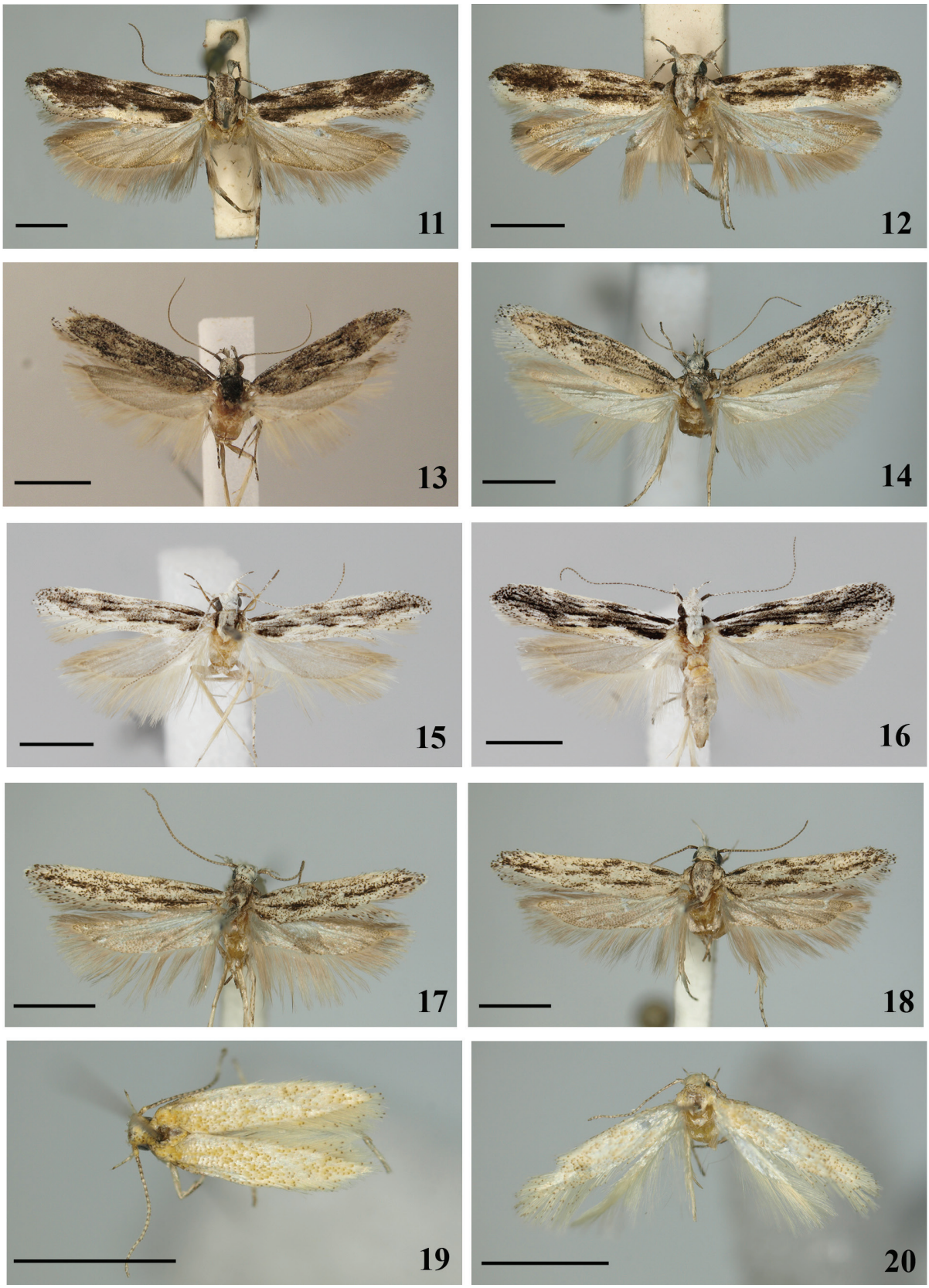

Figures 11–20. Adult of *Tricerophora* spp. **11.** *T. pundamilia* sp. n., HT, ♀, Punda Milia (gen. slide 61/15, O. Bidzilya). **12.** *T.* sp. A, ♂, Wylies Poort (gen. slide 331/14, O. Bidzilya). **13–14.** *T. brumale* sp. n. **13.** HT, ♂, Xaragu Camp (gen. slide 106/12, O. Bidzilya). **14.** PT, ♀, Xaragu Camp (gen. slide 63/18, O. Bidzilya). **15–16.** *T. nigrinervis* sp. n. **15.** HT, ♂, Brandberg (gen. slide 122/05, O. Bidzilya). **16.** PT, ♀, Richtersveld (gen. slide 61/18, O. Bidzilya). **17–18.** *T. acutivalva* sp. n. **17.** HT, ♂, Imam Sade (gen. slide 47/18, O. Bidzilya). **18.** PT, ♂, Imam Sade (gen. slide 1/18, O. Bidzilya). **19–20.** *T. minimorum* sp. n. **19.** HT, ♂, Opuwo (gen. slide 361/14, O. Bidzilya). **20.** PT, ♀, Varianto (gen. slide 536/14, O. Bidzilya). Scale bar = 2 mm

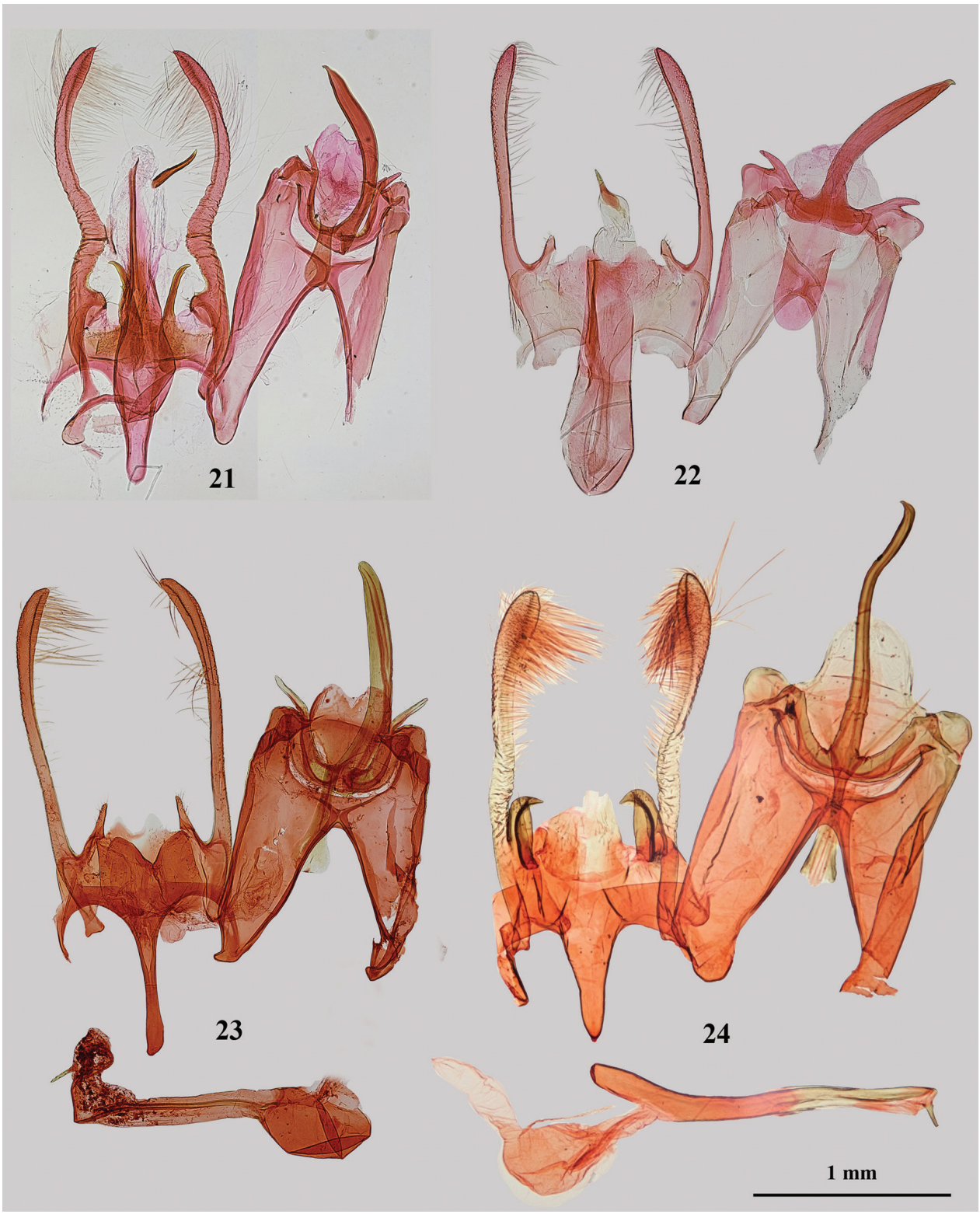

Figures 21–24. Male genitalia of *Tricerophora* spp. **21.** *T. commaculata*, Zimbabwe (gen. slide 322/07, O. Bidzilya). **22.** *T. nigribasis*, Brandberg (gen. slide 117/05, O. Bidzilya). **23.** *T.* sp., Wylies Poort (gen. slide 331/14, O. Bidzilya). **24.** *T. rukinga* sp. n., HT, Rukinga (gen. slide 324/14, O. Bidzilya (= 1542, DJLA)).

same data as for holotype; 1 ♀, same data as for holotype but 11.xi.2012 (Agassiz, Beavan & Heckford) (gen. slide 325/14 (=1543), O. Bidzilya); 1 ♀, KENYA: Coast, Rukinga Estate, same data but 13.xi.2012; 1 ♂, KENYA: Coast, Rukinga Reserve, 520m, 3˚35’15.7S, 38˚44’29.6E, 21.xi.2010 (Agassiz & Ngugi); 1 ♀, KENYA: Coast, Rukinga Reserve, 520m, 3˚35’15.7S, 38˚44’29.6E, 23.xi.2010 (Agassiz & Ngugi) (all DA).

Diagnosis. The new species is characterized externally by predominately black forewing with white pattern along dorsal margin and white blocks on 1/3 and 2/3 of costal margin. It can hardly be distinguished from *T. pundamilia* sp. n. and *T. commaculata* without examination of the genitalia. The male genitalia are very characteristic having a long uncus sub-equal in length with tegumen, a stout sacculus broader than valva and with a pointed, inwardly curved apex as well as the phallus is extremely slender. The rounded, strongly edged ostium with one transverse medial belt, the broad and short antrum, the entirely sclerotized, very short ductus bursae and segment VIII with broad strongly sclerotized anterior margin are characteristic for the female genitalia.

Description. Adult (Figs 7–8): Wingspan 13.2 (♂)-14.0 (♀) mm. Head and thorax covered with white brown-tipped (♀) or grey brown-tipped (♂) scales, labial palpus white, segment 2 with black base and rare brown scales on outer surface, brush of scales underside, segment 3 acute, white mottled with black. Scape brown, flagellum white with brown belts, pubescent on underside in male. Tegulae blackish-grey (♂) or cream-brown (♀). Forewing covered with weakly raised black-tipped scales, diffuse white spots on 1/4 and 1/2 of costal margin, subcostal vein with black interrupted streak from base to 1/2 length, distinct black pattern around fold and in mid width from 2/3 towards to apex, white patch mottled with brown from base to termen along dorsal margin, cilia white, black-tipped. Hindwing and cilia grey.

Male genitalia (Fig. 24): Posterolateral processes of tegumen reduced; uncus very long, narrow; gnathos about two times shorter than uncus, sub-triangular, broadened from base towards trifid apex; tegumen twice as long as broad; valva moderately broad, wrinkled in basal half, distinctly broadened and densely haired in distal 1/3, apex rounded, extending to 2/3 length of uncus; sacculus stout, broader than valva on base, about 1/4–1/5 length of valva, with inwardly curved tip; vinculum two times as broad as long, about 1/3 length of valva, posteromedial lobe irregular, extending to about 1/4–1/5 length of the valva; saccus comparatively short, sub-triangular, gradually narrowed towards slightly pointed apex; phallus very slender, of even width, cornutus short, pointed.

Female genitalia (Fig. 31): Sternum VIII nearly as long as broad, weakly sclerotized, densely covered with fine microtrichia, anterior margin broadly sclerotized; ostium rounded, strongly edged posteriorly, with transverse medial belt; apophysis anterioris about as long as a length of segment VIII; antrum broad, half the length of apophysis anterioris, ductus bursae as long as antrum but narrower, entirely sclerotized; corpus bursae sub-ovate; signum with well serrated arms, the anterior one slightly longer than the posterior one.

Etymology. The species is named after the Rukinga Estate in Kenya, the type locality of the new species.

Distribution. Kenya.

Biology. Adults have been collected in November.

***Tricerophora objecta* (Meyrick, 1921), comb. n.**

Telphusa objecta Meyrick, 1921 – Annals of the Transvaal Museum 8 (2): 70

Type material examined. Holotype of *T. objecta*, ♀: [Zimbabwe] "Salisbury, Rhod., 30.12.'17, A.J.T. Janse" | "*Telphusa objecta* M., TYPE No: 662." | "g. 5546" (TMSA)

Other material examined. 1 ♀, [D.R. Congo] Katanya, Tshinkolobwe, 22.viii.1931 (Romieux) (gen. slide 103/18, O. Bidzilya) (MHNG)

Diagnosis. The species is recognizable externally by the paired white triangular spot in the middle of the costal and dorsal margin of the forewing. The female genitalia are very characteristic having broad, extremely anteriorly prolonged sternum VIII with a large, medial membranous window.

Description. Adult (Figs 9–10): Wingspan 18.0 mm. Head and thorax white, segment 2 of labial palpus white with several brown-tipped scales on outer surface, base black, brush of raised scales underside, segment 3 white mixed with brown, slender, acute. Scape brown mottled with white underside, flagellum light brown with narrow white rings. Tegulae white with brown base. Forewing brown, rarely mottled with slightly raised black-tipped scales, white triangular spot in middle of costal margin and on the opposite side in middle of dorsal margin, another white smaller spot on ¾ of costa, cilia white brown-tipped; hindwing and cilia grey.

Male: Unknown.

Female genitalia (Fig. 32): Sternum VIII about as broad as long, evenly sclerotized in middle, weakly narrowed posteriorly, strongly sclerotized along lateral margins, anterior margin strongly projecting anteriorly forming a stout sub-rectangular lobe with large medial membranous rounded window with uneven edges; apophysis anterioris 3/4 length of segment VIII; antrum very long, tubular, with 15 transverse rings; ductus bursae slightly longer than anterior lobe of sternum VIII, with short sclerotized portion before entrance of corpus bursae, antrum weakly sclerotized, about half the length of ductus bursae, ductus bursae hidden under anterior lobe of sternum VIII but translucent and visible; corpus bursae prolonged; signum with long and broad, serrated arms of equal length.

Distribution. Zimbabwe, D.R. Congo.

Biology. Adults has been collected in December in Zimbabwe and in August in D.R. Congo.

Notes. *Telphusa objecta* was described from the single female holotype collected in Salisbury (Harare), Zimbabwe. Janse (1960: 58) noted that generic position of this species is uncertain and its assignment to *Telphusa* only provisional. The female genitalia of *T. objecta* share with species of *Tricerophora* laterally sclerotized sternum VIII, the long antrum and a signum with long serrated lobes. Despite unknown males, we have no doubt that the species belongs to *Tricerophora*. The ostium with transverse rings indicates the affinity of *T. objecta* to *T. commaculata*, *T. pundamilia* sp. n. and *T. rukinga* sp. n.

***Tricerophora brumale* sp. n.**

http://zoobank.org/E160659A-05A6-4E68-A429-6D9073BA45FF

Type material. Holotype ♂, "Namibia/Namib, Damaralan, Xaragu Camp, 561 m, 7.viii.2007, GEO-WG84, 14˚20'042''E/-20˚24'441''S, leg. Dr. C. Wieser, Kärtner Landesmusem" |"gen. slide 106/12, O. Bidzilya" (KLM). Paratypes: 1 ♀, same data as holotype (gen. slide 63/18, O. Bidzilya) (KLM)

Diagnosis. The new species is defined externally by cream-white forewing gradually mottled with black and brown but without distinct black markings and patterns. *T. nigrinervis* sp. n. differs in the snow-white head without brown scales, more prominent black marking along veins and white area along dorsal margin of the forewing. *T. acutivalva* differs in the less black-irrorated and narrowed after half length of the forewing. The long and broad saccus, triangular gnathos, comparatively broad valva and triangular cornutus separate *T. wieseri* sp. n. from the rest of *Tricerophora*-species. A short antrum in combination with a long ductus bursae, pear-shaped corpus bursae and signum with broad weakly serrated arms are characteristic for the female genitalia.

Description. Adult (Figs 13–14): Wingspan 10.8–11.2 mm. Head, thorax and tegulae covered with white black-tipped scales, frons white, the female paratype with a head completely white. Labial palpus up-curved, far protruding over the head, segment 2 white with black-tipped scales, nearly white in middle with brush beneath, segment 3 narrow, pointed, white with a few black scales mainly in middle. Scape black, antennal segments white with black rings, male flagellum covered beneath with numerous short hairs (ciliated). Forewing cream-white, densely mixed with black, 2–3 diffuse black patches near the base and in cell, cilia white, black-tipped. Hindwing light grey.

Male genitalia (Fig. 25): Posterolateral processes of tegumen short, pointed; uncus long, straight; gnathos slightly shorter than uncus, sub-triangular, broadened from base towards apex; tegumen two times long as broad; valva moderately broad, curved inwards in distal 1/4, haired, slightly extending beyond the top of uncus, apex pointed; sacculus about 1/3 length of valva, straight, apex rounded; vinculum tree times as broad as long and about 1/4 length of valva, posteromedial lobe triangular, extending to about 1/3 length of valva; saccus moderately broad, weakly constricted before apex; phallus weakly swollen on base, cornutus short, triangular.

Female genitalia (Fig. 36): Sternum VIII slightly longer than broad, membranous; ostium indistinct; apophysis anterioris about as long as a length of segment VIII; antrum tubular, 1/3 length of apophysis anterioris; ductus bursae entirely sclerotized, of even width, as long as apophysis anterioris, with distinct transition towards pear-shaped corpus bursae; signum with broad, weakly serrated arms, the anterior one slightly longer and broader than the posterior one.

Etymology. The specific name is derived from Latin "*brumalis*" –, winter-like, and alludes to the winter activity of the adult.

Distribution. Namibia.

Biology. Adults have been collected in early August.

***Tricerophora nigrinervis* sp. n.**

http://zoobank.org/1C6EC60C-4200-4A96-A9D3-C332F200332B

Tricerophora sp. 2 – Bidzilya 2007: 99, figs 31, 35; pl. 7, fig. 3

Type material. Holotype ♂, "Namibia, Brandberg, 1100 m, 1.xii.2000, LF, W. Mey | "gen. slide 122/05, O. Bidzilya" (MfN). Paratypes: 1 ♀, same data as holotype (gen. slide 77/18, O. Bidzilya); 2 ♀, same data, but 800 m, 3.xii.2000 (Mey) (gen. slide 100/05, O. Bidzilya); 1 ♀, same data, but 1400 m, 2.xii.2000 (Mey); 1 ♂, Namibia, Brandberg, Ugab, 30.xi.2000, LF (Mey); 1 ♀, Namibia, Windhoek, Farm Ondekaremba, 18.ii.2008, Turm (Mey) (all MfN); 1 ♀, Namibia/Namib, Damaralan, Xaragu Camp, 561 m, 7.viii.2007, GEO-WG84, 14 20 042 E/-20 24 441 S, leg. Dr. C. Wieser, Kärtner Landesmusem (gen. slide 130/12, O. Bidzilya) (KLM); 1 ♀, RSA, Richtersveld, Numees, Helskloof Gate, 9–12.x.2001, LF (Mey) (gen. slide 61/18, O. Bidzilya) (MfN)

Diagnosis. The new species can be recognized by its relatively small wingspan, snow-white head and thorax and contrast blackish-white forewing distinctly mottled with black mainly along veins and fold. *T. brumale* sp. n. and *T. acutivalva* sp. n. differ in more extensive black irroration on the head, thorax and forewing and less distinct (by *T. brumale* sp. n.) black pattern along veins. The long phallus with two cornuti in combination with long posteromedial lobe of vinculum and comparatively short and broad gnathos are characteristic for the male genitalia. The female genitalia are defined by the long ductus bursae with sclerotized serrated folds, corpus bursae with posterolateral accessory bursa and short arms of the signum.

Description. Adult (Figs 15–16): Wingspan 11.1–11.8 mm. Head and thorax white, labial palpus white, segment 2 with black base and rare brown scales on outer surface, brush of scales underside, segment 3 acute, white mottled with black. Scape brown, flagellum white with brown belts, pubescent by male on underside. Tegulae black. Forewing covered with white, black-tipped scales, diffuse white spots on 1/2 and 3/4 of costal margin, subcostal vein black from base to 1/2 length, black streaks along veins in costal half and in fold, whitish-cream patch mottled with brown in middle from base to nearly 1/2–2/3 of dorsal margin, diffuse white tornal spot on 3/4, cilia white, black-tipped. Hindwing and cilia grey.

Male genitalia (Fig. 27): Posterolateral processes of tegumen short, pointed; uncus long, evenly curved; gnathos half the length of uncus, broad, about of even width, top rounded; tegumen twice as long as broad; val-

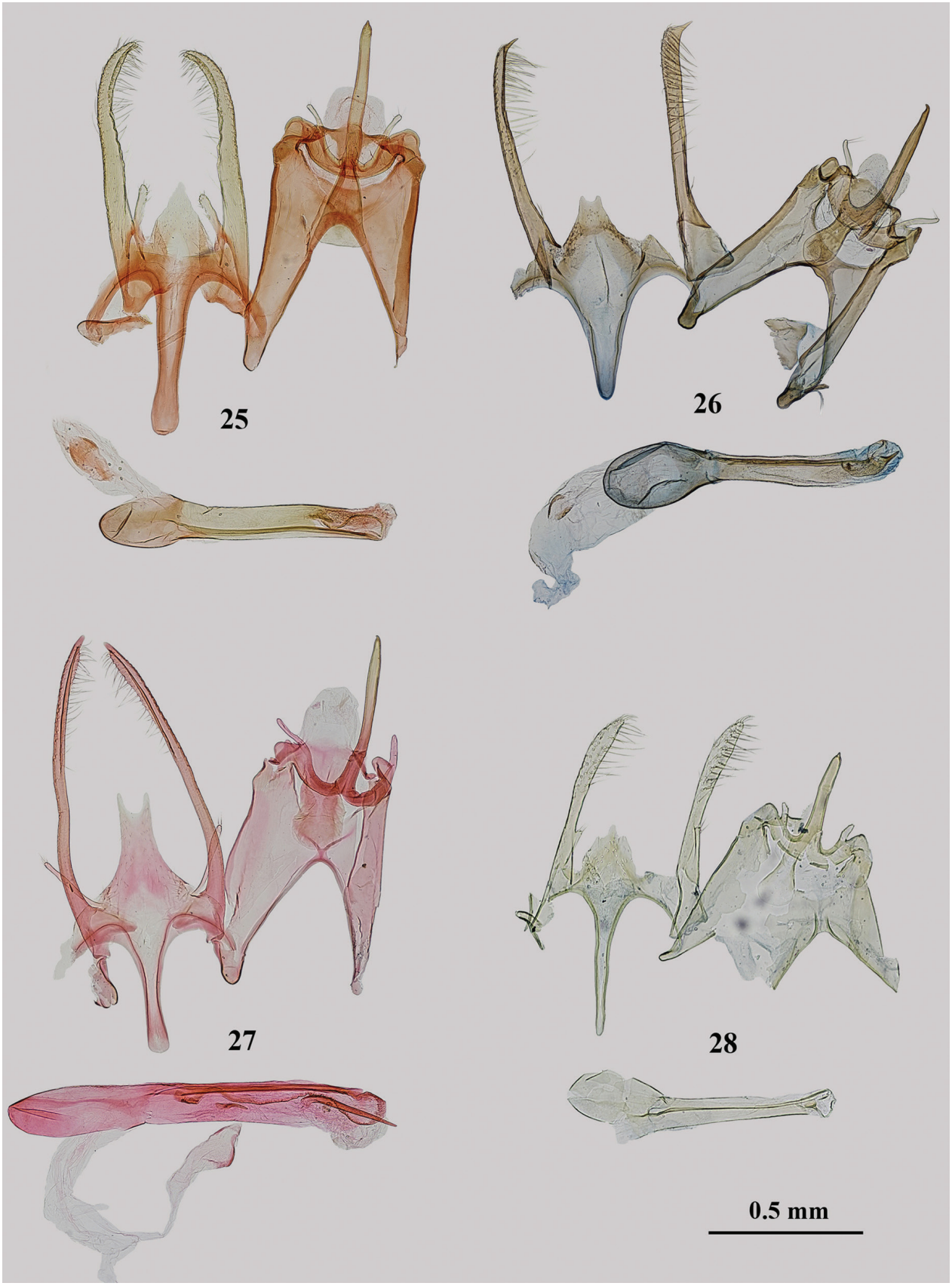

Figures 25–28. Male genitalia of *Tricerophora* spp. **25.** *T. brumale* sp. n., HT, Xaragu Camp (gen. slide 106/12, O. Bidzilya). **26.** *T. acutivalva* sp. n., HT, Imam Sade (gen. slide 47/18, O. Bidzilya). **27.** *T. nigrinervis* sp. n., HT, Brandberg (gen. slide 122/05, O. Bidzilya). **28.** *T. minimorum* sp. n., HT, Opuwo (gen. slide 361/14, O. Bidzilya).

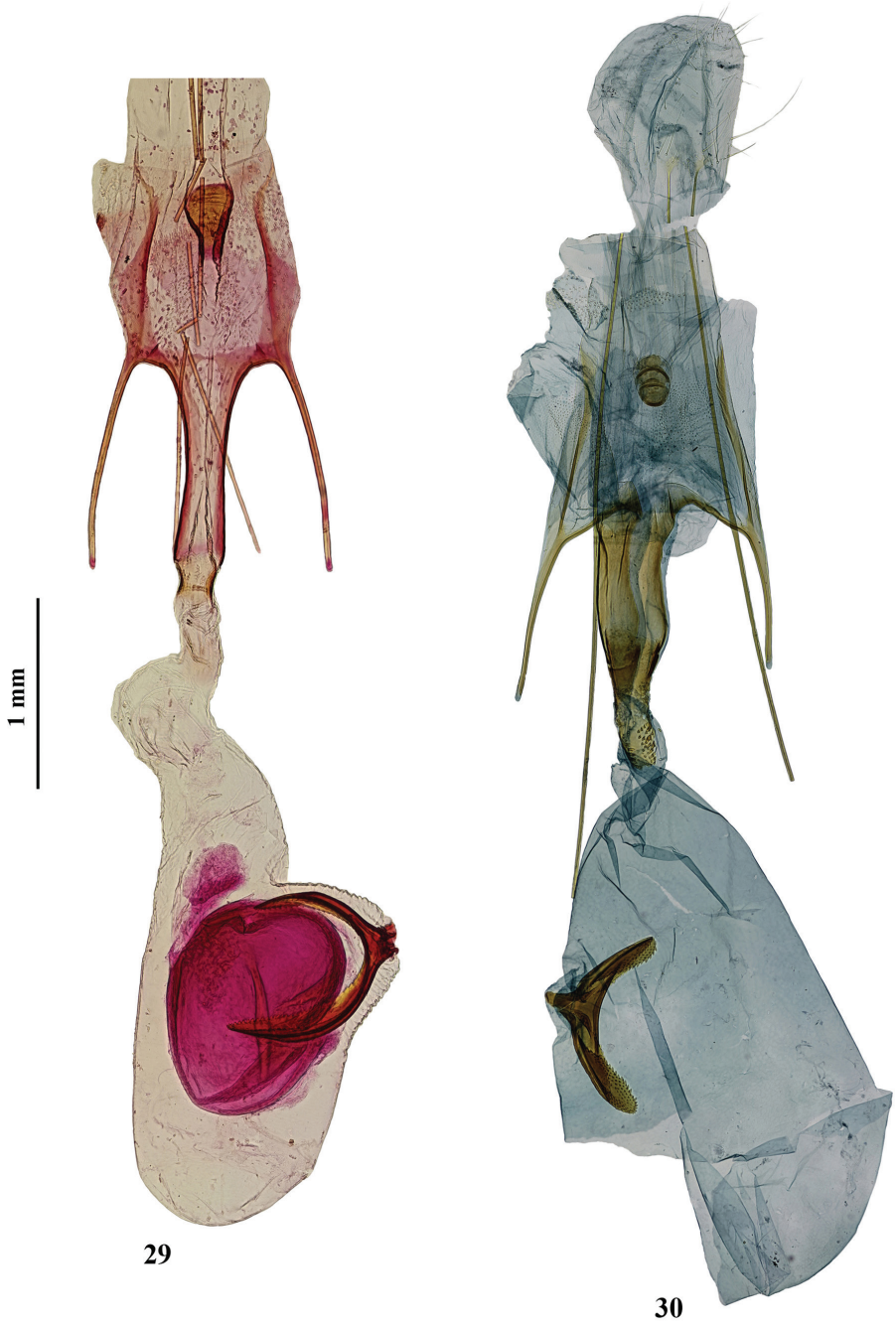

Figures 29–30. Female genitalia of *Tricerophora* spp. **29.** *T. commaculata*, HT, Magude (gen. slide 5544). **30.** *T. pundamilia* sp. n., Punda Milia, HT (gen. slide 61/15, O. Bidzilya).

va nearly straight, narrow, of even width, rarely haired, slightly extending beyond tip of uncus, apex pointed; sacculus about 1/3–1/4 length of valva, very narrow; vinculum three times as broad as long, about 1/6–1/7 length of valva, posteromedial lobe long, extending nearly to half length of the valva, medially with triangular emargination; saccus moderately broad, sligthly narrowed in middle, apex rounded; phallus nearly of even width, as long as tegumen and uncus, medial cornutus short, apical cornutus long and slender, weakly curved at base, than straight, pointed.

Female genitalia (Fig. 35): Segment VIII about as long as broad, sternum VIII membranous, ostium indistinct; apophysis anterioris slightly longer than segment VIII; antrum funnel-shaped, gradually narrowed anteriorly, longer than apophysis anterioris, constricted in the place of connection to ductus bursae; ductus bursae broader and slightly shorter than antrum, with several strongly serrated folds projecting into the corpus bursae; corpus bursae rounded, with broad, partially sclerotized posterior-lateral accessory bursa; signum with very short anterior and posterior arms and broad medial ridge.

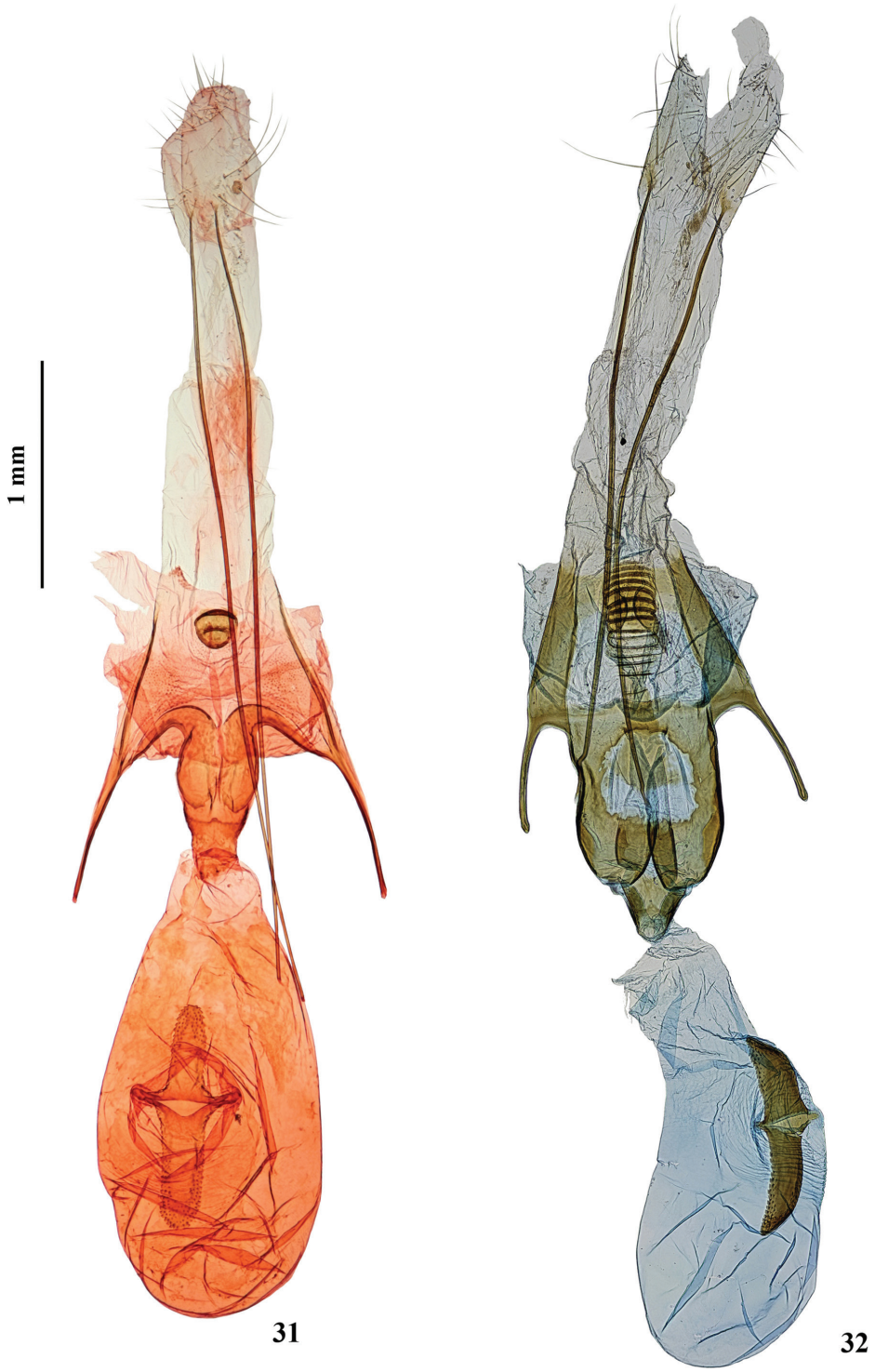

Figures 31–32. Female genitalia of *Tricerophora* spp. **31.** *T. rukinga* sp. n., PT, Rukinga (gen. slide 325/14, O. Bidzilya (= 1543, DJLA)). **32.** *T. objecta*, Kenya, Tschinkolobwe (gen. slide 103/18, O. Bidzilya).

Etymology. The specific name is derived from Latin "*niger*" – black and "*nervus*" – vein, reflecting the characteristic forewing pattern of the new species.

Distribution. Namibia, RSA.

Biology. Adults have been collected in August, October, December and February up to 1100 m elevation at the Brandberg (Namibia).

***Tricerophora acutivalva* sp. n.**

http://zoobank.org/C10FB999-029D-4FCD-8711-4D73DA3B04B9

Type material. Holotype ♂, [Iran], "S-Iran, Strasse Shiraz-Kazerun, Imam Sade, 1200 m, 3.vi.1969, H.G. Amsel leg." | "gen. slide 47/18, O. Bidzilya" (SMNK); Paratypes: 3 ♂, 4 ♀, same data as holotype (gen. slide 1/18♂,

Figures 33–35. Female genitalia of *Tricerophora* spp. **33.** *T. nigribasis*, PT, Abachaus (gen. slide 600/14, O. Bidzilya). **34.** *T.* sp., Brandberg (gen. slide 105/05, O. Bidzilya). **35.** *T. nigrinervis* sp. n., PT, Brandberg (gen. slide 77/18, O. Bidzilya).

77/18♀, O. Bidzilya); 1 ♂, S-Iran, 4–7.vi.1969, Miyan Katal, 1900 m, östl. Kazerun, 51˚40'öL, 29˚30'nB (Amsel) (all SMNK)

Diagnosis. The new species is defined externally by the forewing narrowed in distal half and less extensive black pattern contrary to the other blackish-white *Tricerophora*-species. *T. brumale* sp. n. is more strongly black-irrorated and the forewings are not narrowed in distal half. The apically acute valva with merged sacculus and broad sub-triangular saccus are characteristic for the male genitalia. The female genitalia are distinct by sternum VIII broadly sclerotized laterally in combination with long and broad ductus bursae which is sclerotized in distal half only.

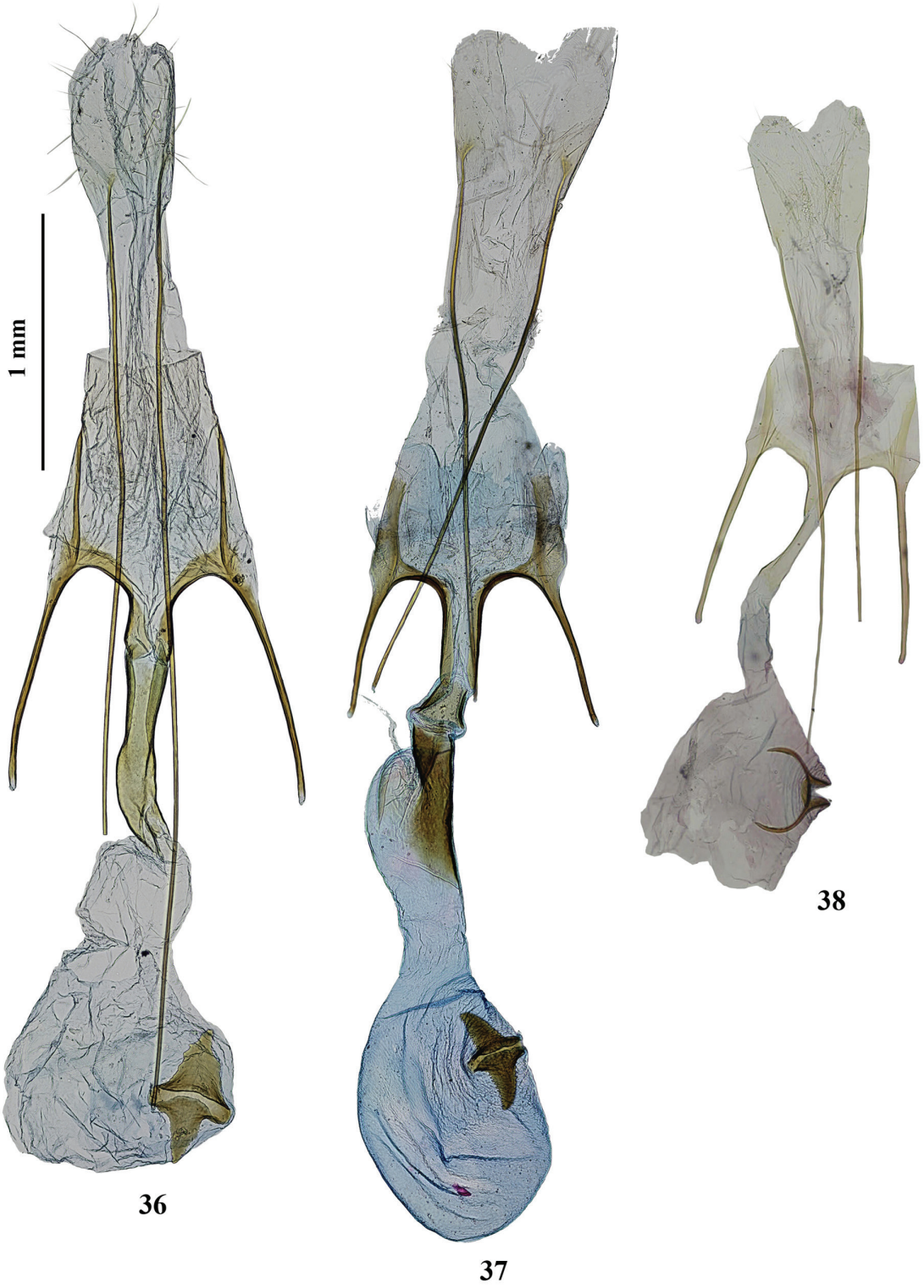

Figures 36–38. Female genitalia of *Tricerophora* spp. **36.** *T. brumale* sp. n., PT, Xaragu Camp (gen. slide 63/18, O. Bidzilya). **37.** *T. acutivalva* sp. n., PT, Imam Sade (gen. slide 77/18, O. Bidzilya). **38.** *T. minimorum* sp. n, PT, Varianto (gen. slide 536/14, O. Bidzilya).

Description. Adult (Figs 17–18): Wingspan 10.0–12.0 mm. Head white with rare black-tipped scales on neck, labial palpus white, segment 2 with black base and rare black scales on outer surface, brush of scales underside, segment 3 acute, white mottled. Scape light brown, flagellum light brown with white belts, pubescent by male on underside. Thorax and tegulae white mixed with black-tipped scales. Forewing white with veins distinctly mottled with black, black streak on mid width from 2/3 length towards apex, cilia white black-tipped. Hindwing and cilia grey.

Male genitalia (Fig. 26): Posterolateral processes of tegumen moderately long, pointed; uncus straight; gnathos about 3/4 length of uncus, weakly constricted in middle, apex broadly rounded; tegumen twice as long as broad; valva moderately broad, of even width, haired, far extending beyond the top of uncus, apex elongated and distinctly pointed; sacculus merged with valva; vinculum four times as broad as long, about 1/6 length of valva, posteromedial lobe trapezoidal, medially broadly emarginated, extending to 1/4 length of valva; saccus broad, sub-triangular, apex rounded; phallus swollen on base, slightly broadened distally, cornutus short, broad on base.

Female genitalia (Fig. 37): Sternum VIII as long as broad, membranous except for strongly sclerotized areas along lateral margins; ostium indistinct; apophysis anterioris slightly longer than segment VIII; antrum tubular, somewhat broadened in distal 3/4, as long as length of apophysis anterioris; ductus bursae 1.5 times as broad as antrum, with sclerotized patch in distal half along right margin, left margin weakly inflated distally, twice as long as apophysis anterioris, with distinct transition towards egg-shaped corpus bursae; arms of signum of equal length and width, gradually narrowed apically, distinctly serrated.

Etymology. The specific name is derived from Latin "acutus" – sharp, and "valva" – clasper, referring the apically pointed valva of the new species.

Distribution. Iran.

Biology. Adults have been collected in early June.

***Tricerophora minimorum* sp. n.**

http://zoobank.org/BA95D532-3209-46D3-8C7C-5274C561D6D9

Type material. Holotype ♂, "Namibia, Opuwo, Op. County Hotel, 2.ix.2012, 1237 m, W. Mey" | "gen. slide 361/14, O. Bidzilya" (MfN). Paratypes: 1 ♀, Namibia, Varianto Farm, Otavi Mountains, 29–31.iii.2003 (Mey) (gen. slide 576/14, O. Bidzilya) (MfN)

Diagnosis. The species is unmistakable separated from rest of *Tricerophora* species by its exceptionally small size and uniformly coloured yellowish-white forewing. The male genitalia are defined by the saccus that is about as long as the length of valva, the uncus that is as long as gnathos and a very short cornutus in the phallus. *T. pundamilia* sp. n. is somewhat similar but the saccus is about half the length of valva. The long apophysis anterioris and ductus bursae equally divided in sclerotized and membranous halves are characteristic for the female genitalia.

Description. Adult (Figs 19–20): Wingspan 7.0 mm. Head and labial palpus yellowish-white, segment 3 mixed with brown on base and before apex. Scape yellow mottled with light brown, flagellum yellow with broad brown rings, pubescent by male on underside. Thorax, tegulae and forewing covered with yellowish-white brown-tipped scales, cilia white. Hindwing and cilia light grey.

Male genitalia (Fig. 28): Posterolateral processes of tegumen short, pointed; uncus straight; gnathos as long as uncus, narrow with distinctly broadened round apex; tegumen 1.5 times as long as broad; valva narrow, straight, weakly broadened and haired dorsally, slightly extending beyond the tip of uncus, apex pointed; sacculus about 1/3 length of valva, very narrow, straight; vinculum 3.5–4 times as broad as long, about 1/4–1/5 times length of valva, posteromedial lobe sub-triangular, extending to 1/3 length of valva; saccus long and narrow, apex rounded; phallus slightly swollen at base, cornutus short.

Female genitalia (Fig. 38): Sternum VIII slightly broader than long, evenly sclerotized, ostium indistinct; apophysis anterioris twice as long as segment VIII; antrum narrow, funnel-shaped, 1/3 length of apophysis anterioris; ductus bursae as long as apophysis anterioris, weakly broadened towards corpus bursae, sclerotized in proximal half; corpus bursae rounded; signum with long, serrated arms of equal length.

Etymology. The specific name refers to the small size of the new species.

Distribution. Namibia.

Biology. Adults have been collected in September and March.

Acknowledgements

We are thankful to Martin Krüger (TMSA), David Agassiz (NHM London, UK), Christian Wieser (KLM) and Bernard Landry (MHNG) for providing access to the collection under their care and for sending additional information on specimens.

The visits of the first author to MfN and TMSA were financially supported by the German Academic Exchange Service (DAAD) and Ernst Mayr Travel Grant from the Museum of Comparative Zoology, Harvard University (USA). Field work in Namibia by the second author was funded by the MfN, DFG and the BIOTA Project (BMBF).

We are thankful to the editor of DEZ and two reviewers, who made constructive suggestions to improve the manuscript. Authors acknowledge the MfN for waiving the authors fees and David Agassiz for the linguistic correction of the manuscript.

References

Bidzilya O (2007) Gelechiidae (Lepidoptera: Gelechioidea). In: Mey W (Ed.) The Lepidoptera of the Brandberg Massif in Namibia. Part 2. Esperiana Memoir 4: 91–118. [pl. 5–8]

Bidzilya O, Li H (2010) Review of the genus *Agnippe* (Lepidoptera: Gelechioidea) in the Palaearctic region. European Journal of Entomology 107: 247–265. https://doi.org/10.14411/eje.2010.033

Huemer P (1988) A taxonomic revision of *Caryocolum* (Lepidoptera, Gelechiidae). Bulletin of the British Museum (Natural History), Entomology 57(3): 439–571.

Huemer P, Karsholt O (1999) Gelechiidae I (Gelechiidae: Gelechiinae, Teleiodinae). In: Huemer P, Karsholt O, Lyneborg L (Eds) Microlepidoptera of Europe. Vol. 3. Apollo Books, Stenstrup, 356 pp.

Janse AJT (1958) Gelechiidae. The Moths of South Africa 6(1): 1–144. [pl. 1–32]

Janse AJT (1960) Gelechiidae. The Moths of South Africa 6(2): 145–240. [pl. 33–129]

Karsholt O, Mutanen M, Lee S, Kaila L (2013) A molecular analysis of the Gelechiidae (Lepidoptera, Gelechioidea) with an interpretative grouping of its taxa. Systematic Entomology 38: 334–348. https://doi.org/10.1111/syen.12006

Kristensen NP [Ed.] (2003) Lepidoptera: Moths and Butterflies 2. Morphology, Physiology and Development. Handbook of Zoology 4(36). Berlin & New York, 564 pp.

Mey W (2011) Basic pattern of Lepidoptera diversity in southwestern Africa. Esperiana Memoir 6: 1–315.

Meyrick E (1921) Descriptions of South African Micro-Lepidoptera. Annals of the Transvaal Museum 8(2): 49–148.

Pitkin L (1986) A technique for the preparation of complex male genitalia in Microlepidoptera. Entomologist's Gazette 37: 173–179.

Dtsch. Entomol. Z. 65 (1) 2018, 99–115 | DOI 10.3897/dez.65.26261

PENSOFT

museum für naturkunde

Review of the flower-inhabiting water scavenger beetle genus *Cycreon* (Coleoptera, Hydrophilidae), with descriptions of new species and comments on its biology

Emmanuel Arriaga-Varela[1,2], Sin Yeng Wong[3,4,5], Alexander Kirejtshuk[6,7], Martin Fikáček[2,1]

1 *Department of Zoology, Faculty of Science, Charles University, Viničná 7, CZ-128 44 Praha 2, Czech Republic*
2 *Department of Entomology, National Museum, Cirkusová 1740, CZ-193 00 Praha, Czech Republic*
3 *Faculty of Resource Science & Technology, Universiti Malaysia Sarawak, 94300 Kota Samarahan, Sarawak, Malaysia*
4 *Harvard University Herbaria, 22 Divinity Avenue, Cambridge, MA 02138, USA*
5 *Ludwig-Maximilians-Universität München, Department Biologie I, Systematische Botanik und Mykologie, Menzinger Straße 67, 80638 München, Germany*
6 *Zoological Institute, Russian Academy of Sciences, Universitetskaya emb., 1, 199034 St. Petersburg, Russia*
7 *CNRS UMR 7205, Muséum national d'histoire naturelle, CP 50, Entomologie 45, rue Buffon, F-75005 Paris, France*

http://zoobank.org/4B756F25-162F-4FDA-BE04-60F397663847

Corresponding author: *Martin Fikáček* (mfikacek@gmail.com)

Received 28 April 2018
Accepted 6 June 2018
Published 12 June 2018

Academic editor:
James Liebherr

Key Words

Sphaeridiinae
Megasternini
flower visitor
Araceae
Schismatoglottideae
new species
Malay Peninsula
Borneo
Oriental Region
pollination

Abstract

The hydrophilid genus *Cycreon* Orchymont, 1919, previously known from two historical specimens only, is reviewed based on the numerous material collected recently from the inflorescences of various Araceae species in the Malay Peninsula and Borneo. Four species are recognized in the genus: *C. sculpturatus* Orchymont, 1919 from Sumatra, *C. armandi* Shatrovskiy, 2017 from Singapore, *C. adolescens* **sp. n.** from peninsular Malaysia, and *C. floricola* **sp. n.** with two subspecies, the nominotypical one from Peninsular Malaysia, and *C. floricola borneanus* **subsp. n.** from Borneo. All species are very similar, differing only by the pronotal punctation, shape of the clypeus and the mentum, and the form of the median lobe of the aedeagus. Specimens of *C. floricola* **sp. n.** and *C. adolescens* **sp. n.** were collected from inflorescences of various genera of the family Araceae. The field observations and analysis of mid gut contents indicates that they feed on organic material on internal organs of the inflorescences, including the pollen of the host plant. They were also observed to carry a large amount of pollen and are likely pollinators of their host species of Araceae.

Introduction

Among the water scavenger beetles (Polyphaga: Hydrophiloidea: Hydrophilidae), the members of the tribe Megasternini stand out in terms of species and morphological diversity, faster speciation rate and the wide array of microenvironments inhabited (Bloom et al. 2014; Fikáček et al. 2009, 2012). Most of the megasternine species are associated with various kinds of decaying organic matter, like mammal dung (e.g., Smetana 1978, Ryndevich 2008, Ryndevich et al. 2017, Arriaga-Varela et al. 2017, 2018), humid forest leaf-litter (e.g., Deler-Hernández et

al. 2015; Fikáček et al. 2009; Fikáček and Short 2006) or rotten seaweed (e.g., Smetana 1978; Ryndevich 2001). In contrast to this general pattern, few genera are known to inhabit the interior of various inflorescences: the Neotropical *Pelosoma* Mulsant has been collected inside *Heliconia* flowers (Archangelsky 1997), and the Neotropical *Nitidulodes* Sharp and Oriental *Cycreon* Orchymont, 1919 were recently reported to be associated to Araceae flowers (Bloom et al. 2014; Low et al. 2016; Hoe and Wong 2016; Hoe et al. 2018). However, very little is known about the biology and the systematics of these genera.

Only two specimens of *Cycreon* are known so far in the literature, representing two different species. The genus was described by d'Orchymont (1919) with *Cycreon sculpturatus* d'Orchymont, 1919 as the only species, based on a single female specimen collected in Palembang, Sumatra without any detailed collecting data. An additional male specimen from Singapore was later examined by d'Orchymont and labeled as '*Cycreon emarginatus* sp. n., however, whether is it not the male of *C. sculpturatus*', but never published. Both specimens were moreover on loan from d'Orchymont collection when M. Hansen was preparing a generic review of the hydrophiloid beetles (Hansen 1991). Shatrovskiy (2017) examined both these specimens and described the second specimen, male from Singapore, as *Cycreon armandi*.

Extensive sampling of insects associated with inflorescences of Malayan aroid plants was performed recently by Low et al. (2014, 2016), Hoe and Wong (2016) and Hoe et al. (2018) in order to study their pollination biology, and Takizawa (2010) in order to study the association of species of *Chaloenus* Westwood, 1861 (Chrysomelidae) with these inflorescences. As a result, a high number of *Cycreon* specimens from both Peninsular Malaysia and Borneo was accumulated. In this study, we use this material to redescribe and illustrate the genus *Cycreon* in detail, to revise the systematics of the genus, and to sum up the available data on the biology of the genus.

Material and methods

Examined specimens and depositories. A total of 1444 specimens of *Cycreon* were examined. Label data are reproduced verbatim; notes on the label data or additional information are written between square brackets []. List of examined specimens is available in DarwinCore-formatted spreadsheet file at Zenodo repository (https://doi.org/10.5281/zenodo.1258208). This file was also used to prepare the distribution map using QGIS software and freely available GLOBE altitude data and DIVA-GIS country borders data. The authors did not examine holotypes of *C. sculpturatus* and *C. armandi* as these are not accessible for the examination, and adopted the information about them from Shatrovskiy (2017). In addition, A. Shatrovskiy kindly provided a new photograph of ventral view of the head of *C. sculpturatus* used to illustrate the shape of the mentum of this species (Fig. 5P).

The examined specimens are deposited in the following collections:

BMNH Natural History Museum, London, United Kingdom (M.V.L. Barclay);
EIHU Hokkaido University Museum, Sapporo, Japan (M. Ôhara);
IBTP BORNEENSIS Collection, Institute for Tropical Biology and Conservation, Universiti Malaysia Sabah (P. Jimbau);
IRSNB Institute Royal des Sciences Naturelles de Belgique, Brussels, Belgium (P. Limbourg);
KMNH Kitakyushu Museum of Natural History and Human History, Kitakyushu, Japan (Y. Minoshima);
NHMW Naturhistorisches Museum, Wien, Austria (M. A. Jäch);
NMPC National Museum, Prague, Czech Republic (M. Fikáček);
SRBC Sergey Ryndevich collection, Baranovichy, Belarus;
ZIN Zoological Institute of the Russian Academy of Science, St. Petersburg, Russia (A.G. Kirejtshuk);
ZMHB Museum für Naturkunde der Humboldt-Universität, Berlin, Germany (J. Frisch, B. Jäger);
ZMUC Zoological Museum, Natural History Museum of Denmark (A.Yu. Solodovnikov).

Morphological studies. Specimens were dissected, with genitalia embedded in a drop of alcohol-soluble Euparal resin on a piece of glass glued to a small piece of cardboard attached below the respective specimen. Habitus photographs were taken using a Canon D-550 digital camera with attached Canon MP-E65mm f/2.8 1–5 macro lens. Pictures of genitalia were taken using a Canon D1100 digital camera attached to an Olympus BX41 compound microscope; combined pictures were were made with Helicon Focus software. Scanning electron micrographs were taken using Hitachi S-3700N environmental electron microscope at the Department of Paleontology, National Museum in Prague. Pictures used for plates were adapted in Adobe Photoshop CS6. All original pictures including additional views not presented in this paper are included in the dataset submitted to the Zenodo archive under doi 10.5281/zenodo.1258208.

All known species of *Cycreon* are very similar and share most structural characters. We therefore provide a generic description which includes shared morphological features, while the species descriptions are restricted mostly to species-specific characters.

Taxonomy

Cycreon Orchymont, 1919

Cycreon Orchymont, 1919: 119.

Types species. *Cycreon sculpturatus* Orchymont, 1919 (by original designation).

Diagnosis. (1) antennal grooves on prosternum small and marked by a weak ridge close to the lateral margins of prosternum (Fig. 2C–D); (2) mentum deeply excised anteromesally (Figs 1J, 2B, 5B, E, H, L, P) ; (3) mesoventral medial elevation reduced to a narrow carina (Fig. 2E–F); (4) grooves for reception of procoxae absent (Fig. 2E–F); (5) metaventrite without abdominal lines or demarcated anterolateral angles (Fig. 2E), (6) abdominal ventrite 1 not carinate medially (Fig. 2G); (7) aedeagus with the median lobe not fused to the bases of parameres, reaching into the phallobase; (8) median portion of male sternite 9 tongue-like (Fig. 3D, H, M).

Note. Orchymont (1919) mentioned the absence of antennal grooves, which were supposed by Hansen (1991) who did not have the chance to study specimens of this genus. Shatrovskiy (2017) revealed that antennal grooves are present although very small, and weakly marked by a faint ridge.

Differential diagnosis. *Cycreon* is distinct among Megasternini in lacking the median carina of abdominal ventrite 1 (Fig. 2G); in this character it only corresponds to the Megasternini genera *Pyretus* Balfour-Browne and *Acaryon* Hebauer. From *Pyretus*, *Cycreon* is easily diagnosed by the narrowly laminate elevation (in contrast to widely pentagonal and widely contacting metaventrite in *Pyretus*), simply carinate median portion of prosternum (forming an elevated prosternal plate in *Pyretus*), and small antennal grooves (antennal grooves are large and reaching lateral pronotal margin in *Pyretus*). The genus *Acaryon* from Madagascar is similar to *Cycreon* in many characters, including the relatively large eyes, simply carinate prosternum, antennal grooves not reaching pronotal margin, narrowly carinate elevation on mesoventrite, metaventrite without additional ridges, and dorsal punctation (with semicircular to circular punctures in *Cycreon*, and circular setiferous punctures intermixed with usual punctation in *Acaryon*). However, *Cycreon* can be distinguished from *Acaryon* by the shape of the mentum (deeply emarginate anteromedially in *Cycreon*, weakly sinuate on anterior margin in *Acycreon*), presence of the grooves for reception of procoxae at sides of the mesoventral elevation (absent in *Cycreon*, present in *Acaryon*) and the dorsal colouration (unicoloured or bicoloured in *Cycreon*, unicoloured yellow with dark central pronotal spot in *Acaryon*).

Description. Body (Fig. 1A–D) 2.2–3.4 mm long, elongate-oval, weakly convex. Colouration more or less reddish-brown, pronotum and underside usually somewhat paler (yellowish-brown), elytra usually darker.

Head. Clypeus with anterior margin with very fine bead, anteromedian margin slightly to strongly emarginate medially (Figs 1E, 5A, D, G, K, O), anterolateral angles rounded, antennal bases exposed; frontoclypeal suture distinct laterally, reduced in medial third; transverse ridges absent. Median portion of frons and clypeus not elevated above remaining surface. Dorsal surface glabrous, with dense punctation composed of shallow circular impressions (incomplete in some species), with a small puncture at anterior margin; interstices between punctures without visible microsculpture (Fig. 4A, D, G). Eyes moderately large, with dorsally visible portion slightly smaller than ventral one, separated by 4.9–5.5× the width of one eye in dorsal view. Labrum (Fig. 1I) ca. 0.4× as wide as head, membranous, largely retracted under clypeus, very weakly bisinuate at anterior margin, moderately densely pubescent dorsally, setae becoming longer on lateral portions. Mandible (Fig. 1F–H) with apex deeply bifid (teeth may be partially abraded in some specimens; compare Fig. 1F, G), curved; its external margin very weekly crenulate at basal half; prostheca with anterior third covered by long thin setae, distal group of these setae facing ventrally and proximal group of them facing mesally (Fig. 1H); mola with fine lamellae having poriferous structure. Maxilla of male with sucking disc on galea (Fig. 2B); maxillary palps with basal palpomere minute, palpomere 2 large, widened at apical half, 1.2× as long as palpomere 3, palpomere 3 slightly shorter than palpomere 4, slightly widening apicad, palpomere 4 fusiform, without digitiform sensilla. Mentum (Figs 1J, 2B, 5B, E, H, L, P) transverse, about twice as wide as long, lateral margins with few sparse setae, anterior margin very deeply emarginate; labial palps trimerous, palpomere 1 transverse, palpomere 2 subequal in width but slightly longer than palpomere 1 and with few long setae, palpomere 3 narrow, slightly longer than palpomere 2. Submentum with moderately dense setiferous punctures, gular sutures vaguely developed, rather widely separated from each other, tentorial pits small, almost rounded. Antenna with 9 antennomeres; scape (antennomere 1) long, cylindrical, constricted medially; pedicel (antennomere 2) rather short, bulbous basally; antennomeres 3–5 short, subequal in length, antennomere 5 much wider than preceding ones; cupule slightly asymmetrical, as long as antennomere 5; antennomeres 7–9 forming an elongate pubescent club (2.2× longer than wide), antennomeres 7–8 subequal in length, antennomere 9 slightly longer, roundly subacuminate at apex; sensorial antennal fields absent. Genal ridge absent.

Prothorax. Pronotum transverse, moderately convex, about as wide as bases of elytra combined; lateral margins minutely bordered; anterior and posterior angles rounded (Fig. 1E); punctation dense, composed of shallow circular impressions with one small puncture at posterior margin, circular impression sometimes incomplete (Fig. 4B, E, H). Prosternum (Fig. 2C) weakly raised medially, with faint longitudinal carina; prosternal process short, almost reaching midlenght of procoxal cavities, not bifurcate; precoxal part short. Procoxal cavities large, open posteriorly. Notosternal suture distinct. Antennal grooves present, very short, vaguely defined by thin ridge parallel to lateral notosternal suture, vanishing posteriad (Fig. 2C–D).

Mesothorax. Mesoventrite completely fused with anepisternum; anterior collar of mesothorax narrow. Median portion of mesoventrite simply tectiform, elevation forming a ridge shortly overlapping anterior margin of metaventrite. Grooves for reception of procoxae absent

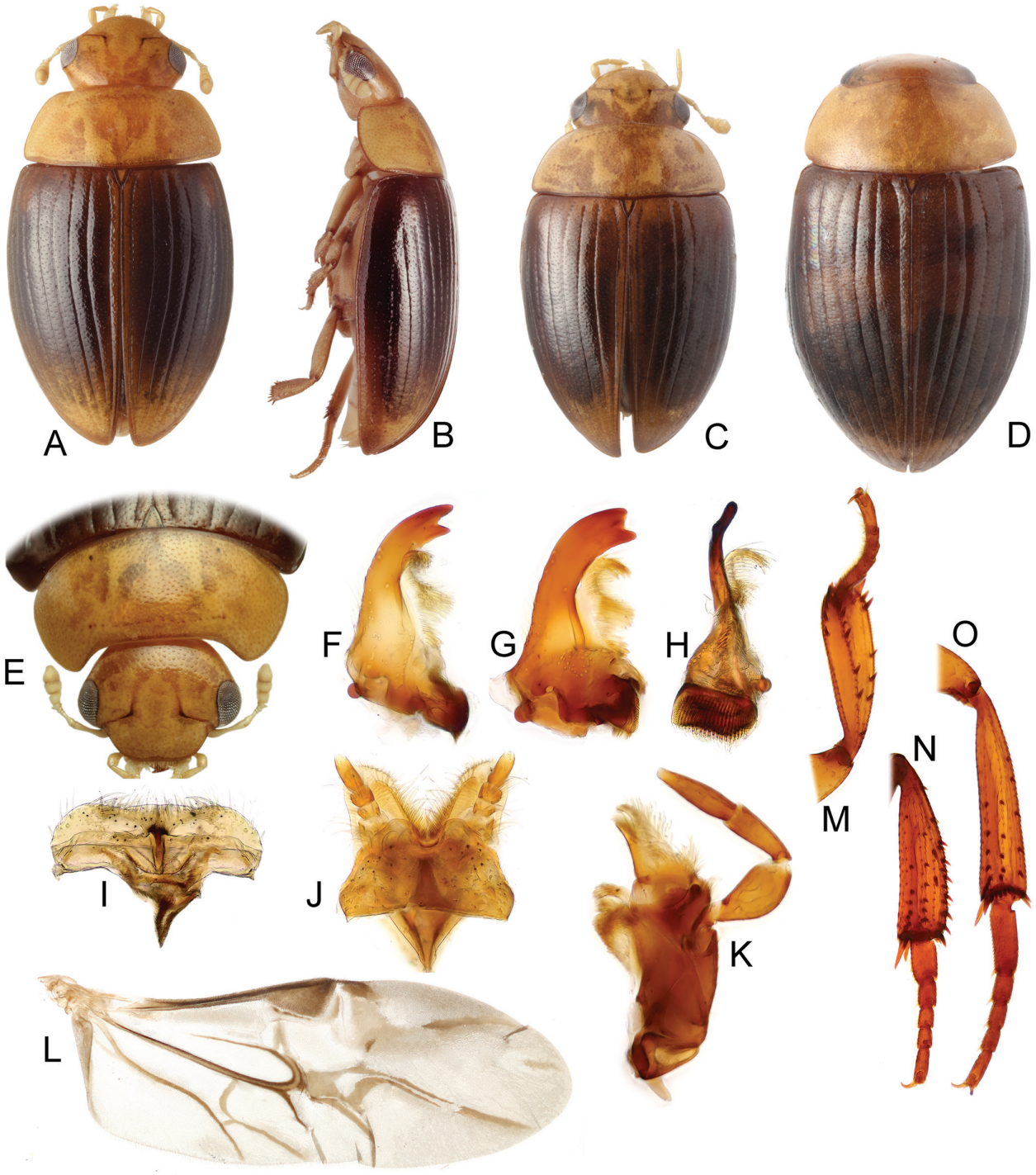

Figure 1. Habitus and morphology of *Cycreon* species. **A–D** – general habitus: **A–B** – *C. floricola floricola* ssp. n. (**A** – dorsal; **B** – lateral); **C** – *C. floricola borneanus* ssp. n., dorsal; **D** – *C. adolescens* sp. n., dorsal. **E–O** – morphology of *C. floricola floricola* ssp. n.: **E** – head and pronotum dorsally. **F–K** – mouthparts (**F** – mandible with unabraded apex; **G** – mandible with abraded apex; **H** – mandible, mesal view; **I** – labium; **J** – labrum; **K** – maxilla. **L** – metathoracic wing. **M–O** – tibiae and tarsi (**M** – prothoracic leg; **N** – mesothoracic leg; **O** – metathoracic leg).

(Fig. 2E–F). Mesepimeron moderately narrow, very weakly widening laterad. Mesocoxal cavities narrowly separated. Scutellar shield small, triangular, 1.1× as long as wide. Elytra weakly convex, weakly bordered laterally, each elytron bearing 10 series, series 1–9 consisting of foveate impressions (punctures) with a setiferous puncture on anterior margin (Fig. 4C, F, I); serial punctures situated in longitudinal sulci; series 1–4 and 9 reaching apex, series 5 and 8 enclosing series 6–7 subapically, series 9 and 10 fainter, series 10 reduced both anteriorly and posteriorly; epipleuron almost horizontal, gradually narrowing posteriad, vanishing behind level of posterior margin of metaventrite, bearing moderately dense short setae (Fig. 2E).

Metathorax. Metaventrite (Fig. 2E) with postcoxal line closely following posterior edge of mesocoxa and slightly deviating only in anterolateral angles; mesal elevate area flat and pentagonal, rather narrow, about as long as wide; lateral portions densely covered with short setae. Femoral lines and anterolateral ridges absent. Metanepisternum ca. 4.5× as long as wide, with anterior oblique ridge, metepimeron with minute ventral portion. Metafurca well developed. Hind wings (Fig. 1L) well developed, with transverse vein r4 arising from basal portion of radial cell, RP rather long, reaching ca. halfway to wing base, basal cubito-anal cell small, closed; wedge cell absent; transverse vein mp-cua joining to MP_{3+4}+CuA_{1+2}; anal lobe not defined.

Legs. Procoxae large, subglobular, transverse, with long setae, junction with trochanter; meso- and metacoxae wide, transverse. Tronchatero-femoral junction straight. Femora flattened, comparatively long, with very short setae; profemur without impressed parts; metafemur 1.1× as long as mesofemur (Fig. 1M–O). Tibiae rather long, triangular, flattened, straight or curved, especially on external margin, with short lateral and mesal spines. Tarsi pentamerous (Fig. 1N–O), tarsomeres densely covered by short stiff setae; metatarsomere 1 longer than metatarsomere 2 and 3 combined, metatarsomeres 2–4 continuously getting shorter, metatarsomere 5 about 0.4× than metatarsomere 1. Claws simple, arcuate; empodium bisetose.

Abdomen with five ventrites. Ventrite 1 without median carina (Fig. 1G), about as long as ventrites 2–4 together. Male sternite IX with tongue-like median projection with round to roundly acuminate anterior margin and rounded posterior margin, lateral struts almost reaching base of median projection (Fig. 3D, H, M). Aedeagus (Fig. 3A, E, J–K) simple; median lobe subparallel-sided to moderately sinuate, in *C. floricola* sp. n. enlarged basally and connected to phallobase by strong muscles; phallobase short, symmetrical to slightly asymmetrical, manubrium present, short; parameres simple. Female genitalia as in *Kanala* (see Fikáček 2010).

Key to the species of *Cycreon*

1 Clypeus strongly emarginated mesally (Figs 5K, O) 2
– Clypeus very weakly emarginated mesally (Figs 5A, D, G) 3
2 Pronotum with dense, completely ring-like impressions (punctures) (Fig. 5C); meso- and metatibiae straight (Fig. 5R) ..... *C sculpturatus* d'Orchymont, 1919
– Pronotum with moderately dense, half-moon shaped impressions (punctures) (Fig. 5M); meso- and metatibiae curved (Fig. 5S) ..... *C. armandi* Shatrovskiy, 2017
3 Pronotum with completely circular impressions (punctures). Mentum less transverse, 1.7× as long as wide (5B), with anteromedial emargination reaching 1/5 of length, and with many ring-like impressions (punctures) in posterior half. Aedeagus with parameres about as long as phallobase; median lobe wide, bluntly pointed at apex (Fig. 3I–J) ..... *C. adolescens* sp. n.
– Pronotum with completely ciruclar or semicircular impressions (punctures). Mentum more transverse, 2.0× as long as wide (Figs 5E, H), with anteromedial emargination reaching 1/3 of length, and with few ring-like impressions (punctures) in posterior half. Aedeagus with parameres longer than phallobase; median lobe abruptly narrowed into a long acute tip at apex (Figs 3A–H). *C. floricola* sp. n. 4
4 Pronotum with incomplete ring-like impressions (punctures) only (Figs 4H, 5I) ..... *C. floricola floricola* spp. n.
– Pronotum with all or vast majority of impressions (punctures) in shape of complete rings (Figs 4E, 5F) ..... *C. floricola borneanus* ssp. n.

Species accounts

Cycreon sculpturatus Orchymont, 1919

Fig. 5O–R

Cycreon sculpturatus Orchymont, 1919: 121.
Cycreon sculpturatus: Shatrovskiy (2017: 589, redescription).

Type locality. Indonesia: South Sumatra: Palembang [ca. 2.9861°S, 104.7555°E].

Material examined. None (information adopted from Shatrovskiy 2017).

Diagnosis. *Cycreon sculpturatus* can be distinguished from other species of the genus by the deeply incised clypeus, pronotum densely covered with complete ring-like impressions (punctures) and straight meso- and metatibiae.

Addition to description. Body 2.6 mm long; colouration light reddish-brown, with slightly darker head and elytra; clypeus about 2.5× as wide as long, with anterior margin conspicuously emarginate medially (Fig. 5O); frons and clypeus with punctation composed of complete circular impressions (punctures); mentum (Fig. 5P) subtrapezoid, widest at posterior fifth, about 2.0× wider than long, anteromedian emargination reaching about 0.2× the mentum length; pronotum with dense and moderately deep punctation consisting of complete circular impressions with a small setiferous puncture in posterior part (Fig. 5Q), punctation of approximately same diameter and density all over pronotum; meso- and metatibiae straight (Fig. 5R); male genitalia unknown (because male remains unknown for this species).

Distribution. Only know by a single female specimen from the type locality (Indonesia, Sumatra, Palembang) (Fig. 7).

Remark. According to Shatrovskiy (2017) the proportions of the clypeus were given as 4× as long as wide, however, the picture in the paper (Shatrovskiy 2017: 591) shows that the ratio is about 2.5×.

Cycreon armandi Shatrovskiy, 2017

Figs 3K–M, 5K–M

Cycreon armandi Shatrovskiy, 2017: 589.

Type locality. Singapore.

Material examined. None (information adopted from Shatrovskiy 2017).

Diagnosis. *Cycreon armandi* can be distinguished from other known species by the deeply incised clypeus, the semicircular impressions (punctures) on the pronotum, and the curved meso- and metatibae.

Addition to description. Body 3.3 mm long; colouration completely light reddish-brown; clypeus about 2× as wide as long, anterior margin of clypeus strongly emarginate medially (Fig. 5K); frons and clypeus with small and not so closely disposed punctures; mentum (Fig. 5L) subtrapezoid, widest at posterior fifth, about 1.8× wider than long, with a deep anteromedian emargination reaching beyond the anterior fourth of length; pronotum with dense and shallow, punctation consisting of small setiferous half-moon shaped punctures (Fig. 5M); meso- and metatibiae curved (Fig. 5S); median projection of sternite 9 rounded apically (Fig. 3M); aedeagus (Fig. 3L) with phallobase 0.6× as long as parameres, almost symmetrical, manubrium narrow and very; parameres continuously narrowing towards apex; median lobe moderately wide (Fig. 3K), slightly constricted in apical fourth; apex acuminate, triagular.

Distribution. Only known from the type locality in Singapore (Fig. 7).

Remarks. According to Shatrovskiy (2017) the proportions of the clypeus are given as 3× as long as wide, however, the picture in the paper (Shatrovskiy 2017: 591) shows that the ratio is closer to 2.0×.

Cycreon adolescens sp. n.

http://zoobank.org/C6503E49-3440-4820-B671-D35E579D6247

Figs 1D, 3I–J, 4J, 5A–C

Type locality. Malaysia, Pahang, Genting Highland [ca. 3.4233°N, 101.7930°E].

Type material. Holotype (male, teneral specimen): "Malaysia, PAHANG / Genting Highland / 24.X.2012 / H. Takizawa" (IBTP). **Paratypes: MALAYSIA: Pahang:** [same data as holotype] (2 females: NMPC, KMNH).

Additional material examined. MALAYSIA: Pahang: Cameron Highlands, Tanah Rata, Robinson Waterfall [ca. 4.461778°N 101.38803°E], in flowers of Araceae, 15.iii.2015, H. Takizawa lgt. (5 females: EIHE, KMNH, NMPC).

Diagnosis. This species is most similar to *Cycreon floricola borneanus* ssp. n. in the very weakly emarginate anterior margin of the clypeus and pronotal punctation consisting of circular punctures, and straight meso- and metatibiae. It differs from the latter in the structure of the male genitalia (relatively longer phallobase and widely pointed apex of the median lobe) and by the less transverse mentum (1.7× wider than long), with many ring-like impressions in posterior half.

Description. *Measurements.* 2.4–3.0 mm long (length of holotype: 2.8 mm), 1.7× as long as wide, widest at basal fifth of elytra; weakly convex, 3.3–3.5× as long as high (height of holotype: 0.82 mm). *Colouration*. Light brown with slightly darker elytra (Fig. 1D).

Head. Clypeus about 2.4× as long as wide, with anterior margin of clypeus margin very weakly emarginate medially. Frons and clypeus with punctation composed of complete circular impressions (punctures) with a small setiferous puncture on anterior margin (Fig. 4A). Interocular distance about 5.5× the width of one eye in dorsal view. Mentum (Figs 4J, 5B) subtrapezoid, widest at posterior fifth, about 1.7× wider than long, with a moderately pronounced emargination reaching about the anterior fifth of mentum length; lateral angles weakly marked; surface with few sparse, moderately long setae in anterolateral angles, posterior half glabrous, punctures moderately large and deep, vanishing mesally, 11–13 punctures close to posterolateral angles with ring-like impressions (punctures).

Prothorax. Pronotum transverse, widest at base 2.2× wider than long; 1.6× wider at base than between anterior angles, 1.7× wider than head including eyes. Punctation dense and shallow, consisting of circular impressions with one small setiferous puncture on posterior margin (Fig. 4B), punctation of approximately same diameter and density all over pronotum.

Pterothorax. Elytra widest at anterior fifth, 1.1–1.2× as long as wide, 2.9–3.0× as long as pronotum, 1.2–1.3× as wide as pronotum. Punctation on intervals composed of semicircular impressions with a setiferous puncture on posterior margin (Fig. 4C). *Legs.* Metatibiae wide and flattened, weakly curved on external margin, 0.35× as long as elytra, 5.0× as long as wide.

Male genitalia (Fig. 3I–J). Phallobase about 1.1× as long as parameres, slightly asymmetrical, manubrium slightly hooked, widely rounded. Parameres continuously narrowing apically, external margins straight, apex rounded. Median lobe wide throughout, apex triangularly acuminate, gonopore rather small, situated subapically. Median projection of sternite 9 not examined.

Etymology. The species name reflects the teneral condition of the holotype (from Latin *adolescens* = growing up, maturing).

Distribution. The species is only known two localities in Pahang province, Malaysia.

Biology. No details about collecting circumstrances are available for type specimens; additional specimens from Tanah Rata were collected from inflorescences of Araceae (H. Takizawa, pers. comm. 2018).

Cycreon floricola sp. n.

http://zoobank.org/16453A2C-31B9-425C-998E-88D0836C8DE7

Figs 1A–C, E-O, 2, 3A–D, E–H, 4G–I, 5D–F, G–I, 6A–B

Description. *Measurements.* 2.2–3.4 mm long (length of holotype: 2.9 mm), 1.8–2.0× as long as wide, widest

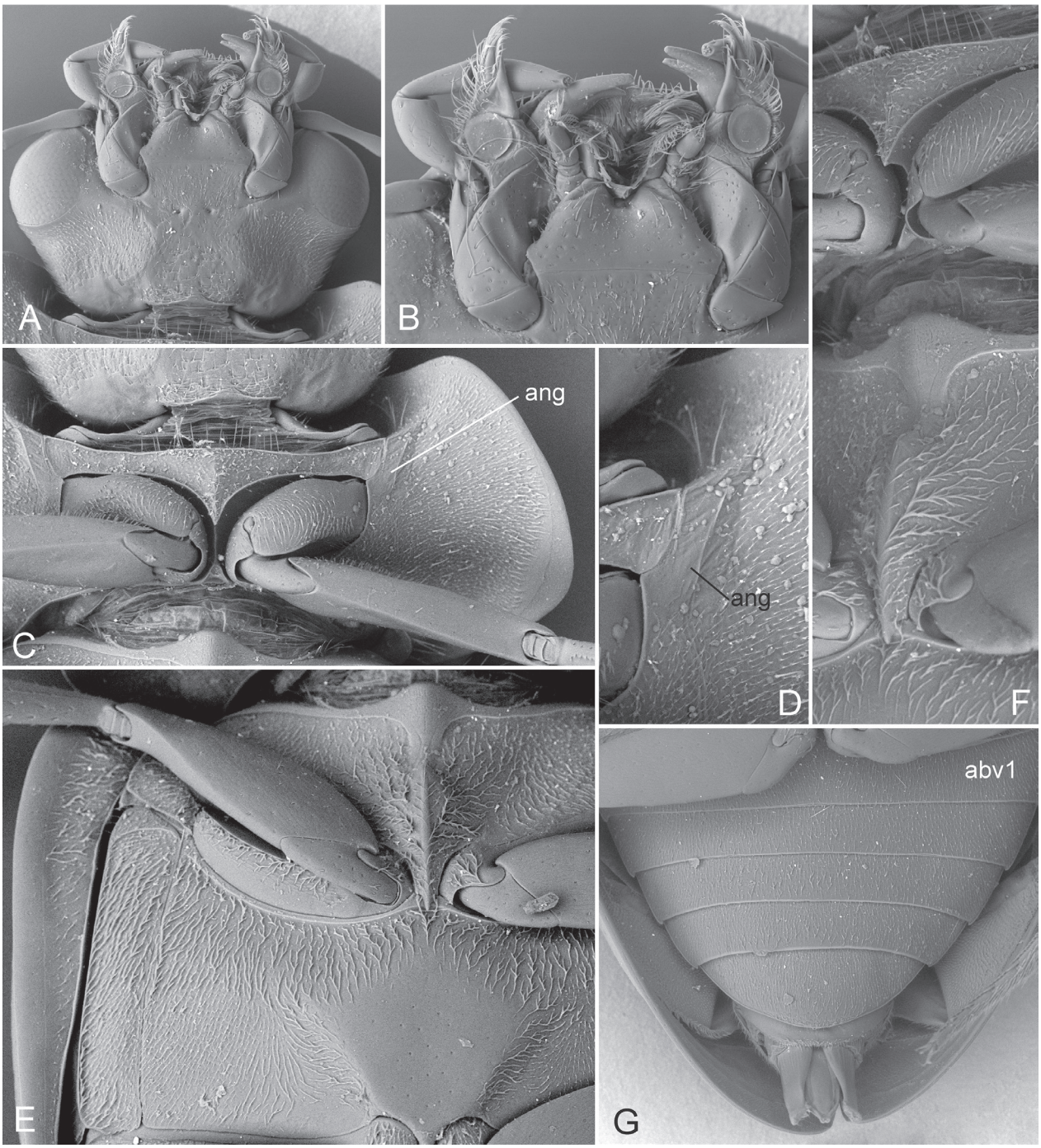

Figure 2. External morphology of *Cycreon floricola floricola* ssp. n. **A**– head, ventral view; **B** – detail of male mouthparts in ventral view; **C** – prothorax in ventral view; **D** – detail of the antennal groove; **E** – meso- and metaventrite; **F** – prosternum and mesoventral elevation in ventrolateral view; **G** – abdominal ventrites. Abbreviations: abv1 – abdominal ventrite 1; ang – antennal grooves.

at basal fifth of elytra; weakly convex, 3.1–3.4× as long as high (height of holotype: 0.9 mm). *Colouration*. Light brown with darker elytra (Figs 1A–C).

Head. Clypeus about 2.5× as wide as long, with anterior margin of clypeus margin very weakly emarginate medially. Frons and clypeus with punctation composed of complete circular impressions (punctures) with one small setiferous puncture on anterior margin (Figs 4G, D). Interocular distance about 4.9–5.2× width of one eye in dorsal view. Mentum (Figs 1J, 2B, 4K, 5E,H) subtrapezoid, widest at posterior fifth, about 2.1× as wide as long, with deep emargination reaching beyond anterior third of mentum length; surface with sparse, moderately long setae in anterior half, posterior half glabrous, punctures moderately large and deep, becoming smaller mesally, with 2–3 punctures with ring-like impressions close to posterolateral angles.

Prothorax. Pronotum transverse, widest at base, 2.2× as wide as long; 1.5–1.6× wider at base than at anterior

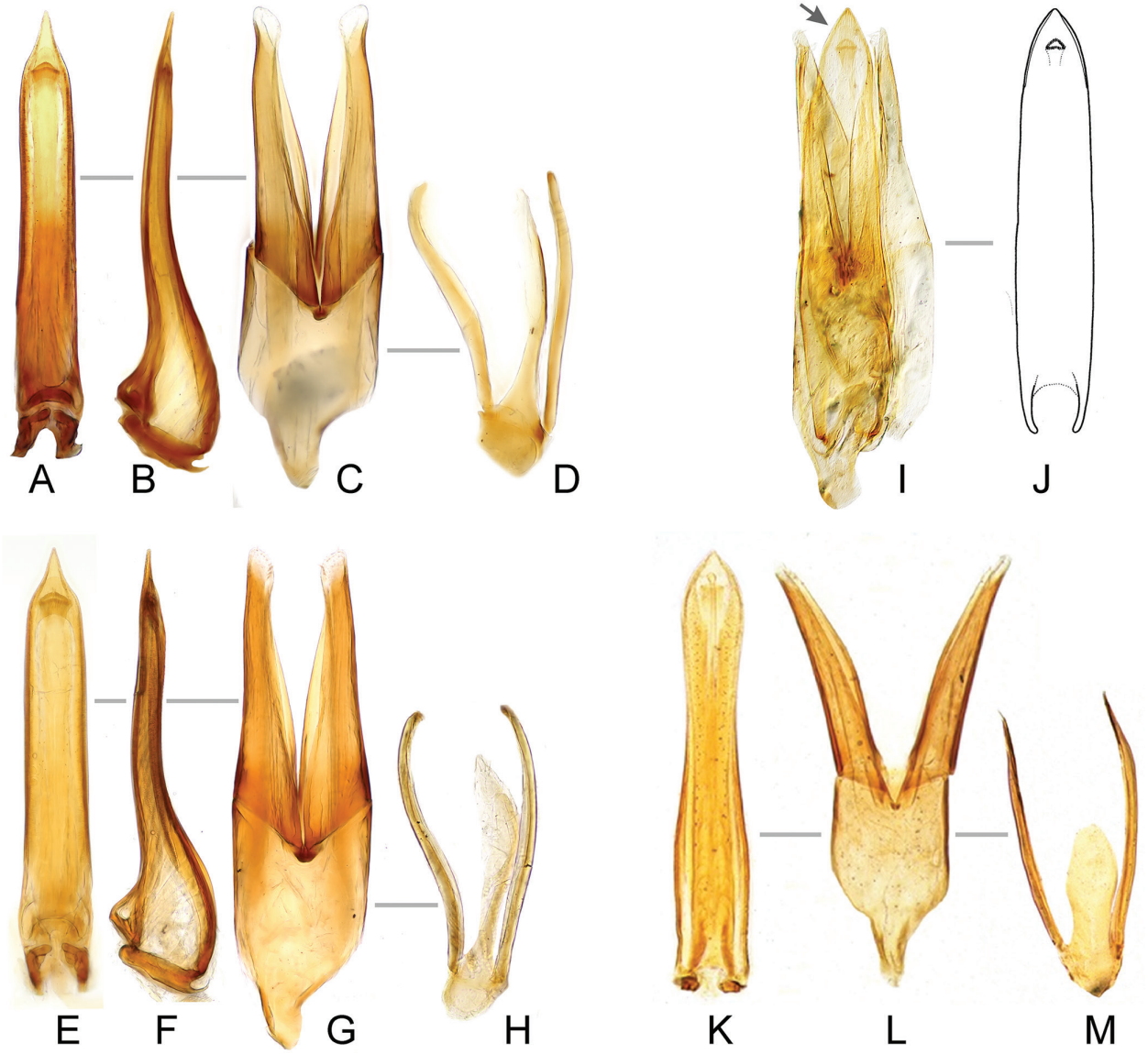

Figure 3. Male genitalia of *Cycreon* species (except *C. sculpturatus* for which male remains unknown). **A–D** – *C. floricola floricola* ssp. n., holotype; **E–H** – *C. floricola borneanus* ssp. n., holotype; **I–J** – *C. adolescens* sp. n., holotype; **K–M** – *C. armandi* Shatrovskiy, 2017, holotype. **A, E, K** – median lobe; **B, F** – median lobe in lateral view; **C, G, L** – tegmen; **D, H, M** – sternite 9; **I** – whole aedeagus; **J** – reconstructed shaped of the median lobe. **K–M** adapted from Shatrovskiy (2017).

angles, 1.6× as wide as head including eyes. Punctation dense and shallow, consisting of semicircular to complete ring-like impressions with a small setiferous puncture on posterior margin (Figs 4E, H, 5F, I), punctation approximately same in size and density all over pronotum.

Pterothorax. Elytra widest at anterior fifth, 1.1–1.2× as long as wide, 2.9–3.0× as long as pronotum, 1.1× as wide as pronotum. Punctation on intervals composed of semicircular impressions with setiferous puncture on posterior margin (Fig. 4F, I).

Legs. Metatibiae wide and flattened, very weakly curved, 0.35× as long as elytra, 4.8× as long as wide.

Male genitalia. Median projection of sternite 9 (Fig. 3D, H) rounded apically, with few short subapical setae, shorter than lateral struts. Phallobase (Fig. 3C, G) about 0.8× as long as parameres, asymmetrically narrowing towards base, manubrium acuminate and slightly hooked, with apex rounded. Parameres continuously narrowing from base to apex, but slightly widened at apex; external margins bisinuate; apex obliquely acuminate. Median lobe moderately wide (Fig. 3A–B, E–F), almost parallel-sided throughout, apex acuminate, with very acute tip, expanded basally and bent dorsally on lateral view, gonopore large, situated subapically.

Etymology. The species name reflects the association of this species with flowers, it consists of *flori-* (from Latin *flos, floris* = flower) and *-cola* (from Latin *incola* = inhabitant).

Comment. This species is composed of two phenotypically distinguishable forms which are geographically exclusive and are here descibed as subspecies. Morphological differences are mainly restricted to punctation on the pro-

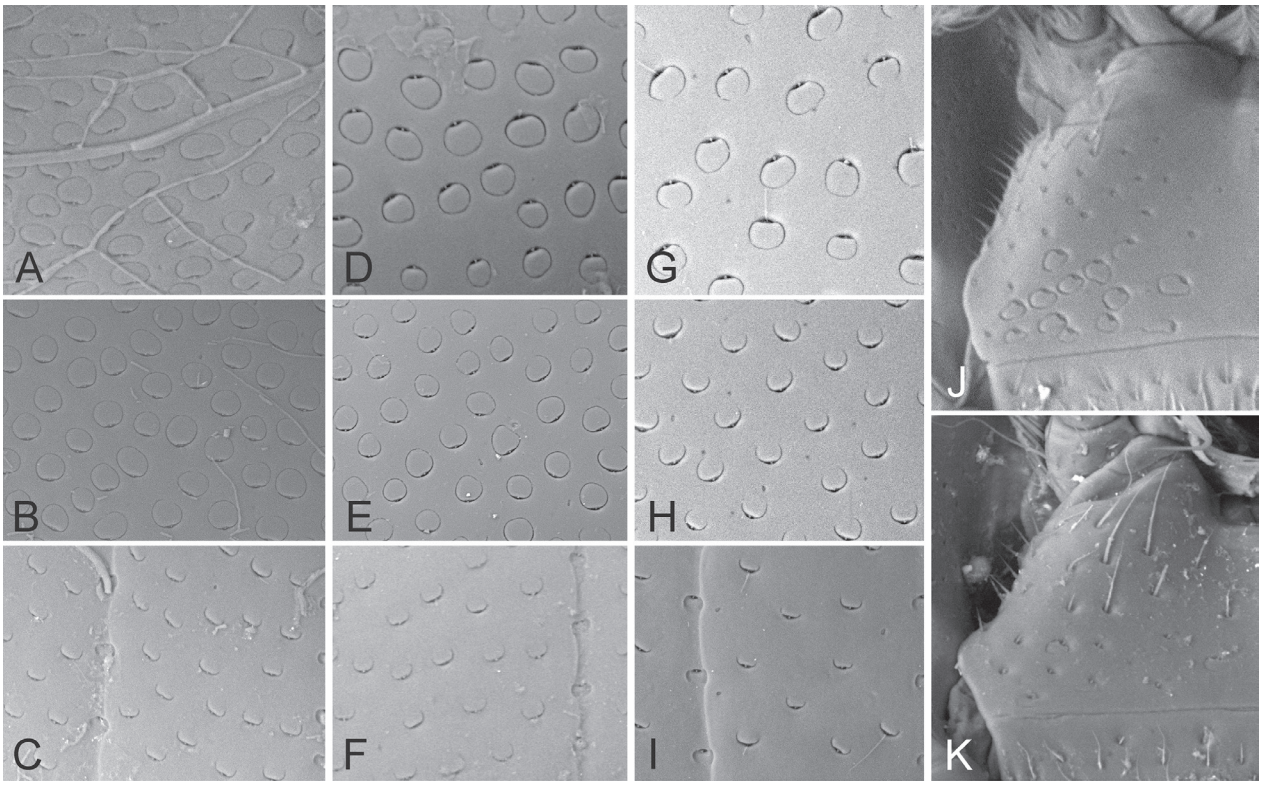

Figure 4. Surface sculptures of *Cycreon* species. **A–C, J** – *C. adolescens* sp. n., holotype; **D–F** – *C. floricola borneanus* ssp. n., paratype; **G–I, K** – *C. floricola floricola* ssp. n., paratype from the type locality. **A, D, G** – head punctation; **B, E, H** – pronotum punctation; **C, F, I** – elytral punctation; **J–K** – punctation of mentum.

notum, which consists exclusively of incomplete ring-like impressions in the mainland form (*C. f. floricola* ssp. n.), and exclusively or mainly of the completely ring-like forms in the specimens from Borneo (*C. f. borneanus* ssp. n.).

Cycreon floricola floricola ssp. n.

http://zoobank.org/953D42A0-7C3B-47BD-A2E5-26CB0ACAB588
Figs 1A–B,E–O, 2, 3A–D, 4G–I, K, 5G–I

Type locality. Malaysia, Kelantan, Guala Musang prov., Kuala Koh district, Taman Negara, 700 m from the entrance, 96 m a.s.l., 4°52.333′N 102°26.872′E.

Type material. Holotype (male: ZIN): "MALAYSIA: Kelantan AR-4332 / Guala Musang prov., Kuala Koh / distr., Taman Negara, 700 m / from entrance, 4°52.333′N / 102°26.872′E, 96m, 11.i.2014 / *Schismatoglottis* sp. HY Chen". **Paratypes: MALAYSIA: Johor:** Endau-Rompin N.P., NERC to Visitor Complex, Stream 1, 80 m, 2°25′12.8 ′ ″N 103°15′41.33″ E, flowering *Kiewia ridleyi*, 22.x.2008, Ooi Im Hin lgt. (AR-2602) (1: ZIN); Kota Tinggi, Hutan Simpan Panti, starting point of the trail to mount Panti, 14 m, 1°48.595′N 103°51.099′E, flowering *Schismatoglottis*, 4.xii.2013, Hoe Yin Chen lgt. (AR-4322) (21: ZIN, NMPC, IBTP); [same locality, except] 16 m, flowering *Schismatoglottis*, 4.xii.2013, Hoe Yin Chen lgt. (AR-4326) (11: ZIN); Kota Tinggi, Hutan Simpan Panti, starting point of the trail to mount Panti, 16 m, 01°48.565'N 103°51.104'E, flowering *Schismatoglottis*, 04.xii.2013, Hoe Yin Chen lgt. (AR-4328) (4: ZIN, NMPC); Kota Tinggi, Hutan Simpan Panti, Starting point of the trail to mount Panti, 16 m, 01°48.565'N 103°51.104'E, flowering *Schismatoglottis*, 13.xii.2013, Hoe Yin Chen lgt. (AR-4328) (6: ZIN, NMPC); **Kelantan:** Gua Musang, Kuala Koh, Taman Negara, 700 m away from the entrance gate (outside the park), 96 m, 4°52.333′N 102°26.872′E, flowering *Schismatoglottis*, 11.x.2014, Hoe Yin Chen lgt. (AR-4332) (237: ZIN, NMPC, IBTP, KMNH, EIHE, NHMW, BMNH, SRBC).

Diagnosis. This subspecies is very similar to *Cycreon floricola borneanus* ssp. n. with which it shares most of the external characters including genital morphology. *Cycreon floricola floricola* can be distinguished by the pronotal punctation consisting exclusively of the incomplete ring-like punctures. The dorsal coloration of the is slightly more contrasting in most specimens of *C. floricola floricola* than in representatives of *C. f. borneanus* ssp. n., with the pronotum darker compared to the elytra.

Description. *Measurements.* 2.4–3.2 mm long (length of holotype: 2.7 mm), 1.9–2.0× as long as wide, widest at basal fifth of elytra; weakly convex, 3.2–3.4× as long as high (height of holotype: 2.7 mm). *Colouration.* Pale yellowish-brown with dark-brown elytra (Fig. 1A–B).

Pronotum 2.2× wider than long; 1.6× wider at base than between anterior angles, with punctation dense and shallow, consisting of semicircular impressions (punctures) with a small setiferous puncture on posterior margin.

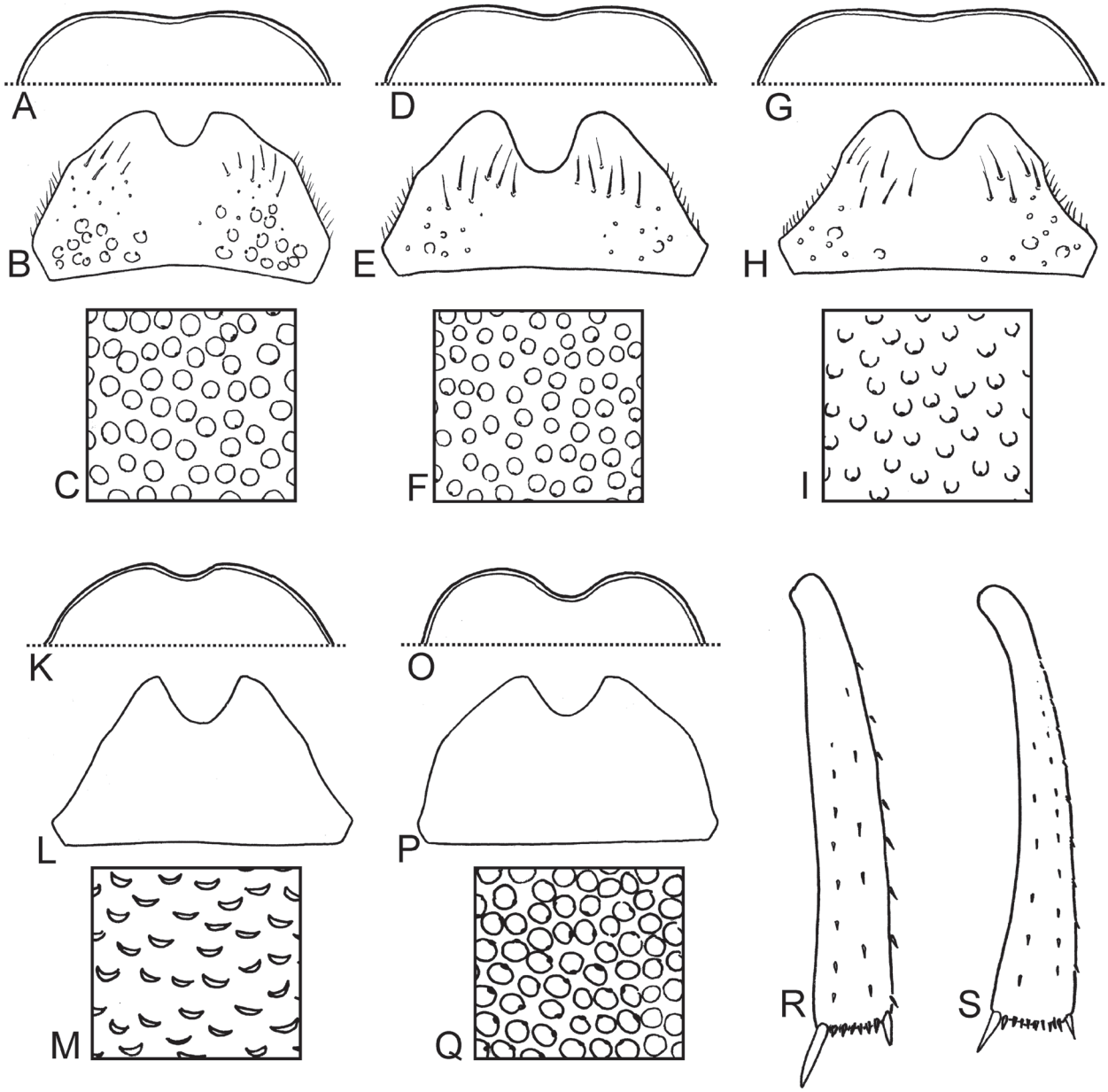

Figure 5. Diagnostic characters of known *Cycreon* species. **A–C** – *C. adolescens* sp. n.; **D–F** – *C. floricola borneanus* ssp. n.; **G–I** – *C. floricola floricola* ssp. n.; **K–L, S** – *C. armandi*; **O–R** – *C. sculpturatus*. **A, D, G, K, O** – anterior margin of clypeus; **B, E, H, L, P** – mentum (superficial sculpture omitted in **L** and **P**); **C, F, I, M, Q** – pronotal punctation; **R–S** – metatibia. **K, M–S** redrawn from Shatrovskiy (2017), **L** based on a photo provided by A. Shatrovskiy (pers. comm., 2017).

Punctation approximately same in size and density all over pronotum.

Elytra widest at anterior fifth, 1.1–1.2× as long as wide, 2.9–3.0× as long as pronotum, 1.1× as wide as pronotum. Punctation on intervals composed of semicircular impressions with one setiferous puncture on posterior margin.

Distribution. The subspecies is known from two regions in Peninsular Malaysia, in provinces of Johor and Kelantan.

Biology. Many specimens of *C. floricola floricola* were collected inside of inflorescences of *Schismatoglottis* species and *Kiewia ridleyi* (Low et al. 2018) (both Araceae).

Cycreon floricola borneanus ssp. n.

http://zoobank.org/ADFC83BC-973B-4A18-AE6F-B906027D49A1
Figs 1C, 3E–H, 5D–F, 6A–B

Type locality. Malaysia, Sabah, Tawau, Lahad Datu, Tawau Hills National Park, Kebun Botani, 305 m a.s.l., 4°23′59.4″N 117°53′17.2″E.

Type material. Holotype (male: ZIN): "MALAYSIA: Sabah AR-2659 / Tawau, Lahad Datu, Tawau Hills / NP, Kebun Botani, 305m / 04°23′59.4N 117°53′17.2E / *Schistamoglottis calyptrata* group, / 8.vii.2016, Wong Sin Yeng, / P. C. Boyce & Zaiety binti Thomas". **Paratypes: INDONESIA**: **Kalimantan Barat:** Bengkayang

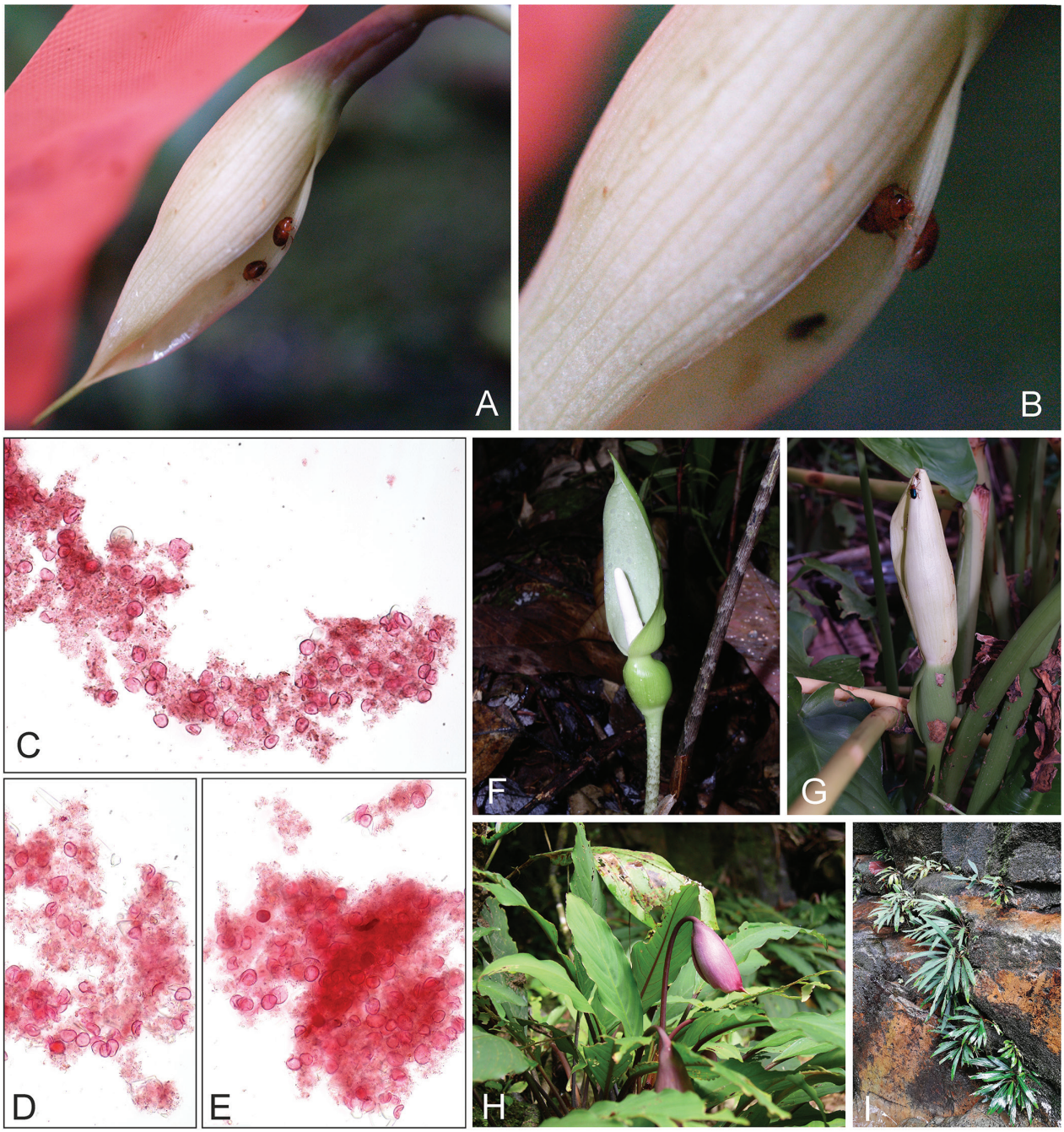

Figure 6. Biology of *Cycreon floricola* sp. n. **A–B** – alive specimens of *C. floricola borneanus* in the inflorescence of *Schottarum sarikeense* at Sebankoi Recreational Park, Betong, Roban, Sarawak in January 2010 (photo by S.-Y. Wong). **C–E** – safranine-dyed gut content of *C. floricola borneanus* collected from *Schismatoglottis calyptrata* complex in Tawau Hills, Kebun Botani on 8th July 2016 (collecting event AR-2659). **F–I** – examples of aroid plants on which the species were collected (**F** – *Alocasia longiloba*; **G** – *Schismatoglottis giamensis*; **H–I** – *Ooia glans*).

Pajintan, Ayer Terjun Sibohe, 80 m, 0°51’55.8”N 109°2’25.1”E, flowering *Schismatoglottis modesta*, 2.ix.2017, Wong & Boyce lgt. (AR-2812) (39: NMPC, ZIN). **Kalimantan Selantan:** ‘S.O. Borneo / Grabowsky S. V.’ (1: ZMNH); Kendangan, 15.5.1882, Grabowsky S. V. [ca.: S 2.592552°, E 115.028244°] (5: ZMNH). **MALAYSIA: Sabah:** Tawau, Lahad Datu, Tawau Hills NP, HQ Area, 304 m, 4°23′51.2”N 117°53′25.1”E, flowering *Alocasia longiloba* complex, 6.vii.2016, Wong Sin Yeng & P.C.Boyce lgt. (AL-315) (1: ZIN); [same locality] flowering *Schismatoglottis calyptrata* complex, 7. vii.2016, Wong Sin Yeng & P.C.Boyce lgt. (AR-2641) (101: ZIN, NMPC, IBTP, KMNH, NHMW); Tawau, Lahad Datu, Tawau Hills NP, Air Terjun Bukit Gelas, 315 m, 4°24′48.4”N 117°53′29.3”E, flowering *Gamogyne loi*, 6.vii.2016, Wong Sin Yeng & P.C.Boyce lgt. (AR-2638) (12: ZIN, NMPC); Tawau, Lahad Datu, Tawau Hills NP, Trail to Bukit Gelas, 319 m, 4°24′37.0”N

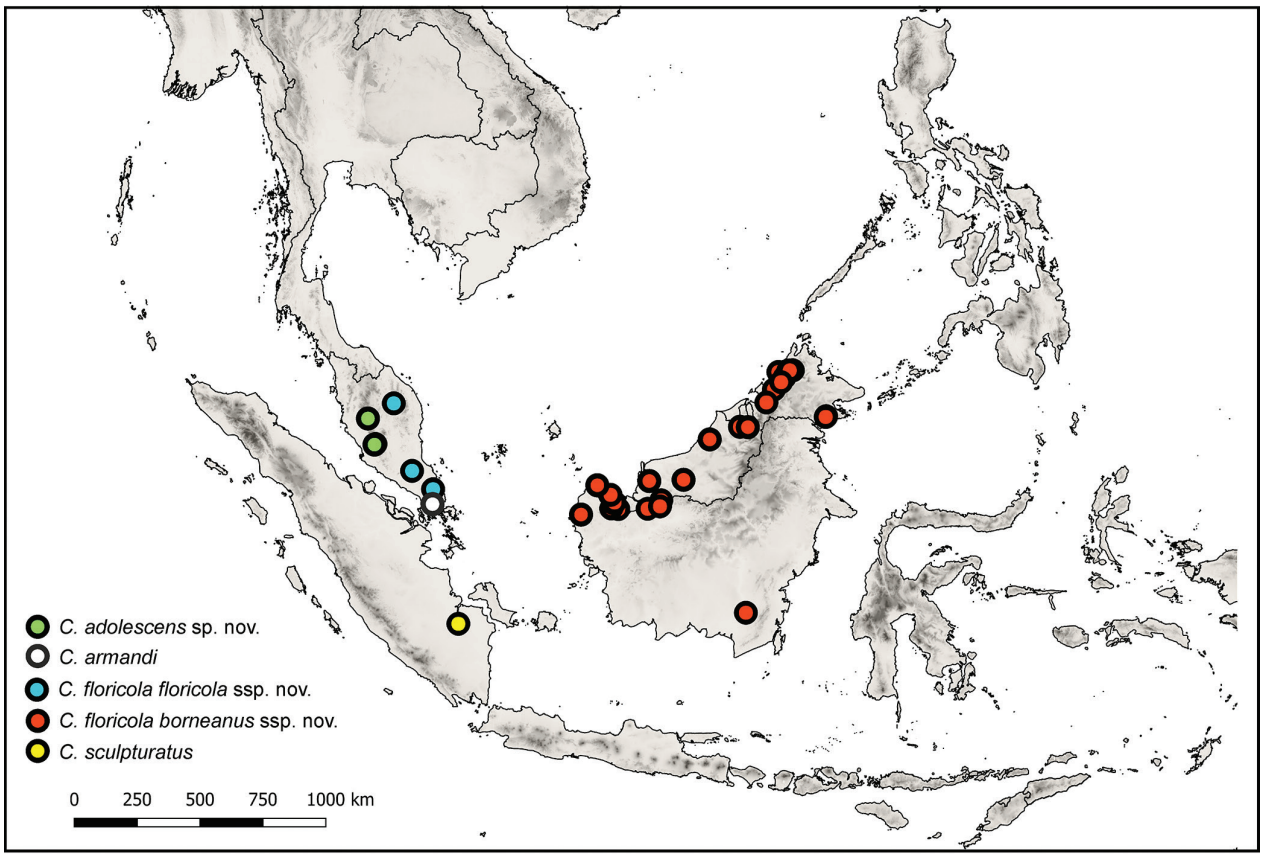

Figure 7. Known distribution of *Cycreon* species.

117°53′38.8”E, flowering *Homalomena hanneae* complex, 6.vii.2016, Wong Sin Yeng & P.C.Boyce lgt. (AR-2636) (18: ZIN, NMPC); [same locality] flowering *Schismatoglottis calyptrata* complex, 7.vii.2016, Wong Sin Yeng & P.C.Boyce lgt. (AR-2652) (36: ZIN, NMPC); Tawau, Lahad Datu, Tawau Hills NP, Kebun Botani, 305 m, 04°23′59.4″N 117°53′17.2″E, flowering *Schismatoglottis calyptrata* complex, 8.vii.2016, Wong Sin Yeng, P.C.Boyce & Zaiety binti Thomas lgt. (AR-2659) (116: ZIN, NMPC, IBTP, KMNH, NHMW, BMNH); Kg. Moyog, Jln. Tambunan, Penampang, 12.xii.2009, H. Takizawa lgt [ca. N 5.888455°, E 116.235335°] (11: EIHE, KMNH, NMPC, IBTP); [same locality and collector] 30.x.2008 (7: EIHE, KMNH); [same locality and collector,] 13.ix.2008 (7: EIHE, KMNH, IBTP); Poring park, Ranau, 19–20.ix.2008, H. Takizawa lgt [ca. N 6.047067°, E 116.703231°] (7: EIHE, KMNH, IBTP); [same locality and collector] 25–26.ix.2008 (5: EIHE, KMNH. IBTP); [same locality and collector] 8–9.i.2010 (7: EIHE, KMNH, IBTP); [same locality and collector] 11.xii.2008 (3: EIHE, KMNH); [same locality and collector] 27.v.2010 (1: EIHE); [same locality and collector] 25.ii.2009 (2: KMNH); [same locality and collector] 10.vii.2008 (1: EIHE); [same locality and collector] 12.iii.2009 (1: KMNH); [same locality and collector] 29.viii.2013 (1: KMNH); [same locality and collector] 12.iii.2009 (1: KMNH); [same locality and collector] 4–5.iv.2008 (3: KMNH, IBTP); [same locality and collector] 7.x.2012 (2: KMNH); Kg. Kiapad, Inanam, Kota Kinabalu, 7.ix.2008, H. Takizawa lgt [ca. N 5.988388°, E 116,190333°] (16: KMNH, EIHE, IBTP, NMPC); [same locality and collector] 2.i.2010 (3: KMNH, EIHE); [same locality and collector] 10.xi.2012 (16: KMNH, EIHE, IBTP, NMPC); [same locality and collector] 6.xii.2008 (18: KMNH, EIHE, IBTP, NMPC); [same locality and collector] 6.iv.2013 (7: KMNH, EIHE, IBTP); [same locality and collector] 5.vii.2008 (22: KMNH, EIHE, IBTP, NMPC); [same locality and collector] 4.x.2008 (3: KMNH); [same locality and collector] 7.xi.2009 (1: KMNH); Ulu Senagang subts., Keningau, 31.i.-2.ii.2011, H. Takizawa lgt. [ca. N 5.362946°, E 116.028679°] (14: KMNH, EIHE, IBTP); [same locality and collector] 24–26.vii.2010 (2: KMNH); Kinabalu PHQ, Ranau, 17–19.iii.2008, H. Takizawa lgt. [ca. N 6.021639°, E 116.542751°] (1: EIHE); Kinabalu Park, HQ, Ranau, 5.iii.2010, H. Takizawa lgt. [ca. N 6.021639°, E 116.542751°] (3: EIHE, KMNH); [same locality and collector] 14.iii.2012 (1: KMNH); [same locality and collector] 8.vii.2010 (2: KMNH); [same locality and collector] 23–25.iii.2010 (1: EIHE); [same locality and collector] 27–28.v.2008 (2: KMNH); [same locality and collector] 13–14.v.2010 (1: EIHE); [same locality and collector] 23–25.viii.2008 (2: KMNH); [same locality and collector] 23–25.vii.2008 (1: KMNH); [same locality and collector] 1.ii.2010 (1: KMNH); [same locality and collector] 23–24.ix.2008 (1: KMNH); [same locality

and collector] 17–19.x.2008 (1: KMNH); Muaya waterfall, Sipitang, 6–9.iii.2009, H. Takizawa lgt. [ca. N 4.903889°, E 115.760278°] (8: EIHE, KMNH, IBTP); Mahua waterfall, Crocker R. P., Tambunan, 26.vii.2011, H. Takizawa lgt [ca. N 5.797627°, E 116.408377°] (1: NMPC); Gn. Bombalai, Tawau Hills park, Tawau, 17. vi.2010, H. Takizawa lgt [ca. N 4.386858°, E 117.879748°] (4: EIHE, KMNH); Pk. Bundu Tuhan Kundasang, Ranau, 6.iii.2010, H. Takizawa lgt. [ca. N 5.996602°, E 116.528987°] (1: NMPC); Mesilau headgate, Kundasang, Ranau, 25.ii.2009, H. Takizawa lgt. [ca. N 6.044605°, E 116.596306°] (1: KMNH); Malangan, Kg. Tikolod, Tambunan, 12–14.iii.2010, H. Takizawa lgt. [ca. N 5.626763°, E 116.286933°] (1: EIHE); Pantai Barat, Kota Kinabalu, Inanam, Kionsom, Kionsom Waterfall, 230 m, 05 57 24.0N 116 12 25.3E, flowering *Schismatoglottis corneri*, 18.iv.2014, Wong Sin Yeng & P.C.Boyce lgt. (AR-4683) (7: ZIN, NMPC). **Sarawak:** Serian, Pichin, between Sugun Karang and Tahang Sipukam, Sungai Kakas, 48 m, 1°06′09.7″N 110°28′11.8″E, flowering *Schismatoglottis bulbifera*, 28.vi.2014, Ooi Im Hin & Jeland ak Kisai lgt. (AR-4832) (1: ZIN); Kuching, Padawan, Puncak Borneo, Jungle Trail, 890 m, 1°07′33.5″N 110°12′57.4″E, flowering *Ooia glans*, 15.ix.2014, Wong Sin Yeng & P.C.Boyce lgt. (AR-93) (92: ZIN, NMPC, IBTP, KMNH, NHMW); Kuching, Padawan, Puncak Borneo, Sungai Semangas, 472 m, 1°08′26.6″N 110°13′36.1″E, flowering *Ooia glans*, 16.ix.2014, Wong Sin Yeng & P.C.Boyce lgt. (AR-4979) (29: ZIN, NMPC, KMNH); Kuching, Matang, Kubah N.P., Sungai Bungen, 230 m, 1°36′30.9″N 110°11′35.0″E, flowering *Ooia glans*, 28.vii.2007, P.C.Boyce, Wong Sin Yeng & S.Maclean lgt. (AR-2118) (27: ZIN, NMPC, IBTP); [same locality] flowering *Schismatoglottis mayoana*, 28.vii.2007, Wong & Maclean lgt. (AR-2122) (1: ZIN); Kuching, Matang, Kubah N.P., Waterfall Trail, 190 m, 1°35′40.2″N 110°10′45.9″E, flowering *Ooia glans*, 28.vii.2007, P.C.Boyce, Wong Sin Yeng & S.Maclean lgt. (AR-2117) (10: ZIN, NMPC); Sri Aman, Lubok Antu, Sungai Engkari, Nanga Segerak, Sungai Serjanggut, 332 m, 1°24′46.5″N 112°00′18.5″E, flowering *Ooia* sp., 17.iii.2015, Wong Sin Yeng, P.C. Boyce & Bada ak Chendai lgt. (AR-5169) (11: ZIN, NMPC); Sri Aman, Lubok Antu, Engkilili, Tempat Rekreasi Sungai Raya, Sungai Raya, 13 m, 1°06′49.2″N 111°30′56.8″E, flowering *Schismatoglottis calyptrata* complex, 9. xii.2005, P.C.Boyce, Jeland ak Kisai, Jipom ak Tisai & Mael ak Late lgt. (AR-1632) (38: ZIN, NMPC, IBTP, KMNH); Sri Aman, Lubok Antu, Sungai Sepipit, 108 m, 1°11′54.9″N 111°57′29.4″E, flowering *Schismatoglottis petradoxa*, 27.vii.2014, Wong Sin Yeng & P.C.Boyce lgt. (AR-4894) (1: ZIN); Kuching, Siburan, Kampung, Giam, Sugun Jawan, 70 m, 1°19′20.7″N 110°16′21.4″E, flowering *Schismatoglottis giamensis*, 20.vi.2009, P.C.Boyce & Wong Sin Yeng lgt. (AR-2549) (56: ZIN, NMPC, IBTP, KMNH); Kuching, Siburan, Kampung Sikog, Air Terjun Baan Gong, 70 m, 1°20′16.1″N 110°20′09.6″E, flowering *Schismatoglottis baangongensis*, 26.vii.2009, P.C.Boyce & Wong Sin Yeng lgt. (AR-2588) (63: ZIN, NMPC, IBTP, KMNH); Miri, Marudi, Long Lama, Mulu N.P., Trail to Deer Cave, 60 m, 4°02′23.8″N 114°48′54.6″E, flowering *Phymatarum borneense*, 5.viii.2006, P.C.Boyce, Wong Sin Yeng, Jeland ak Kisai & Mael ak Litis lgt. (AR-1931) (23: ZIN, NMPC); Miri, Marudi, Long Lama, Mulu N.P., Trail to Deer Cave, 60 m, 4°02′02.0″N 114°49′00.0″E, flowering *Schismatoglottis muluensis*, 6.viii.2006, P.C.Boyce, Wong Sin Yeng, Jeland ak Kisai & Mael ak Litis lgt. (AR-1941) (110: ZIN, NMPC, IBTP, KMNH, NHMW); Kuching, Siburan, Kampung Giam, Air Terjun Giam, 37 m, 01°19’11.2”N 110°16’11.4”E, flowering *Homalomena giamensis*, 07.ii.2016, P.C.Boyce, Jeland ak Kisai & Wong Sin Yen lgt. (AR-1691) (13: ZIN, NMPC); Kampung, Sungai Temaga, trail to Gunung Pueh, 82 m, 01°46’58.6”N 109°43’06.6”E, flowering *Schismatoglottis*, 23.iii.2014, Wong Sin Yeng & P.C.Boyce lgt. (AR-4651) (1: ZIN); Kuching, Siburan, Air Terjun Baan Gong, 70 m, 01°20′16.1″N 110°20′09.6″E, flowering *Homalomena borneensis*, 26.vii.2009, P.C.Boyce & Wong Sin Yeng lgt. (AR-2575) (11: ZIN, NMPC); Kuching, Siburan, Sugun Jawan, 50 m, 01°19’16.1”N 110°16’16.7”E, flowering *Homalomena gastrofructa*, 09.vi.2009, P.C.Boyce & Wong Sin Yeng lgt. (AR-2559) (5: ZIN, NMPC); Miri, Niah N.P., Beside road margin, outside of the main entrance, 13 m, 03°49.598’N 113°45.683’E/03°49.577’N 113°45.710’E, flowering *Schismatoglottis*, 30.iii.2014, Hoe Yin Chen lgt. (AR-4665) (2: ZIN); Kuching, Sematan, Sungai Temaga, trail to Gunung Pueh, 82 m, 01°46’58.6”N 109°43’06.6”E, flowering *Homalomena caput-gorgonis*, 23.iii.2014, Wong Sin Yeng & P.C.Boyce lgt. (AR-4659) (2: ZIN); Kuching, Kampung Sebat Dayak, Air Terjun Sebat, 70 m, 01°48’05.6”N 109°43’09.6”E, flowering *Piptospatha elongata*, 21.iii.2014, Wong Sin Yeng & P.C.Boyce lgt. (AR-4367) (1: ZIN); Betong, Roban, Sebankoi, Taman Rekreasi Sebankoi, 154 m, 01°57′27.4″N 111°26′04.6″E, flowering *Homalomena ibanorum*, 05.xii.2005, P.C.Boyce, Jeland ak Kisai, Jepom ak Tisai, Mael ak Late & Wong Sin Yeng lgt. (AR-1538) (7: ZIN, NMPC); Kuching, Matang, Maha Mariamman Temple, trail to Indian Temple, 350 m, 01°35’25.7”N 110°13’12.8”E, flowering *Homalomena matangae*, 04.iii.2014, P.C.Boyce & Jeland ak Kisai lgt. (AR-230) (7: ZIN, NMPC); Kuching, Bau, Krokong, Gua Peri-peri, 30 m, 01°22’51.9”N 110°07’09.3”E, flowering *Schismatoglottis*, 09.v.2009, P.C.Boyce & Wong Sin Yeng lgt. (AR-2445) (2: ZIN); Kuching, Bau, Gua Angin, 45 m, 01°24’54.8”N 110°08’08.2”E, flowering *Schismatoglottis*, 21.vi.2005, P.C.Boyce & Jeland ak Kisai lgt. (AR-1240) (8: ZIN, NMPC); Roban, Sebankoi, Taman Rekreasi Sebankoi, Site 1, 154 m, 01°57’27.4”N 111°26’04.6”E, flowering *Schismatoglottis sarikeense*, 07.ii.2010, Low Shook Ling lgt. (AR-3001) (4: ZIN); Kuching, Siburan, Kampung Sikog, Air Tejun Baan Gong, 70 m, 01°20′16.1″N 110°20′09.6″E, flowering *Homalomena baangongensis*, 26.vi.2009, P.C.Boyce &

Wong Sin Yeng lgt. (AR-2574) (44: ZIN, NMPC, IBTP, KMNH); Kuching, Matang, Kubah N.P. Sungai Bungen, 230 m, 01°36′30.9″N 110°11′35.0″E, flowering *Ooia glans*, Ooi Im Hin lgt. (AR-2339) (2: ZIN); Kuching, Bau, Gua Angin, 45 m, 01°24'54.8"N 110°08'08.2"E, flowering *Schismatoglottis*, 21.vi.2005, P.C.Boyce & Jeland ak Kisai lgt. (AR-1240) (24: ZIN, NMPC). Miri, Miri, Marudi Long Lama, Mulu National Park, DC limestone, before Kenyalang trail junction, 65 m, 4°02'29.4"N 114°48'44.3"E, flowering *Schismatoglottis muluensis*, 25.xii.2017, SY Wang team lgt. (SK01) (38: NMPC); [same locality] DC limestone, before 2nd shelter, flowering *Schismatoglottis colocasioideae*, 27.xii.2017 (SK03) (11: NMPC); [same locality and host plant] 30.xii.2017 (SK07) (11: NMPC); [same locality] DC limestone, before Kenyalang trail junction, flowering *Schismatoglottis muluensis*, 1.i.2018 (SK10) (11: NMPC); [same locality] DC limestone, near Deer water cave, flowering *Schismatoglottis muluensis*, 1.i.2018 (SK11) (33: NMPC, IBTP); [same locality] DC limestone, canopy trail, flowering *Schismatoglottis colocasioideae*, 7.i.2018 (SK12) (13: NMPC); [same locality] BT right, flowering *Schismatoglottis serratodentata*, 8.i.2018 (SK13) (2: NMPC); [same locality and host plant] 23.i.2018 (SK17) (1: NMPC); [same locality] DC limestone, near Deer water cave, flowering *Schismatoglottis pellucida*, 30.i.2018 (SK18) (3: NMPC); [same locality] flowering *Schismatoglottis multinervia*, 31.i.2018 (SK19) (4: NMPC); [same locality and host plant] 3.ii.2018 (SK21) (3: NMPC); Kapit, Taman Rekreasi Sebabai, 84 m, 1°56'37.5"N 112°54'24.8"E, flowering *Ooia havilandii*, 22.ix.2017, Wong & Boyce lgt. (AR-3635) (23: NMPC, ZIN): Sarikei Bayong, Ulu Sarikei, Lubok Lemba, Rymah Nyuka, 55 m, 1°53'41.3"N 111°30'11.5"E, flowering *Ooia secta*, 3.vi.2017, Wong & Boyce lgt. (AR-2756) (1: NMPC); Kuching Lundu, Gunung Gading NP, waterfall 1, 200 m, 1°41'28.3"N 109°50'43.6"E, flowering *Homalomena*, 27.v.2017, Wong & Boyce lgt. (AR-2757) (3: NMPC); Sarikei Bayong, Ulu Sarikei, Lubok Lemba, Rymah Nyuka, 55 m, 1°53'41.3"N 111°30'11.5"E, flowering *Schismatoglottis erumpens* complex, 3.vi.2017, Wong & Boyce lgt. (AR-2753) (4: NMPC).

Diagnosis. This species is very similar to *Cycreon floricola floricola* with which it shares most external characters and genital morphology. *Cycreon floricola borneanus* ssp. n. can be distinguished from *C. floricola floricola* by the shape of the pronotal punctation consisting only or largely of complete ring-like punctures. The dorsal coloration of *C. floricola borneanus* sp. n. is usually more uniform, with elytral colouration not much darker than pronotal one.

Description. *Measurements.* 2.2–3.4 mm long (length of holotype: 2.9 mm), 1.8–1.9× as long as wide, widest at basal fifth of elytra; weakly convex, 3.1–3.3× as long as high (height of holotype: 2.8 mm). *Colouration.* Pale brown with weakly darker elytra (Fig. 1C).

Pronotum 2.2× wider than long; 1.5× wider at base than between anterior angles, 1.6× wider than head including eyes. Punctation dense and shallow, consisting of complete ring-like impressions with one small setiferous puncture on posterior margin (Figs 4E, 5F), punctation of approximately same in size and density all over pronotum.

Elytra widest at anterior fifth, 1.1–1.2× as long as wide, 2.9–3.0× as long as pronotum, 1.1× as wide as pronotum. Punctation on intervals composed of semicircular impressions with one setiferous puncture on posterior margin (Fig. 4F).

Variation. In most specimens examined from Borneo, the pronotal punctation consists exclusively of completely ring-like punctures. However, in few localities on the north-western coast of Borneo the punctation of 5-20% of specimens shows a mixture of complete and incomplete rings. In the absence of genetic data, we are unable to analyze this variation in detail, and hence temporarily treat even these specimens as *C. floricola borneanus*.

Etymology. The name of this species is derived from Borneo, the historical name of island where all the known specimens of this subspecies were collected.

Distribution. The species seems to be widespread in Borneo, it is recorded from Indonesia: Kalimantan Barat and Kalimantan Selantan and Malaysia: Sabah, Sarawak (Fig. 7)

Biology. This subspecies has been collected in inflorescences of a number of plant species belonging to the Araceae family. It was collected in high numbers in flowers of the genus *Schismatoglottis*: *S. calyptrata*, *S. colocasioideae*, *S. erumpens* complex, S. *giamensis* (Fig. 6G), *S. mayoana*, *S. modesta*, *S. muluensis*, *S. multinervia, S. pellucida*, *S. petradoxa* and *S. serratodentata.* It has been also collected in numbers close to one hundred specimens in an inflorescence of *Ooia glans* (Figs 6H–I) and *O. havilandii.* Other known records of host plants include *Alocasia longiloba* complex (Fig. 6F), *Gamogyne loi*, several species of *Homalomena* (this paper) *Phymatarum borneense* and *Schottarum sarikeense* (Fig. 6A–B) (Low et al. 2016). According to H. Takizawa (pers. comm. 2017), *C. borneanus* can be found in aggregations in a wide range of aroid inflorescences from lowlands to montane areas (ca. between 100–1500 m a.s.l), mainly in flowers on small open places like trail sides in or near well-preserved primary or secondary forests, or along small streams.

Biology of *Cycreon*

All specimens of both subspecies of *C. floricola* have been collected in inflorescences of various Araceae genera, often in high numbers, indicating their tight association with this microhabitat. The fact that there were only two specimens of the genus known up to now likely correspond with the biology of *Cycreon* beetles, since no study of flower-inhabiting beetles associated with Araceae in the Malaysian Peninsula and Sunda islands was performed previously.

Low et al. (2016) studied the biology of insects associated with inflorescences of Araceae in Borneo and demonstrated that *Cycreon floricola borneanus* specimens

are only present in the upper part of the inflorescences of *Phymatarum borneense* and *Schottarum sarikeense*, never in the pistillate zone (= bottom), and that they are not attracted by the smell of the inflorescences, unlike the co-occurring *Chaloenus* beetles (Chrysomelidae) and *Colocasiomyia* flies (Drosophilidae). Observations of few specimens covered by pollen grains were reported, but only *Colocasiomia* flies were considered as pollinators. Subsequent investigations of the pollination biology of the *Schismatoglottis calyptrata* complex (Hoe et al. 2018) revealed that *Cycreon floricola borneanus* visited all the investigated species except *Schismatoglottis calyptrata* and *S. laxipistillata*, but their abundance differed based on host plant species: they were very abundant in *S. giamensis, S. caesia and S. muluensis*, but present in single or few specimens only in *S. pseudoniahensis*, *S. pantiensis*, *S. adducta*, and *S. roh*. *Cycreon* beetles were observed to feed on the exudations from the interpistillar staminodes, mated on the pistillate zone and remained inside the lower spathe chamber. They were also revealed as the most effective pollen carriers, carrying 6–15 times more pollen than *Colocasiomyia* flies and hence considered as secondary pollinators (*Colocasiomyia* flies were 4–6 times more abundant and are hence considered as main pollinators). No hydrophilid larvae were found in the inflorescences, indicating that they may live in different microhabitat.

Mouthparts of *Cycreon* (Fig. 1F–K) are unusual when compared to other members of the tribe Megasternini examined so far, differing from them in three aspects: (1) structure of the mandible with two large teeth on the apex (Fig. 1F–G), (2) excision of the clypeus (varying from weak to very deep, depending of the species; Fig. 5), and (3) shape of the mentum, with deep anterior excision (Figs 1J, 2B, 5). The mandibles of other Megasternini examined so far bear simple apex (e.g., Fikáček 2010, Arriaga-Varela et al. 2018), while those of *Cycreon* have the apex deeply bifid and with two large teeth. When the mandible is examined in mesal view (Fig. 1H), both apical teeth are situated on sides of straight edge, and they become strongly abraded in some specimens (Fig. 1G). This may indicate that mandibular apex is used for processing of some hard/solid material, possibly for scraping organic material from internal parts of the aracean inflorescences, in agreement with the above observations by Hoe et al. (2018). The inspection of the gut contents of *Cycreon floricola borneanus* (Fig. 6C–E) revealed that the midgut contains two components, both stained by safranine dye: (1) pollen grains of the respective plant species and (2) the heterogeneous organic matter which cannot be further identified; it does not seem to be just remains of crushed pollen grains, as no partially crushed pollen grains or remains of their exine were found (safranine stains various organic compounds including cellulose, lignine, glucosamines and cell nuclei, and does not allow detailed identification of this component - it may represent organic detritus scraped by the beetles from interior of the inflorescence). The presence of this unspecified organic matter in the intestines indicates that *Cycreon* beetles are not specialized pollen feeders, but the presence of pollen grains in the midgut content confirms that pollen is part of the diet and may be possibly digested. When compared to specialized pollen-feeding New Zealand genus *Rygmodus* (Hydrophilidae: Cyclominae) analyzed by Minoshima et al. (2018), important differences in mandible morphology can be found, confirming that *Cycreon* is not specialized pollen feeder: (1) mandibular apex is simple and spoon-like in *Rygmodus*, whereas strongly bifid in *Cycreon*, (2) mola is simply tuberculate in *Rygmodus* (a supposed adaptation to disrupt the pollen exina by grinding), but bears poriferous lamellae in *Cycreon* and all other hydrophilids examined. Unlike in *Cycreon*, the midgut of *Rygmodus* contains nearly exclusively pollen grains, with very little fine organic matter (see Minoshima et al. 2018: fig 4).

The excised clypeus and anterior margin of mentum is unusual in the Megasternini. Excised mentum is only known in the Central American genus *Nitidulodes*, which is also associated with aroid inflorescences (Hansen 1991, Bloom et al. 2015). Excised clypeus is only present in *Cycreon*. Moreover, the strong variation of mentum and clypeus shape between different species of *Cycreon* is also unusual within Megasternini. Usually these characters are very similar in congeneric species and differ at most between genera. We suppose that this interspecific variation in *Cycreon* may indicate species-specific food and host-plant preferences. The data by Hoe et al. (2018) indicate some kind of specificity in host plants, which would be in agreement with this assumption. For example, various genera and species of Schismatoglottideae were sampled in Mulu National Park (Malaysia, Sarawak) from December 2017 to February 2018, but *Cycreon* beetles were only found in sampled species of *Schismatoglottis* (beetles were present in all sampled plants), whereas not a single specimen was found in inflorescences of *Anadendrum, Aglaonema, Alocasia, Bucephalandra* and *Lasia.* Additionally, the material collected from various inflorescences of the single aroid tribe Schismatoglottideae by Low et al. (2014, 2016), Hoe & Wong (2016) and Hoe et al. (2018) includes two very closely related subspecies only (*Cycreon floricola floricola* and *C. floricola borneanus*), despite consisting of more than 1000 specimens; not a single specimen of another *Cycreon* species was collected even in peninsular Malaysia, despite the sampled localities were close to those of two other species (*C. armandi* and *C. adolescens*). We suppose this may be caused by the focus on a single narrow group of host plants, and is congruent with the expected species-specific host preferences in *Cycreon* beetles.

Discussion

Interactions of *Cycreon* with aroid inflorescences can be interpreted as an initial stage of development of cantharophyly, i.e. interrelations between beetles and plant reproductive organs, in which only adult are associated with flowers (e.g., Kirejtshuk 1994, 1997). This type of inter-

relations is particularly possible in cases when blossoming period ends by decaying of part of flowers with fungal and microbial infection (Teichert et al. 2012). On the other hand, species of *Chaloenus* beetles (Chrysomelidae: Alticini) co-occurring with *Cycreon* may represents another type of interrelations with plants, connected with a secondary transition of adults from leaf-feeding to flower-feeding. Besides, one sample collected from *Leucocasia giganteum* in peninsular Malaysia included representatives of *Aethina* Erichson (Coleoptera: Nitidulidae: Nitidulinae); some species of the genus are known to be associated with fungi, others to feed on inflorescences (Kirejtshuk 1986). Few examined samples also included few staphylinids, possibly as occasional visitors of decaying aroid inflorescences.

Acknowledgements

We are indebted to H. Takizawa and Y. N. Minoshima (Japan) for providing us with the material from their collections. This work was supported by the European Union's Horizon 2020 research and innovation programme under the Marie Skłodowska-Curie grant agreement No. 642241 to EAV, and by the Ministry of Culture of the Czech Republic (DKRVO 2018/13, National Museum, 00023272) to MF. The work of EAV at the Department of Zoology, Charles University, Prague was partly supported by grant SVV260434/2018. WSY acknowledges the funding from the Ministry of Education of Malaysia through Vote No. NRGS/1089/ 47 2013-(03). The study of AGK was performed in the frames of the state research project AAAA-A17-117030310210-3 and partly supported by the programme of the Presidium of the Russian Academy of Sciences "Evolution of organic world. Significance and influence of planetary processes" and the Russian Foundation of Basic Research (grant No. 18-04-00243–a).

References

Archangelsky M (1997) Studies on the biology, ekology and systematice of the immature stages of New World Hydrophiloidea (Coleoptera: Staphyliniformia). Bulletin of the Ohio Biological Survey, New Series 12(1): 1–207.

Arriaga-Varela E, Seidel M, Deler-Hernández A, Senderov V, Fikáček M (2017) A review of the *Cercyon* Leach (Coleoptera, Hydrophilidae, Sphaeridiinae) of the Greater Antilles. ZooKeys 681: 39–93. https://doi.org/10.3897/zookeys.681.12522

Arriaga-Varela E, Seidel M, Fikáček M (2018) A new genus of coprophagous water scavenger beetle from Africa (Coleoptera, Hydrophilidae, Sphaeridiinae, Megasternini) with a discussion on the *Cercyon* subgenus *Acycreon*. African Invertebrates 59(1): 1–23. https://doi.org/10.3897/AfrInvertebr.59.14621

Bloom D, Fikáček M, Short AEZ (2014) Clade age and diversification rate variation explain disparity in species richness among water scavenger beetle (Hydrophilidae) lineages. PLoS ONE 9(6): e98430. https://doi.org/10.1371/journal.pone.0098430

Fikáček M (2010) Hydrophilidae: The genus Kanala Balfour-Browne (Coleoptera). In: Jäch MA, Balke M (Eds) Water Beetles of New Caledonia, volume 1. Monographs of Coleoptera 3: 365–394.

Fikáček M, Short, AEZ (2006) A revision of the Neotropical genus *Motonerus* Hansen (Coleoptera: Hydrophilidae: Sphaeridiinae). Zootaxa 1268: 1–38.

Fikáček M, Hebauer F, Hansen M (2009) Taxonomic revision of New World species of the genus *Oosternum* Sharp (Coleoptera: Hydrophilidae: Sphaeridiinae). I. Definition of species groups and revision of the *Oosternum aequinoctiale* group. Zootaxa 2054: 1–37.

Fikáček M, Jia FL, Prokin A (2012) A review of the Asian species of the genus *Pachysternum* (Coleoptera: Hydrophilidae: Sphaeridiinae). Zootaxa 3219: 1–53.

Hansen M (1991) The Hydrophiloid beetles: phylogeny, classification and a revision of the genera (Coleoptera, Hydrophiloidea). Kongelige Danske videnskabernes selskab, Copenhagen, 367 pp.

Hoe YC, Wong SY (2016) Floral biology of *Schismatoglottis baangongensis* (Araceae: Schismatoglottideae) in West Sarawak, Borneo. Plant Systematics and Evolution 302: 1239–1252. https://doi.org/10.1007/s00606-016-1329-z

Hoe YC, Wong SY, Gibernau M (2018) Diversity of pollination ecology in the *Schismatoglottis Calyptrata* Complex Clade (Araceae). Plant Biology. doi:10.1111/plb.12687

Kirejtshuk AG (1986) Revision of the genus Aethina Er. (Coleoptera, Nitidulidae) of the fauna of the Oriental and Palaearctic Regions. Proceedings of the Zioological Institute of Academy of Sciences of USSR 140: 44–82. [In Russian]

Kirejtshuk AG (1994) System, evolution of the way of life, and phylogeny of the order Coleoptera. I. Entomological Review 73(2): 266–288 (in Russian). [English translation: 1995, 74: 12–31]

Kirejtshuk AG (1997) On the evolution of anthophilous Nitidulidae (Coleoptera) in tropical and subtropical regions. Bonner Zoologische Beitrage 47(1–2): 111–134.

Low SL, Wong SY, Boyce PC (2014) *Schottarum* (Schismatoglottideae: Araceae) substantiated based on combined nuclear and plastid DNA sequences. Plant Systematics and Evolution 300: 607–617. https://doi.org/10.1007/s00606-013-0906-7

Low SL, Wong SY, Ooi IH, Hesse M, Städler Y, Schönenberger J, Boyce PC (2016) Floral diversity and pollination strategies of three rheophytic Schismatoglottideae (Araceae). Plant Biology 18(1): 84–97. https://doi.org/10.1111/plb.12320

Low SL, Wong SY, Boyce PC (2018). Naming the chaos: generic redelimitation in Schismatoglottideae (Araceae). Webbia 72: 1–100. https://doi.org/10.1080/00837792.2017.1409940

Minoshima YN, Seidel M, Wood JR, Leschen RAB, Gunter NL, Fikáček M (2018) Morphology and biology of the flower-visiting water scavenger beetle genus Rygmodus (Coleoptera: Hydrophilidae). Entomological Science. https://doi.org/10.1111/ens.12316

Orchymont A (1919) Contribution a l'étude des sous-familles des Sphaeridiinae et des Hydrophilinae (Col. Hydrophilidae). Annales de Société Entomologique de France 88 : 105–168.

Ryndevich SK (2001) On identification of species of the Cercyon dux group (Coleoptera: Hydrophilidae). Zoosystematica Rossica 10(1): 79–83.

Ryndevich SK (2008) Review of species of the genus *Cercyon* Leach, 1817 of Russia and adjacent regions. IV. The subgenera *Paracycreon* Orchymont, 1924 and *Dicyrtocercyon* Ganglbauer, 1904 (Coleoptera: Hydrophilidae). Zoosystematica Rossica 17(2): 89–97.

Ryndevich SK, Jia FL, Fikáček M (2017) A review of the Asian species of the Cercyon unipunctatus group (Coleoptera: Hydrophilidae: Sphaeridiinae). Acta Entomologica Musei Nationalis Pragae 57(2): 535–576. https://doi.org/10.1515/aemnp-2017-0089

Shatrovskiy A (2017) A new species of *Cycreon* d'Orchymont, 1919 from Singapore (Coleoptera: Hydrophilidae: Megasternini). Zootaxa 4217 (3): 588–592. https://doi.org/10.11646/zootaxa.4317.3.11

Short AEZ, Fikáček M (2011) World catalogue of the Hydrophiloidea (Coleoptera): additions and corrections II (2006–2010). Acta Entomologica Musei Nationalis Pragae 51: 83–122.

Short AEZ, Fikáček M (2013) Molecular phylogeny, evolution and classification of the Hydrophilidae (Coleoptera). Systematic Entomology 38: 723–752. https://doi.org/10.1111/syen.12024

Smetana A (1978) Revision of the subfamily Sphaeridiinae of America north of Mexico (Coleoptera: Hydrophilidae). Memoirs of Entomological Society of Canada 105: 1–292. https://doi.org/10.4039/entm110105fv

Takizawa H (2010) Revisional notes on the genus *Chaloenus* Westfood (Coleoptera: Chrysomelidae). In: Mohammed HJ, Ipor I, Meekiong K, Sapuan KA, Ampeng A (Eds) Lanjak Entimau Wildlife Sanctuary 'Hidden Jewel of Sarawak'. Proceedings of the Seminar: Lanjak Entimau Scientific Expeditions. Academy of Sciences Malaysia, 347–355.

Teichert H, Dötterl S, Framec D, Kirejtshuk A, Gottsberger G (2012) A novel pollination mode, saprocantharophily, in Duguetia cadaverica (Annonaceae): A stinkhorn (Phallales) flower mimic. Flora (Morphology, Distribution, Functional Ecology of Plants) 207(7): 522–529. https://doi.org/10.1016/j.flora.2012.06.013

Supplementary material 1

List of known specimens of Cycreon in DarwinCore format

Authors: Emmanuel Arriaga-Varela, Sin Yeng Wong, Alexander Kirejtshuk, Martin Fikáček

Data type: occurence

Link: https://doi.org/10.3897/dez.65.26261.suppl1

Liebherr JK
Cladistic classification of *Mecyclothorax* Sharp (Coleoptera, Carabidae, Moriomorphini) and taxonomic revision of the New Caledonian subgenus *Phacothorax* Jeannel 1

Baranek B, Kuba K, Bauder J, Krenn HW
Mouthpart dimorphism in male and female wasps of *Vespula vulgaris* and *Vespula germanica* (Vespidae, Hymenoptera) 65

Mey W
Vansoniella chirindensis gen. n., sp. n. – an unusual taxon with translucent wings from Zimbabwe (Lepidoptera, Limacodidae) 75

Bidzilya OV, Mey W
Review of the genus *Tricerophora* Janse, 1958 (Lepidoptera, Gelechiidae) with description of six new species 81

Arriaga-Varela E, Wong SY, Kirejtshuk A, Fikáček M
Review of the flower-inhabiting water scavenger beetle genus *Cycreon* (Coleoptera, Hydrophilidae), with descriptions of new species and comments on its biology 99

Deutsche Entomologische Zeitschrift

65 (1) 2018

http://dez.pensoft.net

Leibniz Association